University of Brighton

Preparation of surfactant incorporated third-generation solid dispersion formulations for curcumin to enhance drug solubility and oral bioavailability

This thesis is submitted to school of applied science,

University of Brighton, for the degree of Doctor of Philosophy

Zhenqi Liu

December 2022

Abstract

One of the endless challenges in the pharmaceutical industry is the poor oral bioavailability of drugs associated with poor solubility. Curcumin, a yellow-orange substance that is extracted from the spice turmeric (*Curcuma longa, Zinziberaceae*), has been attributed with a wide range of pharmacological activities for the prevention and treatment of many diseases. However, its potential for use as an orally delivered medicinal product is hindered by its extremely poor aqueous solubility and oral bioavailability. Many techniques have been applied to overcome the bioavailability problem of curcumin and solid dispersions were reported to be one of the most promising strategies to improve the solubility, dissolution rate and bioavailability of curcumin.

The objective of this study was to develop novel polymer-surfactant-based solid dispersion formulations for curcumin to increase its aqueous solubility and potentially increase oral bioavailability. Through a series of screening processes, a curcumin + Soluplus + Vitamin E TPGs (1:10:10) solid dispersion prepared by solvent evaporation + freeze-drying method was selected as the novel curcumin solid dispersion formulation, and it was named “Solucumin”. It has significantly increased the solubility of curcumin, with solubility study results showing the curcumin solubility 582-fold and 937-fold higher than commercial grade curcumin in pH 1.2 and 6.8 aqueous solutions, respectively. *In vitro* dissolution study, *in vitro* Caco-2 cell permeability and uptake studies and characterisation studies (FTIR, DSC, XRD, DLS, Zeta-potential and a short-term physical stability test) were conducted for Solucumin and it was compared with two marketed curcumin products (Longvida® and Nacumin®) and a polymer-surfactant-based solid formulation of curcumin (Mexcumin).

Solucumin has exhibited significantly higher dissolution, cellular

permeation and uptake of curcumin than all the comparators and commercial curcumin powder. Interestingly, it was found to be less effective in improving the dissolution of other curcuminoids (demethoxycurcumin and bisdemethoxycurcumin) compared with Mexcumin. XRD and DLS confirmed the amorphisation of curcumin and particle size reduction in Solucumin, which could be the main reasons for the improved curcumin solubility and dissolution. FTIR showed no curcumin in Solucumin was adhered to the surface of the excipients. DSC revealed that Vitamin E TPGs in Solucumin melted at human body temperature (37ºC) and it could dissolve curcumin. In the short-term stability test, Solucumin showed it has a degradation-resistant effect for at least a month.

In addition to curcumin, Solucumin technology has also been tested on other poorly water-soluble drugs/natural compounds to investigate its effect on drug/compound dissolution. It was found that Solucumin has significantly improved the dissolution of niclosamide, nitrofurantoin, terbinafine, quinine and quercetin in a pH 6.8 dissolution medium.

Overall, it can be concluded that Solucumin, the novel solid dispersion formulation developed in this study, succeeded in significantly improving the aqueous solubility, dissolution and permeability of curcumin. It is a promising formulation for improving the oral bioavailability not only of curcumin but also of other drugs/natural compounds with poor water solubility.

Table of Contents

Table of Figures

List of Tables

Abbreviations

5-LOX	Arachidonate 5-lipoxygenase)
λmax	Wavelength of maximum absorption
ß-NAD	Nicotinamide adenine dinucleotide
A-B	Apical side to basolateral side
AD	Alzheimer's disease
ANOVA	Analysis of variance
API	Active ingredient
ASBT	Apical sodium–bile acid transporter
AUC	Area under curve
B-A	Basolateral side to apical side
BCRP	Breast cancer resistance protein
BCS	Biopharmaceutical classification system
C_0	Initial drug concentration measured in the donor chamber
C_{max}	Maximum plasma concentration
C_s	*Solute concentration at the particle surface*
C_t	*Bulk concentration of solute*
C-LPNCs	Curcumin loaded phosphatidylcholine-maltodextrin based nanoparticles
CO2	Carbon dioxide
COX-2	Prostaglandin-endoperoxide synthase 2
CRSD	Controlled release solid dispersions co-amorphous CUR-PIP	Co-amorphous curcumin-piperine solid dispersion
CMC	Critical micelle concentration
CNELNs	Novel lipid nanoemulsion containing curcumin
CYP1A	Cytochrome P450 1A
DLS	Dynamic light scattering

DSC	Differential scanning calorimetry
DMEM	Dulbecco's modified Eagle's medium
DMSO	Dimethyl sulfoxide
E1E	(Z)-di-tert-butyl3,3 -((3-
112(oleoyloxy)propyl)azanediyl)dipropanoate	
EC	Ethyl cellulose
EGCG	Epigallocatechin gallate
EGR-1	Early growth of the response-1-gene product
EMC	Electronic medicines compendium
FBS	Fetal bovine serum
FDA	Food and Drug Administration
FTIR	Fourier transform infrared spectroscopy
GERD	Gastroesophageal reflux disease
GI	Gastrointestinal
GSTs	Glutathione S-transferases
HBSS	Hank's balanced salt solution
HBV	Hepatitis B
HEPES	4-(2-hydroxyethyl)-1-piperazineethanesulfonic acid
HIV	Human immunodeficiency viruses
HIV-1	Human immunodeficiency viruses 1
HIV-2	Human immunodeficiency viruses 2
HLB	Hydrophilic–lipophilic balance
HME	Hot melt extrusion
HPLC	High-performance liquid chromatography
HPC	Hydroxypropyl Cellulose
HPMC	Hydroxyprophylmethyl cellulose
HPMCAS	Hypromellose Acetate Succinate
HSV-1	Herpes simplex virus 1
ICH	The International Conference of Harmonization

IR	Infrared
IL1β	Interleukin 1β
IL1	Interleukin 1
IL6	Interleukin 6
IL8	Interleukin 8
IP	Intraperitoneal
IV	Intravenous
Ka	Mean absorption constants
LDH	Lactate dehydrogenase
LogP	Logarithm of the partition coefficient
LTR	Long terminal repeats
MAPK	Mitogen-activated protein kinases
MCC	Microcrystalline cellulose
Mct-1	Monocarboxylic acid transporter 1
MMP-3	Matrix metalloprotease 3
MMP-9	Matrix metalloprotease 9
MPD	Microprecipitated bulk powder
MPMS	1-methoxyphenazine methosulfate
MRP	Multidrug resistance-associated protein
MTT	3-(4,5-Dimethylthiazol-2-yl)-2,5-diphenyltetrazolium
bromide	
Na2GA	Disodium glycyrrhizin
NaCl	Sodium chloride
NaOH	Sodium hydroxide
NADPH	Nicotinamide adenine dinucleotide phosphate
$NaHCO_3$	Sodium bicarbonate
NEAA	Non-Essential Amino Acids
NCC	N-carboxymethyl chitosan
NCF	Novel self-nanomicellising solid dispersion

NFκB	Nuclear factor κB
NOAEL	No-observed-adverse-effect level
NPSSD	Novel polymeric-surfactant solid dispersions
OATP-1A2	Anion-transporting polypeptide 1A2
OATP-2B1	Anion-transporting polypeptide 2B1
OCTN2	Organic cation/carnitine transporter
OSTα-OSTβ	Organic solute transporter alpha-beta
Papp	Apparent permeability coefficient
PBS	Phosphate-buffered saline
PdI	Polydispersity index
Peff	Effective permeabilities
PEG	Polyethylene Glycol
PEG400	Polyethylene Glycol 400
PEG1000	Polyethylene Glycol 1000
PEPT1	Human peptide transporter 1
PD	Parkinson's disease
P-gp	P-glycoprotein
PUD	Peptic ulcer disease
PVP	Poly (vinylpyrrolidone)
PVPVA	Polyvinylpyrrolidone/vinyl acetate
PVA	Polyvinyl alcohol
RH	Relative humidity
ROS	Reactive oxygen species
R_{TOTAL}	Resistance values of the cell monolayers on the permeable membrane
R_{BLANK}	Resistance values of the permeable membrane with no cells
R_{TISSUE}	The specific cell resistance values
SAS	Supercritical anti-solvent

SCC	Squamous cell carcinoma
SD	Standard deviation
SF	Solvent evaporation+ freeze drying
SFD	Spray freeze drying
SGF	Simulated gastric fluid
SIF	Simulated intestinal fluid
SME-Cur	Self-microemulsifying curcumin
SNEDDS	Self-nanoemulsifying drug delivery system
SLCP	Solid lipid curcumin particle
SLN	Solid lipid nanoparticles
SULTs	Sulfotransferases
TDSS	Transdermal drug delivery system
TEER	Transepithelial electrical resistance
Tg	Glass transition point
TPGS 2K	di-tocopherol polyethylene glycol 2000 succinate
Tris-HCl buffer	Trizma hydro-chloride buffer solution
TNFα	Tumour necrosis factor 1α
UGTs	UDP-glucuronosyltransferases
USP	United States Pharmacopoeia
URF	Ultra rapid freezing
UV-vis	Ultraviolet-visible
WHO	World Health Organization
XRD	X-ray powder diffraction
Z ring	FtsZ ring

Acknowledgements

First and foremost, I am extremely grateful to my supervisor, Dr Ananth Pannala and Prof. John Smart for their invaluable advice, continuous support and patience during the courses of my study. They have given me complete freedom and respected my routines. Their vast knowledge, wealth of experience, fantastic creativity and excitement for science has inspired me to move further in my research and daily life. Additionally, I would like to express my gratitude to Dr Alison Lansley for her invaluable support in developing the methodology for my cell culture experiments. I would also like to thank the pharmaceutical and tissue culture laboratory teams, particularly Mrs Christine Smith, Dr Angela Quadir and Dr Petra Kristova for their wonderful technical support and assistance. Your generosity and kindness have made my study at University of Brighton a wonderful time. Special thanks to Dr Gary Parkinson from UCL School of Pharmacy for generously allowing me to use their X-ray diffractometer to test my samples, which was vital for my project.

I would particularly like to thank the most important people in my life, my parents, Xuhai Liu and Xiaohua Wei. My parents have been my role models since I was a child. They both work in the field of pharmaceutical research and have achieved countless successes in their areas. It was their dedication to research that inspired my determination to pursue a PhD. They are the people who raised me, educated me and made me a better person. They always respect my decisions and provide as much support as possible. Words cannot express how grateful I am to them. Without their tremendous understanding and encouragement at all times, I could not have gotten this far.

Declaration

I declare that the research contained in this thesis, unless otherwise formally indicated within the text, is the original work of the author. The thesis has not been previously submitted to this or any other university for a degree and does not incorporate any material that already submitted for a degree.

Zhenqi Liu

University of Brighton

December 2022

Chapter 1. Curcumin and its oral bioavailability problems

1.1. Introduction

Curcumin is a natural substance extracted from the roots of turmeric (*Curcuma longa*). Decades of scientific research have confirmed its ability to act as a potential therapeutic agent against numerous diseases. To this day, curcumin continues to attract the attention of researchers all over the world. However, despite its excellent medical potential, curcumin is still not approved for use as a medicine due to its extremely poor bioavailability.

This chapter will provide a comprehensive overview of curcumin including its origin, chemical structure, chemical properties, stability, physical appearance and potential medical benefits. It will also explain curcumin's oral bioavailability problems and the factors that contribute to it. Furthermore, the approaches developed for improving curcumin's bioavailability will be discussed briefly. At the end of this chapter, the hypothesis and aims proposed for developing a novel formulation to improve curcumins aqueous solubility and oral bioavailability will be discussed.

1.2. A brief introduction to turmeric

Turmeric (*Curcuma longa, Zingiberaceae*) is the plant from which curcumin is extracted from its roots. It is a member of the ginger family (*Zingiberaceae*). It is a rhizomatous, monocotyledonous perennial herb. The strong yellow fleshy tuber of turmeric is very similar in appearance to the roots of branching finger-like ginger (Esatbeyoglu et al., 2012). Turmeric requires plenty of water, hot and humid climate to grow. Therefore, most of the turmeric is cultivated in tropical and subtropical regions, particularly in India and South-East Asia (Scartezzini & Speroni, 2000). The rhizomes of turmeric can be boiled in water and dried, after which they are ground into deep orange-yellow coloured powders. Turmeric powder has long been used as a spice, a medicinal herb and a dye in Asia (Anand et al., 2007). In the 13th century, Arabian merchants brought turmeric from India to the European market (Aggarwal et al., 2007). The Latin name of turmeric “Curcuma” was derived from the Arabic word "Kourkoum", which is the original name of saffron. Due to its golden colour and exotic flavour, turmeric is also known as Indian saffron in Europe (Esatbeyoglu et al., 2012). In the West, turmeric is approved as a food additive and supplement. It is also commonly used as a colouring agent for foods, cosmetics, hair, textiles and furs (Grant & Schneider, 2000).

The use of turmeric for medical treatment in Asia can be traced back thousands of years (Araiza-Calahorra et al., 2018). Turmeric has been widely used since ancient times as a herbal medicine for treating many conditions such as cough/inflammation, respiratory diseases, flu, sinusitis, liver disorders, rheumatism and abdominal pain (Ravindranath & Chandrasekhara, 1980; Shoba et al., 1998; Wahlström & Blennow, 1978). In India, turmeric is traditionally used for treating infections, sprains/swelling and healing burn wounds (Araújo et al., 2001), while in China turmeric is regularly used as a herbal medication for treating diseases that are associated with abdominal pain

(Aggarwal et al., 2004). With the advancement of science and technology, it had been discovered that curcumin is the key ingredient that contributes to most of the therapeutic effects of turmeric (Mukundan et al., 1993; Pal et al., 2001).

The curcuminoids content of turmeric varies between 2-9% depending on its geographical origin and soil conditions (Priyadarsini, 2014). The term "curcuminoids" denotes a group of compounds including curcumin, demethoxycurcumin, bisdemethoxycurcumin and cyclic curcumin. Out of them, curcumin is the major component (50-60%) (Chaudhary et al., 2010). The bright orange-yellow colour of turmeric is derived from the curcuminoids (Esatbeyoglu et al., 2012).

1.3. A brief introduction to curcumin

Curcumin is a yellowish crystalline, odourless powder that is obtained from the roots of turmeric (Esatbeyoglu et al., 2012). Chemically, curcumin is known as diferuloylmethane ($C_{21}H_{20}O_6$) with a molecular mass of 368.37 g/mol. It is a polyphenol compound and has a melting point of 183 °C. LogP or octanol-water partition coefficient, is a measure of how hydrophilic or hydrophobic a molecule is. A negative LogP value indicates the compound is more hydrophilic while a positive LogP value means the compound is more lipophilic. Curcumin has a LogP value of 3.0, which indicates it is predominately dissolved in lipid (lipophilic). As a result, it is almost insoluble in water and readily soluble in polar solvents like DMSO, methanol, ethanol, acetonitrile, chloroform, acetone, etc.(Priyadarsini, 2014). The IUPAC name of curcumin is 1,7-bis (4- hydroxy-3-methoxy phenyl)-1,6-heptadiene-3,5-dione (1E-6E). The two aryl rings in curcumin contain *ortho*-methoxy phenolic groups that are symmetrically linked to a β-diketone moiety (Anand et al., 2007; Araiza-Calahorra et al., 2018; Carolina Alves et al., 2019). Polymorphism is the ability of a substance to crystallize into different crystalline forms. In general, there is an inverse relation between stability and solubility among polymorphic crystals, and the less stable polymorph is more soluble/has faster dissolution rate (Pudipeddi & Serajuddin, 2005). Curcumin exists in different polymorphic forms, of which Form 1 is monoclinic while other one (Form 2) is orthorhombic. It was reported that the metastable polymorph (Form 2) of curcumin showed almost 2-fold higher aqueous solubility than the thermodynamically more stable one (Form 1) (Sanphui et al., 2011). According to biopharmaceutical classification system (BCS) classification, pharmaceutical compounds with poor solubility can be classified into BCS class II (low solubility and high permeability) or BCS class IV (low solubility and low permeability) compounds (Tsume et al., 2014). Curcumin is a substrate for P-glycoprotein (P-gp), an ATP-dependent transmembrane drug efflux pump that is widely expressed in the intestine. This

results in a large amount of curcumin being expelled from the intestinal epithelium, leading to poor permeability (Song et al., 2016). As a result, curcumin can be classified as a BCS IV compound.

Curcumin exhibits a pH keto–enol tautomerism and it is depended on the pH and polarity of the solvent. Curcumin exists in the enol form in nonpolar solvents due to the intramolecular hydrogen bond formation, whereas in polar solvents it exists in keto form. In an acidic or neutral solution, the keto form of curcumin is predominant. Curcumin is most stable at this form but its aqueous solubility is very poor. On the other hand, when in an alkaline medium, the enol form of curcumin becomes predominant which is less stable but has higher aqueous solubility. However, it is very prone to degradation (Figure. 1.1) (Anand et al., 2007; Bernabé-Pineda et al., 2004; Jovanovic et al., 1999). The colour of curcumin also changes at different pH levels. At pH < 1, curcumin displays a red colour as it is in the protonated state. At pH 1–7, it exhibits a bright yellow colour as it exists in the neutral state. At pH > 7, curcumin is deprotonated and exhibits a red colour again in solution(Anand et al., 2007; Bernabé-Pineda et al., 2004).

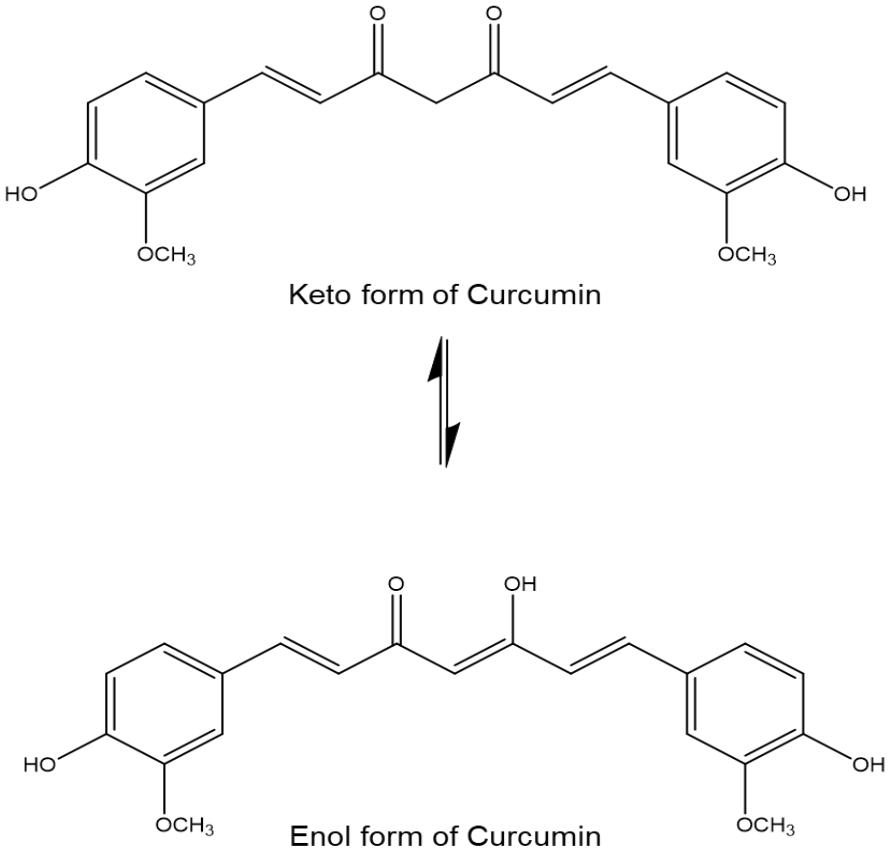

Figure 1.1. Keto-Enol tautomerism of curcumin

The two phenolic groups in curcumin act as active sites for reacting with free radical oxidants and converting them into less reactive species. During the reaction with free radical oxidants, curcumin undergoes oxidation by hydrogen atom transfer (HAT) or sequential electron and proton transfer (SET) from the phenolic OH groups (Priyadarsini, 2013). For example, the reaction of peroxy radicals with curcumin produces curcumin phenoxy radicals that are less reactive than peroxy radicals, thereby reducing the oxidative stress induced by free radical oxidants. The reduction in oxidative stress is thought to be responsible for the antioxidant effect of curcumin.(Priyadarsini, 2014).

1.4. The safety of curcumin

The safety of curcumin was proven in several animal tests and human studies (Lao et al., 2006b; Lao et al., 2006a; Sharma et al., 2004; Siviero et al., 2015). An oral dose as high as 12 g per day was shown to be well tolerated in humans (Lao et al., 2006a). However, despite its wide pharmacological potential and high dose tolerance, curcumin is still not approved as a therapeutic agent for oral delivery. The main reason is that curcumin has very poor oral bioavailability so it can be barely absorbed in the human body (Anand et al., 2007). Curcumin plasma concentration was under the detection limit at an oral dose of 12 g in an *in vivo* study on healthy male human (Klickovic et al., 2014). To overcome curcumin's problem of bioavailability, numerous research studies have been reported every year. In this introduction, factors that account for the poor oral bioavailability of curcumin are first explained in detail followed by a review of recent efforts in improving curcumin's oral bioavailability.

1.5. The medical potentials of curcumin

Curcumin was found to have a wide spectrum of pharmacological activities. Several studies on curcumin showed that it has anti-inflammatory (Srimal & Dhawan, 1973), antimicrobial (Kim et al., 2003; Kuttan et al., 1985; Prasad & Tyagi, 2015; Reddy et al., 2005), antirheumatic (Senft et al., 2010), immunomodulatory (Jantan et al., 2012) and anti-tumour effects (Hatcher et al., 2008). The anti-tumour effect of curcumin is associated with the suppression of early growth of the response-1-gene product (EGR-1), protein tyrosine kinase cascade and mitogen-activated protein kinases (MAPK) pathway (Khan et al., 2018). As mentioned in section 1.3, curcumin demonstrates antioxidant properties based on its ability to scavenge free radicals due to the electron-donating property of the phenolic group (Khopde et al., 1999; Mukundan et al., 1993; Ruby et al., 1995; Sharma, 1976; Sugiyama et al., 1996). The anti-inflammatory effect of curcumin is associated with its ability to inhibit NFκB (Nuclear factor κB) to bind with DNA. The inhibition of NFκB-DNA binding led to the suppression of pro-inflammatory molecules MMP-3 (matrix metalloprotease 3) and MMP-9 (matrix metalloprotease 9). It also results in a reduction in pro-inflammatory cytokines, such as TNFα (tumour necrosis factor 1α), IL1β (interleukin 1β) and IL8 (interleukin 8) (Esatbeyoglu et al., 2012). In addition, curcumin also exerts anti-inflammatory effects by binding to proteins COX-2 (prostaglandin-endoperoxide synthase 2), which leads to a reduction in COX-2 expression, prostaglandin and thromboxane synthesis. Subsequently, curcumin inhibits the activity of 5-LOX (Arachidonate 5-lipoxygenase) and leukotriene synthesis. The decreased expression of these compounds attributes to the anti-inflammatory effects of curcumin (Hong et al., 2004). The anti-bacterial effect of curcumin is believed to be associated with its ability to inhibit the formation of the FtsZ ring (Z ring) at the site of a division of bacterial cells, which disrupts this process (Rai et al., 2008). Curcumin also showed an anti-viral effect on several viruses such as HIV, influenza, HSV-1,

coxsackievirus and HBV. The anti-viral activities of curcumin include inhibiting the HIV-1 LTR-directed gene expression, HIV-1/HIV-2 proteases, haemagglutination, reducing HSV-1, coxsackievirus and HBV replication (Zorofchian Moghadamtousi et al., 2014). The pharmacological effect of curcumin on rheumatic diseases like osteoarthritis is based on its ability to inhibit the expression of MMP3. MMP3 is highly expressed in synovial cells in patients with osteoarthritis, which results in the degradation of connective tissue components. By inhibiting the expression of MMP3, curcumin inhibits the proliferation of osteoarthritis synovial cells, increases the cell apoptosis, and eventually eases the inflammation and cartilage degradation of osteoarthritis (M. Yang et al., 2019). Although the exact mechanisms are still unknown, the immunomodulatory effects of curcumin are most likely due to its ability to inhibit NF-κB target genes that are involved in inducing immune responses (Yadav et al., 2005). Additionally, activity in protecting the heart and kidney against oxidative injury was reported in several studies(Saeidinia et al., 2018; Venkatesan, 1998; Venkatesan et al., 2000). Curcumin shows heart-protecting effects through several mechanisms that include inhibiting cardiomyocyte fibrosis, increasing ventricular hypertrophy and related-gene expression (Saeidinia et al., 2018). Curcumin protects against renal injury by suppressing oxidative pressure in the kidney. It also increases levels of natural antioxidants, kidney glutathione content and glutathione peroxidase activity in kidney tissues, which restores kidney functions(Venkatesan et al., 2000). Curcumin also showed therapeutic activity in diabetes due to its effect in increasing sensitivity to insulin and reducing blood glucose levels in humans (Parsamanesh et al., 2018). Other studies showed that curcumin could be a promising drug candidate for treating or preventing neurodegenerative diseases such as Alzheimer's disease (AD) (Mutsuga et al., 2011; Ray et al., 2011), Parkinson's disease (PD) and brain tumours (Hatcher et al., 2008; Mythri et al., 2011). It has been reported that curcumin suppresses the formation of amyloid β protein

aggregates in the brain. The suppression of amyloid β protein aggregates leads to the reduction of reactive oxygen species (ROS) and cytochemokines, which decreases oxidative stress-induced damage and neuroinflammation to the brain (Mutsuga et al., 2011; Mythri et al., 2011; Ray et al., 2011).

1.6. Routes of administration reported for curcumin

The reported delivery routes of curcumin include oral administration, intravenous (IV) injection, nasal administration, topical administration, subcutaneous delivery and intraperitoneal (IP) administration (Prasad et al., 2014). Among the delivery routes, oral delivery is regarded as the most accepted route for drug administration. It is also the most preferred administration route over other delivery routes due to its convenience, high patient compliance, cost-effectiveness and ease of production (Gupta et al., 2009). Besides, oral administration is the most studied delivery route for curcumin. In most of studies, curcumin was delivered to the subjects (either humans or animals) through oral administration (Prasad et al., 2014). Orally delivered curcumin has exhibited various pharmacological effects such as anti-inflammatory, anti-tumour, antioxidant, antimicrobial, antidiabetic, immunomodulatory, etc. For IV administration, curcumin can be formulated into liposomes or emulsions (Li et al., 2005; Kiss et al., 2022) and saline is normally used as the carrier solution (Anderson, 2017). IV administration (Injection or infusion) helps curcumin bypass the physiological barriers against drug absorption, leading to the highest bioavailability and fastest effect among all delivery routes. However, compared with the oral route, IV administration of curcumin has some major drawbacks such as poor patient adherence, inconvenience, needle-associated pain, risk of unsafe needle use and the need for trained healthcare personnel (Homayun et al., 2019). Topical delivery is the administration of drugs directly onto the body surfaces such as skin or mucous membranes. Compared with oral administration, curcumin delivered through

the topical route showed pharmacological effects related mostly to the skin conditions such as skin inflammation, wound healing and skin cancer among others (Dovigo et al., 2013; López-Jornet et al., 2011; LoTempio et al., 2005; Sun et al., 2013). Nasal delivery is a drug administration route where the drug is insufflated through the nose and absorbed via the nasal mucosa. Curcumin was used in nasal administration for better brain targeting and it showed pharmacological effects on neurodegenerative diseases such as Alzheimer's and Parkinson's diseases (Prasad et al., 2014). Nasal delivery is an easier way of delivering curcumin when compared with IV injection. However, it is still relatively inconvenient when compared to the oral delivery route since there is a possibility of nasal irritation for some patients (Türker et al., 2004). Intraperitoneal injection is an administration route where the drug is injected directly into the peritoneum (body cavity) and in subcutaneous injection, the drug is injected into the tissue layer between the skin and the muscle. These two delivery routes were reported more often and used in the administration of curcumin to animals than to humans (Prasad et al., 2014). The routes of administration played important roles in the therapeutic effects of a drug substance. Among all the delivery routes of curcumin, oral administration is an effective route to deliver curcumin with numerous advantages over other administration routes. Therefore, it is suggested to focus more on the studies of the oral administration of curcumin and the development of curcumin formulation for oral delivery.

1.7. Factors that account for curcumin's poor oral bioavailability

Curcumin could be classified as a class IV substance since it has poor aqueous solubility and limited permeability across the intestinal membranes (Paolino et al., 2016; Wahlang et al., 2011). Apart from the poor solubility and intestinal permeability, curcumin also has low serum concentration, poor pH-dependent aqueous stability and rapid metabolism in animals and humans, which are believed to be the main reasons that account for the poor oral bioavailability of curcumin (Gantait et al., 2011; Holder et al., 1978; Ireson et al., 2001; Kunnumakkara et al., 2008; Kurien et al., 2007; Modasiya & Patel, 2012; Murugan & Pari, 2006; Perkins et al., 2002; Pfeiffer et al., 2007; Ravindranath & Chandrasekhara, 1981; Sandur et al., 2007; Song et al., 2016; Suresh & Nangia, 2018; Wang et al., 1997).

1.7.1. Poor aqueous and gastro-intestinal fluid solubility

Curcumin is hydrophobic with extremely poor water solubility (Lao et al., 2006a). Its aqueous solubility is also pH dependent. At acidic or neutral pH, it is practically insoluble. The maximum solubility of curcumin in an aqueous solution at pH 5 was only 11 ng/ml (Gantait et al., 2011; Holder et al., 1978). It was reported that the solubility increased to 0.1 μg/ml at pH 6.8. However, it dropped to 0.06 μg/ml when the pH was increased to 7.4 (Song et al., 2016). This is problematic for the absorption of curcumin since for any orally administrated drug to be absorbed, it needs to first dissolve in the gastrointestinal (GI) fluids. Curcumin has a low plasma concentration even after administering a high oral dose. In a clinical trial conducted in healthy human males even after an oral dose of curcumin as high as 12 g the plasma curcumin concentration was too low to be detected (Klickovic et al., 2014). In contrast, when 1 g/kg of curcumin was delivered orally to Sprague– Dawley rats and measuring plasma curcumin concentration showed that the amount of curcumin present in the plasma was less than 1% of the administrated dose (Wahlström

& Blennow, 1978). A similar result was also reported by Chang et al., after an oral dose of 1 g/kg of curcumin in rodents resulted in a curcumin plasma concentration of 15 ng/ml after 50 min. When at the same dose, humans showed much lower curcumin plasma concentration than rats (Chang et al., 2013). In another study, the same dose of curcumin (2 g/kg) was delivered orally to rats and humans respectively. The maximum plasma concentration (C_{max}) in rats was found to be 1.35 ± 0.23 μg/ml measured 50 min after taking the dose, whereas the C_{max} of curcumin in humans was only 0.006 ± 0.005 μg/ml measured 1 h after administration (Shoba et al., 1998). The results from these studies further suggest that curcumin has a very poor plasma concentration even after a high oral dose in both rodents and humans. When the same oral dose was administered, rats were found to have higher plasma concentrations of curcumin than humans.

1.7.2. Low permeability (absorption)

Apart from solubility, permeability is another main factor that affects oral drug administration since the absorption of drugs depends on their permeability across the biological membrane of the GI tract after dissolution (Parikh et al., 2016). Experimental results in *in vivo* animal models and simulated human intestinal epithelium barrier have shown that curcumin is poorly permeable across intestinal membranes even after dissolution (Gao et al., 2013; Righeschi et al., 2016; Volpe et al., 2007; Wahlang et al., 2011). It was found that in the rat small intestine, curcumin was best absorbed at the duodenal segment, followed by the jejunum and colon. The absorption of curcumin in the ileum was the poorest (Wang et al., 2017a).

Caco-2 cell lines (Figure. 1.2) possess the same cell polarity and compact single-cell layer as human intestinal epithelial cells and as a result, they are commonly used as the cell model for testing the intestinal

permeability/absorption of drugs (Artursson & Karlsson, 1991; Parikh et al., 2018; Sambuy et al., 2005; Xue et al., 2017).

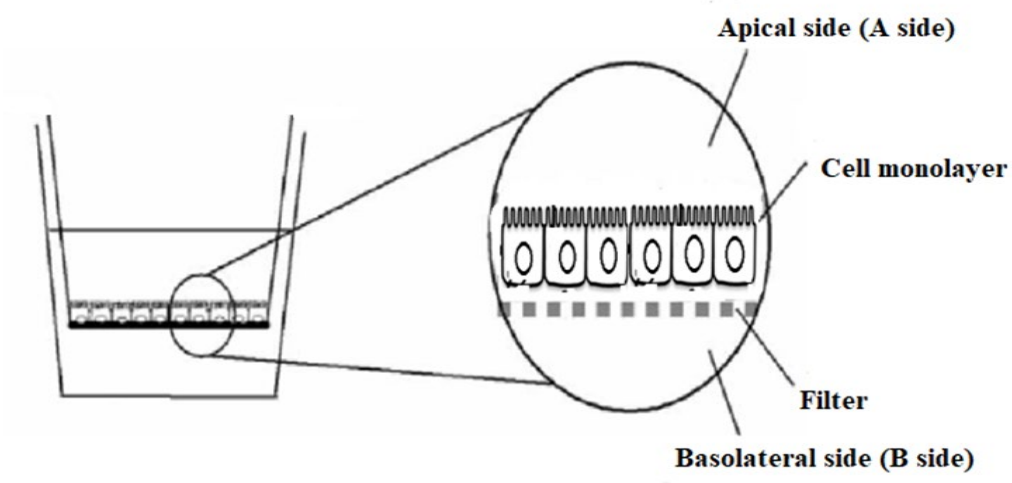

Figure 1.2. The structure of Caco-2 cell monolayer grown at a permeable filter support.

The results from the permeability test for curcumin reported by Zeng et al. (Zeng et al., 2017a) in Caco-2 cell lines exhibited that there was a decrease of permeability from the apical side to the basolateral side (A to B direction) with an increase in curcumin concentration. Conversely, permeability from the basolateral side to the apical side (B to A direction) increased along with an increase in the concentration of curcumin added. The apical and basolateral sides represent the luminal and blood/mesenteric lymph sides of the small intestinal tract, respectively (Artursson et al., 2001; van Breemen & Li, 2005). When curcumin at a concentration of 5 μg/ml, the value of Papp (A-B) was greater than Papp (B-A) which indicated an increased absorption of curcumin. However, when the curcumin concentration was increased to 10 μg/ml and 20 μg/ml, the value of Papp (A-B) became lower than Papp (B-A), indicating that the amount of curcumin that is being moved back into the intestinal lumen is higher than the amount being absorbed in this concentration range. It also showed that the intestinal permeability of curcumin does not increase in a concentration-dependent manner for curcumin (Zeng et al., 2017a). In transcellular studies, the apparent permeability coefficient (Papp) was used to represent the amount of compound transported per unit of time (Wang et al., 2017a). It was reported that the value of Papp is correlated to the extent of drug molecules that penetrate the intestinal tract of the drugs (Artursson & Karlsson, 1991; Ozeki et al., 2015). However, in another curcumin permeability study conducted using the Caco-2 cell line, it was reported that efflux pathways do not play a role in curcumin intestinal permeability. This observation was based on Papp (A-B) value ($2.93 \pm 0.94 \times 10^{-6}$ cm/s) was found higher than the value of Papp (B-A) ($2.55 \pm 0.02 \times 10^{-6}$ cm/s) at curcumin concentration of 62.6 μg/ml (170μM) (Wahlang et al., 2011). An efflux pump like P-glycoprotein could also affect the permeability of curcumin. P-glycoprotein is an ATP-dependent efflux pump that can pump drugs out of the cells thus reducing the bioavailability. In the small intestine, the expression of P-glycoprotein is present at the ileum and

jejunum (Canaparo et al., 2007). An *in vitro* study using Caco-2 cells showed that co-administration of P-glycoprotein inhibitors such as verapamil along with curcumin could increase the rate of absorption of curcumin (Xue et al., 2017). This indicated that curcumin could potentially be a P-glycoprotein substrate and blocking P-glycoprotein can help improve the permeability and drug absorption in the intestinal tract. Wang et al. (Wang et al., 2017a) investigated a concentration-dependent effect of verapamil on the absorption of curcumin in rat intestines. No obvious change to the absorption of curcumin was observed when verapamil concentration was increased from 0.05 mmol/l to 0.1 mmol/l. When verapamil concentration was increased to 0.5 mmol/l, the rate of curcumin absorption was increased by approximately 3%. This showed that a P-glycoprotein inhibitor like verapamil is capable to improve both the rate and the amount of curcumin absorbed in the small intestines (Wang et al., 2017a). Overall, from these studies, it can be concluded that curcumin has poor permeability across intestinal barriers even after dissolution, thus confirming that curcumin can be classified as a class IV drug according to the biochemical classification scheme (poorly soluble and poorly permeable).

1.7.3. High metabolism rate of curcumin

Curcumin delivered orally undergoes extensive metabolic reduction and conjugation, which result in poor bioavailability (Garcea et al., 2004). The mechanisms of curcumin metabolism are shown in Figures 1.3 and 1.4. Phase I metabolism includes the reduction of the four double bonds of the heptadiene-3, 5-dione structure of curcumin. The reduced curcumin metabolites dihydrocurcumin, tetrahydrocurcumin, and hexahydrocurcumin were detected in plasma (rats and humans) following curcumin oral supplementation. The reduction processes were catalysed by NADPH-dependent curcumin reductases that exist in the liver (Hoehle et al., 2007; Ireson et al., 2001). *E. coli*, the microorganism that commonly exists in the small intestine and colon, was found to have the ability to catalyse the metabolic reduction processes of curcumin (Hassaninasab et al., 2011). During Phase II metabolism, glucuronidation and sulfation of curcumin and the reduced metabolites take place. The conjugation activities are catalysed by UDP-glucuronosyltransferases and sulfotransferase respectively (Ireson et al., 2002). The conjugated metabolites include curcumin sulfate, curcumin glucuronide sulfate, curcumin glucuronide, dihydro curcumin glucuronide, tetrahydro curcumin glucuronide and hexahydro curcumin glucuronide. *In vivo* studies in rats and humans showed that the curcumin glucuronide and curcumin glucuronide/sulfate conjugates were found in the plasma, jejunum and livers (Asai & Miyazawa, 2000; Hoehle et al., 2007; Ireson et al., 2001; Ireson et al., 2002).(Ireson et al., 2001; Ireson et al., 2002). An *in vivo* study conducted in rats showed that the UDP-glucuronosyltransferases and sulfotransferase enzymes activities were found in the livers, kidneys, small intestine mucosa and colon intestinal mucosa; no conjugated enzyme activities were found in the plasma (Asai & Miyazawa, 2000). These observations might indicate that the conjugated curcumin metabolites are probably produced in these tissues before presenting in the plasma circulation. The glucuronidation activity was found to

occur more extensively in human intestines compared to rats, while it became less extensive in human liver than in rats. The difference in metabolism extent may be due to the differences in conjugation-hydrolysing enzymes content in the intestines & livers of humans and rats (Garcea et al., 2004; Ireson et al., 2001; Ireson et al., 2002).

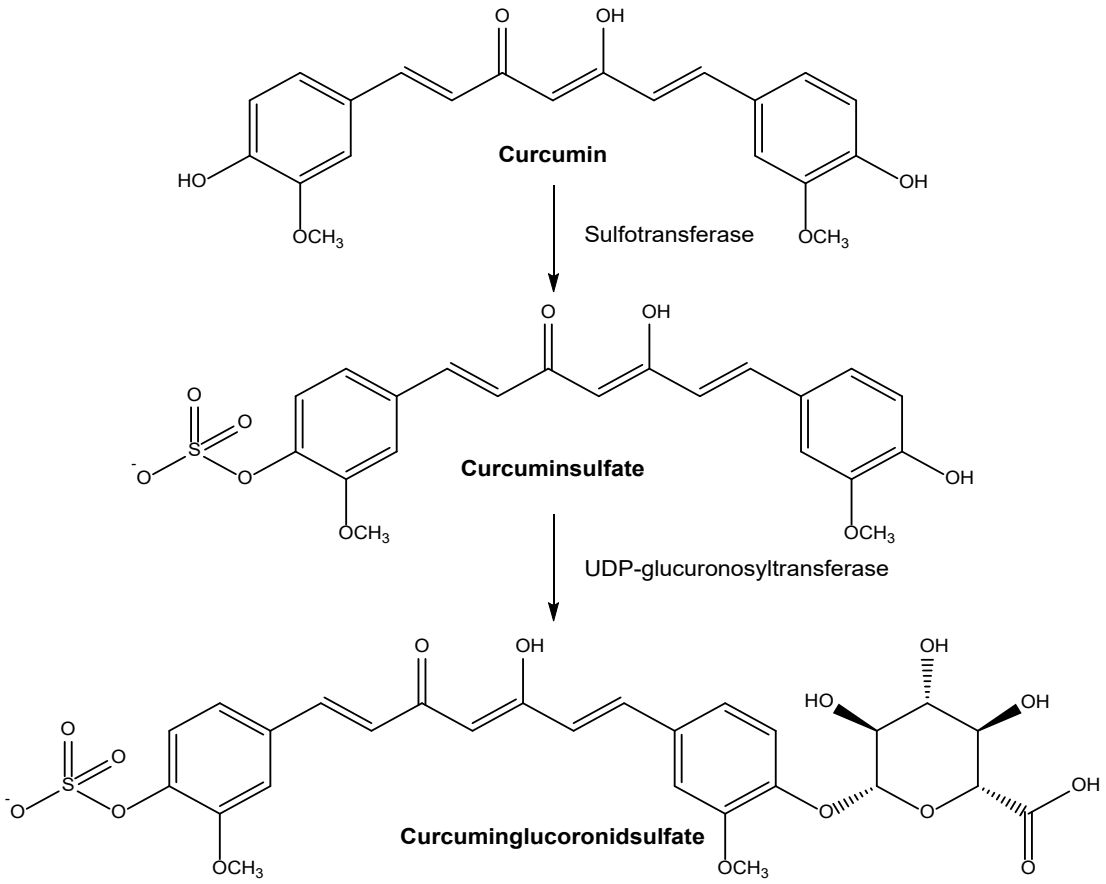

Figure 1.3. Sulphation and glucuronidation of curcumin (adapted from Esatbeyoglu et al., 2012)

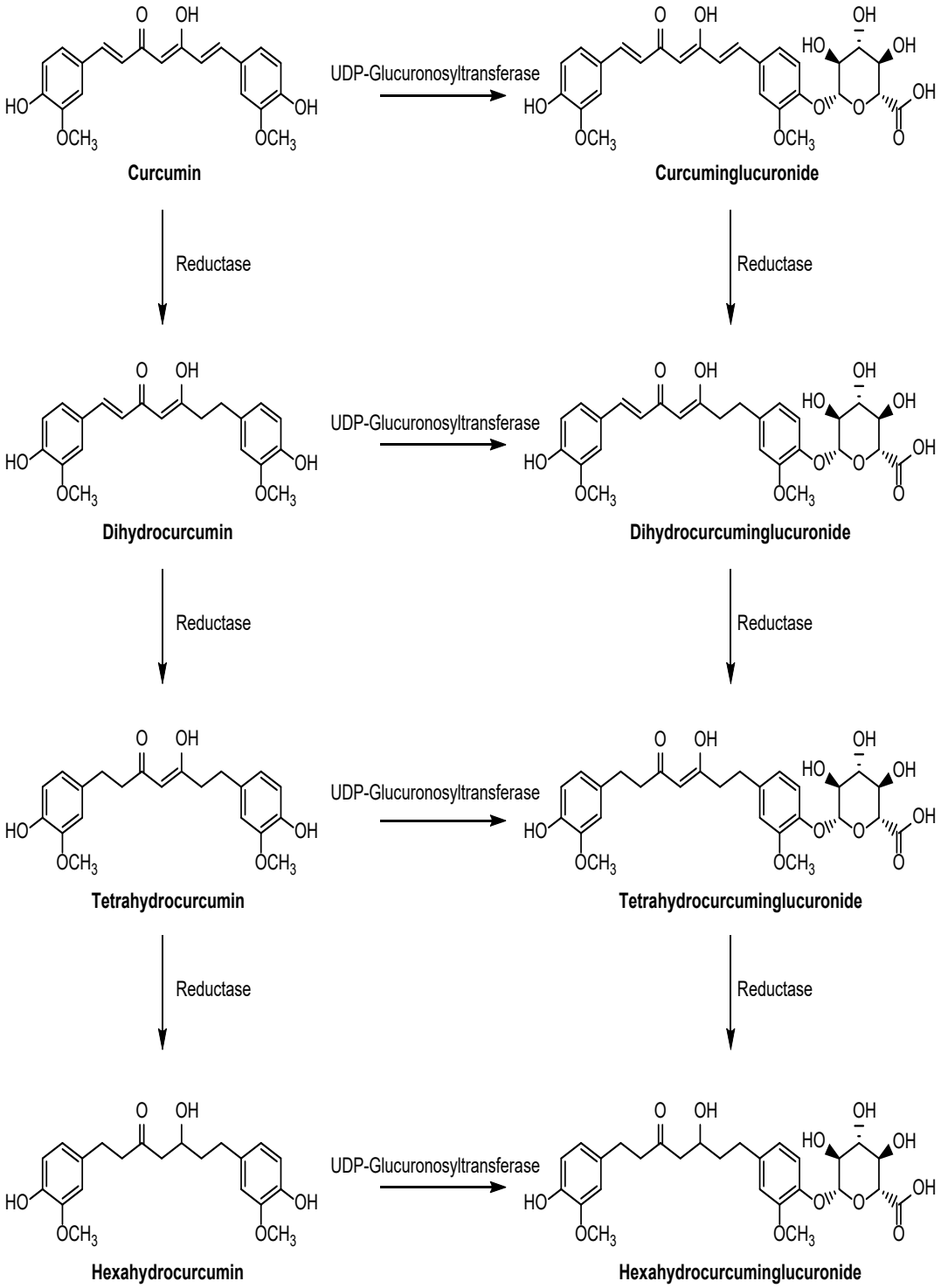

Figure 1.4. Reduction and glucuronidation of curcumin (adapted from Esatbeyoglu et al., 2012)

1.7.4. Chemical stability of curcumin

Like its aqueous solubility, the chemical stability of curcumin in an aqueous solution is affected by changes in pH. Curcumin is most stable at pH 1–6, when in the environment of the stomach or small intestine. However, the aqueous solubility becomes extremely poor at this pH range while the stability of curcumin decreases significantly when the pH is above 7 (Esatbeyoglu et al., 2012; Wang et al., 1997). In a stability test, using 5 mM curcumin solution (dissolved in methanol and added to 0.1 M phosphate buffer at pH 7.2) incubated at 37 °C for different lengths of time and analysed by HPLC, the results showed that 90% of the curcumin was degraded within 30 minutes to various degradation products including vanillin, ferulic acid and feruloyl methane (Figure. 1.5)**.** Vanillin was identified to be the major degradation product in this assay, the reaction following first-order kinetics (Wang et al., 1997).

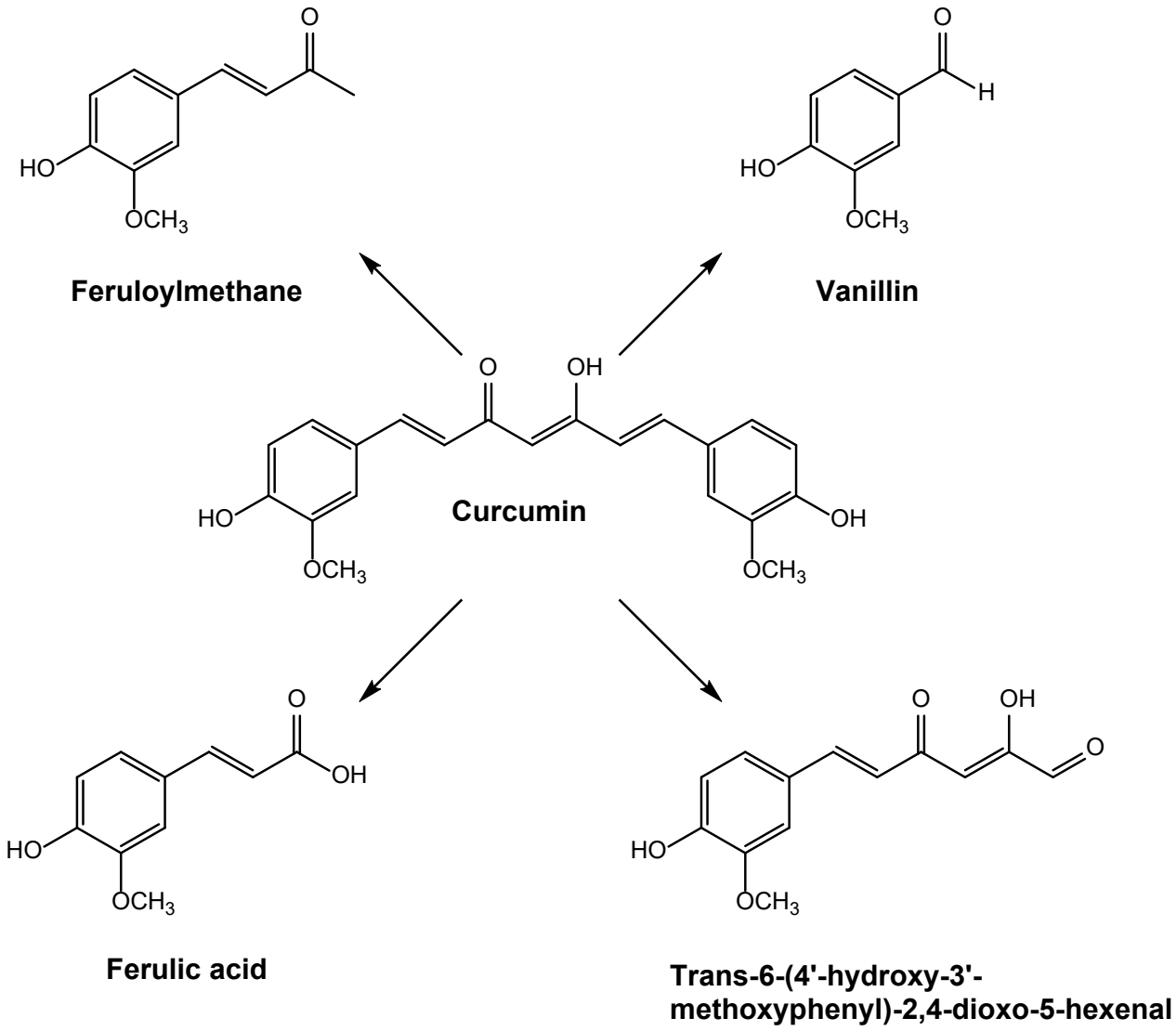

Figure 1.5. Degradation products of curcumin (adapted from Wang et al., 1997)

1.8. Strategies for improving curcumin's oral bioavailability

Numerous efforts have been made to find a way to overcome the low oral bioavailability of curcumin and a great number of novel formulations have been developed by researchers to achieve this goal. Details of strategies for improving the poor oral bioavailability of curcumin are discussed in the following sections. A summary of these developments is given in Table 1.1. The effect on the oral absorption of curcumin from the formulation is summarised and compared in Figure 1.6.

Subjects	**Amount of curcumin administrated**	**Formulation**	**Improved the oral bioavailability of curcumin**	**References**
Humans	2 g	2 g of curcumin + 5mg of piperine was delivered orally simultaneously	2-fold	Anand et al., 2007
Rats	200 mg/kg	Pre-administration of 20mg/kg piperine, then 200mg/kg curcumin after 6 hours	97-fold	Zeng et al., 2017b
Albino Wister rats	50 mg/kg	Curcumin loaded phosphatidylcholine-maltodextrin based nanoparticles(C-LPNCs)	55.2-fold	Chaurasia et al., 2015
Male SD (Sprague Dawley) rats	50 mg/kg	Curcumin-loaded nanosuspension, prepared by citric acid and Brij78	3.7-fold	Y. Wang et al., 2017
Humans	100 mg	Curcumin-loaded, Alginate and polysorbate nanoparticles	5-fold	Govindaraju et al., 2019
Male SD rats	50 mg/kg	Curcumin-loaded solid lipid	9.5-fold	Baek and Cho, 2017

		nanoparticles (SLN) with N-carboxymethyl chito san (NCC) coating		
Caco-2 cells	4µg/ml	The curcumin-loaded hybrid liposomal formulation consists of chitosan and phospholipid	1.256-fold higher 4h after incubation.	Peng et al., 2017
Male wistar rats	10 mg/kg	Curcumin-loaded mixed micelle (consisting of Pluronic F-127 and Gelucire® 44/14)	55-fold	Patil et al., 2015
Male SD rats	100 mg/kg	Curcumin-loaded sophorolipid-based nanomicelle	3.6-fold	Peng et al., 2018
Rats	50 mg/kg	Self-assembled, polymeric curcumin-loaded micelles, consisting of TPGS2 K, HS15 and Pluronic F127	2.87-fold	Wang et al., 2015
Male Wistar albino rats	8 mg/kg	Thiol modified chitosan coated, curcumin-piperine loaded, oil-in-water	64-fold	Vecchione et al., 2016

		nanoemulsion		
Male SD rats	100 mg/kg	Curcumin-loaded self-nano emulsifying drug delivery system (SNEDDS) , consisting of ethyl oleate, tween 80 and PEG 600	1.94-fold	Wan et al., 2016
Rats	100 mg/kg	Curcumin-phospholipid complex, entrapped in a self-nanoemulsion that consists of caster oil, Tween 80 and PEG 400	52.55-fold	Shukla et al., 2016
Rats	50 mg/kg	Self-emulsifying curcumin-loaded microemulsion that consists of E1E, Solutol HS and Transcutol HP	73-fold	Dhumal et al.,2015
Adult male Wistar rats	12.5 mg/kg	Self-microemulsifying curcumin (SME-Cur) wrapped in a hydroxyprophylmeth	5-fold	Petchsomrit et al., 2015

		yl cellulose (HPMC)-based sponge		
Male SD rats	47 mg/kg	Self-nanomicellizing curcumin-loaded Soluplus solid dispersion	117-fold higher than that of 150mg/kg curcumin suspension	Parikh et al., 2018
Male S D rats	150 mg/kg	Ball milled curcumin loaded disodium glycyrrhizin (Na2GA) solid dispersion	19-fold	Zhang et al., 2018
Male SD rats	30 mg/kg	Curcumin-loaded ternary solid dispersion system, prepared with Mannitol and TPGs	65-fold higher than 200mg/kg oral dose of pure curcumin	Song et al., 2016
Rats	500 mg/kg	Curcumin-Gelucire 50/13 solid dispersion	5.5-fold	Teixeira et al., 2015
Rats	100 mg/kg	curcumin-piperine solid dispersion	1.92-fold	Wang et al., 2019

Table 1.1. A summary of the novel formulations for improving curcumin's oral bioavailability

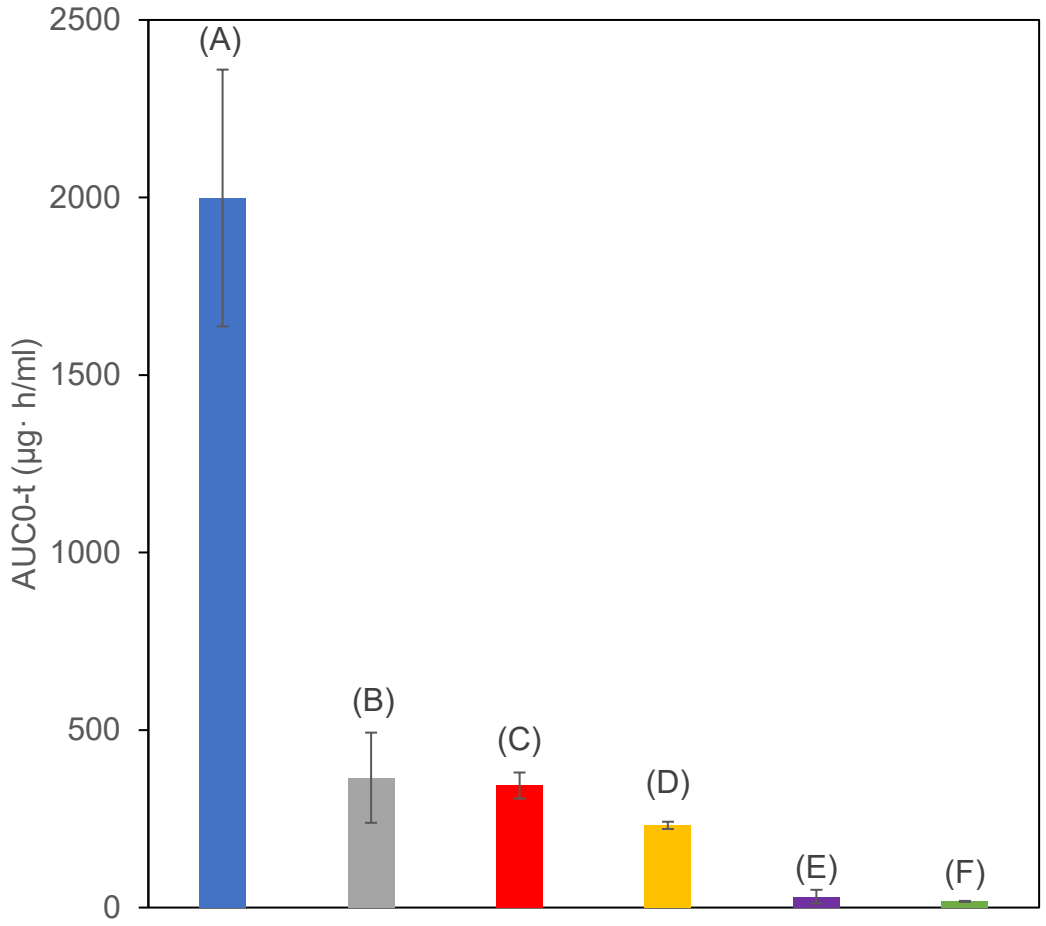

Figure 1.6. Comparison of curcumin oral absorption results of the different curcumin oral bioavailability enhancement strategies, at the curcumin oral doses of: (A) 47 mg/kg for the Soluplus containing self-nanomicellising solid dispersion (Parikh et al., 2018), (B) 50 mg/kg for the Nanosuspension prepared by CO_2-assisted in situ nano-amorphisation methods (Wang et al., 2017a), (C) 8 mg/kg for curcumin+piperine loaded nanoemulsion with thiol modified chitosan coating (Vecchione et al., 2018), (D) 100 mg/kg for the co-amorphous curcumin-piperine solid dispersion (Wang et al., 2019) and (E) 50 mg/kg for the self-emulsifying microemulsion(Dhumal et al., 2015)

1.8.1. Co-administration of adjuvants

Some adjuvants can decrease the metabolism of curcumin which can help to improve the bioavailability of curcumin. Piperine (Figure. 1.7) is an alkaloid naturally present in black pepper (from Piper nigrum) and is the substance that gives black pepper (*Piper nigrum*) its pungency.

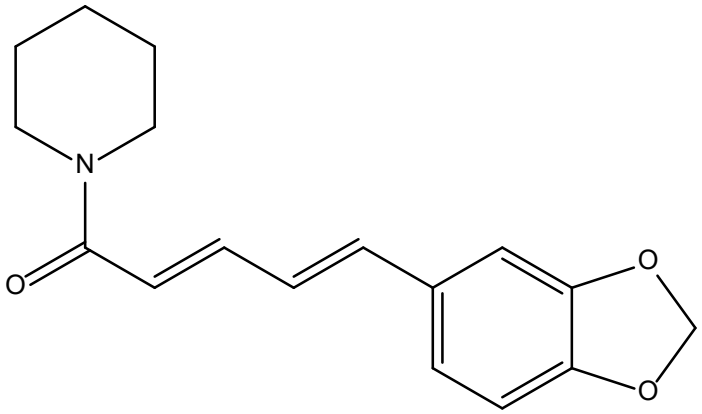

Piperine

Figure 1.7. Chemical structure of piperine

Co- administration of piperine with curcumin was found to improve the bioavailability of curcumin (Atal et al., 1985). Piperine inhibits the enzyme UDP-glucuronyltransferase in the liver thereby limiting the extent of curcumin glucuronidation. Because of this process, more curcumin is available for absorption (Zeng et al., 2017b). An *in vivo* study was conducted in both rats and humans at an oral dose of 2 g/kg of curcumin with 20 mg/kg piperine, administered simultaneously (Shoba et al., 1998). The relative bioavailability of curcumin in rats was increased by 1.54-fold while in the human volunteers it increased by 20-fold. However, even though the extent of increase of bioavailability of curcumin was higher in humans than in rats, the amount of curcumin being absorbed was in fact higher in rats (Figure 1.8). In another clinical trial, 2 g of curcumin and 5 mg of piperine were co-administered orally to healthy human volunteers (Anand et al., 2007).

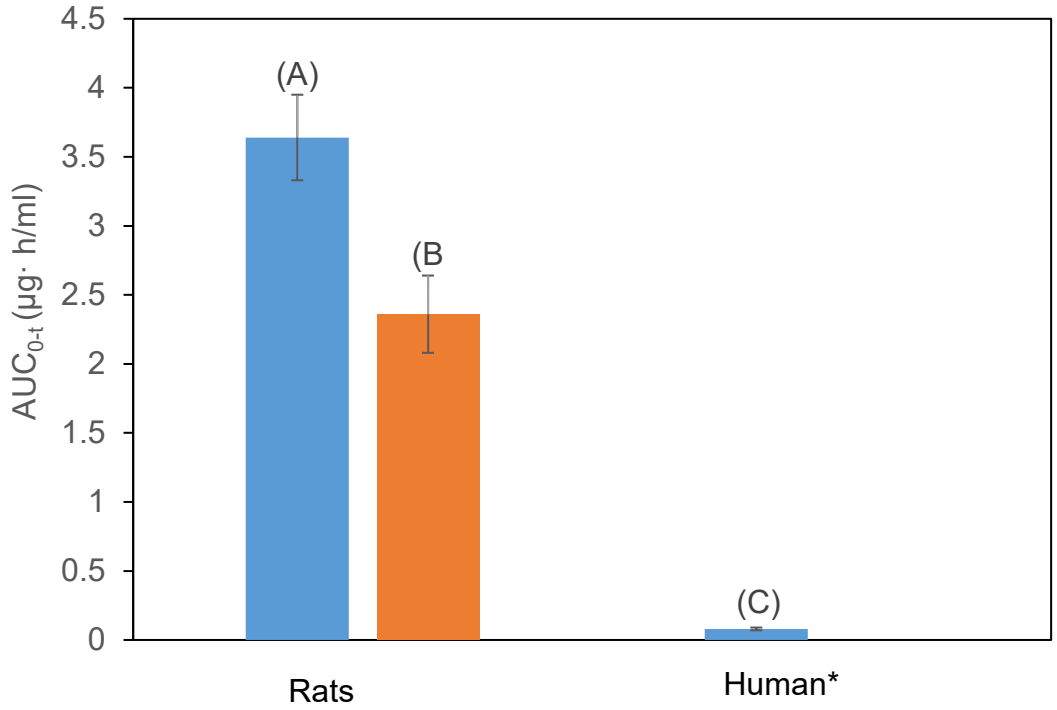

Figure 1.8. Comparison of curcumin oral absorption results of the curcumin + piperine co-administration strategy in rats and humans. (A) 2 g/kg curcumin with 20 mg/kg piperine and (B) 2 g/kg curcumin control administered in rats; (C) 2 g/kg curcumin with 20 mg/kg piperine administered to human volunteers; *: Pure curcumin absorption in humans was reported to be below the detection limit (Shoba et at., 1998)

The test results revealed that there was an increase in the absorption of curcumin by 200%, compared with that of taking curcumin alone (Figure 1.9). Another study by Zeng et al. (Zeng et al., 2017b) investigated the effect of the pre-administration of piperine on the oral bioavailability of curcumin. In this study, rats received 20 mg/kg of piperine initially followed by curcumin (200 mg/kg) at various time intervals between 0.5 and 8 hours after piperine administration. The rats that received pre-administration of piperine before the curcumin all showed remarkable enhancement in curcumin oral bioavailability, especially at 6 h after taking piperine with AUC_{0-t} increased 97-fold when compared to curcumin alone. In contrast, rats that received the same oral dose of piperine and curcumin at the same time exhibited much lower enhancement in AUC_{0-t}, by a 1.67-fold relative to pure curcumin (Figure 1.10). It was also found that piperine causes time-dependent and selective suppression of UDP-glucuronyltransferase and sulfotransferases, which reduces curcumin metabolism (Volak et al., 2008; Zeng et al., 2017b).

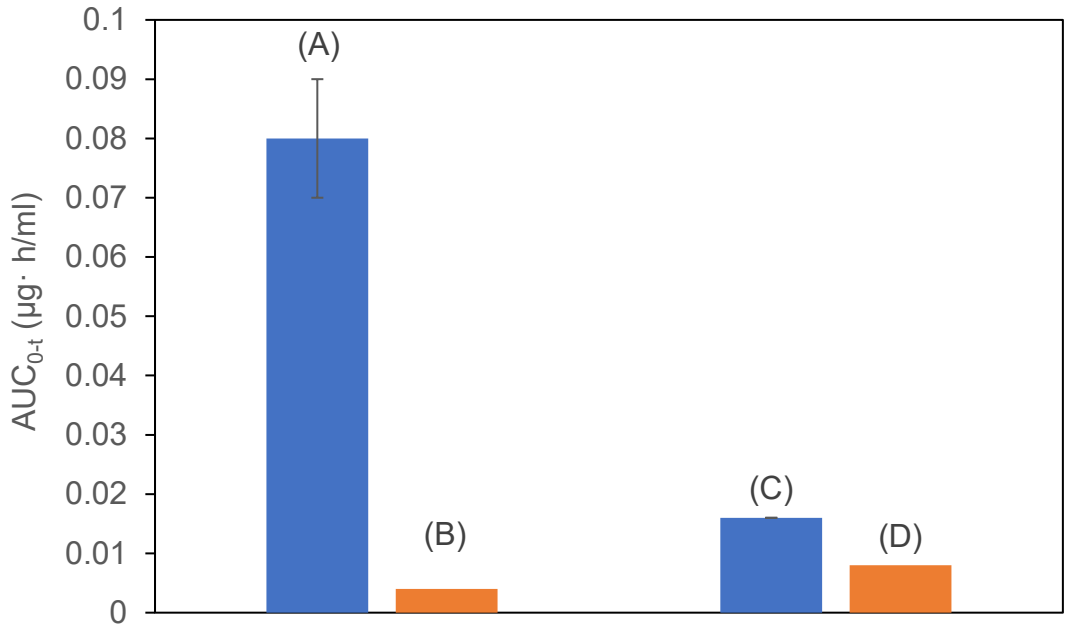

Figure 1.9. Comparison of curcumin oral absorption results of different piperine strategies tested in healthy human volunteers. (A) 2 g/kg curcumin with 20 mg/kg piperine and (B) 2 g/kg curcumin control administered in rats (Shoba et at., 1998); (C) 5 mg piperine along with 2 g of curcumin and (D) 2 g curcumin control (Anand et al., 2007)

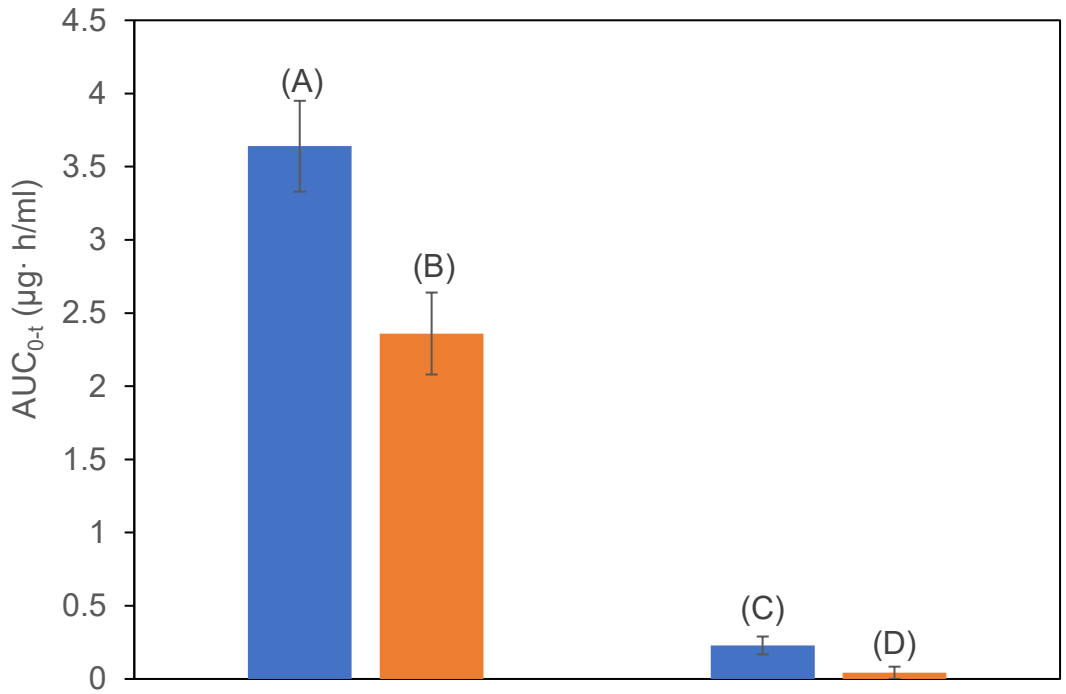

Figure 1.10. Comparison of curcumin oral absorption results of two different piperine strategies tested in rats. (A) 2 g/kg curcumin with 20 mg/kg piperine and (B) 2 g/kg curcumin control administered in rats (Shoba et at., 1998); (C) initial dose of 20 mg/kg piperine followed by 200 mg/kg of curcumin after six hours and (D) 200 mg/kg curcumin control (Zeng et al., 2017b)

Apart from piperine, several other natural compounds such as silibinin and quercetin have been shown to inhibit the effects of UDP-glucuronyltransferase (Grancharov et al., 2001; J. A. Williams et al., 2002). Quercetin is a plant flavonol that is present in many fruits, vegetables and grains (Lund & Pantuso, 2014). Silibinin is a flavonoid that is extracted from the medicinal plant *Silybum marianum* (milk thistle). The effect of co-delivering natural curcumin metabolism enzyme inhibitors on the oral bioavailability of curcumin was studied using a self-emulsion formulation of curcumin. The self-emulsion formulation (containing 100 mg/kg curcumin) was delivered orally to mice with or without either piperine (125 mg/kg), quercetin (100 mg/kg), or silibinin (100 mg/kg). The pharmacokinetic results showed that piperine co-administration showed the highest C_{max} of curcumin. However, curcumin concentration in the plasma was highly variable (0–2.4 μM curcumin plasma levels), which was deemed unacceptable. Co-administration of quercetin or silibinin showed much more stable plasma levels of curcumin and both increased the average C_{max} of curcumin. Silibinin co-delivery resulted in higher C_{max} of curcumin than quercetin so the bioavailability study was only conducted for silibinin. The results reported that co-administration of silibinin improved the overall bioavailability of curcumin by approximately 3.5-fold ($AUC_{0–6}$ 0.2613 ± 0.0368 Vs. 0.0808 ± 0.0469 h μmol/l for SMEDDS without adjuvant co-delivery) (Grill et al., 2014). An *in vitro* Caco-2 cell monolayer permeability study examined how oral co-administration of piperine, quercetin or resveratrol can affect the intestinal absorption of curcumin. Resveratrol (*trans*-3,5,4′ - trihydroxystilbene), is a natural plant compound that is present in grapes, berries and other plants. All three compounds showed an increase in curcumin permeability across the Caco-2 cell monolayers. Quercetin and resveratrol increased the curcumin permeability by 1.46- fold and 1.25-fold, respectively. The highest effect on curcumin permeability was from piperine, which increased the permeability by 2.33-fold. Interestingly, when quercetin and resveratrol were combined with

curcumin, the permeability increased by 1.85-fold. This indicated that there is an additive effect of resveratrol and quercetin on curcumin absorption (Lund & Pantuso, 2014). Co-delivery of natural compounds like piperine, quercetin, resveratrol and silibinin decreased the metabolism of curcumin which eventually increased the absorption of curcumin. It is a promising and easy way to improve the oral bioavailability of curcumin and could be investigated further in the development of novel drug delivery systems.

1.8.2. Nanoparticles

The nanoparticle-based delivery system is another effective strategy to improve the oral bioavailability of poorly water-soluble drugs. The nano-size of the particle (10–1000 nm) leads to a greater surface area for the drug particles thereby increasing the area of physical interaction with the solvent. According to the Noyes-Whitney equation ($dC/dT = kS(Cs-Ct)$), the dissolution rate (dC/dT) is directly proportional to the surface area (S). Therefore, nano-sized drug particles with a higher surface area are likely to be dissolved more rapidly(Jahagirdar et al., 2019; Merisko-Liversidge et al., 2003; Müller et al., 2011).

A list of approved nanodrugs is shown in Table 1.2. In comparison with the conventional formulations, these nanodrugs benefited from increased dissolution rate and saturation solubility, which leads to higher bioavailability (Junghanns & Müller, 2008). Nanoparticle technology is widely used for delivering poorly-water soluble drugs or substances (Bisht et al., 2007; Ensign et al., 2012; Singh & Lillard Jr, 2009; Lisha Zhang et al., 2008). Curcumin-loaded lipopolysaccharide nanoparticles (C-LPNCs) were developed to improve the oral bioavailability of curcumin (Chaurasia et al., 2015). Soluthin® MD, a phosphatidylcholine-maltodextrin based hydrophilic lipopolysaccharide, was used as the nanocarrier to load curcumin. Poloxamer 188 was added as a

stabilizer to prevent aggregation and size growth of the C-LPNCs. A graphical scheme of this formulation is shown in Figure 1.11.

Trade name	**Generic name**	**Route of administration**	**Indication**
Emend®	Aprepitant as nanocrystal	Oral	Preventing nausea and vomiting
Megace ES®	Megestrol acetate as nanocrystal	Oral	Treating loss of appetite and wasting syndrome in people with acquired immunodeficiency syndrome (AIDS).
Rapamune®	Rapamycin (sirolimus) as nanocrystals formulated in tablets	Oral	Immunosuppressant
Tricor®	Fenofibrate as nanocrystals	Oral	Treating hypercholesterolemia and hypertriglyceridemia
Triglide®	Fenofibrate as nanocrystals	Oral	Treating hypercholesterolemia and hypertriglyceridemia

Table 1.2. A List of FDA-approved nanodrugs (Junghanns & Muller, 2008)

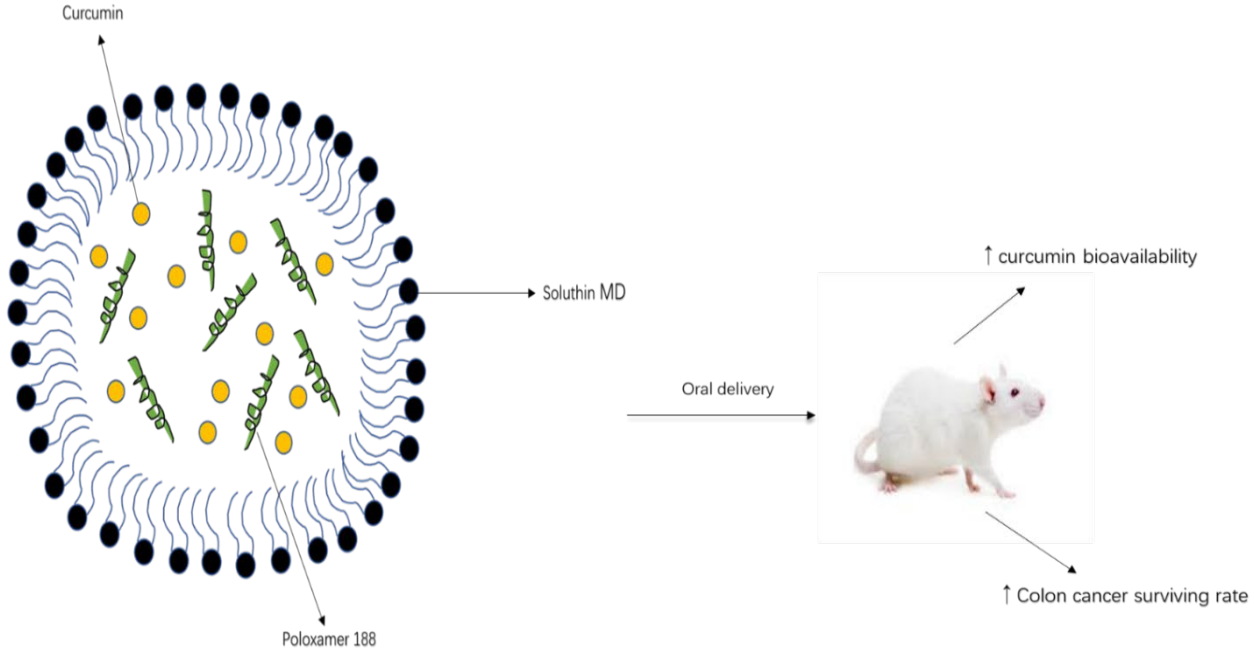

Figure 1.11. Graphic scheme of the Curcumin loaded phosphatidylcholine-maltodextrin based lipopolysaccharide nanoparticles (C-LPNCs) formulation (adapted from Chaurasia et al., 2015)

Burst dissolution of the curcumin was observed in the first 30 minutes at pH 7.4 buffer solution, which was due to the amorphous distribution of the curcumin particles in the C-LPNCs. Subsequently, the dissolution rate was reported to gradually reduce and became relatively stable after 12 hours. After 24 hours, 80% of the curcumin in the C-LPNCs dissolved in the solution. The C-LPNCs were evaluated *in vivo* to investigate their effect on the oral bioavailability. A curcumin equivalent dose of 50 mg/kg was administrated orally to Albino Wister rats. The C_{max} and AUC_{0-t} of curcumin were found to have increased by 104.8-fold and 55.2-fold respectively when administrated as the C-LPNCS, compared with the unformulated curcumin. Lymphatic transport was found to be involved in the oral absorption of C-LPNCs, which can reduce curcumin hepatic metabolism in the liver thus contributing to the increase in curcumin bioavailability. In addition, maltodextrin in the formulation can protect curcumin from degradation in the harsh environment of the gastrointestinal tract, which could be another reason for the improvement of the oral bioavailability. Anticancer activity of C-LPNCs against colon cancer was investigated *in vivo* in colon-26 tumour-bearing rats. A curcumin equivalent dose of 50 mg/kg was delivered orally daily to the rats for 30 days. At the end of the study, 100% survival rate was observed in the group being treated with the C-LPNCs while 33.33% survival rate was observed in the group receiving pure curcumin (Chaurasia et al., 2015). In another study, a simple method called CO_2-assisted in situ nano-amorphization was used to prepare curcumin-lipopolysaccharide based oral nanosuspension to improve the bioavailability and anticancer efficacy of curcumin (Wang et al., 2017b) In this method, curcumin, citric acid and a stabilizer, Brij78, were first dissolved in ethanol. The solvent was then removed via evaporation, resulting in the formation of a solid mixture. Subsequently, a carbonated solution was added to the solid mixture to form the curcumin-loaded nanosuspension. In an *in vivo* test in rats, it was reported that the oral bioavailability of curcumin had improved by 3.70-fold from the

CUR/Brij78 nanosuspensions compared with that of free curcumin suspension. Another novel curcumin-loaded nanoparticle was developed by using an ionotropic gelation method. Alginate and polysorbate combinations were used to form the nanoparticles to entrap curcumin (Govindaraju et al., 2019). This formulation showed a low release of curcumin in gastric and intestinal environments and a sustained release within the colon. This phenomenon was due to colonic microflora, which helped to digest the alginate thus allowing curcumin to be released from the nanoparticles. In the human body, at a curcumin dose of 100 mg, the nanoparticle formulation increased the oral bioavailability of curcumin by 5-fold more than that of free curcumin suspension. Since most of the curcumin was released and absorbed in the colon, this formulation might be a promising approach for the oral delivery of curcumin for targeting colonic diseases. Applying a coating to the surface of nanoparticles may help to prevent agglomeration to occur. Commonly used polymers for such coating are polyethylene glycol (PEG), poly (vinylpyrrolidone) (PVP), dextran, chitosan, pullulan etc. Surfactants like sodium oleate and dodecylamine have also been used for nanoparticle coating (De Jong & Borm, 2008). In another study, a curcumin-loaded solid lipid nanoparticles (SLNs) with N-carboxymethyl chitosan (NCC) coating were prepared through a modified hot homogenization and sonication method (Baek & Cho, 2017). The NCC-coated SLN samples exhibited 9.5-fold higher oral bioavailability than that of curcumin solution. Inhibition of burst release (over-rapid release) of curcumin was observed in NCC-coated SLNs in simulated gastric fluid (pH1.2) thus indicating that NCC coating was able to address the burst release problem that SLNs usually have in an acidic environment. Among the nanoparticle formulations mentioned above, the nanosuspension prepared by CO_2 assisted in situ nano-amorphization method (Wang et al., 2017b) exhibited the highest curcumin oral bioavailability with the $AUC_{0\text{-}t}$ value of 365.73 μg h/ml in rats. A comparison of the curcumin oral absorption data between each nanoparticle formulation is

shown in Figure 1.12.

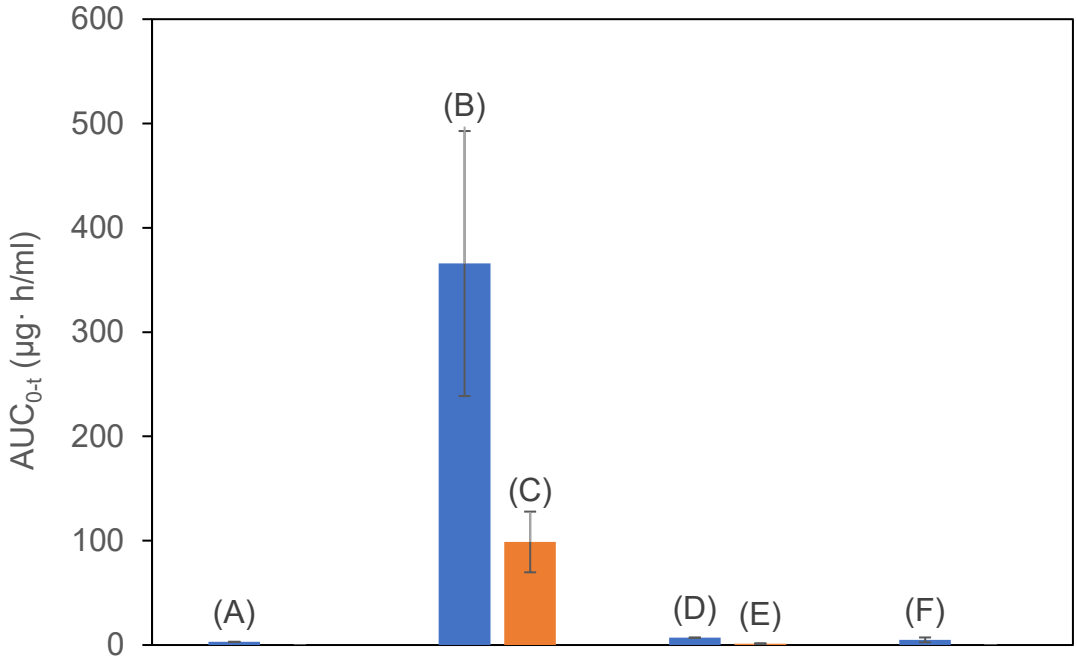

Figure 1.12. Comparison of curcumin oral absorption results of the novel curcumin-loaded nanoparticle formulations at the curcumin equivalent oral doses of (A) 50 mg/kg for the curcumin-loaded lipopolysaccharide nanoparticles, curcumin control concentrations below the limit of detection in this study (Chaurasia et al., 2015); (B) 50 mg/kg for the nanosuspension prepared by CO2-assisted in situ nano-amorphization methods and (C) curcumin control (Y-H.Wang at al., 2017); (D) 100 mg for the Alginate-polysorbate 80 nanoparticles and (E) (Govindaraju et al 2019); and (F) 50mg/kg for the solid lipid nanoparticles (SLNs) with N-carboxymethyl chitosan (NCC) coating, tested in rats, curcumin control concentrations were reported to be below the limit of detection (Baek & Cho,2017)

1.8.3. Liposomes

Liposomes are a type of drug delivery system which contain a phospholipid bilayer structure giving them the ability to encapsulate both hydrophilic and hydrophobic substances (Anand et al., 2007). As a drug delivery approach, liposomes have the advantage of being biodegradable, non-toxic, and remarkably biocompatible (Li et al., 2018). A hybrid liposomal formulation that consisted of chitosan and soybean lecithin was developed as a drug vehicle for curcumin (Peng et al., 2017). The bioavailability of curcumin from the liposomal formulation was tested using caco-2 cells. The hybrid liposomes exhibited a higher cellular uptake rate than that of phospholipid liposomes, 1.66-fold higher at 0.5 hours after incubation and 1.256-fold higher after 4 hours of incubation. The researchers reported a sustained release of curcumin, increased positive charge and decreased hydrophobicity from the hybrid liposomal formulation were the main reasons for the increased curcumin bioavailability. In another study, a liposomal formulation coated with chitosan was tested in simulated gastric fluid (pH between 2 and 3) and simulated intestinal fluid (pH 7). It was reported that around 80% of the curcumin loaded in the liposome dissolved in the simulated gastric and the simulated intestinal fluids (Cuomo et al., 2018). In the research area of curcumin liposomal formulation, the current trend is to use hybrid liposomal formulations to help to improve the bioavailability of curcumin. The studies mentioned above showed that the hybrid liposomal formulations have better performance in improving the bioavailability of curcumin than the conventional curcumin-loaded liposomes and the unformulated curcumin.

1.8.4. Micelles and polymer micelles

Micelles are spherical aggregates of surfactants that form spontaneously when the surfactants reach a critical micelle concentration (CMC) at a certain temperature in an aqueous solution (Xu et al., 2013). The size of micelles normally ranges between 20 and 80 nm. Typical micelles are comprised of an

outer shell formed by hydrophilic head groups and a core formed by hydrophobic tail groups. Micelles can be used as vesicles to load and deliver poorly water-soluble drugs. The hydrophobic core can encapsulate the lipophilic drugs and the hydrophilic outer shell to protect the drugs from being inactivated in the gastrointestinal environment. As a result, the solubilisation and stability of the drugs are improved (Haley & Frenkel, 2008). A novel curcumin-loaded mixed micelle (CUR-MM) that consists of two surfactants (Pluronic F-127 and Gelucire® 44/14) was developed (Patil et al., 2015). The formulation showed that it can enhance the oral bioavailability of curcumin and its anti-cancer effect. The optimised CUR-MM formulation with the size of 188 ± 3 nm and an entrapment efficiency of 76.45 ± 1.18% w/w exhibited significant enhancement in the oral bioavailability of curcumin (by approximately 55-fold) and cytotoxicity to human lung cancer cell line A549 (by approximately 300%), in comparison with free curcumin. The improved oral bioavailability and anti-cancer effects of curcumin were attributed to the controlled release of curcumin from the CUR-MM, an increase of curcumin solubility from micellization and inhibition of P-glycoprotein by the surfactants. In another study, a sophorolipid nano-micelle formulation was prepared by using a 'pH-driven method' (Peng et al., 2018). *In vivo* test results showed that it increased curcumin's oral bioavailability by 3.6-fold compared with the unformulated curcumin. This proves that biosurfactants like sophorolipid, obtained from natural sources, could be used for formulating drug delivery systems to enhance the oral bioavailability of curcumin. The preparation method used in this study, the pH-driven method, does not require heat and organic solvents, thus making it a simple and cost-effective way for producing nano-sized curcumin products. A clinical trial was conducted among 23 healthy human candidates (13 male and 10 female) to assess a micellar curcumin formulation that composed of micronised curcumin powder and Tween-80 (Schiborr et al., 2014). The result of pharmacokinetics studies showed that the ingestion of a single oral dose of

500 mg micelle encapsulated curcumin (equivalent to 410 mg curcumin) resulted in a C_{max} of 3.228 µmol/l compared to 0.007 µmol/L of free curcumin powder. Both male and female subjects have almost the same T_{max}, but the female subjects exhibited a higher C_{max} of 3.701 µmol/l in comparison with 2.612 µmol/l for male subjects, indicating that women might be absorbing more curcumin than men in this study. A novel self-assembled, curcumin-loaded polymeric micelle was developed for improving curcumin oral absorption (Wang et al., 2015). It consisted of di-tocopherol polyethylene glycol 2000 succinate (TPGS2 K), octadecanoic acid, Solutol HS15 and Pluronic F127. Both *in vitro* and *in vivo* test results revealed that the micelle system provided a better intestinal absorption of curcumin relative to free curcumin. Oral administration of the micelle formulation in rats resulted in higher AUC_{0-t} of curcumin (870.2 ± 466.78 mg h/l) compared with curcumin alone (AUC_{0-t} of 303.58 ± 294.31 mg h/l). Furthermore, lymphatic transport pathways were found to be involved in the absorption of the micelle system, which helps curcumin avoid first-pass metabolism. Overall, a major increase in the oral bioavailability of curcumin was demonstrated in the recently developed novel micelles formulations. These results indicate that micelles are a promising way of delivering curcumin orally and are worthy of further studies in the future. A comparison plot to describe the results of curcumin oral bioavailability from different micellar formulations is shown in Figure 1.13.

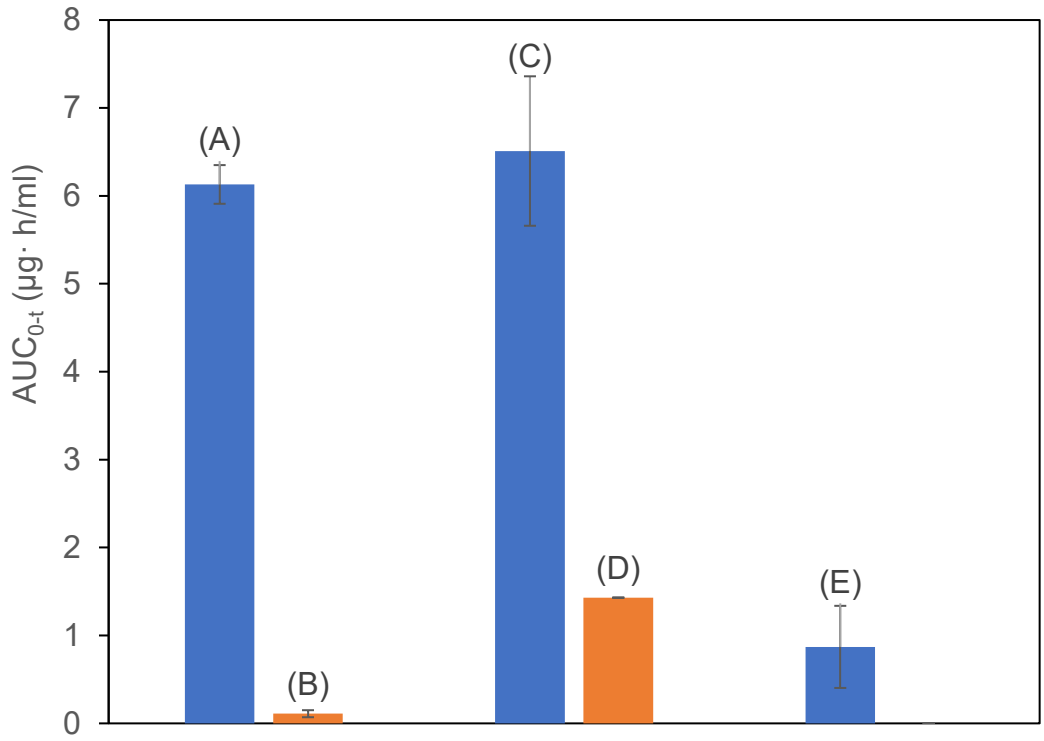

Figure 1.13. Comparison of curcumin oral absorption of curcumin loaded micelles formulation (A) curcumin oral doses of 10 mg/kg for curcumin-loaded mixed micelle and (B) curcumin control (Patil et al., 2015); (C) 100 mg/kg for the curcumin loaded sophoroliplid-coated nanomicelles and (D) curcumin control (Schiborr et al., 2014); (E) 50 mg/kg for the self-assembled curcumin-loaded polymeric micelle, the concentration of curcumin from the control sample was reported to be below the limit of detection (Wang et al., 2015)

1.8.5. Curcumin-loaded nano and micro-emulsions

Nanoemulsions, also known as submicron emulsions, are another type of nano-sized drug delivery system. They are single-phase, isotropic thermodynamically stable systems that consist of emulsified oil, water and amphiphilic molecules (surfactants). The size of the emulsion droplets typically ranges between approximately 10–1000 nm (Gurpreet & Singh, 2018). A Thiol modified chitosan-coated, curcumin-piperine loaded oil-in-water nanoemulsion was developed (Vecchione et al., 2016). The optimised formulation has a nano-droplet size of 110 nm, a weight ratio of curcumin: piperine in 100 to 1 and a chitosan thiolation level of 14–15%. At an oral dose equivalent to 8 mg/kg of curcumin, the $AUC_{0\text{-}t}$ value of curcumin increased by 64-fold (343.3 μg h/ml) than standard curcumin (5.4 μg h/ml). Compared with the two piperine strategies that were reviewed in section 1.4.1 (Shoba et al., 1998; Zeng et al., 2017b), the optimised curcumin-piperine loaded nanoemulsion formulation is 94-fold and 1505-fold higher in terms of the $AUC_{0\text{-}t}$ values. This indicates that the combination of piperine with the nanoemulsion technology is much more effective than only using piperine alone in improving the oral bioavailability of curcumin. In another study, a novel lipid nanoemulsion containing curcumin (CNELNs) was prepared and tested for changes in bioavailability in *in vitro* and *in vivo* models (Wan et al., 2016). The mean absorption constants (Ka) and effective permeabilities (Peff) over the whole intestine system were increased by 2.98-fold and 6.65-fold, respectively. The relative bioavailability of CNELNs to standard curcumin was 733.59%, which was possible due to the increase in intestinal absorption. CNELNs also displayed a stronger effect in suppressing the growth of human lung cancer cell A549. In another study, a nanoemulsion was developed by mixing a curcumin-phospholipid complex with castor oil, Tween 80 and PEG 400 (Shukla et al., 2017). The curcumin-phospholipid loaded nanoemulsion showed a significantly higher serum concentration of curcumin than free curcumin and the curcumin-phospholipid complex not being

loaded into the nanoemulsion. Using an oral dose of 100 mg/kg in rats, the C_{max} of curcumin from the combined formulation was 487.7 ± 53.4 ng/ml, compared to 21.6 ± 3.6 ng/ml for free curcumin and 54.6 ± 3.7 ng/ml for the curcumin-phospholipid complex. The relative bioavailability of curcumin from the combined formulation was 7.67-fold and 52.55-fold higher than that of curcumin-phospholipid complex and unformulated curcumin. Several research studies have been carried out to study the potential for using a nanoemulsion strategy to improve the oral bioavailability of curcumin. The results of these studies demonstrated that it is a promising strategy to fulfil the goal of improving curcumin's oral bioavailability. Among the nanoemulsion formulations reviewed, piperine loaded in an oil-in-water nanoemulsion with modified chitosan coating (Vecchione et al., 2016) showed the highest curcumin oral absorption with the AUC_{0-t} value of 343.8 μg h/ml. In contrast, the other two nanoemulsion formulations (Shukla et al., 2017; Wan et al., 2016) have much poorer curcumin bioavailability with AUC_{0-t} value of 0.7 μg h/ml and 2.97 μg h/ml (Figure 1.14).

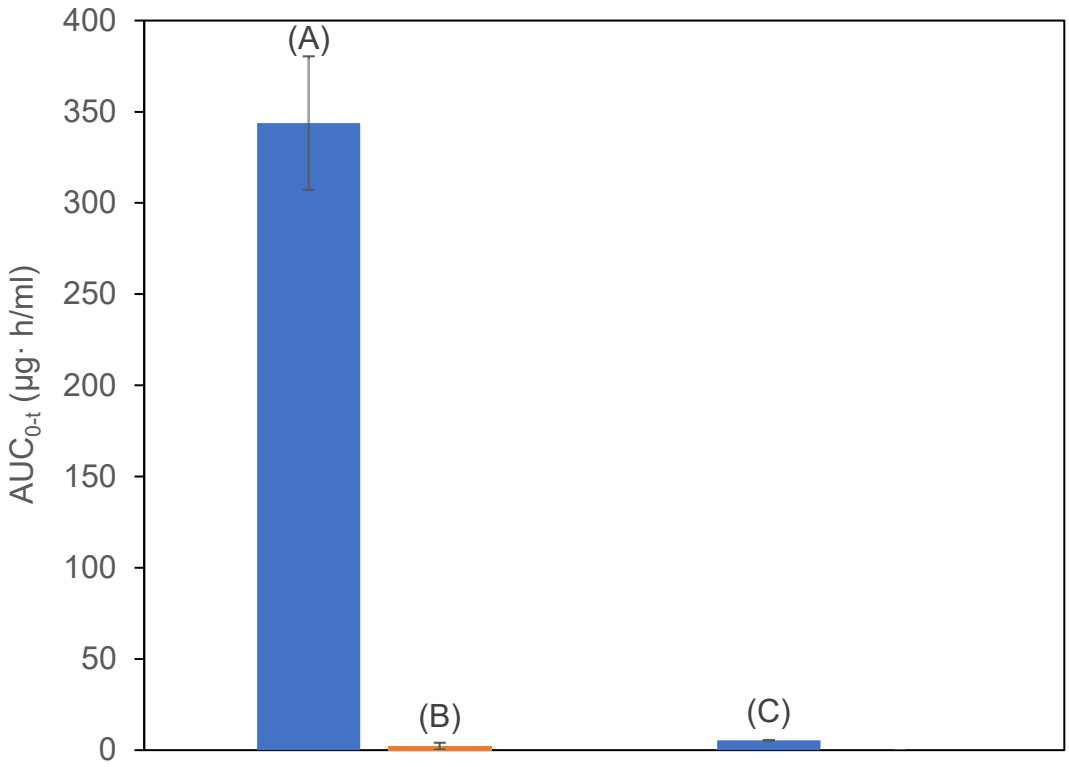

Figure 1.14. Comparison of curcumin oral absorption results of the novel nanoemulsion formulations (A) at an oral dose of 8 mg/kg for Chitosan coated, piperine-loaded oil in water nanoemulsion (B) curcumin control (Vecchione et al., 2016) and (C) oral dose of 100 mg/kg of curcumin-phospholipid complex incorporated self-nanoemulsion, curcumin control values were reported to be below the limit of detection (Shukla et al., 2016)

The microemulsion is an isotropic colloidal system of micron-sized droplets that consists of water, oil, surfactant and cosurfactants. When in a microemulsion system, drug compounds can be entrapped within the oil droplets, which protect them from both enzymatic and chemical degradations thus increasing the residence time and bioavailability of the drugs (Constantinides, 1995). Interestingly, the droplet size of the microemulsion is not in micrometers but between 10 and 100 nm. A microemulsion is fairly similar to a nanoemulsion in terms of structure. What differentiates it from a nanoemulsion is that a microemulsion is thermodynamically stable whereas a nanoemulsion is not. Also, microemulsions normally have a narrow particle size distribution compared to nanoemulsions (McClements, 2012). Microemulsion is thermodynamically stable because it is in a state of minimum free energy. This means that the system has reached a state where the interfacial tension between the two immiscible liquids is minimised. The emulsifying agent in microemulsions is typically a surfactant, which reduces the interfacial tension between the oil and water phases, allowing them to mix more easily (Lawrence, 1994; Schulman et al.,1959). On the other hand, nanoemulsion is not thermodynamically stable because the interfacial tension between the two immiscible liquids is higher compared to microemulsion. This means that the system is not at a state of minimum free energy, and there is a tendency for the droplets to coalesce over time. Therefore, nanoemulsion requires higher amount of emulsifiers and energy input to form and maintain their stability (McClements & Rao, 2011; Solans et al., 2005).

A self-emulsifying microemulsion drug delivery system (SMEDDS) was developed to improve the oral bioavailability of curcumin (Dhumal et al., 2015). A semi-synthetic bicephalous hydrolipid known as E1E was used in this formulation, along with Solutol HS15 (a surfactant) and Transcutol HP (a cosurfactant) to form the microemulsion encapsulating curcumin. An optimised

SMEDDS formulation with a drug loading efficiency of 70.52 ±2.46 mg/g was orally administrated to rats at a curcumin dose of 50 mg/kg. Plasma analysis showed that the C_{max} and AUC_{0-t} of curcumin from the SMEDDS were 4.921 ± 0.42 (μg/mL) and 17.30 ± 1.50 (μg h/ml) respectively, in comparison with free curcumin suspension with 0.186 ± 0.006 (μg/ml) and 0.234 ± 0.023 (μg.h/ml) respectively. T_{max} remained unchanged in both SMEDDS and the free curcumin suspension 60 minutes after oral administration. In another study, self-microemulsifying curcumin (SME-Cur) entrapped in a hydroxypropylmethyl cellulose (HPMC)-based sponge was developed to study oral absorption of curcumin (Petchsomrit et al., 2016). The *in vivo* study was performed in rabbits at a curcumin-equivalent oral dose of 12.5 mg/kg. The HPMC sponge entrapped SME-Cur showed significantly higher C_{max} and AUC_{0-t} (1.77 ±0.13 mg/ml and 2615.68 ± 97.79 ng/h/ml, respectively) than unformulated curcumin at a dose of 50 mg/kg (0.30 ±0.03 mg/ml and 509.49 ± 47.77 ng· h/ml, respectively). The *in vitro* drug release test found that the HPMC-based sponges entrapped SME-Cur provided a sustained release of curcumin and led to a higher percentage release compared with the unwrapped SME-Cur and free curcumin. The improved drug release could be attributed to the drug-polymer interaction leads to the inhibition of precipitation and crystallization of curcumin in solution. Compared to nanoemulsions, microemulsions have received less attention since there were only a few studies on their use in improving the oral bioavailability of curcumin (Figure 1.15). However, the studies of microemulsions reviewed in this article both showed considerable improvement in curcumin's oral bioavailability (Dhumal et al., 2015; Petchsomrit et al., 2016). All of these indicate that microemulsions are still a potent and promising technology to overcome curcumin's oral delivery problems and it is worthy of further studies in the future.

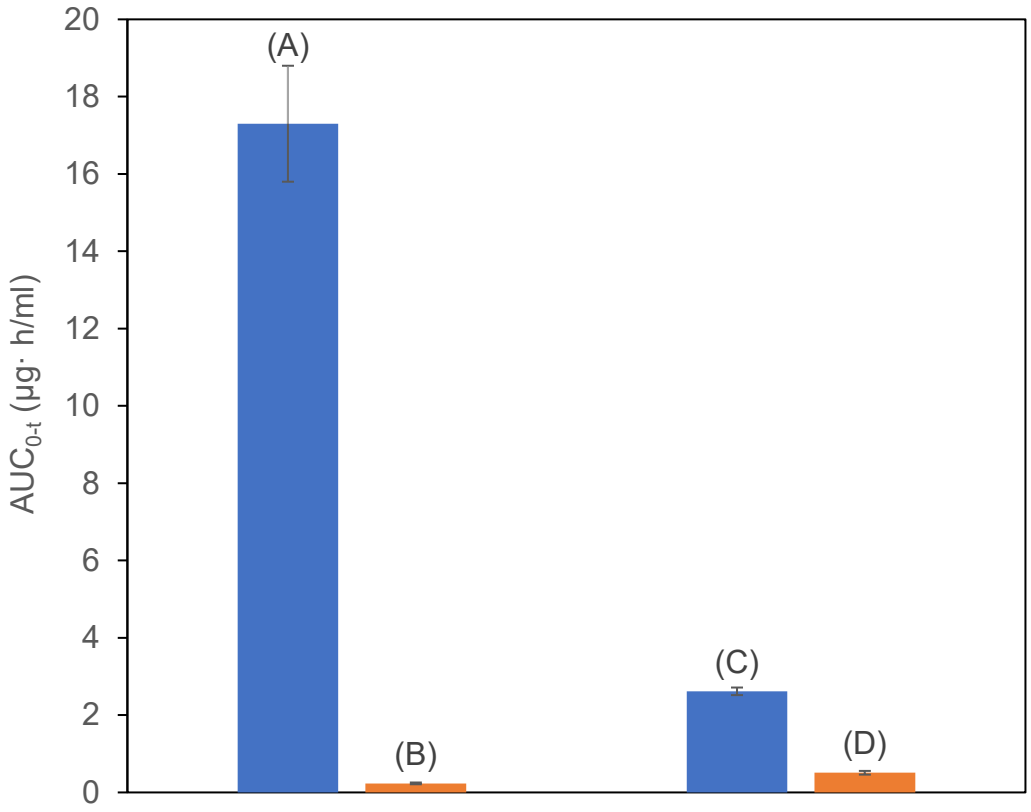

Figure 1.15. Comparison of curcumin oral absorption results of the novel microemulsion formulations at the curcumin equivalent doses of (A) 50 mg/kg for the self-emulsifying microemulsion and (B) curcumin control (Dhumal et al.,2015) and (C) 12.5 mg/kg for the HPMC sponge entrapped self-microemulsifying curcumin and (D) curcumin control (Petchsomrit et al., 2015)

1.8.6. Solid dispersions

A solid dispersion is a solid product where at least one drug is dispersed in a hydrophilic polymeric carrier and the drug(s) are molecularly dispersed in the polymeric matrix (Chiou & Riegelman, 1971). The principle of solid dispersion to improve the drug bioavailability was to first rapidly release the drug particles from the polymeric carrier to create a supersaturated solution after which the concentration is maintained long enough for the drug to be absorbed (Craig, 2002; Kumar & Gupta, 2013; Vasconcelos et al., 2007). Drugs in a supersaturation state tend to precipitate rapidly before the absorption takes place which results in reduced bioavailability. Polymeric matrix in solid dispersion can inhibit crystal growth and nucleation of the drug by binding to the drug molecules and preventing their aggregation. This can help to maintain the drug in a solubilised state and prevent precipitation when supersaturation is reached (Vasconcelos et al., 2007). The exact mechanism of how polymers prevent precipitation and prolong drug supersaturation is still not fully understood. Nevertheless, it is generally believed to be a result of hydrogen bond formation between the polymers and the drugs, based on the observation that polymers are effective in inhibiting the precipitation of drugs rich in hydrogen-bond acceptors (Bevernage et al., 2011; Gao et al., 2009; Miller et al., 2008). Solid dispersion continues to be a widely studied strategy to improve the oral bioavailability of poorly water-soluble drug candidates (Chuah et al., 2014; Onoue et al., 2010; Seo et al., 2012). A list of FDA-approved solid dispersion drugs is shown in Table 1.3.

Trading name	**Active ingredient**	**Carrier**	**Preparation method**	**Dosage form**
Kalydeco®	Ivacaftor	HPMCAS	Spray drying	Tablet
Zelboraf®	Vemurafenib	HPMCAS	Coprecipitation	Tablet
Incivek®	Telaprevir	HPMCAS	Spray drying	Tablet
Intelence®	Etravirine	HPMC	Spray drying	Tablet
Novir®	Ritonavir	PVP/PA	Melt extrusion	Tablet
Kaletra®	Lopinavir	PVP/PA	Melt extrusion	Tablet

Table 1.3. A list of FDA-approved solid dispersion drugs (Baghel et al.,2016)

A recent study combined a solid dispersion strategy with nanotechnology and developed a novel self-nanomicellising solid dispersion (NCF) for delivering curcumin orally (Parikh et al., 2018). Soluplus (polyvinyl caprolactam-polyvinyl acetate-polyethylene glycol graft copolymer) was used as a carrier for curcumin in the NCF formulation. NCF exhibited a significant increase in the aqueous solubility of curcumin (over 20,000-fold higher than the curcumin control). Considerable improvements in dissolution rate and small-intestinal permeability of curcumin were also found with the NCF formulation. Furthermore, improved curcumin stability in an alkaline environment was found. As a result of the increased dissolution, solubility, permeability and alkaline solution stability, the oral bioavailability of curcumin from the NCF was significantly enhanced by 117-fold compared with pure curcumin. In another study, an amorphous curcumin solid dispersion was prepared with disodium glycyrrhizin (Na2GA) via ball milling (Q. Zhang et al., 2018). Na2GA was able to form micelles when dissolved in water and encapsulate the amorphous curcumin particles. *In vivo* evaluation showed that the self-micelle forming solid dispersion provided a 19-fold increase in curcumin oral bioavailability over free curcumin. In addition, the solid dispersion formulation improved curcumin

permeability across the gastrointestinal membranes. A curcumin-loaded ternary solid dispersion system was prepared by using mannitol as the hydrophilic carrier and D-α-Tocopheryl polyethylene glycol 1000 succinate (Vitamin E TPGs) as the surfactant (Song et al., 2016). TPGs was selected due to their safety and potential to inhibit P-glycoprotein efflux. The aqueous solubility of curcumin from the solid dispersion formulation remained stable across a pH range from 1.2 to 7.4, which diminished the pH-dependent solubility pattern in pure curcumin powder. Pharmacokinetics studies revealed that the C_{max} and AUC_{0-t} of curcumin were increased by 86- and 65-fold respectively, in comparison with pure curcumin powder. The solid dispersion formulation also exhibited an inhibition effect on p-glycoprotein and this was believed to be the main reason for the increased curcumin intestinal absorption observed from the solid dispersion system. A curcumin-loaded solid dispersion formulation was developed by using Gelucire 50/13 (a non-ionic water-dispersible surfactant) as the carrier material (Teixeira et al., 2016). The solid dispersion formulation was prepared by spray drying. The aqueous solubility of curcumin was significantly increased by the solid dispersion (2700 μg/ml), which was 3600-fold higher than the unformulated curcumin (0.75 μg/ml). The solid dispersion demonstrated rapid release of curcumin at 10 min, with 90% and 73% of curcumin being released at pH 1.2 and 7.4, respectively. The percentage of curcumin released was also considerably higher than pure curcumin. Results from rat plasma sample analysis indicated a 5.5-fold increase in curcumin plasma concentration from the solid dispersion compared with the unformulated curcumin under the same oral dose (500 mg/kg). Since spray drying is a technique that is suitable for scaled-up production, the solid dispersion formulation developed in this study could be a promising way to improve curcumin bioavailability from an industrial perspective. In another study, an excipient-free co-amorphous curcumin-piperine solid dispersion (co-amorphous CUR-PIP) was prepared by melting and quench cooling method (Wang et al., 2019). This formulation has

a combined solid dispersion effect of increasing drug dissolution along with piperine's effect of inhibiting the glucuronidation of curcumin *in vivo*. In this study, a higher dissolution rate and longer-lasting supersaturated curcumin concentration were observed from the co-amorphous CUR-PIP. This could be due to piperine's effects to suppress UDP-glucuronyltransferase and sulfotransferases in the intestines and liver (Zeng et al., 2017b). In addition, the permeability of curcumin across the gastrointestinal membrane was elevated by 2.67-fold compared with pure curcumin, which was linked to piperine's ability to inhibit curcumin glucuronosyltransferases. As a result of faster, longer-lasting supersaturation dissolution and higher GI permeability, the oral bioavailability of curcumin was enhanced by 2.16- and 1.92-fold with the co-amorphous CUR-PIP relative to the crystalline and amorphous curcumin. Compared with the previously mentioned strategies that used piperine for curcumin, the co-amorphous CUR-PIP showed around 8-fold and 134-fold higher $AUC_{0\text{-}t}$ values than the curcumin-piperine co-administration strategy (Shoba et al., 1998) and the pre-treatment of piperine strategy (Zeng et al., 2017b). However, it is around 11-fold lower compared to the curcumin-piperine loaded nanoemulsion (Vecchione et al., 2016). A comparative graph between the solid dispersion formulation and the nanoemulsion formulation is shown in Figure 1.16. The results from the studies mentioned above suggest that the solubility and dissolution of curcumin can be greatly improved by solid dispersion strategies, thus leading to an improvement in curcumin's oral bioavailability. The selection of carriers and surfactants also plays a vital role in the performance of solid dispersion formulations in improving the oral bioavailability of curcumin. Among all the solid dispersion formulations reviewed in this article, the self-nanomicellising solid dispersion prepared using Soluplus (Parikh et al., 2018) exhibited significantly higher curcumin oral absorption compared with the other solid dispersion formulations. A comparative graph is shown in Figure 1.17.

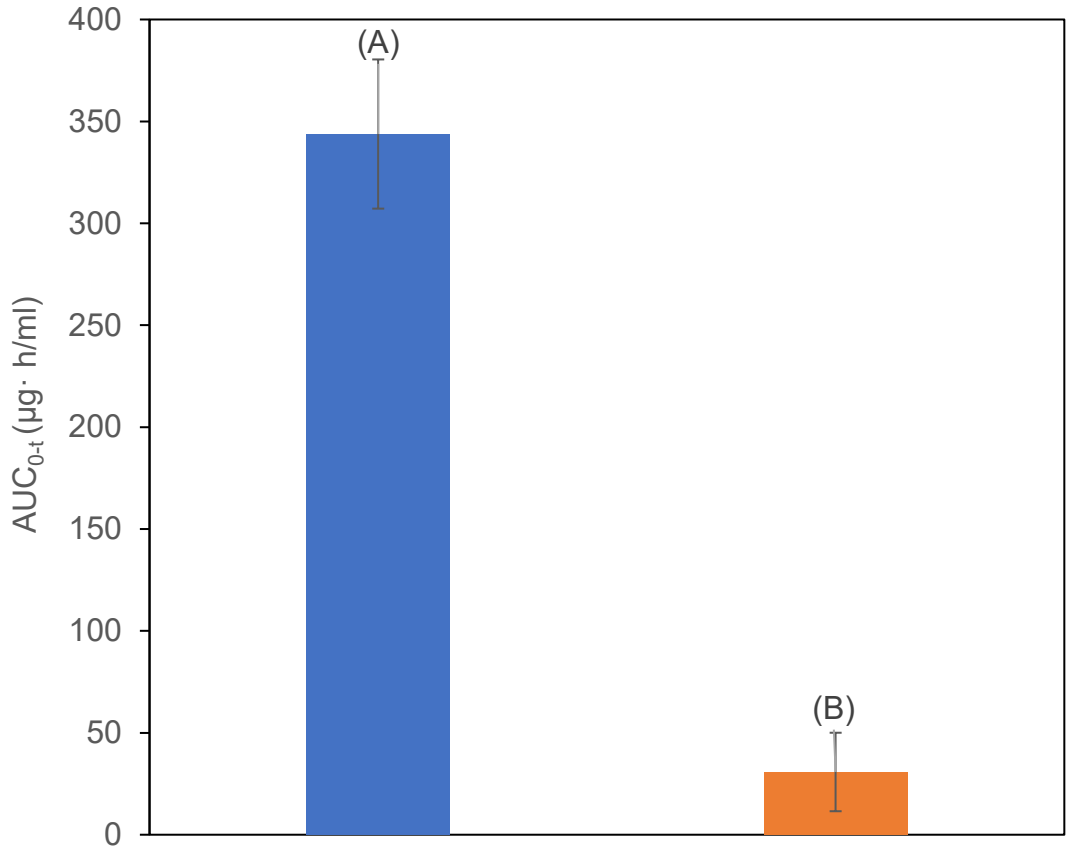

Figure 1.16. Comparison of the curcumin oral absorption results at the curcumin equivalent oral doses of (A) 8 mg/kg for the curcumin-piperine loaded nanoemulsion formulation (Vecchione et al., 2016) and (B) 100 mg/kg for the curcumin-piperine loaded solid dispersion formulation (Wang et al., 2019)

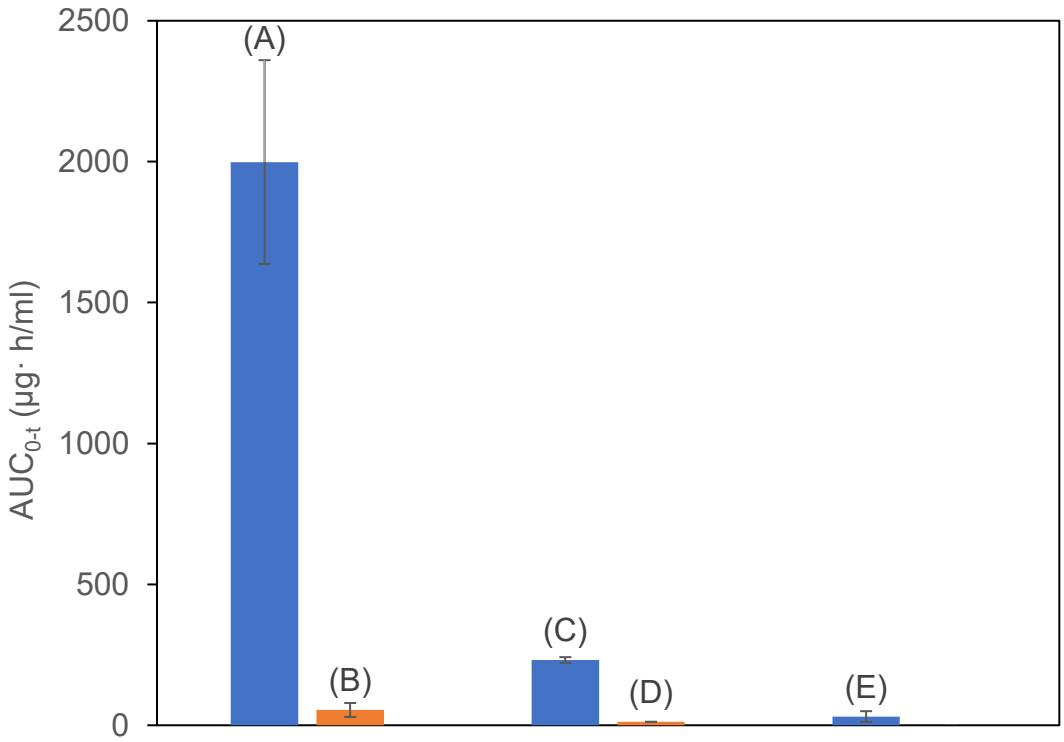

Figure 1.17. Comparative graph of curcumin oral absorption results of the novel solid dispersion formulations at the curcumin equivalent oral doses of: (A) 47 mg/kg for Soluplus containing self-nanomicellizing solid dispersion and (B) curcumin control (Parikh et al., 2018a); (C) 150 mg/kg for ball milled curcumin mixed with Na_2GA in a solid dispersion and (D) curcumin control (Zhang et al., 2018) and (E) 100 mg/kg for co-amorphous curcumin-piperine solid dispersion, curcumin levels from the control sample were below the limit of detection; The AUC_{0-t} values of the pure curcumin(control) of this study was reported to be below the limit of detection (Wang et al., 2019)

1.9. Study hypothesis

For any orally administrated drug to be absorbed, it first needs to be dissolved in the fluids of the gastrointestinal (GI) system. As a result, the poor aqueous solubility of curcumin makes it practically insoluble in the GI system which limits its oral bioavailability.

In this study, the researcher has proposed a hypothesis of using polymer and surfactants to form a simple solid dispersion formulation for curcumin in order to improve the poor aqueous solubility and dissolution of curcumin, which can potentially improve the drug permeability as there is an increase of the concentration gradient of the drug across the cell membrane, which can enhance drug transport through passive diffusion. When a drug exhibits higher solubility and permeability across cell membranes in the gastrointestinal tract, it has the potential to achieve better oral bioavailability as a greater proportion of the drug can enter the systemic circulation.

Polymers have been used for formulation development in the pharmaceutical industry for decades and a wide range of them showed remarkable performance in improving the solubility of poorly soluble drugs (Gullapalli & Mazzitelli, 2015; Linn et al., 2012). They are often used in combination with non-ionic surfactants to promote the absorption of sparingly soluble substances. It has been reported that the incubation of surfactants can further improve the drug solubility of polymer-containing formulations and reduce the risk of drug precipitation (Lee et al., 2015; Nandi et al., 2003; Tønsberg et al., 2010; Tønsberg et al., 2011).

The rationale of solid dispersion to improve bioavailability is that within a solid dispersion system, the drug can be molecularly distributed in the carrier as solid solution or randomly distributed in the carrier as the amorphous form.

When a hydrophilic drug carrier is dissolved in the aqueous medium, the amorphous drug can be easier to dissolve due to the higher surface area and no crystal lattice interactions or bonds that need to be broken during the dissolution process (Solanki et al., 2019). The addition of surfactant to the solid dispersion formulation could further improve the solubility and dissolution of curcumin by facilitating the drug release process at the solid/liquid interface and micelle solubilisation in the bulk (Rahman et al., 2009).

1.10. Aims

The main aim of this study is to develop a novel polymeric-surfactant based solid dispersion formulation for curcumin to improve its aqueous solubility and bioavailability. It will also study the formulation's potential to be applied to other poorly soluble drugs. To achieve these, the following aims will be targeted:

- To select the appropriate ingredients and techniques for preparing the novel curcumin solid dispersion formulation via literature review screening and solubility study.
- To assess whether the novel formulation improves the solubility, dissolution, intestinal permeation and cellular uptake of curcumin and compare these aspects with other curcumin formulations and curcumin supplement products available in the market.
- To characterise the novel solid dispersion formulation for its thermal property, particle size, crystallinity and chemical composition.
- To determine the stability change of the novel formulation under different storage conditions.
- To assess the effect of the novel solid dispersion formulation on drugs other than curcumin, which include terbinafine, niclosamide, nitrofurantoin, omeprazole, quinine, quercetin and rutin. They are selected based on their poor aqueous solubility.

Chapter 2. Screening of the excipients and preparation methods for the novel curcumin solid dispersion formulation

2.1. Introduction

Chapter 2 consists of two parts. Firstly, it will start with a detailed introduction to solid dispersions, providing more information about what solid dispersions are, what types of solid dispersions are available and how they can improve the solubility and oral bioavailability of poorly soluble drugs. Different preparation methods for curcumin and their advantages & disadvantages will also be discussed. Furthermore, it will provide a brief introduction of the excipients candidates (Soluplus, HPMCS and Vitamin E TPGs).

The second part will discuss the process of screening the excipients for preparing the novel solid dispersion formulation of curcumin in details. The screening process consists of two parts: the preliminary screening study and the secondary screening study. In the preliminary screening, a literature review of solid dispersion curcumin was carried out to select the excipients candidates. During the secondary screening study, curcumin solid dispersion samples were prepared using the excipient candidates and then underwent a solubility test. The results of the solubility test were used to determine the final excipient, preparation method and the drug: excipients ratio for the novel curcumin formulation.

2.1.1. A detailed introduction to solid dispersion

As described in section 1.8.6, a solid dispersion is a solid product where at least one drug is dispersed in a solid matrix which can either be a polymer or a small molecule (Chiou & Riegelman, 1971). When the drug and matrix are in intimate contact then the drug occupies void spaces between the matrix constituents. When the solid dispersion is exposed to an aqueous medium, the hydrophilic matrix is dissolved and the drug is released as fine colloidal particles. Solid dispersions were first studied in 1961 where they were found to significantly improve the dissolution and absorption of sulfathiazole (Sekiguchi & Obi, 1961). Subsequently, solid dispersion technology was used as a promising approach for improving the bioavailability of poorly soluble drugs. When solid dispersions are made as pharmaceutical formulations, the active ingredients are mostly poorly water-soluble drugs (Kim et al., 2011). The purpose of this is to disperse the drug into a hydrophilic matrix which can dissolve before the drug particles contact the gastrointestinal fluid when the solid dispersion formulation is taken orally. The dispersed drug particles can then rapidly dissolve and reach supersaturation (having more dissolved solute in a solution than that is required for saturation) in the gastrointestinal fluid, which improves the efficiency of drug absorption through the membranes of the gastrointestinal tract(Kim et al., 2011).

There are 4 possible ways for the drug to be distributed within a solid dispersion and they are shown in Figure 2.1(a,b,c and d). In these figures, the oval symbols represent the drug molecules and the curves represent the matrix in solid dispersions.

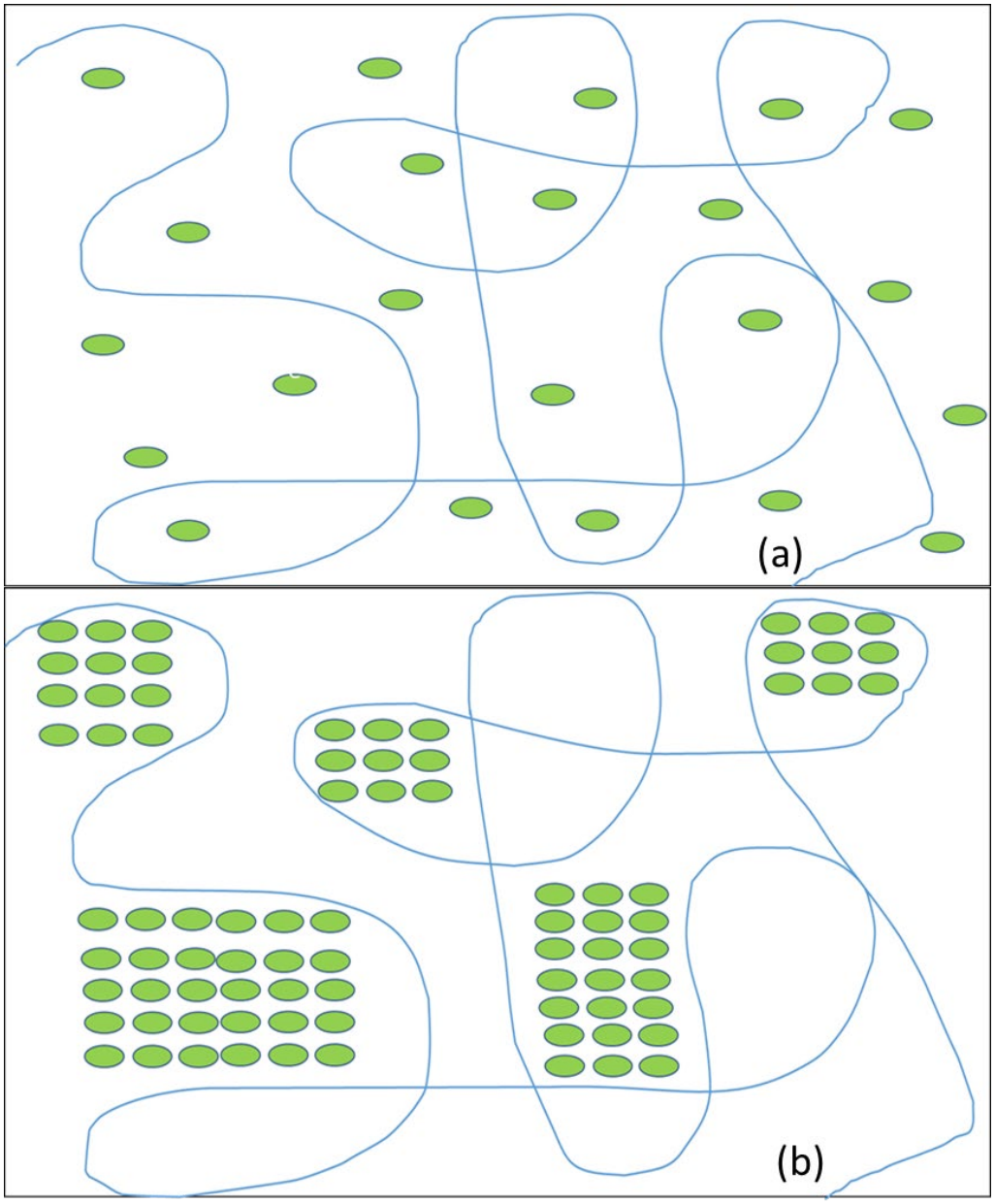
(a)
(b)

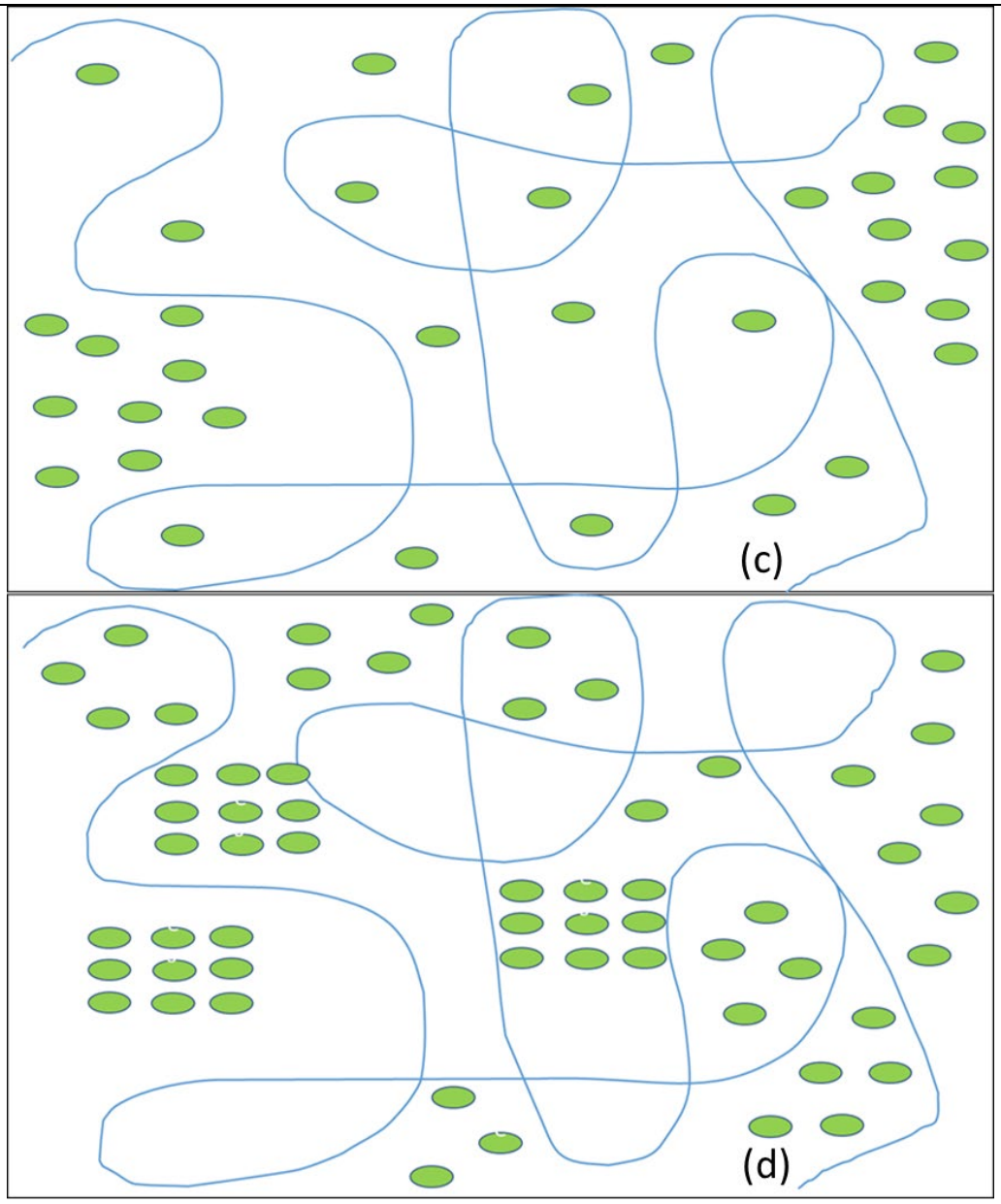

Figure 2.1. The structure of a solid dispersion that contains: (a) The “perfect structure “for a solid dispersion is where all the drug molecules are homogenously and molecularly dispersed in a hydrophilic matrix (b) a dispersion of crystalline drug particles in a hydrophilic matrix (c) a dispersion of crystalline drug particles in a hydrophilic matrix and (d) both amorphous drug clusters and crystalline drugs dispersed in a hydrophilic matrix

It is worth mentioning that the 'perfect structure' for a solid dispersion showed in Figure 2.1(a) is very rare to happen in real life. This is because such dispersion of the drug molecules only occurs when there is a very low drug loading with a high temperature when the solid dispersion was prepared (Huang & Dai, 2014). Furthermore, even if such a structure is formed, when the temperature drops, the molecularly dispersed drug in the matrix will convert into crystalline drug particles (Huang & Dai, 2014). As a result, the drugs in solid dispersions are mostly either dispersed in crystalline form, amorphous form or a mixture of both (Vo et al., 2013). The matrix can also be in a crystalline or amorphous state (Kim et al., 2011).

2.1.1.1. Classification of solid dispersion

Solid dispersion can be classified into four generations based on their physical states and the excipients used.

2.1.1.1.1. First generation of solid dispersion

The first generation of solid dispersions is crystalline solid dispersions prepared using crystalline carriers (Kim et al., 2011), typically sugar or urea (Bindhani & Mohapatra, 2018). A eutectic mixture is formed when the drug and carrier both in the melted state are mixed to produce a homogenous mass. (Kim et al., 2011). It is worth noting that eutectic mixture should not be confused with cocrystal. Both are solid state mixtures with two or more components, but there are distinct differences. As shown in Figure 2.2, eutectic mixture is formed by the melting of two or more components and mixing them in specific proportions. A new solid phase is formed after cooling down at a certain temperature. The components of a eutectic mixture are typically fully soluble in each other in the liquid state. The resulting solid phase is a homogeneous mixture of the components in a specific ratio, with no fixed crystalline structure. In other words, the individual components in a eutectic mixture do not form a defined crystal

lattice structure, but rather a disordered structure (Balakrishnan et al., 2020; Cherukuvada & Guru Row, 2014). In contrast, a cocrystal is a solid form that is formed by the combination of two or more components in a crystalline lattice structure, held together by non-covalent interactions such as hydrogen bonds. The components in a cocrystal form a well-defined, ordered crystalline structure, where each molecule is held in a specific position relative to the other molecules. Cocrystal is typically formed by a slow, controlled crystallisation process from a solution containing the components in specific ratios. Unlike a eutectic mixture, the components of a cocrystal are not necessarily fully soluble in each other in the liquid state (Vishweshwar et al., 2006).

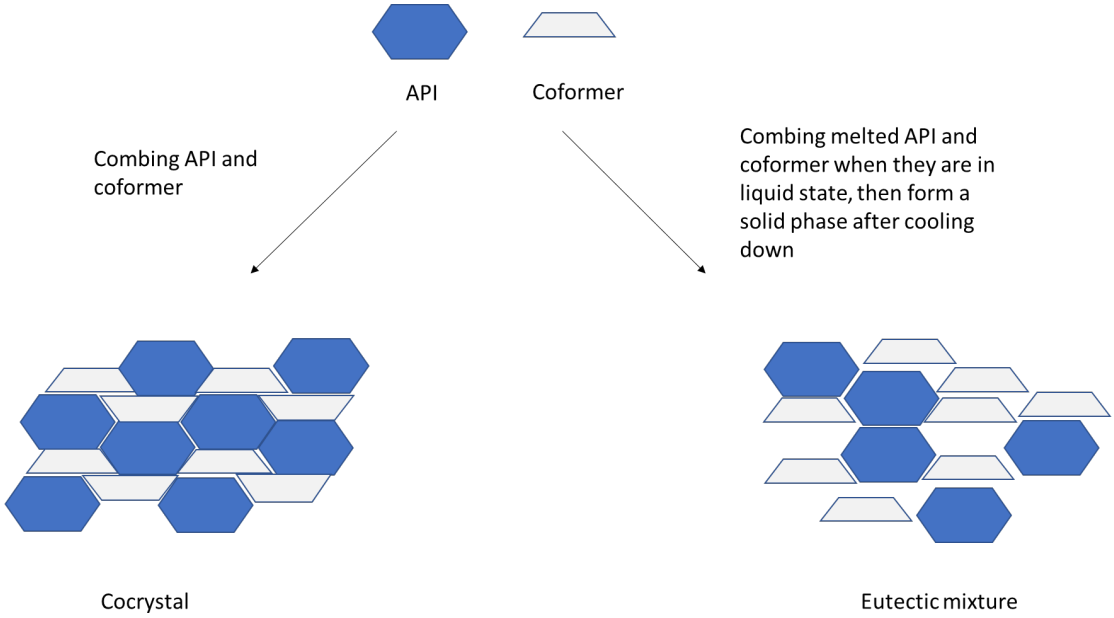

Figure 2.2. Pictorial representation of the differences between cocrystal and eutectic mixture

These become crystallised simultaneously when cooled and it then consists of fine crystals of the drug and the carrier material with a larger surface area than their original forms (Tekade & Yadav, 2020). This leads to better wettability, more rapid drug dissolution and more efficient drug absorption in the gastrointestinal tract (Chiou & Riegelman, 1971).

The first reported the first generation of solid dispersion was a eutectic mixture of sulfathiazole and urea made by Sekiguchi et al. in 1961 (Sekiguchi & Obi, 1961). Since that eutectic mixture was further applied in formulation development. In 2012, Goud et al. developed a series of eutectic mixture formulations for curcumin including binary eutectic mixtures of curcumin : nicotinamide (1:2), curcumin: ferulic acid (1:1), curcumin: hydroquinone (1:1), curcumin: p-hydroxybenzoic acid (1:1), and curcumin: L-tartaric acid (1:1). In an *in vitro* dissolution test conducted in paddle dissolution apparatus, the powders of the binary eutectic mixtures were directly poured into the dissolution medium (40% ethanol: water, 37ºC). The dissolution experiments were continued for 4 hours and all the eutectic mixture samples showed a higher concentration of curcumin dissolution than the curcumin control at every time point. All the samples reached the peak curcumin dissolution at 120 minutes and they were ranked from high to low as followed: curcumin: ferulic acid (244 mg/l) > curcumin: L-tartaric acid (226 mg/l) > curcumin: hydroquinone (219 mg/l) > curcumin: p-hydroxybenzoic acid (214 mg/l) > curcumin:nicotinamide (197 mg/l) > curcumin control (99 mg/l) (Goud et al., 2012).

Due to their crystalline structure, the first-generation solid dispersions have the advantage of being thermodynamically stable. However, this also leads to a slower release of the drug than amorphous forms of solid

dispersions(Vasconcelos et al., 2007).

2.1.1.1.2. Second generation of solid dispersion

For the second generation of solid dispersions, they are prepared using amorphous carriers instead of crystalline ones. Using amorphous carriers increase the wettability and dispersibility of the drug. These properties, together with the low thermodynamic stability of the amorphous carrier, are contributed to the enhancement of the drug solubility and dissolution rate (Vo et al., 2013).

Amorphous carriers are mostly polymers and they are characterised based on their origin. One type of polymeric carrier is fully synthetic polymers that include povidone (PVP), polyethyleneglycols (PEG) and polymethacrylates (Saffoon et al., 2011). The other ones are natural product-based polymers, such as cellulose derivatives, (such as hydroxypropylmethylcellulose (HPMC) and ethylcellulose) and cyclodextrins (Saffoon et al., 2011). Sugar glasses such as trehalose and sucrose are also used to prepare solid dispersions due to their extremely fast dissolution rates (Vo et al., 2013).

Drugs can be dispersed in second-generation solid dispersions in the crystalline form, amorphous form or a mixture of both. Depending on the molecular interaction of the drug and the carrier, the amorphous solid dispersions can be classified into three types: amorphous solid solutions, amorphous solid suspensions and mixtures of both (Bindhani & Mohapatra, 2018; Kim et al., 2011). In an amorphous solid solution, the drug is fully dissolved and molecularly dispersed in an amorphous polymeric carrier, forming a homogeneous mixture. In this type of solid dispersion, only one phase is present and only one glass transition point (T_g) will be observed (Van Drooge et al., 2006). Amorphous solid suspensions are usually made when the drug has very low solubility in the carrier material or it has a very high melting point

(Chiou & Riegelman, 1971). It consists of an amorphous carrier in which the drug is usually dispersed as amorphous clusters. It does not form homogeneous structures and thus has two phases and two glass transition points ($T_{g\ drug}$ and $T_{g\ carrier}$).(Van Drooge et al., 2006). As for the mixture of both amorphous solid solution and solid suspension, it contains two phases: one consists of the drug which is molecularly dispersed in the carrier while the other consists of the drug dispersed as amorphous clusters (Van Drooge et al., 2006). Which one of the three types of second-generation amorphous solid dispersion is obtained depends on the miscibility of the drug and carrier and the preparation method(Breitenbach et al., 1999).

Although the second generation solid dispersions can increase drug solubility and dissolution rate, the subsequent supersaturation of the drug may lead to drug precipitation and recrystallisation especially in amorphous solid dispersions thus decreasing the solubility and bioavailability of the drug. This is particularly common among sugar glass-based solid dispersions (Vo et al., 2013). Furthermore, the amorphous drug may recrystallise into the crystalline form during preparation (cooling or solvent removal) or storage. Prevention of recrystallisation of drugs in the preparation, storage and dissolution process can be achieved by using polymers with high viscosity. However, they tend to hinder the dispersion of drugs in carriers and delay the dissolution of the drugs in an aqueous medium (Tekade & Yadav, 2020). Therefore, an ideal polymeric carrier or second-generation solid dispersion should be able to keep a good balance between the anti-recrystallisation effect and drug dissolution.

2.1.1.1.3. Third generation of solid dispersion

The third generation of solid dispersions either uses a surfactant as the carrier, or a mixture of amorphous polymer and surfactant as carrier. The

introduction of surfactants in solid dispersions has shown a significant effect in overcoming the drug precipitation and recrystallisation problems that occur in second-generation solid dispersions (Vo et al., 2013).

Surfactants with amphiphilic structures can improve the miscibility of drugs and carriers thus reducing the rate of drug recrystallisation. In addition, surfactants can prevent the drug precipitation from supersaturation by either adsorbing the outer layer of drug particles or forming micelles to entrap the drug (Tekade & Yadav, 2020; Vo et al., 2013). Commonly used surfactants include poloxamer 407(Kim et al., 2011), poloxamer 188, gelucire 44/14 (Saffoon et al., 2011), HPMC poloxamer and HPMC-polyoxyethylene hydrogenated castor oil (Won et al., 2005), PEG and polysorbate 80 mixtures (Dannenfelser et al., 2004), polyethylene glycol-HPMC (Janssens et al., 2008).

The third generation solid dispersions are intended to achieve the highest degree of bioavailability and stability (Vasconcelos et al., 2007). However, the addition of surfactants can sometimes have a negative influence on the stability of solid dispersions. It was reported that some surfactants such as polysorbate 80, poloxamer 188 and sodium dodecyl sulfate accelerate the nucleation of celecoxib from an amorphous solid dispersion during the dissolution process (J. Chen et al., 2015) Therefore, when selecting a surfactant as the carrier, careful consideration needs to be given to its effect on the stability of solid dispersion formulations.

2.1.1.1.4. Fourth generation solid dispersions

The fourth generation solid dispersions can be referred to as controlled-release solid dispersions (CRSD). This formulation was developed for poorly water-soluble drugs with a short biological half-life, aiming to improve the solubility and provide extended release in a controlled manner. In CRSD, drugs

are dispersed in either a hydrophilic carrier or hydrophobic carrier (Huang et al., 2006). The carriers for CRSD need to be able to delay the drug release in the dissolution medium so that an adequate amount of drug can be delivered for an extended period of time (Vo et al., 2013). The extended drug release properties of CRSD provide several advantages such as improved patient compliance due to reduced dosing frequency, decreased side effects, more consistent or prolonged therapeutic effect (Desai et al., 2006; Iqbal et al., 2002). Commonly used carriers for extended release of poorly water-soluble drugs in CRSD include ethyl cellulose (EC) (Desai et al., 2006), HPC (Tanaka et al., 2006), Eudragit® RS, RL (Cui et al., 2003; Huang et al., 2006), poly(ethylene oxide) (PEO) and carboxyvinylpolymer (Carbopol®) (Ozeki et al., 2000). These materials are polymers that do not dissolve in water or dissolve very slowly, so they can maintain a constant release of drugs.

2.1.1.2. Preparation methods for solid dispersions

There are four major methods for preparing solid dispersions: the melting method, solvent method, melting solvent method and mechanochemical activation method. A branch tree of each method is shown in Figure 2.3.

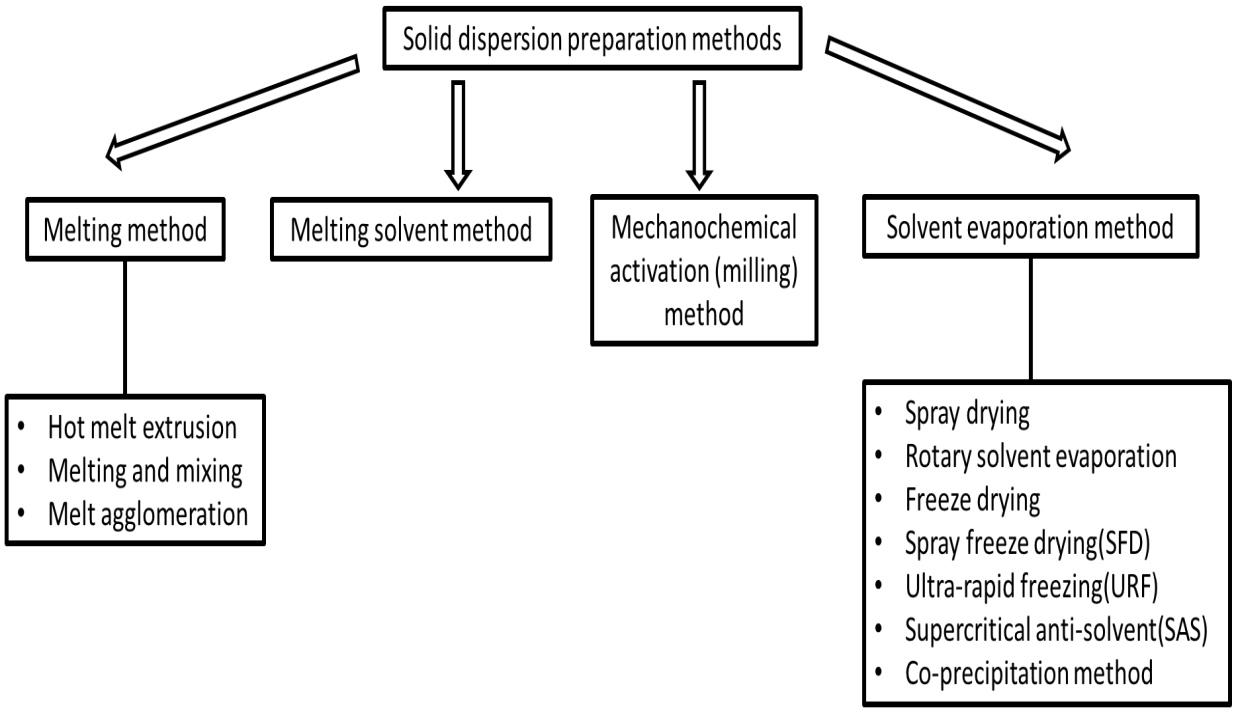

Figure 2.3. A branch tree of solid dispersion preparation methods

2.1.1.2.1. Melting method

The melting method for preparing solid dispersions include melting and mixing, hot melt extrusion and melt agglomeration. A major advantage of the melting method is that no solvents are required during preparation, thus avoiding any residual solvent in the final product.

The first solid dispersion is a eutectic mixture prepared by a melting and mixing method (Sekiguchi & Obi, 1961). Here, the drug and the carrier are melted and mixed at a specific ratio to form a homogenous mixture. The mixture is subsequently cooled to form a solid product (Chiou & Riegelman, 1971). Slow cooling the mixture often produces drugs in crystalline state, while fast cooling may yield drugs in amorphous state(Vo et al., 2013). An important prerequisite for the use of the melting and mixing method for preparing solid dispersion is that the drug and the carrier must be miscible in the molten state so that a homogeneous mixture can be obtained. Therefore, only carrier and drug with similar physicochemical properties can be used in this method, otherwise it will result in inhomogeneous solid dispersions (Vo et al., 2013). PEG and poloxamer are two materials that are commonly used as carriers to prepare solid dispersions by this method due to their relatively low melting points (Barmpalexis et al., 2011; Damian et al., 2000; Kolašinac et al., 2012).

Hot melt extrusion is an established process which was originally used in the plastics and food industries since the 1930s. Now this method has become one of the most common methods for solid dispersion preparation with many such products available in the market, such as Cesamet®, Rezulin®, Kaletra®, Novir® and Isotip® (Chokshi & Zia, 2004; Maniruzzaman et al., 2012). In the hot melt extrusion method, APIs and polymers are fed into an extruder which consists of one or two rotating screws (either corotating or counter rotating)

inside a stationary cylindrical barrel. Intense mixing and agitation forced by the rotating screw causes the drug particles to break down and dissolve in the molten polymers at a controlled temperature, resulting in a homogeneous dispersion. Then the dispersion flow through a die and extruded into a product with uniform density and shape (Crowley et al., 2007). It is worth noting that the contact parts of the extruders used in pharmaceuticals must not be reactive nor may they release components into the product(Maniruzzaman et al., 2012; Vo et al., 2013). Hot melt extrusion of miscible drugs and polymers have a high probability of forming amorphous solid dispersions (Vo et al., 2013). When selecting the appropriate polymer for hot melt extrusion method, the Hansen solubility parameter can be used to predict the miscibility of the drug with the polymer (Moes et al., 2013). Hot melt extrusion is an efficient and easy scale-up method to produce highly thermodynamic stable solid dispersions. However, like other melting methods, it has some common problems such as the high requirement for the miscibility of drugs and carriers as well as needing high temperatures in the preparation process(Saerens et al., 2011).

Amorphous solid dispersions prepared by the hot melt method are usually viscous like, with poor flowability and poor compressibility, which hinders their use in making tablets (Vo et al., 2013). Melt agglomeration is a melting method that can counter these problems. It uses the carriers as a meltable binder to hold drugs and other excipients together, making sure the tablets remain intact after compression (Gupta et al., 2002; Seo et al., 2003). In this method, a mixture of drug-carrier-other excipients is processed in a high shear mixer or rotary processor. The mixture can be prepared by three different ways(Gupta et al., 2002; Passerini et al., 2002; Seo et al., 2003): 1) the molten carrier is added to a heated mixture of the drug and excipients. 2) the molten carrier is mixed with the drug and then added to the heated excipients. 3) A mixture of the drug-carrier-excipients is heated at a temperature with or above the melting

point of the carrier. Several researchers have used melting agglomeration method to prepare agglomerates containing solid dispersions (Gupta et al., 2002; Passerini et al., 2002; Seo et al., 2003; Vilhelmsen et al., 2005). These studies showed a significant increase in the dissolution rate of drugs due to a high degree of dispersion.

2.1.1.2.2. Solvent method

In the solvent method, as the name implies, solid dispersions are obtained after the removal of solvent from the solution containing a drug and carrier (Chiou & Riegelman, 1971). An important prerequisite for this method is that both the drug and carrier need to be fully soluble in the solvent selected(Leuner & Dressman, 2000).Commonly used solvents include acetone, ethanol, ethyl acetate, methanol, methylene chloride and water. Sometimes a mixture of two or more solvents are used in solvent evaporation method (Vo et al., 2013). The solvents used to dissolve the drug and the excipients could significantly affect the stability and dissolution rate of the solid dispersions prepared. The impacts were believed to be due to the interactions between the drug molecule or carrier with the solvent (Bikiaris, 2011). Similar to the melting method, the solidification rate in the solvent method determines the physical state of the drug in the solid dispersion. To ensure the amorphous state of the drug, a rapid solidification is always preferred (Vo et al., 2013).

Unlike melting methods, the solvent method can be carried out at relatively low temperatures without heating, thus avoiding the decomposition of the drug and the carrier at higher temperatures. This allows some polymers that are rarely chosen as carriers for preparing solid dispersions in the melting method due to their high melting points to be used in solvent method. However, there is a disadvantage to this method, there can be residual solvent remaining after

the removal process and it may lead to toxicity. In addition, the solvent method has environmental concerns because of the large quantity of solvent needed in large scale production which can be a threat to the environment.

The solvent method can be sub-classified as follows: rotary solvent evaporation (Ceballos et al., 2005; Wang et al., 2005), spray drying (Li et al., 2011), freeze drying (lyophilisation) (García-Rodriguez et al., 2011), spray freeze drying (Lim et al., 2010), ultra-rapid freezing (Overhoff, Engstrom, et al., 2007) and supercritical anti-solvent (SAS) (Won et al., 2005).

Rotary solvent evaporation is a solvent removal technique using a rotary evaporator (sometimes known as a rotovap). In this method, the drug-carrier solution is loaded in a vessel (Usually a round-bottomed flask with a volume at least twice the volume of the solution), then the solution-containing vessel is rotated under vacuum while being heated by a water bath. This step continues until the solvent has evaporated and the solid product has been produced. Rotary solvent evaporation increases the rate of evaporation of the solvent in three ways (1) reducing the pressure exerted on the surface of the solvent, the energy needed to break the intermolecular bonds decreases, which facilitates the transition of the molecules into the gas phase (2) rotating the solution to increase the surface area for evaporation (3) heating the solution with the water bath (Bhujbal et al., 2021). Rotary solvent evaporation is easy to perform and can be carried out at a low to moderate temperature so that the degradation of drugs and carriers at high temperatures can be avoid (Vo et al., 2013). After the solvent evaporation process, the resultant solid dispersions can be stored in a vacuum desiccator for complete removal of the residual solvent (Kim et al., 2011).

Spray drying is a well-established technique for preparing solid dispersions

as it allows extremely rapid evaporation of the solvent (Paudel et al., 2013). In this technique, the drug-carrier solution or suspension is loaded from a container into the nozzle inlet via a pump system and atomised into fine droplets with a large surface area. The fine droplets lead to rapid evaporation of the solvent and formation of solid particles. The size of these particles can be customised by adjusting the droplet size via the nozzle to meet the formulation requirements (Vo et al., 2013). Typically, spray-dried solid dispersions are amorphous due to their rapid solidification (Bikiaris, 2011). Spray drying has the advantages of being easy to produce continuously and on a large scale, while providing good uniformity of molecular dispersion (Bikiaris, 2011; Vo et al., 2013). Some solid dispersion products prepared by spray drying are commercially available in the market such as Intelence®, which is an amorphous solid dispersion of Etravirine using (Hypromellose) HPMC as the carrier (Litou et al., 2020).

Different solvents used in spray drying can result in a different stability and dissolution rate of the solid dispersions (Al-Obaidi et al., 2009). In addition, the concentration of the drug and the polymers dissolved in the solvent can affect the crystallinity of the solid dispersions prepared by spray drying. Less concentrated drug-carrier solutions, while maintaining constant ratio of drug:carrier, tend to form smaller sized solid dispersions with slower structural relaxation rates. Compounds that do not show rapid relaxation tend not to crystallise from the amorphous form (Hasegawa et al., 2009). This indicates the importance of controlling spray drying conditions when preparing solid dispersions in order to obtain more stable and faster dissolving products.

Freeze drying is another technique for preparing solid dispersion via solvent

removal. It was generally used for removal of aqueous solutions like water. Theoretically, organic solvents could also be removed by freeze drying, but in reality, it is much more changeling than the removal of water. The low freezing temperature and triple points of many organic solvents so the freeze driers must be able to maintain a low enough temperature and pressure to avoid the organic solvents from melting. In addition, many laboratory freeze dryers are equipped with acrylic drying chamber. The presence of organic solvents in the vapour stream or in the condensate can cause damage to acrylic and eventually cause leakage issues (MillrockTechnology, 2020).

Freeze drying includes three stages: freezing, primary drying and secondary drying (Jakubowska & Lulek, 2021). The resulting freeze dried product is commonly known as a freeze dried ‘cake’ (Hottot et al., 2007). During the freezing stage, the drug-carrier solution is frozen at a temperature below the freezing point of the solvent. The drug and carrier are concentrated, while the solvent is crystallised and the phases are separated (Jakubowska & Lulek, 2021). At the primary drying stage, the frozen sample is loaded into the freeze dryer. During the drying process, the pressure is reduced by a vacuum which causes sublimation of the frozen solvent. To increase the rate of sublimation, the temperature in the freeze dryer can be increased. The sublimation of the frozen solvent is responsible for the porous structure of the dried product. It was noted that when increasing the temperature, care must be taken to avoid temperatures increased too much and quickly so that the ‘cake’ can undergo collapse: this can cause detrimental defects such as physical collapse or micro collapse within the product, loss of activity and a high moisture content (Siow et al., 2016). Finally, at the secondary drying stage, in which the temperature of the freeze-dried cake is increasing slowly to remove the unfrozen solvent remained. Once again, the temperature must not be raised too quickly otherwise the cake collapse can occur (Tang & Pikal, 2004). The advantage of

freeze drying is that it minimises the risk of phase separation. However, it has the disadvantage that most organic solvents have a very low freezing temperature and will not remain frozen during sublimation. Therefore, if samples need to be lyophilised at low temperatures, the process will take longer (Vo et al., 2013).

With the development of technology, enhanced methods for freeze drying have been applied to the preparation of solid dispersions. These methods are spray freeze drying (SFD) and ultra-rapid freezing (URF) which have faster freezing rate compared to the conventional freeze drying method (Vo et al., 2013). This makes them more efficient in terms of processing times when preparing solid dispersions.

SFD is a combination of spray drying and freeze drying methods where a feed solution that contain the poorly water soluble drug and hydrophilic excipients is sprayed into liquid nitrogen or low temperature dry air to form frozen droplets which are then lyophilised to form solid products (Hu et al., 2002). The solvent for preparing feed solution is normally a mixture of a water miscible organic solvent and water, such as tetrahydrofuran–water which can dissolved both hydrophobic drugs/compounds and hydrophilic excipients (Hu et al., 2002). Like spray drying, SFD produces fine droplets with a large surface area. In addition, the direct contact with the cooling agents results in rapid vitrification (transformation of liquid into an amorphous glass), thus reducing the risk of phase separation to a minimum. It also able to customise the particle size by adjusting the droplet size via the nozzle. Since no elevated temperatures are required in SFD, this technique is suitable for thermolabile drugs/compounds. SFD normally produces solid dispersions in an amorphous

state because the rapid freezing rate can prevent molecular arrangement into crystalline domains (Hu et al., 2003; Tong et al., 2011). In addition, drug stability in SFD solid dispersions is considerably better compared to solid dispersions prepared by conventional freeze-drying methods. This is due to the higher cooling rate of SFD, resulting in more drug incorporation into the matrix, especially at high drug loads (van Drooge et al., 2005).

During URF, the poorly water soluble drug and the hydrophilic carrier are first fully dissolved in either an organic solvent (such as *tert*-butanol and acetonitrile) or a solvent consists of a water miscible organic solvent and water. Then the solution contains the drug and excipients is spread on a cold solid surface to form a thin film that freezes in less than 1 second and the solvent is removed by lyophilisation (Overhoff, Moreno, et al., 2007) . As the freezing process in URF is extremely fast, the risk of nucleation of the drug particles is minimised, making them stay in the amorphous form after lyophilisation (Yu, 2001).

Supercritical anti-solvent (SAS) is a unique solvent method because it uses supercritical carbon dioxide (CO_2) as an anti-solvent. Supercritical carbon dioxide is a fluid form of carbon dioxide where it is held at or above its critical temperature (31.0 °C) and critical pressure (7.377 MPa)(Xu & Liu, 2013). In this method, the drug and carrier are dissolved in a minimal volume of solvent and the solution is sprayed into a vessel containing supercritical carbon dioxide. When the solution encounters the supercritical carbon dioxide, the solvent is rapidly extracted which resulting in the precipitation of solid dispersed particles (Sethia & Squillante, 2004). Compared to traditional anti-solvent precipitation methods, SAS requires less organic solvent and it is more environment friendly (Karanth et al., 2006). In addition, supercritical carbon dioxide can be easily and completely removed from the final product by pressure reduction, in

contrast to the complex purification methods often required when using organic anti-solvents (Mezzomo et al., 2012).

Co-precipitation is a solvent method in preparing solid dispersions for drugs and carrier with poor aqueous solubility (Shah et al., 2013). In this method, the drug and carrier are completely dissolved in an organic solvent and the solution is then added to an anti-solvent (usually water). Due to the poor water solubility of the drugs and carriers, they can be simultaneously precipitated in water. The resulting suspension is filtered, washed to remove residual solvent and dried under vacuum. The co-precipitated material obtained after filtration and drying is known as microprecipitated bulk powder (MPD) which is a solid dispersion of the drug and carrier (Vo et al., 2013). The advantage of this method is that it does not require elevated temperatures which reduce the risk of degradation of the drug or carrier (Sertsou et al., 2002). In addition, the solvent can be removed by washing so it may have less equipment and energy requirements. It is worth noting that the solvent and anti-solvent used in co-precipitation can sometimes act as plasticizers which result in high molecular mobility and molecular rearrangement including crystallisation (Sertsou et al., 2002). Therefore, careful consideration must be taken for the selection of the solvent and anti-solvent used in co-precipitation, as they are vital for the success of the final products.

2.1.1.2.3. Melting solvent method

Melting solvent method is, as the name suggests, a combination of melting and solvent methods. When preparing solid dispersions by this method, the drug is first dissolved in a suitable solvent while the carrier is molten. Then the drug solution is mixed with the molten carrier, followed by solvent removal and solidification to form solid dispersions (Sareen et al., 2012). Since drugs do not need to be melted in this method, it protects them from thermal degradation. In

addition, the melting solvent method requires lower temperature and mixing times than other melting methods. All these make this method particularly suitable for drugs that are thermolabile or have high melting points such as etravirine (it degrades upon melting at 246 °C) (Huang et al., 2019). Another advantage is that the molten form of the carrier is better dispersed in the solvent than the solid form, making the dissolution process easier and faster (Vo et al., 2013). However, since this method is a combination of melting and solvent methods, more equipment and energy may need to be used. Also, costs may be higher because of the need for heating and the use of solvents.

2.1.1.2.4. Mechanochemical activation method

Mechanochemical activation, also known as milling, is a solid-state method that is commonly used for preparing solid dispersions. The milling process can be carried out in either a dry or wet environment, depending on the nature of the material and the desired product characteristics. This method involves subjecting the drug and excipients to high-energy mechanical forces, such as grinding, milling, or ball-milling, which cause the drug molecules to be trapped within the polymer matrix, leading to the formation of a solid dispersion. The high-energy mechanical forces generated during milling can promote the formation of amorphous solid dispersions by disrupting the crystal lattice of the drug (Loh et al., 2015; Mai et al., 2020).

The mechanochemical activation method offers several advantages over traditional solvent-based methods of preparing solid dispersions. It is a solvent-free process, which eliminates the need for costly and time-consuming solvent evaporation steps and reduces the risk of residual solvent contamination (Jug & Mura, 2018). Furthermore, the method can be easily scaled up for industrial production (Loh et al., 2015). However, the mechanochemical activation method also has some limitations and challenges. One major challenge is the

potential for degradation or decomposition of the drug and excipients due to the heat generated by the high-energy mechanical forces during the milling process (Bikiaris, 2011). Additionally, the method requires careful optimisation of milling parameters, such as milling time, speed, and milling media, to achieve uniform and stable solid formulations with improved drug solubility and dissolution (Karakucuk & Celebi, 2020).

2.1.1.2.5. Advantages of solid dispersions

Solid dispersions show many important advantages over other techniques for improving the solubility and bioavailability of poorly water-soluble drugs, such as particle size reduction (milling or micronisation), salt formation, and solubilisation (co-solvents, micelles, emulsions), making it a very promising strategy. In addition, solid dispersions can be formulated in solid oral dosage forms which are more favoured for patients than liquid products produced by methods like emulsion and co-solvent (Karavas et al., 2006; Serajuddin, 1999).

Comparing with conventional particle size reduction methods like micronisation where the particle size is limited to around 2-5 μm, it is possible for solid dispersion to reduce the size of drug particles to the molecular level (Vo et al., 2013). It is true that nanosizing techniques can produce extremely small, nano-sized drug particles in solid form, but the preparation process may be long and complicated. In addition, nanoparticles require stabilizers to inhibit the over-growth of the nanoparticles and prevent them from aggregation/coagulation (Tuomela et al., 2016). Sometimes special equipment is required to produce nano-sized particles like high-speed homogenisation or ultrasonication while solid dispersions can be produced by relatively easy and commonly available equipment such as rotary evaporators, freeze driers or

spray driers. In solid dispersions, the interaction between the drug and carrier can prevent the precipitation/re-crystallisation of drug particles that may occur during the dissolution process or storage. The drug in solid dispersion can be released in supersaturation state which is favoured for rapid absorption (Leuner & Dressman, 2000). Even precipitation does occur during the dissolution process, the precipitated drugs are likely to exist in amorphous or metastable crystalline forms which have lower thermodynamic stability (higher energy state) than the original crystalline formed drug particles, which still result in faster and better drug dissolution (Vo et al., 2013).

Salt formation is a method of increasing the solubility of a drug by forming an ionic compound as a result of an acid-base reaction. In general, the salt form of drugs has higher solubilities than their corresponding acid or base forms (Serajuddin, 2007). When compared to the formation of salt formation, solid dispersion methods have the advantage that they can be applied for a wider range of ionisable drugs since salt formation is not feasible for neutral compounds. In addition, the improvement in dissolution rate and oral bioavailability may not be achieved by salt formation because the drug salts can precipitate out in the GI fluid into their respective acid or base form of the drugs (Serajuddin, 1999).

In addition to reducing particle size, maintaining supersaturation during dissolution and the ability to prevent drug precipitation, solid dispersions can also improve drug dissolution and bioavailability by improving wettability and porosity and causing polymorphic changes of the drugs. In first, second and third generation solid dispersions, the hydrophilic carrier molecules form a matrix that surround the drug particles. The matrix can dissolve rapidly when they encounter dissolution medium which improves the wettability of the drug, especially when a surfactant or emulsifier is used in the solid dispersion. This

reduces the risk of agglomeration of the drug particles in the dissolution medium and improves the dissolution rate of the drug (Vo et al., 2013). Solid dispersions also have a highly porous structure, especially those prepared by a solvent method. The fast solvent removal could leave some channels in the solid dispersion structure, thus increasing the porosity and surface area of the drug which contribute to the improvement in dissolution rate (Zhang et al., 2012). It was suggested that solid dispersions using linear polymers as carriers often have a higher porosity than those prepared using reticular polymers (Vo et al., 2013). As for the ability to change polymorphic state of drugs, second, third and fourth generation solid dispersions are able to transform drugs from their crystalline form to amorphous form. The reduction of the crystallinity makes the drugs easier and faster to dissolve because less energy is required to break the lattice structure during the dissolution process (Taylor & Zografi, 1997).

In conclusion, the numerous advantages of solid dispersion technology make it one of the most promising strategies for improving the oral bioavailability of poorly water-soluble drugs.

2.1.1.2.6. Disadvantages of solid dispersion

Despite the numerous advantages of solid dispersions in improving the bioavailability of poorly water-soluble drugs, it still has several problems. The use of different methods of solid dispersion preparation can lead to various problems such as thermal degradation/instability of the drugs and carriers when using melting methods, environmental and safety issues with the use of organic solvents in solvent methods, inhomogeneity of drug dispersion during solidification process and the cost in terms of energy and processing times. Another major problem is that it is possible for amorphous state drugs in solid dispersions to convert to the crystalline form during storage, which results in a

shorter shelf-life (Baird & Taylor, 2012).The recrystallisation of amorphous drugs is related to the glass transition point (T_g) and the molecular mobility of the drug. During storage, moisture in the air can act as a plasticiser and usually decreases the T_g of amorphous drugs, resulting in increased molecular mobility which leads to an increased tendency for amorphous drugs to crystallise (Duddu & Sokoloski, 1995; Hancock & Zografi, 1994). An increase in temperature can also enhance the molecular mobility of the amorphous drugs which leads to recrystallisation. Therefore, moisture level and temperature during storage are main factors that influence the physical stability of amorphous drugs in a solid dispersion system (Vasconcelos et al., 2007).

To overcome this problem, carriers with higher T_g than the drug can be used in solid dispersion preparation because they can decrease the molecular mobility of drug by increasing the T_g of the solid dispersion. The formation of hydrogen bonding between the drug and carrier can also help to hinder the drug recystalisation by increasing the miscibility between the drug and carrier (Taylor & Zografi, 1997). Furthermore, the addition of surfactants and emulsifiers to solid dispersion systems helps to improve drug-polymer miscibility because of their amphiphilic structure, thus reducing the tendency for drug recrystallisation (Vo et al., 2013). It is worth noting that some carrier materials, especially polymers, are hygroscopic and the water absorbed by the carriers can cause increases in molecular mobility (Vo et al., 2013). Therefore, an ideal carrier should have high T_g, able to form strong hydrogen bonding interaction with the drug and low hygroscopicity in order to produce stable solid dispersions. In conclusion, solid dispersions do have some drawbacks, but these may be avoided or mitigated if careful consideration is given to the choice of excipients, preparation method and storage conditions.

2.1.2. A brief introduction of the excipient candidates

2.1.2.1. Soluplus

Soluplus is an amorphous, amphiphilic polyvinyl caprolactampolyvinyl acetate-polyethylene glycol graft copolymer developed by BASF, a German multinational chemical company. It is branded as “polymeric solubilizer and matrix forming polymer” (Alopaeus et al., 2019; BASF, 2019; Caron et al., 2013; Linn et al., 2012) . The molecular weight of Soluplus ranges from 90,000–140,000 g/mol and the hydrophilic/lipophilic balance value is approximately 14, indicating its hydrophilic nature (BASF, 2019). Soluplus is also a surface active agent with critical micelle concentration (CMC) of 0.82 mg/ml (Tanida et al., 2016). This polymer has a hydrophilic polyethylene glycol (PEG) backbone with one or two lipophilic sidechains consisting of vinyl acetate randomly co-polymerised with vinyl caprolactam (Alopaeus et al., 2019).

It was originally developed as an excipient for hot-melt extrusion due to its glass transition temperature of around 70°C and no chemical degradation even after extrusion at 220°C (BASF, 2019). Based on a toxicological assessment conducted by BASF, doses of up to 8000 mg Soluplus per healthy human volunteer were regarded as safe. For a subject of 70 kg body weight, this translates into an oral Soluplus dose of 114 mg/kg (BASF, 2019).

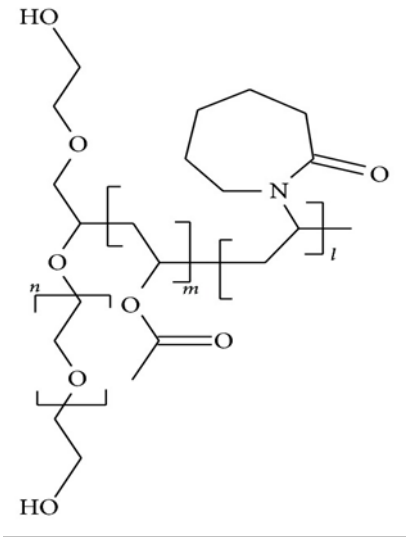

n=13, m=30, l=57

Figure 2.4. Chemical structure of Soluplus

2.1.2.2. HPMCAS

HPMCAS (hypromellose acetate succinate) is an amorphous synthetic polymer derived from cellulose which appears as a fine white powder (Friesen et al., 2008). It has three different grades (L, M and H), based on the % of the hydrophobic acetyl group(-COCH3) and the hydrophilic succinyl group (-COCH2CH2COOH) in the molecule. L grade having the highest succinyl (14-18%) and lowest acetyl groups (5-9%) while. H grade possesses the lowest succinyl (4-8%) and highest acetyl groups (10-14%). M grade groups of succinyl and acetyl are intermediate (10-14% and 7-11% respectively) (Adhikari & Polli, 2020). The molecular weight of HPMCAS ranged from 17,000 to 20,000 g/mol (Fukasawa & Obara, 2004). All three grades of HPMCAS have a glass transition point at around 120°C (Ashland, 2019).

HPMCAS is an approved pharmaceutical excipient for oral dosage forms. No adverse effects were found in several toxicological studies in mice, rats, guinea pigs, rabbits, dogs and frogs (Cappon et al., 2003).

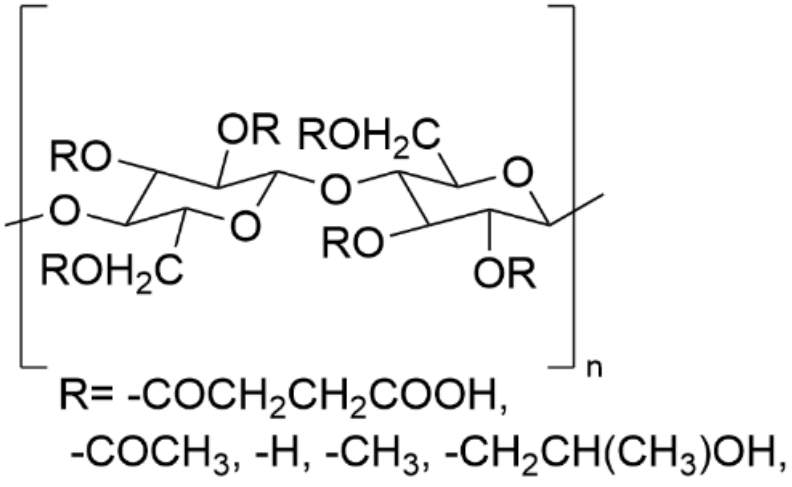

Figure 2.5. Chemical structure of HPMCAS (hypromellose acetate succinate)

2.1.2.3. Vitamin E TPGs

Vitamin E TPGs or tocophersolan (D-α-Tocopheryl polyethylene glycol 1000 succinate) is a water-soluble derivative of natural Vitamin E that is formed by esterification of Vitamin E succinate with polyethylene glycol (PEG)1000. It consists of a hydrophilic head (PEG1000) and a hydrophobic tail (Vitamin E) and they are linked by succinic acid. Vitamin E TPGs is a nonionic surfactant with an average molecular weight of 1513 g/mol. It is a waxy solid at room temperature (Melting points ranged from 37 to 41 °C) (Guo et al., 2013) The hydrophilic/lipophilic balance value is 13.2 which means it is more hydrophilic. It has a low critical micelle concentration (CMC) of 0.2mg/ml (Kumbhar et al., 2022). Vitamin E TPGs remains stable at pH 4.5–7.5, only 10% was hydrolysed when kept for 3 months in neutral aqueous buffer It is also a FDA approved safe pharmaceutical adjuvant(FDA, 2019). Vitamin E TPGs is very versatile and can be used as an absorption enhancer, emulsifier, solubiliser, penetration enhancer and stabiliser. (Kumbhar et al., 2022). The maximum doses of Vitamin E TPGs approved by FDA is shown in Table 2.1. From toxicology studies in animals (rats and rabbits), the European Food Safety Authority concluded that an overall no-observed-adverse-effect level (NOAEL) of 1g/kg body weight per day was reported (Krasavage & Terhaar, 1977).

Dosage form	**Maximum amount of Vitamin E TPGs included per unit dose**
Tablet	42.5 mg
Solution	300 mg/ml
Capsule	300 mg
Film coated tablet	28.33 mg

Table 2.1. The maximum amount of Vitamin E TPGs used per unit dose in FDA approved drug products (FDA, 2019)

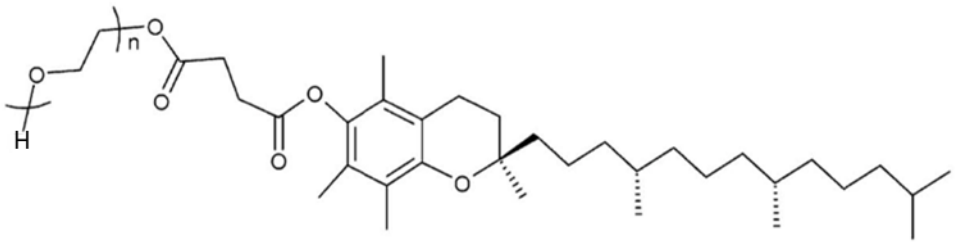

n= 22 (averagely)

Figure 2.6. Vitamin E TPGs chemical structure

2.2. Aims

- To carry out a preliminary screening study (Literature review) to select the candidate excipients.
- To prepare binary solid dispersion samples for solubility studies (Secondary screening study).
- To prepare ternary solid dispersion samples for solubility studies (Secondary screening study).
- To confirm the excipients, ratio of drug: excipients and preparation method for making the novel solid dispersion of curcumin formulation, based on the secondary screening study results.

2.3. Materials and method

2.3.1. Materials

Commercial grade curcumin powders (*Curcuma Longa*) were obtained from Techbifarm (Hanoi,Vietnam). Soluplus was provided by BASF SE (Ludwigshafen, Germany). Vitamin E TPGs was purchased from Sigma-Aldrich company Ltd (Gillingham, Dorset, UK). M, H and L grades of HPMCAS were purchased from Ashland (Wilmington, US). HPLC grade acetone was acquired from Fisher Scientific Ltd. (Loughborough, UK). Sodium chloride, hydrochloride acid, potassium phosphate monobasic and sodium hydroxide were all obtained from Fisher Scientific Ltd. (Loughborough, UK).

2.3.2. Method

2.3.2.1. Preliminary screening study

A literature review of polymers and surfactants was conducted to investigate and compare their performance in improving the aqueous solubility and *in vivo* bioavailability of curcumin when used as excipients in solid dispersion formulations. Polymers and surfactants that showed considerable improvement effect were selected as the excipient candidates for the secondary screening study, which was a solubility study.

2.3.2.2. Solid dispersion preparation methods

Two solid dispersion preparation methods:1) solvent evaporation combined with freeze drying and 2) hot melt extrusion were used for preparing the curcumin solid dispersion samples for the secondary screening study. It was worth noted that since 100% pure curcumin was extremely rare and expensive in the market, in this study, commercial grade curcumin powder containing mainly curcumin (≥ 80%) and a small proportion of other curcuminoids

(demethoxycurcumin and bis-demethoxycurcumin) was used to prepare samples of curcumin solid dispersions.

For solvent evaporation+freeze drying method, solid dispersion samples were prepared in a two-step procedure, consisting of solvent evaporation and freeze-drying. A mixture of curcumin and the excipients were dissolved in 100ml acetone in a round bottom flask. The ratios of the drug:excipients are shown in Table 2.2. The reason for using acetone is that curcumin, Soluplus, HPMCAS (L, M and H grades) and Vitamin E TPGs can all dissolve in this solvent. The solvent was then removed from the solution by rotary evaporation at (40^0C, 250 mbar, 200 rpm) using the rotary evaporator (IKA Rotary evaporator RV 3 V-C, Germany). A thin waxy film was then formed, water was sprayed onto the film and sonicated for 10 minutes in an ultrasonic bath (Fisherbrand™ S-Series Heated Ultrasonic Bath) to allow the thin film to detach from the inner wall of the flask. The separated thin film was transferred into a 200 ml beaker and placed at -80°C in an ultra-low temperature freezer (Haier Biomedical -86°C ultra-low temperature Freezer) until the liquid was fully frozen. It was then placed in a freeze-drier (Christ Alpha 2-4, Germany) at -70ºC and 0.2 mbar. The process of lyophilisation lasted 24 hours to remove remaining moisture. After lyophilisation, a dry, brittle yellowish freeze-dried cake was formed. It was then crushed into powders by mortar and pestle, covered with aluminium foil to protect and stored in a desiccator at room temperature until further use.

More than 10 parts of Soluplus with 1 part of curcumin was not considered in this study because it has been observed that when above this ratio, Soluplus starts to form a gel network in aqueous solution. Shi et al. reported that the formation of the gel network can increase the viscosity of the solution and it increased the diffusion layer thickness surrounding the drug particles thus delaying the dissolution of the drug (Shi et al., 2018).

According to a study performed by Song et.al., the maximum ratio of curcumin to Vitamin E TPGs was suggested to be 1: 10 (w/w) in solid dispersion formulations (Song et al., 2016). As a result, the maximum ratio of curcumin to Vitamin E TPGs in this study was selected as 1 to 10.

As for hot melt extrusion method, when preparing solid dispersion samples containing only Vitamin E TPGs, Vitamin E TPGs was first melted at 60^{o}C and then mixed with curcumin and either Soluplus or HPMCAS (M, L or H) to generate a blend. The blend was further mixed using Turbula® Shaker-Mixer for 15 minutes. The ratios for the API and excipients were the same as the solvent evaporation + freeze drying method. The blended powders were fed into a 10mm twin-screw hot-melt extruder equipped with a 2mm round-shaped die (Twintech, UK). The hot-melt extruder consisted of 5 heating zones and the temperatures at each zone were maintained as shown in Figure 2.7. The speed of the screw was set at 150 rpm. Extrudates that were generated were allowed to cool to room temperature and then crushed into powders using a blender (Haden Chester 1.5 L Turbo Table Blender).

For preparing the solid dispersion samples without Vitamin E TPGs, curcumin and Soluplus or HPMCAS powders were blended for 15 minutes in a Turbula® Shaker-Mixer and then follow the same steps as above. The ratios of the drug:excipients for HME samples were the same as those used in the solvent evaporation + freeze drying method.

The HME process temperature was selected at 150°C. In general, the temperature of the melting zone is normally set at least 15-60℃ above the melting point or the glass transition temperature of polymeric excipients, in

order to attain suitable plasticity and hence enable melt flow within the extruder barrel(Crowley et al., 2007). The HME process temperature is also recommended to be set 20-30 ºC lower than the melting point of the drug to make sure the drug is being thermally stable at the processing temperature(Alshetaili et al., 2020; Djuris et al., 2013). It was reported that when the HME process temperature below 120º C, the machine would stop working due to the high viscosity of Soluplus (torque overload, over 100%)(Gupta et al., 2016). As a result, the HME process temperature was set to be 150°C. It was much higher than the glass transition point of Soluplus (70°C)(Alshahrani et al., 2015) and melting points of Vitamin E TPGs (37 to 41°C) (Guo et al., 2013) and at least 20ºC lower than the melting point of curcumin (170-175℃)(Esatbeyoglu et al., 2012).

Curcumin	Carrier (Soluplus or HPMCAS)	Surfactant (Vitamin E TPGs)
1	3	———
1	5	———
1	10	———
1	———	1
1	———	5
1	———	10
1	10	1
1	10	5
1	10	10

Table 2.2. Curcumin to excipient(s) weight ratios in each solid dispersion samples

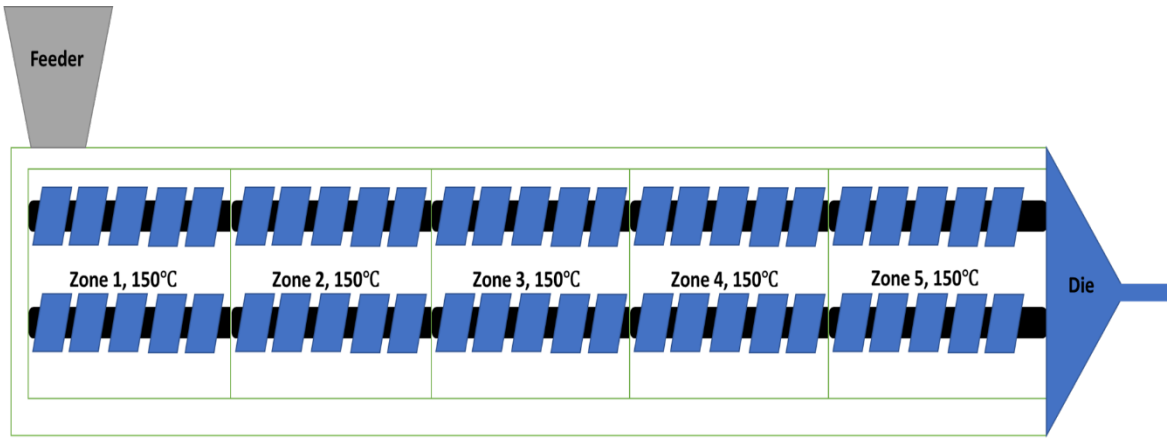

Figure 2.7. HME process temperature at each heating zone of the hot melt extruder

2.3.2.3. Preparation of pH1.2 and pH6.8 buffer

Buffer of pH1.2 and pH6.8 were prepared to mimic the pH environment of stomach and small intestine during the drug dissolution process after oral administration. The preparation method for pH1.2 adopted from Pan et al. (Pan et al., 2015) while pH 6.8 buffer was adopted from Stippler et al. (Stippler et al., 2004).

The pH1.2 buffer (35mM) was prepared by dissolving NaCl (3 g) in 1450 ml of ultra-pure water and then adjusted pH to 1.2 ± 0.1 with 0.1M HCl solution. The pH6.8 buffer (50mM) was prepared by adding potassium phosphate monobasic (6.805 g) and sodium hydroxide (0.896 g) in 1000 ml of ultra-pure water and adjusted the pH to 6.8 ± 0.1, with 1 M NaOH solution. In the end, the volume of each buffer was adjusted to 1500 ml using ultra-pure water.

2.3.2.4. Determination of the wavelength of maximum absorbance (λmax) of curcumin

A 10 µg/ml standard solution of commercial curcumin was prepared by using acetone. Wavelength of maximum absorption (λmax) of curcumin was determined by scanning the standard solution of curcumin using UV-visible spectrophotometer (Lambda 265 UV/Vis Spectrophotometer, Perkin Elmer) between 400-600 nm.

2.3.2.5. Secondary screening study (Solubility study)

Binary solid dispersion samples, ternary solid dispersion samples and the curcumin control containing equivalent curcumin dose of 10mg were added to glass vials containing 10ml of pH1.2 buffer respectively then left on an orbital shaker at 37°C for 24 hours. 4ml of suspension sample was collected and filtered by 0.45 µm syringe filter (Fisherbrand™, Non-sterile PTFE 0.45 µm Syringe Filter). The filtered liquid was analysed in the UV spectrophotometer (Lambda 265 UV/Vis Spectrophotometer, Perkin Elmer) to determine the drug

concentration. The concentration of drug detected was considered as the saturation solubility of the drug from each formulation sample. The same procedure was followed for solubility study in pH 6.8 buffer. 3 replicates were made for each test samples and each experiment was repeated on three different days. The solubility test results presented were the average of three individual experiments and expressed as mean ± standard deviation (n=9). A new calibration curve for curcumin with concentration ranged from 0.01 to 10 µg/ml was plotted each time the UV spectrophotometer was switched off and on. All the curves showed a linear relationship with a correlation coefficient of $R^2 > 0.995$. An example of the calibration curve for curcumin is shown in Figure 2.8 for exhibition purpose.

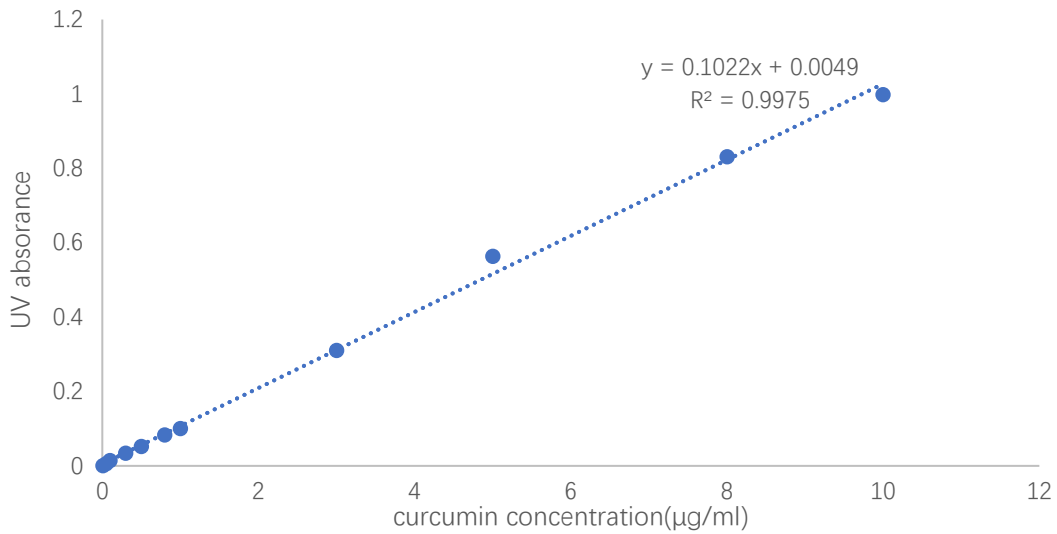

Figure 2.8. Curcumin calibration curve with concentrations from 0.01 to 10 µg/ml

2.3.2.6. Statistical analysis

One-Way analysis of variance tests (ANOVA) was performed for statistical analysis. Post hoc test (Tukey test) was carried out after the ANOVA analysis for analysing the solubility test results. The observations would be considered as significantly different with p-value ≤ 0.05. ANOVA and Tukey test were performed using IBM SPSS Statistics software (Version 24.0; IBM Corp, Armonk, NY, USA).

2.4. Results

2.4.1. Preliminary screening study

There are many research studies on using solid dispersions for improving the oral bioavailability of curcumin. However, most of the studies only conduct *in vitro* assays and did not perform *in vivo* pharmacokinetic studies on the solid dispersion formulations developed. *In vitro* assays do not always correlate with *in vivo* pharmacokinetic results or give a correct indication of the bioavailability of the formulation (Vo et al., 2013). Therefore, only studies that performed *in vivo* pharmacokinetic studies were reviewed and compared in preliminary screening study because they provided a more reliable indication of the actual oral bioavailability. Among the numerous research studies on solid dispersion formulations of curcumin, 10 studies have performed *in vivo* pharmacokinetics studies in animal models via oral drug administration. A summary of these curcumin solid dispersion formulations is shown in Table 2.3. Comparison the oral bioavailability of each curcumin solid dispersion formulation in animal models was shown in Figure 2.9.

Formulation	**Amount of curcumin**	**AUC_{0-t}**	**C_{max}**	**Increase in solubility**	**Subjects**	**Reference**
Curcumin-PVP(1:3) solid dispersion prepared by solvent evaporation	40 mg/kg	45.7 ± 27.4 µg h/ml	99.98 ± 68.09 µg/l	200-fold increase in water solubility for curcumin	Male Sprague-Dawley rat	(Gao et al., 2019)
Curcumin-PVP k 30-α-glucosyl stevia (1:5:10) solid dispersion prepared by freeze drying	20 mg/kg	5.06 µg min/ml	86.6 ng /ml	13,000-fold higher than native cur equilibrium solubility	Male Sprague-Dawley rat	(Kadota et al., 2016)
Curcumin: PEG 4000:PVP K30 solid dispersions (1:7:3) prepared by solvent evaporation	2g/kg	5765.73 ± 441.94 ng h/ml	0.91 ± 0.031 µg/ml	4000-fold increase in curcumin solubility at pH1.2	Albino wistarrats	(Kumavat et al., 2014)
Hot melt extrusion solid dispersion consists of curcumin (10%), HPMC (75%), lecithin (10%) and isomalt (5%)	20 mg curcumin/rat	20470 ± 834 ng min/ml	184 ± 14 ng/ml	Over 1000-fold increase in water solubility	Male Sprague–Dawley rats	(Chuah et al., 2014)
Curcumin (200 mg) and HPMC-AS (800 mg) solid	20 mg curcumin/kg	27.1 ± 6.7 µg min	147 ± 53 ng/ml	No solubility test	Male Sprague–Dawley rats	(Onoue et al., 2010)

dispersion prepared by freeze drying		/ml				
Curcumin-cellulose acetate-manitol (1:10:10) sustained release solid dispersion prepared by solvent evaporation	50 mg/kg	1,094.79 ± 195.02 ng h/m/	187.03 ± 34.59 ng/ml	4.2-fold increase in curcumin water solubility	Male Wistar rats	(Wan et al., 2012)
Curcumin-soluplus (1:3) self-micelling solid dispersion prepared by solvent evaporation	47 mg/kg	33,310.05 ± 6025.34 ng min/ml	523.64 ± 123.53 ng/ml	20,000-fold higher than the curcumin control	Male Sprague-Dawley rats	(Parikh et al., 2018)
Solid dispersion of curcumin, D-α-tocopheryl polyethylene glycol 1000 succinate (Vitamin E TPGs) and mannitol at a ratio of 1:10:15, prepared by solvent evaporation method	30 mg/kg	240 ± 30.2 ng·h/ml	233 ± 62.4 ng/ml	Over 40,000-fold higher than curcumin control at pH ranged from 1.2 to 7.2	Sprague Dawley rats	(Song et al., 2016)
Curcumin-Solutol ® HS15 (1:10)	50 mg/kg	72.84 ± 36.4	95.60 ± 53.8	Approximately 2.5-fold higher curcumin	Male Sprague–Dawley	(Seo et al., 2012)

solid dispersion prepared by solvent evaporation		ng h/ml	ng/ml	solubility in pH 1.2, 6.8 and 7.4 buffer respectively	rats	
Curcumin and Eudragit® EPO solid dispersion prepared by co-precipitation	150 mg/kg	81.9 ± 11.47 µg h/ml	4.7 ± 2.17 µg/ml	20,000-fold higher than the curcumin control	BALB/C mice	(Kumar et al., 2016)

Table 2.3. A summary of the curcumin solid dispersion formulations reviewed in initial screening study

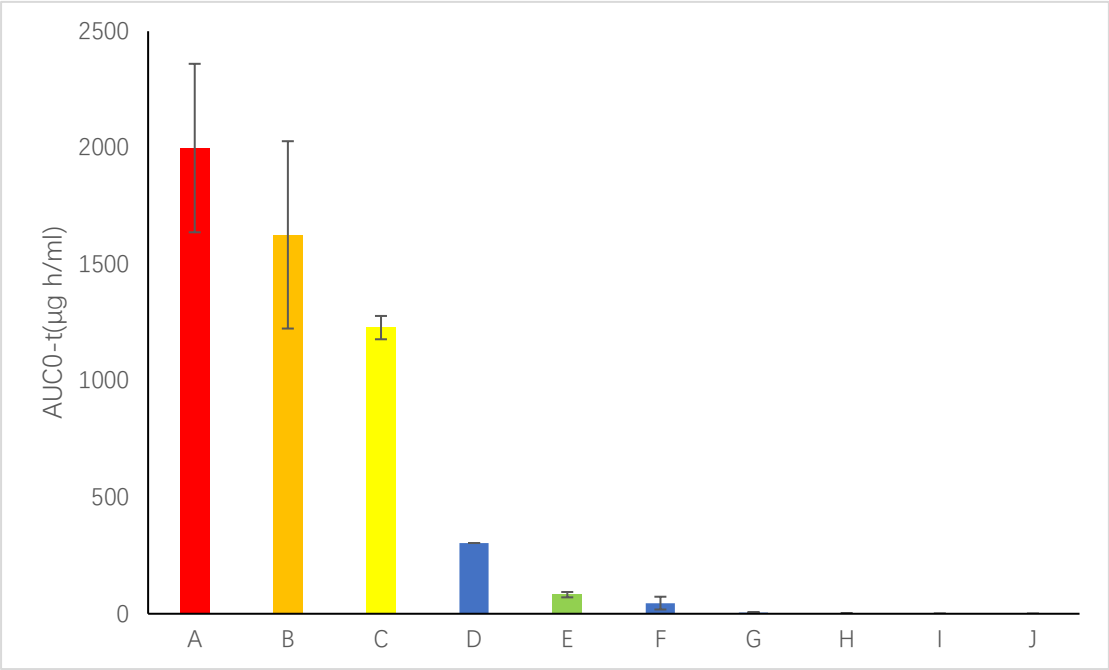

Figure 2.9. Comparison of in vivo curcumin oral bioavailability results of the different curcumin solid dispersion formulations, at the curcumin oral doses of: (A) 47 mg/kg for curcumin-soluplus (1:3) self-nanomicellising solid dispersion prepared by solvent evaporation (Parikh et al., 2018) (B) 20 mg/kg for curcumin-HPMCAS(1:4) solid dispersion prepared by freeze drying (Onoue et al., 2010) (C) 20 mg /rat for Hot melt extrusion solid dispersion consists of curcumin (10%), HPMC (75%), lecithin (10%) and isomalt (5%) (Chuah et al., 2014) (D) 20 mg/kg for curcumin-PVP k 30-α-glucosyl stevia (1:5:10) solid dispersion prepared by freeze drying (Kadota et al., 2016) (E) 150 mg/kg for Curcumin and Eudragit® EPO solid dispersion prepared by co-precipitation (Kumar et al., 2016) (F) 40 mg/kg for curcumin-PVP(1:3) solid dispersion prepared by solvent evaporation (Gao et al., 2019) (G) 2g/kg for curcumin: PEG 4000:PVP K30 solid dispersions (1:7:3) prepared by solvent evaporation (Kumavat et al., 2014) (H) 50 mg/kg for curcumin-cellulose acetate-manitol (1:10:10) sustained release solid dispersion prepared by solvent evaporation (Wan et al., 2012) (I) 30 mg/kg for solid dispersion of curcumin, D-α-tocopheryl polyethylene glycol 1000 succinate (Vitamin E TPGs) and mannitol at a ratio of 1:10:15, prepared by solvent evaporation (Song et al., 2016).(J) 50 mg/kg for curcumin-Solutol ® HS15 (1:10) solid dispersion prepared by solvent evaporation (Seo et al., 2012)

In *in vivo* pharmacokinetics studies, bioavailability usually refers to the fraction of a drug that is absorbed into the system and therefore available for biological effect. This is usually measured by quantifying the "area under the curve (AUC_{0-t}), which indicates the concentration of the drug in plasma across an interval of definite time (Hung et al., 2018). As shown in Figure 2.8, based on the value of AUC_{0-t}, the curcumin solid dispersion formulations were ranked as follows: Parikh et al's formulation > Onoue et al 's formulation > Chuah et al.'s formulation > Kadota et al. 's formulation > Kumar et al. 's formulation > Gao et al's formulation > Kumavat et al's formulation > Wan et al's formulation > Song et al's formulation > Seo et al's formulation.

By comparing the curcumin solid dispersion formulations, it was found that Soluplus and HPMCAS are the polymeric carriers that demonstrated the strongest effect in enhancing the oral bioavailability of curcumin. As a result, they were selected as the candidate carriers to be assessed in the secondary screening study. As for the surfactant candidate, Vitamin E TPGs or tocophersolan (D-α-Tocopheryl polyethylene glycol 1000 succinate) was selected. The reason for choosing it is because it has demonstrated considerable effect in improving the solubility of curcumin. Also, it was the only excipient used as a surfactant among the ten studies reviewed.

2.4.2. Appearance and texture of the solid dispersion samples

In this study, solvent evaporation was combined with freeze drying method. The reason for combining the two techniques together is that samples stayed attached to the inner walls of the glass round-bottom flask after solvent evaporation and they were very difficult to collect. It was found that a subsequent freeze-drying step allowed the samples to be collected without adhering to the inner walls of the container and so was easy to collect. With the exception of the curcumin: Vitamin E TPGs samples, all solid dispersion

samples prepared by solvent evaporation + freeze-drying method were in a powder form with a bright yellow colour. An example is shown in Figure 2.10b. For the curcumin-Vitamin E TPGs samples prepared by solvent evaporation freeze drying, they all expressed a waxy-like appearance with a sticky texture as shown in Figure 2.10a. Such texture presented a problem in handling.

Curcumin solid dispersion samples were also prepared by HME method. For the HME solid dispersion samples without Vitamin E TPGs also existed in powdered form, but the colours were dark orange. An example is shown in Figure 2.11a. Unfortunately, the combination of curcumin with Vitamin E TPGs was not able to form a proper solid form product using the HME method. After adding the blend consisting of curcumin and melted Vitamin E TPGs into the HME machine, it resulted in a thick, sticky gel with a deep-red colour as shown in Figure 2.11b. The texture of the products makes them difficult to handle. In addition, the yield was extremely low, with an average of only 0.38 mg of HME curcumin: Vitamin E TPGs product produced from 11 g of the blend mixture. Due to the extremely poor yield, not enough HME curcumin-Vitamin E TPGs samples can be produced for the solubility test in the secondary screening study.

(a) **(b)**

Figure 2.10. Appearance and texture of (a) Curcumin + Vitamin E TPGs 1:10 sample prepared by solvent evaporation + freeze drying (b) Curcumin + Soluplus + Vitamin E TPGs 1:10:10 sample prepared by solvent evaporation + freeze drying

(a) **(b)**

Figure 2.11. Appearance and texture of (a) Curcumin + Soluplus+Vitamin E TPGs 1:10:10 sample prepared by HME (b) Curcumin + Vitamin E TPGs 1:10 sample prepared by solvent HME

2.4.3. Determination of the wavelength of maximum absorbance (λmax) of curcumin

As shown in Figure 2.12, the UV spectrophotometry test result of the commercial curcumin powder showed a characteristic peak at the wavelength of 424.3 nm. This UV wavelength value, 424.3 nm, was used for evaluating the commercial curcumin content of the samples.

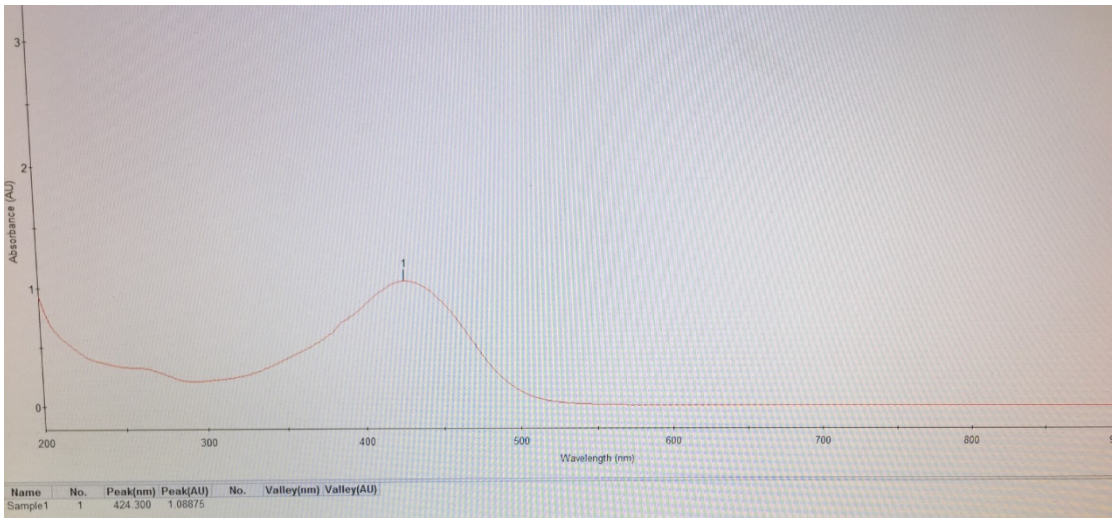

Figure 2.12. UV spectrum of commercial curcumin (no interference in spectrum)

2.4.4. Secondary screening study (Solubility study)

A summary of solubility test results of binary and ternary solid dispersion samples prepared by solvent evaporation + freeze drying and HME methods is shown in Table 2.4. A binary solid dispersion consists of one API and one excipients (carrier or surfactant) while a ternary solid dispersion consists of one API and two excipients (carrier and surfactant). According to ANOVA and the Post hoc test (Tukey test), all solid dispersion samples have shown significantly higher solubilities for curcumin at pH1.2 and pH6.8 relative to the curcumin only control ($p \leq 0.05$).

		Ratio		Curcumin concentration (μg/ml）	
Sample	**Curcumin**	**Soluplus or HPMCAS**	**Vitamin E TPGs**	**pH1.2**	**pH6.8**
Commercial curcumin (control)	1	*	*	0.032 ± 0.004	0.075 ± 0.005
Curcumin+HPMCAS (M), SF	1	3	*	0.105 ± 0.003*	0.161 ± 0.015*
	1	5	*	0.188 ± 0.014*	0.653 ± 0.093*
	1	10	*	0.208 ± 0.034*	0.949 ± 0.161*
Curcumin+HPMCAS (L),SF	1	3	*	0.101±0.032*	0.128 ± 0.018*
	1	5	*	0.148±0.028*	0.407 ± 0.018
	1	10	*	0.160±0.013*	0.789 ± 0.103*
Curcumin+HPMCAS (H),SF	1	3	*	0.106 ± 0.018*	0.141 ± 0.125*
	1	5	*	0.161 ± 0.025*	0.546 ± 0.133*
	1	10	*	0.185 ± 0.026*	0.907 ± 0.101*
Curcumin+Soluplus, SF	1	3	*	0.373 ± 0.049*	0.818 ± 0.088*
	1	5	*	0.668 ± 0.048*	1.589 ± 0.109*
	1	10	*	0.884 ± 0.068*	3.761 ± 0.867*
Curcumin+Vitamin E TPGs, SF	1	*	3	0.292 ± 0.047*	1.395 ± 0.153*
		*	5	1.443 ± 0.443*	6.454 ± 1.242*
		*	10	3.214 ± 1.040*,**	14.443 ± 4.443*,**
Curcumin+HPMCAS (M), HME	1	3	*	0.128 ± 0.021*	0.488 ± 0.004*
	1	5	*	0.111 ± 0.025*	0.512 ± 0.006*
	1	10	*	0.138 ± 0.016*	0.617 ± 0.113*
Curcumin+HPMCAS (L),HME	1	3	*	0.076±0.004*	0.145 ± 0.038*
	1	5	*	0.079±0.009*	0.398 ± 0.025*
	1	10	*	0.107±0.013*	0.413 ± 0.031*
Curcumin+HPMCAS (H),HME	1	3	*	0.093 ± 0.014*	0.388 ± 0.034*
	1	5	*	0.095 ± 0.014*	0.431 ± 0.046*
	1	10	*	0.106 ± 0.024*	0.467 ± 0.123*
Curcumin+Soluplus, HME	1	3	*	0.134 ± 0.013*	0.435 ± 0.038*
	1	5	*	0.215 ± 0.058*	0.845 ± 0.085*
	1	10	*	0.286 ± 0.081*	1.346 ± 0.321*
Curcumin+HPMCAS (M)+Vitamin E TPGs, SF	1	10	1	0.238 ± 0.065*	0.864± 0.065*
	1	10	5	2.405 ± 0.421*	6.405 ± 2.543*
	1	10	10	4.305 ± 1.436*	10.305 ± 4.266*
	1	10	1	0.188 ± 0.046*	0.676± 0.088*
	1	10	5	1.105 ± 0.075*	3.581 ± 0.710*

Curcumin+HPMCAS (L)+Vitamin E TPGs, SF	1	10	10	2.183 ± 0.562*	6.405 ± 2.321*
Curcumin+HPMCAS (H)+Vitamin E TPGs, SF	1	10	1	0.434 ± 0.102*	3.692± 0.231*
	1	10	5	2.066 ± 1.463*	7.724 ± 0.132*
	1	10	10	3.218± 1.327*	11.405 ± 2.321*
Curcumin+Soluplus+ Vitamin E TPGs,SF	1	10	1	1.146±0.642*	5.343 ± 1.464*
	1	10	5	8.381±2.353*	24.185 ± 6.941*
	1	10	10	18.631±2.421*,#	70.325 ± 10.255*,#
Curcumin+HPMCAS (M)+Vitamin E TPGs, HME	1	10	1	0.185±0.032*	0.632±0.211*
	1	10	5	1.532±0.464*	3.852±0.986*
	1	10	10	2.045±0.853*	7.245±2.583*
Curcumin+HPMCAS (L)+Vitamin E TPGs, HME	1	10	1	0.236±0.042*	0.845±0.183*
	1	10	5	1.462±0.873*	5.842±2.631*
	1	10	10	3.952±1.635*	8.752±2.331*
Curcumin+HPMCAS (H)+Vitamin E TPGs, HME	1	10	1	0.346±0.056*	1.853±0.745*
	1	10	5	1.754±0.673*	3.852±1.832*
	1	10	10	3.514±1.325*	7.623±2.593*
Curcumin+Soluplus+ Vitamin E TPGs,HME	1	10	1	0.656 ± 0.121*	3.573 ± 1.783*
	1	10	5	4.823±1.335*	16.358 ± 6.335*
	1	10	10	10.343 ± 4.464*	37.643 ± 9.911*

Table 2.4. A summary of solubility test results of binary and ternary solid dispersion samples (n=9, mean ± SD). * denotes statistically significant difference of solid dispersion samples and the curcumin control (p≤ 0.05).** denotes statistically significant difference of curcumin + Vitamin E TPGs, SF, (1:10) and other binary solid dispersion samples (p≤ 0.05). # denotes statistically significant difference of Curcumin+Soluplus+Vitamin E TPGs, SF, (1:10:10) and all other solid dispersion samples (p≤ 0.05)

SF=Solvent evaporation+ freeze drying method

HME=Hot melt extrusion method

2.4.4.1. Comparison of binary solid dispersion samples prepared by solvent evaporation + freeze drying method

All binary solid dispersion samples prepared by SF (solvent evaporation + freeze drying) method were compared with each other in terms of the solubility of curcumin at pH1.2 and pH6.8.

Within this group, the effect of the excipients to increase solubility at both the pH level was ranked from highest to lowest as follows: Vitamin E TPGs > Soluplus > HPMCAS (M) > HPMCAS (H) > HPMCAS (L). In addition, it was observed that the solubility of curcumin of the SF solid dispersion samples increased in an excipient dose dependent manner. Among the all the binary samples prepared by SF method listed in Table 8, curcumin + Vitamin E TPGs, SF, (1:10) has the highest solubility of curcumin, with 3.214 ± 1.040 μg/ml and 14.443 ± 4.443 μg/ml at pH1.2 and 6.8 respectively, which were 100-fold and 193-fold higher than commercial curcumin powder.

2.4.4.2. Comparison of binary solid dispersion samples prepared by hot melt extrusion method

All the binary solid dispersion samples prepared by HME method were compared for the solubility of curcumin at pH1.2 and pH6.8. Curcumin + Vitamin E TPGs solid dispersion sample prepared by HME were not included in the solubility study since there was not sufficient product produced due to the extremely low yield. This is similar to the samples prepared by SF method, the solubility of curcumin in the HME solid dispersion samples also increased along the increase in the drug-excipient ratio. As a result, the optimal ratio of curcumin to excipient was determined to be 1:10 (w/w) since this is the ratio that maximises the solubility of curcumin.

In this group, the ranking for the ability of the excipients to increase solubility

was shown from highest to lowest as follows: Soluplus > HPMCAS(M) > HPMCAS(H) > HPMCAS(L). Among the binary HME samples shown in Table 8, the one with the highest curcumin solubility was curcumin + Soluplus, HME, (1:10), with 0.286 ± 0.08 µg/ml and1.346 ± 0.321 µg/ml at pH1.2 and pH 6.8 respectively, which were 9-fold and 18-fold higher than commercial curcumin powder.

2.4.4.3. Comparison of binary solid dispersion samples with API:Excipient ratio of 1:10

All the binary solid dispersion samples with API: Excipient ratio of 1:10 were compared in terms of the solubility of curcumin at pH1.2 and pH6.8. By comparison, samples prepared by SF method all showed significantly higher solubility of commercial curcumin than those prepared by HME method, at both pH1.2 and pH6.8. Among all the binary solid dispersion samples, curcumin + Vitamin E TPGs, SF, (1:10) showed significantly higher solubility of curcumin than others, based on Post hoc Tukey test result ($p \leq 0.05$). However, its sticky and waxy texture makes it difficult to handle and it cannot be ground to a fine powder. The textural problem may be the reason why Vitamin E TPGs have never been used as the sole excipient for the preparation of solid dispersions of insoluble drugs. Despite its significant solubility enhancing effect, Vitamin E TPGs is not suitable for use as the sole excipient for the preparation of solid dispersions.

In section 2.4.4.4 and 2.4.4.5, curcumin + Soluplus+ Vitamin E TPGs and curcumin + HPMCAS (M, H or L) + Vitamin E TPGs solid dispersion samples were prepared and assessed by the solubility study to see if the combination of vitamin E TPGs with another polymer can produce a solid dispersion product without texture problems and with higher drug solubility than binary solid dispersion samples.

2.4.4.4. Comparison of ternary solid dispersion samples prepared by solvent evaporation + freeze drying method

The proportion of Vitamin E TPGs content in the ternary solid dispersion samples showed a positive relationship with the solubility of curcumin at both pH1.2 and pH 6.8. The drug: excipients ratio of 1:10:10 (w/w) is the ratio that maximises the curcumin solubility. Among all the ternary SF samples, curcumin + Soluplus + Vitamin E TPGs, SF, (1:10:10) showed the highest curcumin solubility of 18.631 ± 2.421 μg/ml and 70.325 ± 10.255 μg/ml at pH1.2 and pH6.8 respectively, which were 582-fold and 937-fold higher than that of commercial curcumin powder.

2.4.4.5. Comparison of ternary solid dispersion samples prepared by hot melt extrusion method

The same trend was found here, where solubility of commercial curcumin increased in a Vitamin E TPGs concentration dependent manner. Based on the results, the optimal drug: excipients ratio for ternary solid dispersions is 1:10:10 (w/w) since this ratio maximises the solubility of curcumin. Among all the ternary HME samples, curcumin + Soluplus + Vitamin E TPGs, HME (1:10:10) showed the highest solubility of 10.343 ± 4.464 μg/ml and 37.643 ± 9.911 μg/ml at pH1.2 and pH6.8 respectively, which were 323-fold and 502-fold higher than commercial curcumin powder.

2.4.4.6. Comparison of Curcumin+Soluplus(1:10), Curcumin+Vitamin E TPGs (1:10) and Curcumin+Soluplus+Vitamin E TPGS (1:10:10)

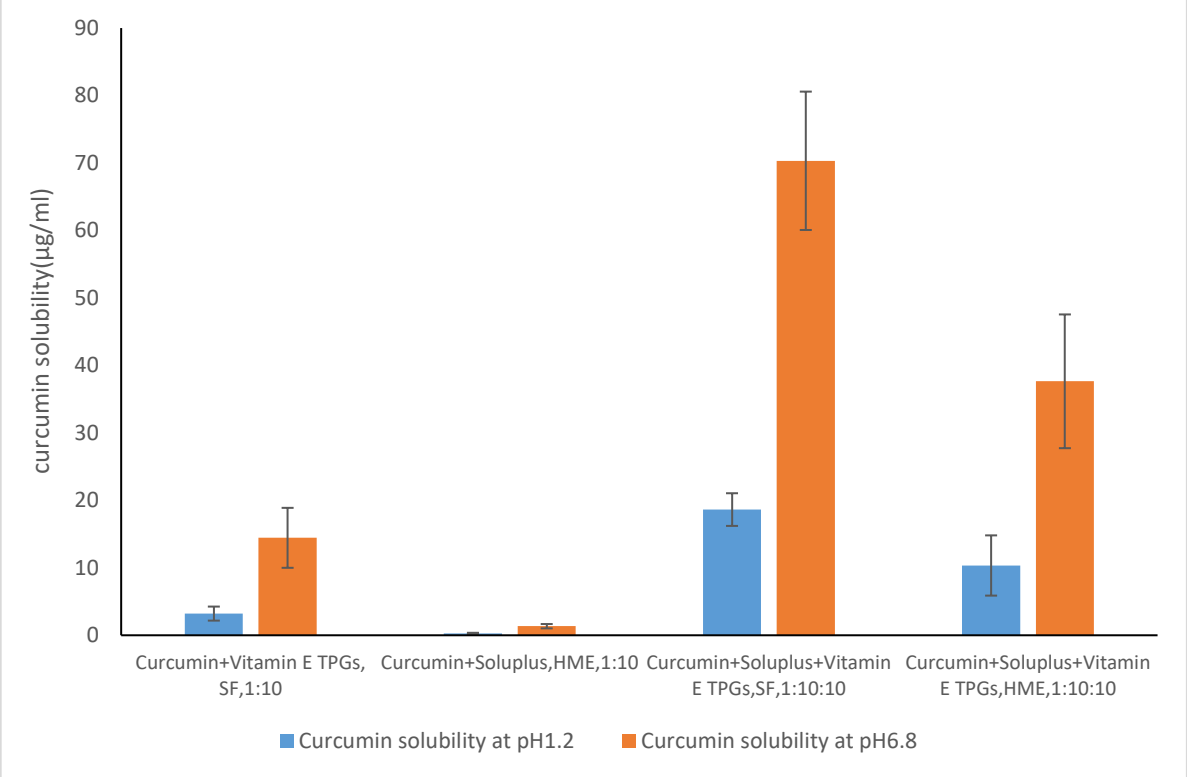

Figure 2.13. Comparison of binary and ternary solid dispersion samples prepared by SF (solvent evaporation + freeze drying) and HME (hot melt extrusion) methods (n=9, Mean ± SD)

The binary solid dispersion samples and the ternary solid dispersion samples with the highest solubility of curcumin were shown and compared in Figure 2.13, to find out which sample was the one with the highest solubility of curcumin among all the samples tested in the solubility study.

Curcumin + Soluplus + Vitamin E TPGs, SF, (1:10:10) was the sample with the highest solubility of curcumin at both pH1.2 and pH6.8, which were significantly higher than any other samples. As a result, it was named as “Solucumin”, implicating that it is a highly soluble curcumin product. The solubility of curcumin at pH 6.8 was significantly higher than at pH 1.2, based on Post Hoc Tukey test ($p \leq 0.05$). This suggests that Solucumin would be more suitable for absorption in the small intestinal fraction than stomach.

2.5. Discussion

2.5.1. Excipients selected from preliminary screening study

From the literature review conducted in preliminary screening study, Soluplus and HPMCAS (M, L and H grades) were selected as the candidate carriers while Vitamin E TPGs was chosen as the surfactant to be assessed in the secondary screening study.

The solid dispersion formulation developed by Parikh et al. have shown that Soluplus as the carrier, was able to lead to considerable increase in both aqueous solubility and oral bioavailability of curcumin, as a result of amorphisation of curcumin, drug-polymer hydrogen bonding interaction, and micellisation (Parikh et al., 2018). In addition to curcumin, Soluplus-based solid dispersions have also shown effect in improving the aqueous solubility and bioavailability of other poorly water-soluble drugs such as atorvastatin, alprazolam, carvedilol, efavirenz and valsartan (Ha et al., 2014; Lavra et al., 2017; Lee et al., 2015; Liu et al., 2015; Parikh et al., 2018; Shamma & Basha, 2013). Soluplus has low hygroscopicity, which means it is less likely to absorb moisture from the air and cause recrystallisation of the amorphous drugs. This property enables it to stabilise amorphous solid dispersions during storage (Alshahrani et al., 2015). Furthermore, it was reported that Soluplus has a strong inhibition effect of the precipitation and crystallisation of solid dispersions that can occur in supersaturation. This is due to its ability to form strong hydrogen bonding interactions with drugs (Liu et al., 2020; Rahman et al., 2020).

HPMCAS was originally developed as an aqueous enteric coating material (Tanno et al., 2004). but it has now been successfully used as a carrier to make solid dispersions of poorly water-soluble drugs such as itraconazole and paclitaxel (DiNunzio et al., 2010; Miao et al., 2019; Onoue et al., 2010; Qian et

al., 2012). The ability to formulate an amorphous solid dispersion and significantly improve the oral bioavailability of curcumin has been well demonstrated by Onoue et al. (Onoue et al., 2010). Like Soluplus, it is also an effective precipitation and recrystallisation inhibitor in amorphous solid dispersions of the poorly soluble drug (Pinto et al., 2018; Tanno et al., 2004). However, HPMCAS is hygroscopic which can hydrolyse into acetic acid and succinic acid over time during storage. This property of HPMCAS is likely to be detrimental to the stability of the solid dispersions made from it.

In Song et al.'s study for developing a solid dispersion of curcumin, mannitol was used as the hydrophilic carrier and Vitamin E TPGs was used as the surfactant. It was found that the solubility of curcumin increased dramatically by Vitamin E TPGs and it was associated with the formulation of micelles. On the other hand, mannitol did not show any effect on the increase of solubility of curcumin as the curcumin-mannitol-Vitamin E TPGs solid dispersion did not show higher solubility than the curcumin-Vitamin E TPGs solid (Song et al., 2016). Apart from curcumin, Vitamin E TPGs can also be used as a surfactant in the polymer-surfactant solid dispersions to improve the solubility and bioavailability of other poorly soluble drugs such as eprosartan and valsartan (Ahn et al., 2011; Lee et al., 2015; Song et al., 2016). In addition, it was reported that Vitamin E TPGs has an inhibitory effect of P-glycoprotein (P-gp) which can contribute to an increase in the oral absorption of drugs (Guo et al., 2013).

2.5.2. Secondary screening study (Solubility study)

By definition, drug solubility is the maximum concentration of a substance that can be completely dissolved in a given solvent at a certain temperature and pressure level (Coltescu et al., 2020). For orally administered drugs, they must be dissolved in the gastrointestinal tract before it can be absorbed and

circulated in the bloodstream.(Salehi et al., 2021). Solubility is a critical factor that determines the oral bioavailability of drugs. In fact, poor drug solubility is one of the most frequent causes for low oral bioavailability (Savjani et al., 2012). Due to the significance of drug solubility on the bioavailability of orally administered drugs, the solubility of the drug for the solid dispersion formulation samples was chosen as the criterion in the secondary screening study.

In this study, the curcumin solubility was determined by UV spectrophotometry. It was worth noting that UV spectrometry does not differentiate curcumin, demethoxycurcumin and bisdemethoxycurcumin in the commercial curcumin. Nevertheless, as curcumin makes up the majority of commercial curcumin (≥ 80%), the results measured by UV spectrometry were considered to reflect the solubility of curcumin.

All samples, including commercial curcumin powder, showed higher solubility in pH 6.8 than when in pH1.2, which is consistent with previous studies (Song et al., 2016). This suggests that orally administered curcumin is likely to be more soluble in the small intestine than stomach. Among all the samples tested in the secondary screening study, Curcumin + Soluplus + Vitamin E TPGs (1:10:10) prepared by solvent evaporation + freeze drying showed the highest solubility of curcumin in both pH1.2 and pH6.8. It is possible that the combination of Soluplus and Vitamin E VTPGs created a matrix that allows curcumin to disperse and exist in an amorphous state This capability was demonstrated in another formulation of Soluplus-Vitamin E TPGs solid dispersion of valsartan (Lee et al., 2015). Amorphous drugs generally possess higher dissolution rates than their crystalline counterparts due to the lack of uniformed molecular arrangement which provides them with higher molecular mobility and free energy (Vo et al., 2013). Vitamin E TPGs also has a lower CMC than Soluplus, which means that it can form micelles more readily in

aqueous media and this can help to solubilise poorly soluble drugs in the micellar core thus improving drug solubility (Rangel-Yagui et al., 2005). In addition, the combination of Soluplus and Vitamin E TPGs might increase the formulation of hydrogen bonding between the drug and carrier as there are more hydrogen bond forming functional groups involved in the solid dispersion system. This is because both Soluplus and Vitamin E TPGs contain functional groups that can form hydrogen bonds with the drug molecule. Soluplus contains hydroxyl and amide groups, while Vitamin E TPGs contains hydroxyl and carbonyl groups. The hydroxyl and carbonyl groups contain oxygen atoms with lone pair of electrons, that can form hydrogen bonding with hydrogen atoms in curcumin molecule. The nitrogen atom in amide group has a lone pair of electrons, which can form a hydrogen bond with the oxygen atoms in curcumin molecule. The hydrogen bonding interaction can help to hinder the drug recrystallisation/precipitation by increasing the miscibility between the drug and carrier This reduces the risk of a subsequent decrease in the solubility of the drug. (Taylor & Zografi, 1997). Finally, including surfactants to solid dispersion system helps to lower surface tension and improve drug wettability thus further increasing the dissolution of poorly water-soluble drugs (Saharan et al., 2009) The addition of surfactants also helps to improve drug-polymer miscibility because of their amphiphilic structure, thus reducing the tendency for drug recrystallisation (Vo et al., 2013).

HPMCAS (L, M and H grades) has shown a weaker solubility enhancement effect than Soluplus and Vitamin E TPGs. Among the three grades of HPMCAS, the M grade is the one with the best solubility improvement ability when forming solid dispersions for curcumin. It was reported that succinyl groups (hydrophilic region) of HPMCAS can facilitate aqueous solvation while the acetyl groups

(hydrophobic regions) can interact with the drug which prevent precipitation of the drug to occur (Sarabu et al., 2020). This could be the reason why M grade of HPMCAS has better solubility improvement ability than the other two grades, since it has a more balanced ratio of the hydrophilic succinyl groups and the hydrophobic acetyl groups. HPMCAS is practically insoluble in gastric fluid, but can swell and dissolve in the environment of small intestine. This explained the very poor curcumin solubility from HPMCAS solid dispersion samples at pH1.2 (Ashland, 2019).

As for the solid dispersion preparation methods, hot melt extrusion has the advantage of being easy to produce in scale and saving production time. But the solid dispersion samples prepared by solvent evaporation + freeze drying method have shown much higher drug solubilities than those prepared by HME. Since the screening criterion in the secondary screening study is the solubility of curcumin, the solvent evaporation + freeze drying method was chosen as the method for the preparation of the novel curcumin solid dispersion formulation.

It was worth noting that HME solid dispersions of curcumin and Vitamin E TPGs showed dark-red colour and remained in molten form at room temperature. This could be due to the formation of a eutectic mixture of curcumin and Vitamin E TPGs. The eutectic mixture can lower the melting point of curcumin because it disrupts the intermolecular forces between curcumin molecules and Vitamin E TPGS molecules. The new solid phase formed by the eutectic mixture should have a lower melting point than either of the two components alone (Liu et al., 2018). Vitamin E TPGs has melting point of ranged from 37 to 41 °C (Guo et al., 2013). It was reasonable for its eutectic mixture with curcumin to remain melted at room temperature. The formation of a eutectic mixture can also change the colour of API due to changes in its molecular structure (Figueirêdo et al., 2017). In the case of curcumin, its yellow

colour is due to the presence of double bonds conjugated with the carbonyl moiety (Adriani et al., 2020). Changes in structure by eutectic mixture might alter the length of the conjugated part of the molecule, in turn shifting the wavelengths of light that it absorbs, causing the colour change from yellow to red.

No cryoprotectant was added to the curcumin formulation in this study and the resulted freeze-dried product was a yellowish, brittle cake which needed to be crushed into powders by mortar and pestle. In order to get fluffy powder instead of a compact cake as the freeze-dried product, cryoprotectants could be added to the formulation. It was reported that the addition of cryoprotectants such as such as mannitol, lactose and trehalose provided protection from the stress during freezing and drying steps which resulted in fluffy dry powders at the end of the lypholisation (Patil et al., 2010). The optimisation of the curcumin formulation by adding cryoprotectants could be studied in the future.

Based on the screening results, curcumin + Soluplus + Vitamin E TPGs (1:10:10) prepared by solvent evaporation + freeze drying method, now known as Solucumin, was selected as the novel curcumin solid dispersion formulation for further studies. In this formulation, Soluplus was used as the primary carrier to make an amorphous solid product without textural issues, while Vitamin E VTPGs was used as a secondary carrier/surfactant to further enhance the solubility and oral bioavailability of curcumin.

2.6. Conclusion

Overall, through the preliminary and secondary screening studies, a solid dispersion formulation consisted of curcumin + Soluplus + Vitamin E TPGs (1:10:10) prepared by solvent evaporation + freeze-drying was selected as the novel curcumin solid dispersion formulation due to its significant improvement on the solubility of curcumin at pH1.2 and pH6.8. The formulation was named Solucumin, which implied its ability to improve the solubility of curcumin. It showed a higher solubility of curcumin at pH 6.8 than at pH 1.2, suggesting that the curcumin it contains might be more soluble in small intestinal fluids than in gastric fluids.

The increased solubility of curcumin in Solucumin was possibly caused by several factors, including the conversion of crystalline curcumin to amorphous form, the formation of micelles by Vitamin E TPGs and potential drug-excipient hydrogen bonding interactions. The novel curcumin solid dispersion formulation, now known as Solucumin, will be further studies in the following chapters to investigate its effect on curcumin dissolution, intestinal curcumin permeability, drug crystallinity, particle sizes and drug stability.

Chapter 3: *In vitro* dissolution study of Solucumin and the comparators

3.1. Introduction

In the previous chapter, excipients screening studies were carried out and a solid dispersion formulation of curcumin + Soluplus + Vitamin E TPGs (1:10:10) prepared by solvent evaporation+freeze drying method, named as 'Solucumin', was chosen as the novel curcumin solid dispersion formulation. In this chapter, an *in vitro* dissolution test was carried out to determine the dissolution profiles of curcumin, demethoxycurcumin and bisdemethoxycurcumin from Solucumin. Two marketed curcumin products (Longvida® and Nacumin®) and a polymeric-surfactant based curcumin solid formulation known as Mexcumin were used as the comparators in the dissolution test. Commercial curcumin was used as the control.

3.1.1. A brief introduction of demethoxycurcumin and bisdemethoxycurcumin

Obtaining curcumin in the pure form is very rare and expensive. As a result, commercially available curcumin powder is not 100% pure curcumin but a mixture of curcuminoids containing approximately 77% curcumin, 17% demethoxycurcumin and 3% bisdemethoxycurcumin (Esatbeyoglu et al., 2012). Demethoxycurcumin and bisdemethoxycurcumin are some of the curcuminoids present in turmeric. The molecular weight of demethoxycurcumin ($C_{20}H_{18}O_5$) and bis-demethoxycurcumin ($C_{19}H_{16}O_4$) is 338.359 g mol^{-1} and 308.333 g mol^{-1}, respectively. Like curcumin, they are practically insoluble in water and readily soluble in organic solvents like DMSO, ethanol and acetone (Kurien et al., 2017).

Curcumin is the major curcuminoid that occurs naturally in turmeric and has been shown to be responsible for its wide spectrum of health benefits such as anti-inflammatory (Srimal & Dhawan, 1973), anticancer, antimicrobial (Kim et

al., 2003), antirheumatic (Senft et al., 2010) and anti-tumour effects (Hatcher et al., 2008). However, some studies have shown that demethoxycurcumin and bisdemethoxycurcumin can be more effective than curcumin when used as anticholinesterases, antidiabetics (Kalaycıoğlu et al., 2017), anti-inflammatory, anti-proliferative agents (Sandur et al., 2007) and gastro protective agents (Orona-Ortiz et al., 2021).

The chemical structures of curcumin, demethoxycurcumin and bisdemethoxycurcumin (bis(4-hydroxycinnamoyl)methane) are illustrated in Figure 3.1. The three curcuminoids have similar chemical structures and the only difference is that curcumin has two methoxyphenol groups while demethoxycurcumin has one and bisdemethoxycurcumin has none. Studies have shown that the phenolic methoxy groups exert antioxidant effect and this is why curcumin has stronger antioxidant effect than demethoxycurcumin and bisdemethoxycurcumin (Ahsan et al., 1999; Youssef et al., 2004). However, bisdemethoxycurcumin was reported having higher resistance to degradation in an alkaline environment than curcumin and demethoxycurcumin and this was linked to the absence of the two methoxy groups. Owing to its strong degradation resistance in alkaline environments, bisdemethoxycurcumin is often added to foods to improve colour stability (Esatbeyoglu et al., 2012).

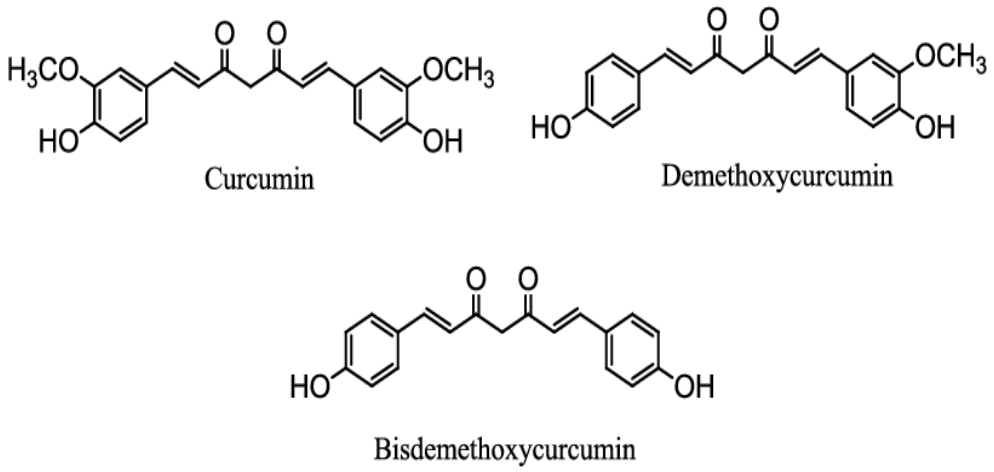

Figure 3.1. Chemical structures of curcumin, demethoxycurcumin and bisdemethoxycurcumin

3.1.2.A brief introduction of Longvida®, Nacumin® and Mexcumin

Two commercially available over-the-counter curcumin supplement products (Longvida® and Nacumin®) and a polymer-based curcumin formulation developed in a previous study (named as Mexcumin) were selected for comparison against Solucumin in terms of solubility and the *in vitro* release of curcumin.

Longvida® is a solid lipid curcumin particle (SLCP) based formulation developed by Verdure Sciences (Noblesville, USA) in collaboration with scientists from University of California (Los Angeles, USA) (Gupte et al., 2019; vs-corp, 2020). The curcumin percentage in Longvida® was reported to be 20% to 30% (Jamwal, 2018). Longvida® is currently marketed as 400 mg and 500 mg capsules and is promoted as a "highly stable and highly soluble product, optimised to deliver free curcumin". (vs-corp, 2020). The SLCP complex reduces the particle size of curcumin, making it easier to dissolve and pass through the intestinal cell membrane (Stohs et al., 2020). It also protects curcumin from rapid degradation and excretion thus improving the curcumin absorption and half-life (Jamwal, 2018) It was reported that Longvida® has over 100-fold higher oral bioavailability when compared to unformulated curcumin in human volunteers during a single-dose, crossover, double-blind, comparative pharmacokinetic study (Gota et al., 2010).

Nacumin® is a novel nano-curcumin formulation developed by TECHBIFARM, in collaboration with scientists from Vietnam and the UK. It is marketed as a product “containing super-soluble nano-size natural curcumin” and is sold as capsules, tablets and water-soluble powders in the market (Techbifarm, 2020). There is not much detailed information about Nacumin® since currently there is no published study or report regarding the curcumin content, solubility, dissolution, physical and chemical properties, bioavailability and efficacy of this product.

Mexcumin is a polymer-based solid formulation of curcumin, developed in

previous project by the research group. This formulation was designed to improve the drug dissolution and oral bioavailability of curcumin. It is in powdered form and it is prepared using polyethylene glycol 400 (PEG400) and Poloxamer 407 and a melting and mixing method. Its name “Mexcumin” implies that it is a curcumin formulation prepared by melt and mixing method. Since Mexcumin is a curcumin formulation consisting of a polymer and a surfactant, it was added as another comparator to compare with Solucumin in the *in vitro* dissolution test. PEG 400 and poloxamer 407 are commonly used materials in melting and mixing methods due to their relatively low melting points (Barmpalexis et al., 2011; Damian et al., 2000; Kolašinac et al., 2012). PEG 400 and Poloxamer 407 are GRAS (generally recognised as safe) excipients widely used in the pharmaceutical industry (FDA, 2022a; Giuliano et al., 2018). According to FDA inactive ingredient database, the maximum daily oral dose of PEG 400 and Poloxamer 407 were reported to be 2813 mg and 495 mg, respectively (FDA, 2022b). PEGs are widely used in pharmaceutical products as water soluble bases, solvents, and vehicles. They are miscible with aqueous fluids at all proportions and can be used as a solvent for dissolving a wide range of sparingly aqueous soluble compounds. These features make PEG an ideal delivery vehicle for poorly water-soluble compounds (Gullapalli & Mazzitelli, 2015). In addition, it was reported that the inclusion of surfactants could help to further improve the drug solubility in PEG containing formulations and reduce the risk of drug precipitation (Nandi et al., 2003; Tønsberg et al., 2010; Tønsberg et al., 2011). As an amphophilic non-ionic copolymer, poloxamer 407 is often used as a surfactant and combined with other polymers in formulations to enhance solubilisation and prolonged drug release of poorly water-soluble drugs such as nifedipine, etoricoxib, nimesulide, cilostazol and danazol (Chowdary & Prakasarao, 2011; Chutimaworapan et al., 2000; Dimitrova et al., 2000; Jin et al., 2021; Rogers et al., 2003). However, it was reported to be less effective when used alone (Dumortier et al., 2006).

3.1.3. Models of drug dissolution and *in vitro* dissolution test

When a solid drug is administered orally it needs to undergo dissolution in the stomach and/or small intestine before it can pass across the gastrointestinal

(GI) membrane and reaches the systemic circulation. If the rate of drug dissolution is slower than the drug permeability rate, it will become the rate limiting step for the drug absorption and oral bioavailability (Lee et al., 2008).

Dissolution is the process in which a substance enters a solvent and transfers from solid state to solution. The process is fundamentally controlled by the affinity between the solid material and the solvent. It consists of two successive steps:

1） Molecules of the solute liberated from the solid phase and move into the liquid layer near the solid surface (solid-liquid interface). In other words, this is an interfacial reaction between the solid surface and the solvent.

2） Then the solutes are transported from the solid-liquid interface into the bulk solution.

The dissolution process of drugs is a complex phenomenon that involves several factors. One of the most important factors is the rate of the drug dissolves in the solvent, which is governed by two fundamental theories: Noyes-Whitney equation and Fick's law of diffusion.

The Noyes-Whitney equation suggests that the dissolution rate of a solute is directly proportional to the solute's surface area and the concentration gradient, and inversely proportional to the thickness of the diffusion layer. The equation is expressed below:

$$dC/dt=(DA(Cs-C))/h$$

Equation 3.1

dC/dt = The rate of dissolution

D = The diffusion coefficient

A = The surface area of the solute

Cs = The saturation solubility of the solute

C = The concentration of the drug in the solvent

H = The thickness of the diffusion layer

Fick's law of diffusion describes the rate of diffusion of solutes move from an area of high concentration to an area of low concentration. In the context of drug dissolution, it explains how the drug molecules move from the solid state to the solution state by diffusion through the solvent. The law states that the rate of diffusion is directly proportional to the concentration gradient, the diffusion coefficient and the surface area, and inversely proportional to the thickness of the diffusion layer. The law is expressed below:

$$J = -D(dc/dx)$$

Equation 3.2

J = The rate of diffusion
D = The diffusion coefficient
c = The concentration of the solute
x = The distance travelled by the solute

The impact of diffusion on the dissolution process is critical, as it determines the rate of the drug molecules move from the solid-state to the solution phase. The process of dissolution involves the diffusion of the drug molecules through the diffusion layer and then into the bulk of the solvent. The rate of diffusion depends on the thickness of the diffusion layer, which is governed by the agitation of the solvent and the properties of the drug (Gao et al., 2021).

Dissolution models for solid substances are usually based on these two transport steps. There are three models to describe the process of dissolution: diffusion layer model, interfacial barrier model and the Danckwerts model (Lee et al., 2008).

The diffusion layer model proposed originally by Nernst and Brunner in 1904 to describe the dissolution of pure solid substances. In this model, it assumes the dissolution process consists of two steps:

1) *A thin stagnant film or diffusion layer surrounds the surface of a solute particle. The interfacial reaction between the solid surface and the solvent is assumed to be instantaneous. There is an equilibrium that exists at the interface so the solute concentration at the particle surface (Cs) is the saturated solubility of the solute*
2) *Once the solute molecules diffuse through the diffusion layer and reach the liquid film–solvent interface, rapid mixing will take place and lead to a uniform bulk concentration of solute (Ct). This step is slower, and it is the rate determining step for the drug dissolution.*

As shown in Fig. 3.2, dissolution rate is determined entirely by the thickness of the diffusion layer and the solute concentration gradient within the diffusion layer.

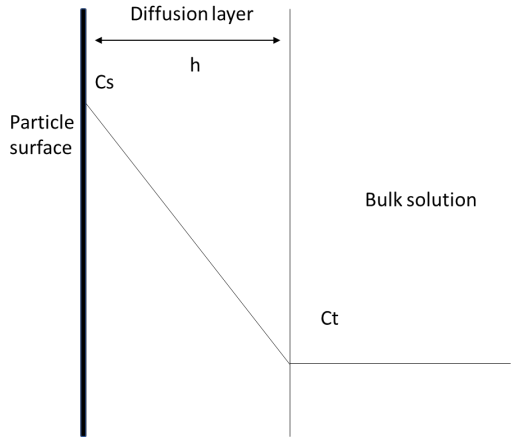

Figure 3.2. Schematic of diffusion layer model for solid drug dissolution

The interfacial barrier model was developed by Higuchi in 1961. Like the diffusion layer model, it assumes there is a diffusion layer surrounding the surface of a solute particle. However, the interfacial barrier model believed that there is no equilibrium at the solid-liquid interface and the liberation of solutes at the solid–liquid interface controls the overall rate of the solute transport process. The schematic of interfacial barrier model is shown in Figure 3.3.

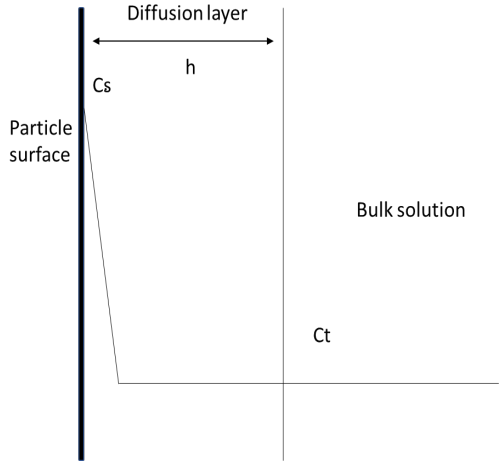

Figure 3.3. Schematic of interfacial barrier model for solid drug dissolution

Danckwerts model was developed by Danckwerts in 1951. Unlike the diffusion layer model and the interfacial barrier model, it does not include a diffusion layer surrounding a solute particle. Instead, it assumes that there are several macroscopic packets of solvent present in the agitated liquid. They reach the solid surface, absorb the solute by diffusion and transport it into the bulk of solution. These packets get continuously replaced by new ones and attach to new solid surface each time and dissolution rate is correlated to the rate of surface renewal. As a result, this model is also known as surface renewal model. This transport phenomenon is shown in Figure 3.4.

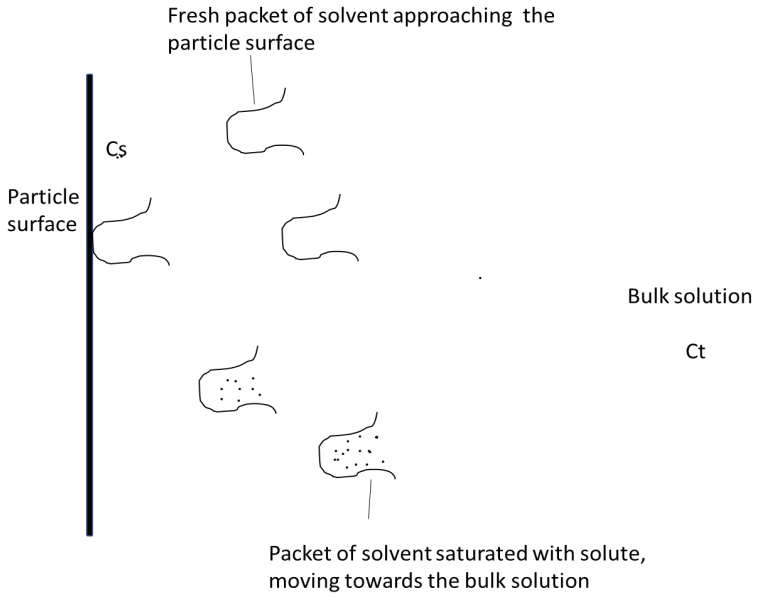

Figure 3.4. Schematic of Danckwerts model for solid drug dissolution

These three dissolution models can be used alone or in combination to describe the mechanism of dissolution of a solid substance. Among them, the diffusion layer model is the simplest and most commonly used model to describe the dissolution process of a pure substance (Lee et al., 2008). Sink condition, a situation when the volume of dissolution medium is at least three times the saturation volume. In other words, if the maximum concentration of the drug in the dissolution medium is less than 1/3 of the saturation solubility, it is in sink conditions. This is important in dissolution studies because it helps to prevent saturation of the dissolution medium and ensure the concentration gradient remains constant during the dissolution, which helps to maintain a steady state of drug dissolution (Liu et al., 2013). The impact of sink conditions on drug dissolution kinetics depends on the order of the kinetics. In zero-order kinetics, the rate of dissolution is constant and independent of the concentration gradient. As a result, sink conditions would have no impact on the rate of dissolution in this case. In contrast, first-order kinetics are concentration-dependent and the rate of dissolution is proportional to the concentration gradient (Paarakh et al., 2018). Therefore, sink conditions can help to maintain a constant concentration gradient and rate of dissolution in first order kinetics. *In vitro* dissolution test measures the rate of dissolution under controlled laboratory conditions. Dissolution rate of drugs can be used as a parameter to forecast the *in vivo* performance. When developing the method for an *in vitro* dissolution test, careful consideration must be taken in selecting the appropriate equipment, techniques, dissolution medium and the stirring speed. For solid dosage forms, the industry standard dissolution test methods are the United States Pharmacopoeia (USP) Apparatus 1 (basket) and the USP Apparatus 2 (paddle). Floating capsules and tablets are generally used with the USP Apparatus 1 basket while immediate release tablets, modified release tablets and extended-release tablets are typically tested using the USP Apparatus 2 paddle. When Apparatus 1 or 2 is not suitable for the dissolution test, other dissolution equipment includes USP 3 (reciprocating cylinder), USP 4 (flow-through-cell), USP 5 (paddle- over-tray), USP 6 (cylinder) and USP 7 (reciprocating disk) can be considered (USP, 2011, 2013). More details of the USP dissolution apparatus are listed in Table 3.1 below:

Name	**Type of apparatus**	**Dosage form that can be applied**	**Stirring speed**
USP Apparatus 1	Basket	Capsules, beads, delayed release / enteric coated formulations, floating formulations	50-120 rpm
USP Apparatus 2	Paddle	Tablets, capsules, beads, delayed release formulations, enteric coated formulations	25-50 rpm
USP Apparatus 3	Reciprocating cylinder	Tablets, beads, controlled release dosage forms	6-35 rpm
USP Apparatus 4	Flow through cell	Powders, implants, suppositories, controlled release formulations	N/A
USP Apparatus 5	Paddle over disk	Transdermal drug delivery system (TDDS) and ointments	25-50 rpm
USP Apparatus 6	Cylinder	Transdermal drug delivery system (TDDS)	N/A
USP Apparatus 7	Reciprocating disk	Extended-release formulations	30 rpm

Table 3.1. List of UPS dissolution apparatus for testing the dissolution rate of solid dosage forms. The temperature of the dissolution medium should be maintained at 37°C ± 0.5°C

If possible, *in vitro* dissolution test should be performed at the temperature of 37 ± 0.5°C using simulated gastric or intestinal fluids as the dissolution medium to mimic the physiological conditions in human gastrointestinal tract. Maintaining a sink condition is desirable but not mandatory (FDA, 1997; WHO, 2020). A dissolution medium of pH 6.8 should be used to simulate intestinal fluid (SIF) while a dissolution medium of pH 1.2 should be used to simulate gastric fluid (SGF). Enzymes are not normally added to SIF or SGF unless there is a valid reason to do so. When using water as the dissolution medium, some test conditions like pH level and surface tension may vary depending on the water source. As a result, water is not encouraged to be used as the dissolution medium for *in vitro* dissolution test (FDA, 1997). During an *in vitro* dissolution test, samples are collected from the apparatus at set time points. The samples are then filtered and analysed for drug concentration by HPLC to a UV-visible detector or by UV-visible spectrophotometry. When designing the method for a dissolution test, a decision must be made whether to replace the dissolution medium after sampling at each time point. According to USP guidelines, medium replacement is not recommended because the dose units may be disturbed during the replacement of the medium. However, if maintaining of sink condition is required but it is difficult to do so, replacement of medium may be necessary (USP, 2013). Dissolution results can be evaluated as either cumulative dissolution rate or fractional dissolution rate. Cumulative dissolution rate represents the sum of all drug dissolution occurring within a time interval while fractional dissolution rate represents the drug dissolution at a specific time point or during a portion of the total test time. Typically, the profile of drug dissolution will be expressed as mass or percentage of dissolved drug (up to 100%) vs time (USP, 2013).

3.2. Aims

- To prepare Solcumin and Mexcumin samples.
- To determine curcumin, demethoxycurcumin and bisdemethoxycurcumin concentration in commercial curcumin powder.
- To determine curcumin, demethoxycurcumin and bisdemethoxycurcumin concentration in Solcumin, Mexcumin, Longvida® and Nacumin ®.
- To conduct *in vitro* dissolution tests at pH1.2 and 6.8 to determine the dissolution profiles of curcumin, demethoxycurcumin and bisdemethoxycurcumin from Solcumin, Mexcumin, Longvida®, Nacumin® and commercial curcumin powder (the control).

3.3. Materials and method

3.3.1. Materials

Commercial curcumin powder was obtained from Techbifarm (Hanoi, Vietnam). Curcumin and demethoxycurcumin (purity ≥ 98%) were purchased from Sigma-Aldrich Ltd. (Gillingham, Dorset, UK). Bisdemethoxycurcumin (purity ≥ 98%) was purchased from TCI (Tokyo, Japan). Soluplus was provided by BASF SE (Ludwigshafen, Germany). Polyethylene glycol (PEG) 400, Poloxamer 407, Vitamin E TPGs, and Microcrystalline cellulose (MCC) were obtained from Sigma-Aldrich Ltd. (Gillingham, Dorset, UK). Magnesium stearate was purchased from Merck (Dorset, UK) and Aerosil from Evonik (Essen, Germany). Longvida® Optimised Curcumin 500 mg capsules were purchased from Igennus Healthcare Nutrition (Cambridge, UK). Nacumin® capsules with average weight 420 mg per capsule was a gift from Techbifarm (Hanoi, Vietnam).

HPLC grade acetone, ethanol, acetonitrile and orthophosphoric acid solution were acquired from Fisher Scientific Ltd. (Loughborough, UK).

3.3.2. Method

3.3.2.1. Preparation of Solcumin

Solucumin was prepared by the same method that covered in section 2.3.2.2.

3.3.2.2. Preparation of Mexcumin

Mexcumin was prepared in a two-step procedure involving melting and mixing. 2 g of commercial curcumin powder, 1 g PEG 400 (used as water miscible solvent) and 1.8g Poloxamer 407 (used as surfactant) were weighed into a beaker. The beaker was placed on top of a stainless-steel steam water bath and slowly melted by the heat produced with the steam. The mixture was continuously stirred until it resulted in the formation of a thick golden coloured mixture. The curcumin-PEG400-Poloxamer 407 mixture was then cooled to

room temperature followed by the addition of 11.2 g of microcrystalline cellulose (MCC), included to give the formulation a more solid-like texture, and mixed vigorously with a spatula. To this mixture, 0.2 g of magnesium stearate and 0.2 g of aerosil (colloidal silicon dioxide) were added to promote granule flow. The mixture was transferred into a mortar and mixed thoroughly using a pestle, which resulted in the formation of granules.

3.3.2.3. HPLC analysis method

Samples were analysed using a SphereClone™ C-18 reverse phase silica column (SphereClone™, 150 x 4.6 mm, 5 µm particle size) on an Algient 1100 HPLC system (Agilent Technologies, US) with a solvent cabinet, pump system, UV-visible detector and manual injection valve. 20 µl of each sample was injected manually onto the HPLC system using a manual syringe (Agilent, needle length 50 mm, volume 100 µl, Agilent Technologies, US). The mobile phase consisted of a 55:45 mixture of 0.1% v/v orthophosphoric acid and acetonitrile solutions, with an isocratic flow rate of 0.8 ml/min and a run time of 15 minutes for each sample. The separated curcuminoids were detected at 430 nm using a UV-visible detector.

3.3.2.4. Determining the curcuminoids content in commercial curcumin

To determine curcuminoid content, 5 mg of commercial curcumin powders were dissolved in 50 ml ethanol resulting in a 0.1 mg/ml stock solution. It was then diluted using a 50:50 mixture of 0.1% v/v orthophosphoric acid and acetonitrile to obtain a 0.05 mg/ml standard commercial curcumin solution. The standard solution was then analysed by HPLC to determine the content of curcumin, demethoxycurcumin and bisdemethoxycurcumin in the commercial curcumin powders (n=3). Standard solutions of curcumin, demethoxycurcumin and bisdemethoxycurcumin over a concentration range of 1 to 100 µg/ml were prepared in ethanol and analysed by HPLC. Calibration curves showed a linear relationship with a correlation coefficient of $R^2 > 0.995$ over the entire range for all three compounds. Examples of the calibration curves of the curcuminoids were shown in Figures 3.5,3.6 and 3.7.

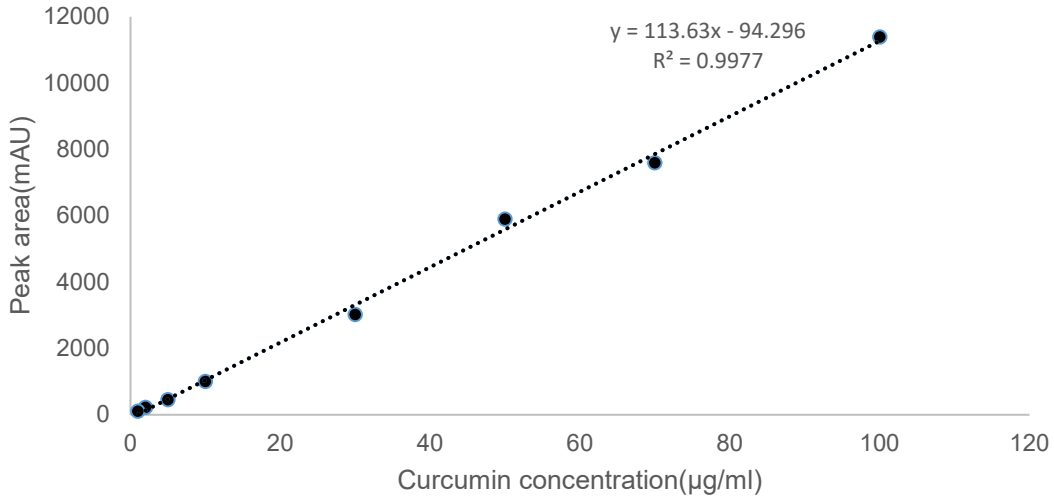

Figure 3.5. Calibration curve of curcumin used for the curcuminoids content determining test

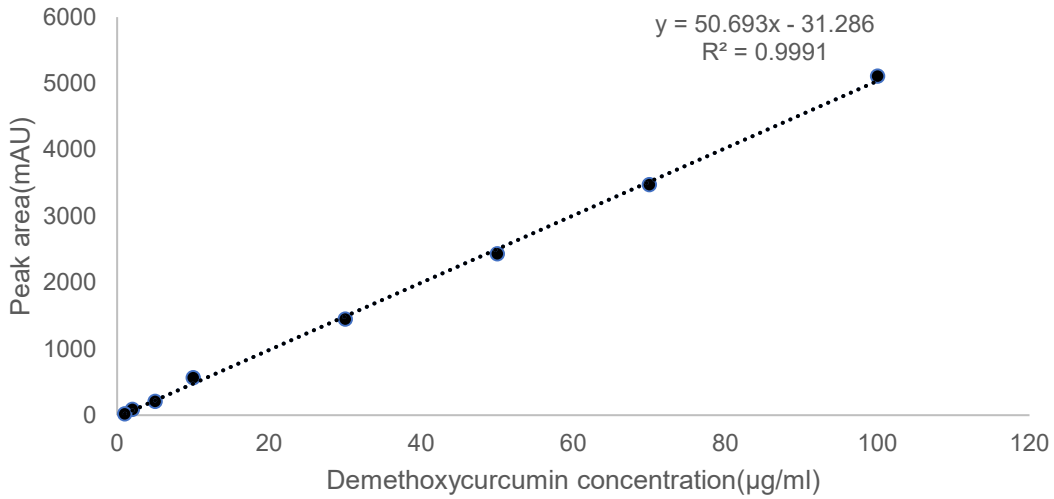

Figure 3.6. Calibration curve of demethoxycurcumin used for the curcuminoids content determining test

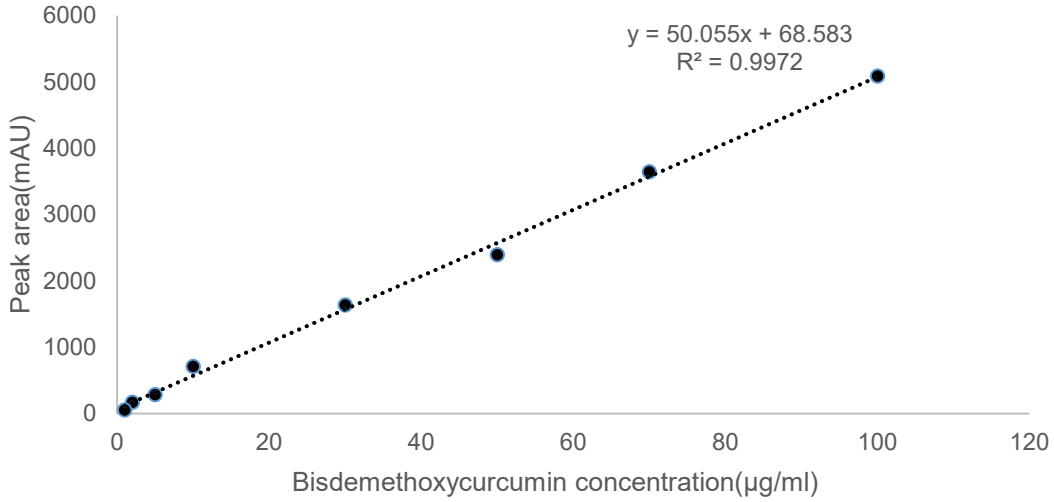

Figure 3.7. Calibration curve of bisdemethoxycurcumin used for the curcuminoids content determining test

3.3.2.5. Determining curcuminoid content in Solucumin, Mexcumin, Longvida® and Nacumin®

5 mg each of Solucumin and Mexcumin were weighed and placed into a 50 ml conical flask, separately. To obtain the powder from Longvida® and Nacumin® capsules, the capsules were opened, and 5 mg powders of each product were collected from the inside and transferred into a 50 ml conical flask separately. 50 ml of ethanol was added to each conical flask, resulting in 0.1 mg/ml stock solutions. The stock solutions were then diluted using 50:50 mixture of 0.1% v/v orthophosphoric acid and acetonitrile solutions to form 0.05 mg/ml standard solutions of Solucumin, Mexcumin, Longvida® and Nacumin®. The standard solutions were analysed by HPLC to determine the concentration of curcumin, demethoxycurcumin and bisdemethoxycurcumin contained in these preparations (n=3). The same curcuminoid calibration curves (Figure 3.5, 3.6 and 3.7) were used for determining curcuminoid content in commercial curcumin were used for Solcumin, Mexcumin , Longvida® and Nacumin®.

3.3.2.6. *In vitro* dissolution study

The dissolution profiles of Solucumin, Mexcumin , Longvida®, Nacumin® and commercial curcumin powder were determined by using the USP dissolution basket apparatus. Solucumin, Mexcumin and commercial curcumin powders alone were weighed to provide the equivalent to 40 mg of curcumin and were filled in size 0 gelatine capsules. Longvida® and Nacumin® capsules were used directly for the dissolution test. Each capsule was placed into a dissolution mesh basket. The baskets were attached to the basket shifts of the dissolution apparatus. During the dissolution test, the capsule-loaded baskets were immersed in 900 ml of 0.1M HCl dissolution medium (pH1.2, to mimic stomach pH) and phosphate buffer dissolution medium (pH6.8, to mimic small intestine pH), separately, at 37ºC and 100 rpm rotation. The same method mentioned in section 2.3.2.3 was used to prepare pH6.8 phosphate buffer dissolution medium. Sample solutions (2 ml) were collected using a 2 ml syringe at each time point (10, 30, 60, 120, 180, 240 and 360 minutes) and filtered through 0.45 µm PTFE syringe filters (Fisherbrand™, Non-sterile PTFE 0.45 µm Syringe Filter). The dissolution medium was not replaced during the test.

20 µl of each filtered sample solution was injected directly on to the HPLC to determine the concentrations of curcumin, demethoxycurcumin and bisdemethoxycurcumin (n=6). The results were expressed as the % drug release of the total content of the curcuminoid in the formulation.

Calibration curves were plotted for curcumin with the concentration range from 0.05 to 5 µg/ml. For demethoxycurcumin and bisdemethoxycurcumin, calibration curves were plotted with the concentration range from 0.05 to 1 µg/ml. All calibration curves showed a linear relationship with a correlation coefficient of $R^2 > 0.990$. The calibration curves of the curcuminoids are shown in Figure 3.8. 3.9 and 3.10.

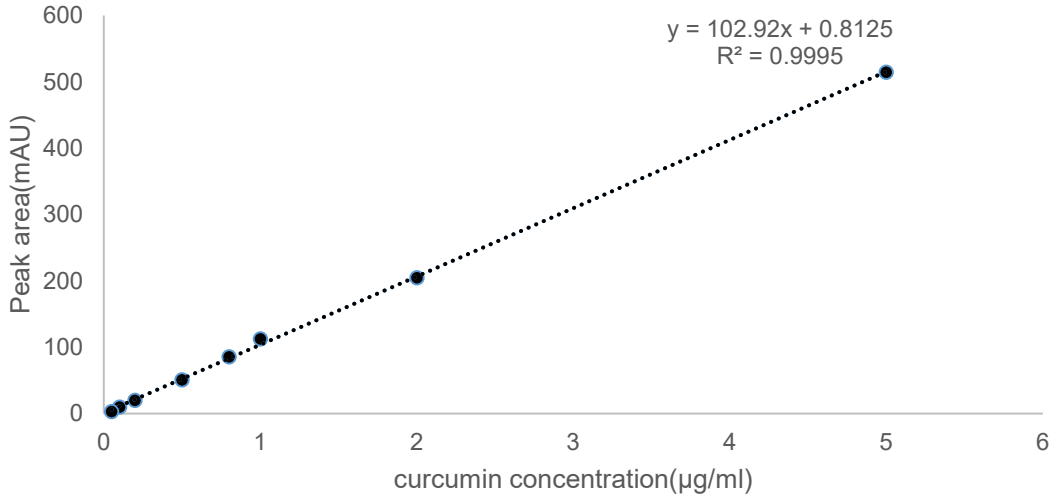

Figure 3.8. Calibration curve of curcumin used in the *in vitro* dissolution test

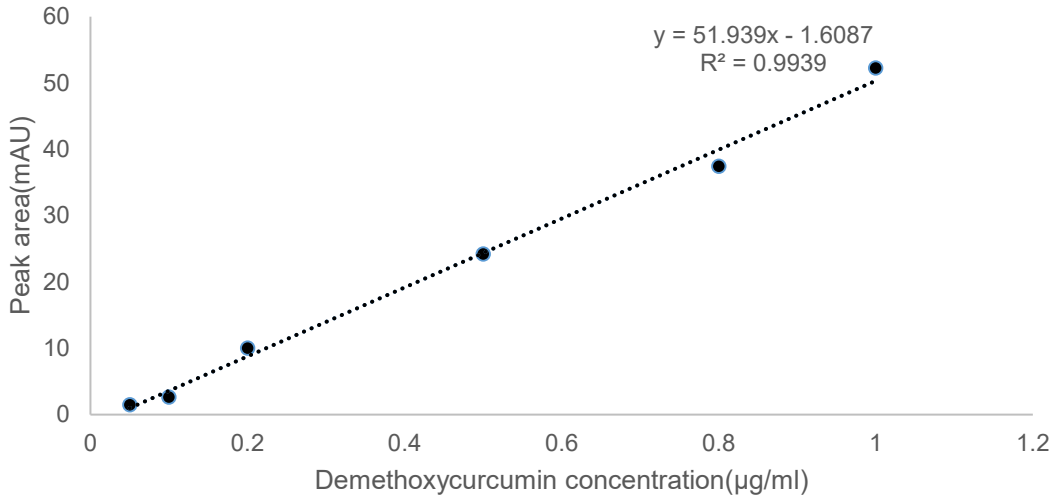

Figure 3.9. Calibration curve of demethoxycurcumin used in the *in vitro* dissolution test

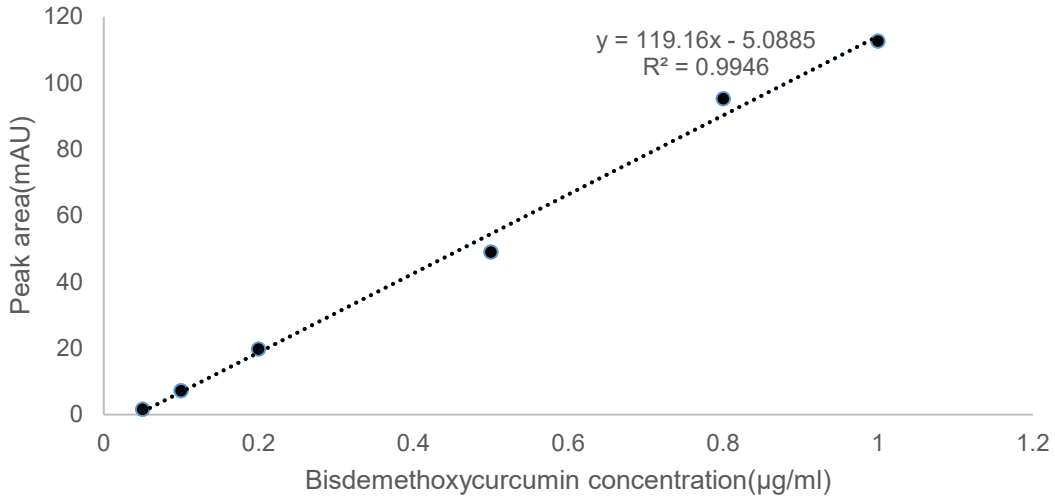

Figure 3.10. Calibration curve of bisdemthoxycurcumin used in the *in vitro* dissolution test

3.3.2.7. Statistical analysis

To compare the dissolution profiles of the test samples, one-way analysis of variance tests (ANOVA) was performed to compare the dissolution of the curcuminoids of each sample at each time point. Post hoc (Tukey) tests were carried out after the ANOVA analysis. Tukey's method was selected since it is the most common for comparing all possible group pairings (Day & Quinn, 1989). The observations would be considered as significantly different with p-value ≤ 0.05. ANOVA and Tukey test were performed using IBM SPSS Statistics software (Version 24.0; IBM Corp, Armonk, NY, USA).

3.4. Results

3.4.1. Determining curcuminoids content in commercial curcumin

In this study, commercial curcumin powder was used for the formulation preparation and dissolution studies. It contains three notable curcuminoids: curcumin, demethoxycurcumin and bisdemethoxycurcumin. Since it is not 100% pure curcumin, it is important to know the actual content of curcumin, as well as the other two curcuminoids, in the commercial curcumin powder before further studies.

The HPLC chromatogram of commercial curcumin powder is shown in Figure 3.11a. Three peaks were observed, which represented curcumin, demethoxycurcumin and bisdemethoxycurcumin. The retention times of the three peaks were compared with the retention time of the representative peaks of demethoxycurcumin (Figure 3.11c) and bisdemethoxycurcumin (Figure 3.11d). It was worth noting that the characteristic peaks for demethoxycurcumin and bisdemethoxycurcumin can still be observed in the HPLC chromatogram of curcumin (≥ 98% purity) (Figure 3.11b).

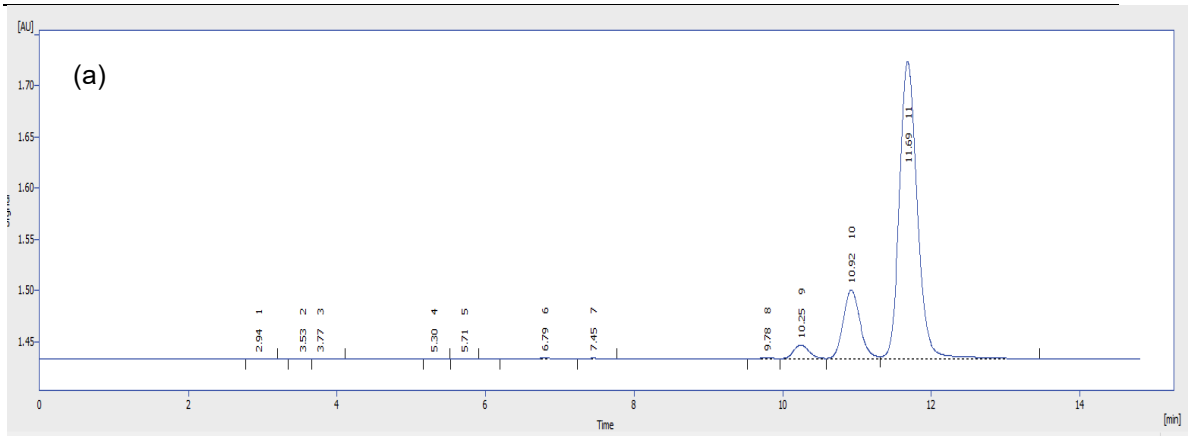
(a)
[AU]
1.70
1.65
1.60
1.55
1.50
1.45
2.94 1
3.53 2
3.77 3
5.30 4
5.71 5
6.79 6
7.45 7
9.78 8
10.25 9
10.92 10
11.69 11
0
2
4
6
8
10
12
14
Time
[min]

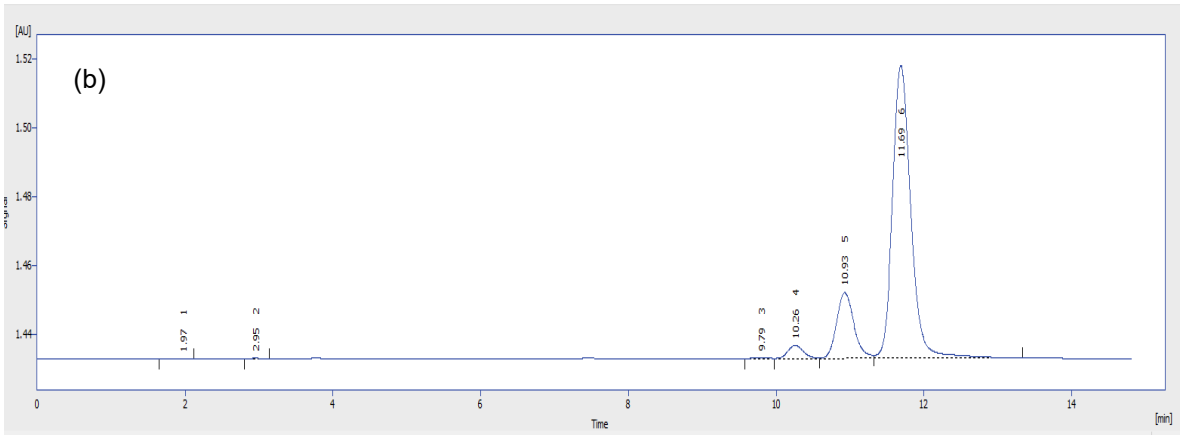
(b)
[AU]
1.52
1.50
1.48
1.46
1.44
1.97 1
2.95 2
9.79 3
10.26 4
10.93 5
11.69 6
0
2
4
6
8
10
12
14
Time
[min]

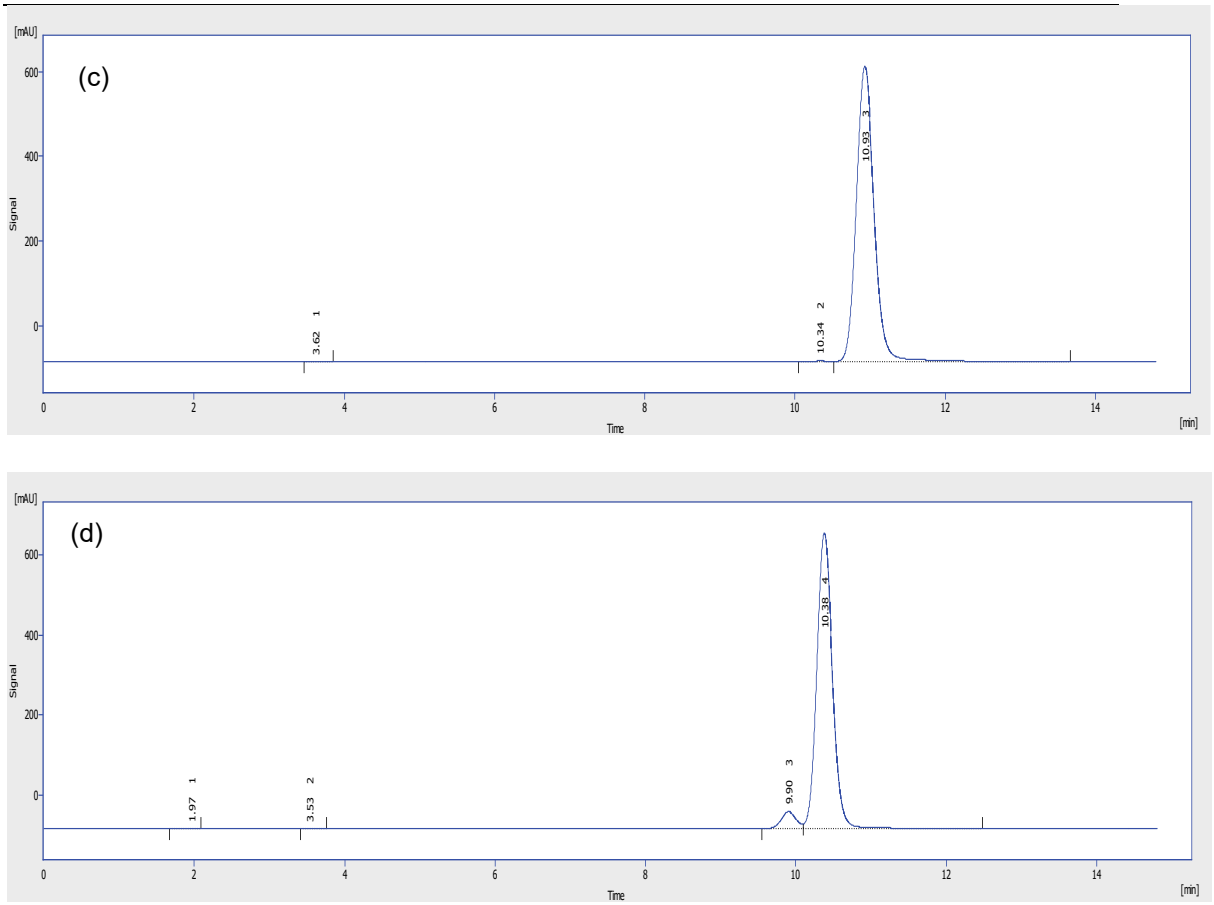

Figure 3.11. HPLC chromatogram of (a) commercial curcumin powder, which showed three peaks at 10.25, 10.92 and 11.69 minutes corresponding to bisdemethoxycurcumin, demethoxycurcumin and curcumin, respectively (b) curcumin(≥ 98% purity), which showed three peaks at 10.26, 10.93 and 11.69 minutes, corresponding to bisdemethoxycurcumin, demethoxycurcumin and curcumin, respectively (c) demethoxycurcumin(≥ 98% purity), which showed a peak at 10.93 minutes corresponding to demethoxycurcumin and (d) bisdemethoxycurcumin(≥98% purity) showed a peak 10.38 minutes corresponding bisdemethoxycurcumin. The identity of the small peak showed at 9.90 minutes was unknown, but it was likely caused by the impurity in the bisdemethoxycurcumin powder

As shown in Figure 3.11(a), the peaks with average retention time of 11.73 ± 0.04 minutes represented curcumin, 10.97 ± 0.03 minutes and 10.31 ± 0.34 minutes represented demethoxycurcumin and bisdemethoxycurcumin, respectively. With the peak area the average percentages of each curcuminoid in commercial curcumin powder can be calculated by Equation 3.3.

$$\%\ \text{Curcuminoid content} = \frac{\text{Peak area of curcuminoid}}{\text{Sum of peak areas of all curcuminoids}}\ \text{X}\ 100$$

Equation 3.3

The percentages of curcumin, demethoxycurcumin and bisdemethoxycurcumin in commercial curcumin powder and the formulations are shown at Table 3.2 in section 3.4.2.

3.4.2. Determining curcuminoids content in Solucumin, Mexcumin, Longvida® and Nacumin®

The actual curcuminoids content in Solucumin, Mexcumin, Longvida® and Nacumin® was measured before the *in vitro* dissolution study. Average weight (n=3) of ingredients per capsule was found to be 480 mg for Longvida® and 420 mg for Nacumin®. With the peak areas of each curcuminoid obtained from HPLC, the percentage of curcumin, demethoxycurcumin and bisdemethoxycurcumin contained in commercial curcumin powder, Solucumin, Mexcumin , Longvida® and Nacumin® was calculated. As shown in Table 3.2, of all the curcuminoids contained in the formulations and commercial curcumin powder, curcumin has the highest percentage, followed by demethoxycurcumin and finally bisdemethoxycurcumin. Longvida® has the highest curcuminoids content among all the formulation samples with 30.67 ± 1.33% of curcumin, 15.71 ± 0.53 % of demethoxycurcumin and 1.02 ± 0.04 % bisdemethoxycurcumin. It was followed by Mexcumin with 8.91 ± 0.85 % of curcumin, 2.98 ± 0.35 % of demethoxycurcumin and 0.31 ± 0.07 % of bisdemethoxycurcumin, Nacumin® with 7.15 ± 0.15 % of curcumin, 2.81 ± 0.18 % of demethoxycurcumin and 0.24 ± 0.01 % of bisdemethoxycurcumin and finally Solucumin with 6.74 ± 0.45 % of curcumin, 2.02 ± 0.05 % of demethoxycurcumin and 0.21±0.09 % of bisdemethoxycurcumin.

	Curcumin (%)	**Demethoxycurcumin (%)**	**Bisdemethoxycurcumin (%)**
Commercial curcumin	81.46±2.19	16.37±0.74	2.15±0.23
Longvida®	30.67±1.33	15.71±0.53	1.02±0.04
Nacumin®	7.15±0.15	2.81±0.18	0.24±0.01
Solucumin	6.74±0.45	2.02±0.05	0.21±0.09
Mexcumin	8.91±0.85	2.98±0.35	0.31±0.07

Table 3.2. Percentage of curcumin, demethoxycurcumin and bisdemethoxycurcumin in commercial curcumin, Solucumin, Mexcumin , Longvida® and Nacumin® (n=6, mean ± SD)

3.4.3. *In vitro* dissolution study

Curcuminoid release and dissolution profile from all the formulations at pH 6.8, with the exception of commercial curcumin powder, can be observed in Figure 3.13, 3.14 and 3.15. The amount of each formulation sample added for the dissolution study was shown in Table 3.3. Dissolution of curcumin, demethoxycurcumin or bisdemethoxycurcumin was not observed from any of the samples at any time point at pH 1.2. This observation showed that pH of the dissolution medium can affect the dissolution of the curcuminoids from the formulations.

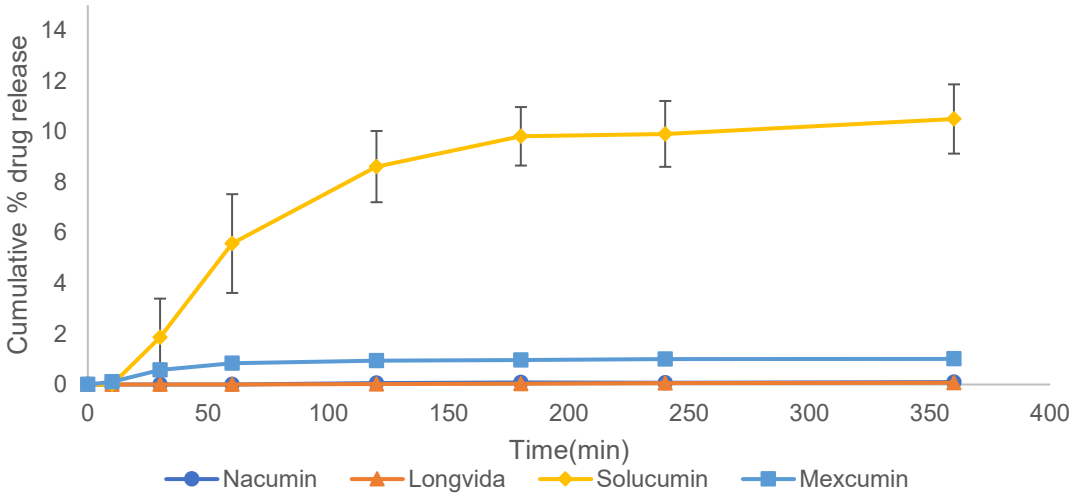

Figure 3.12. Dissolution profile of curcumin release in pH 6.8 from Nacumin® (●), Longvida® (▲), Solucumin (♦) and Mexcumin (■) (n=6, mean ± SD)

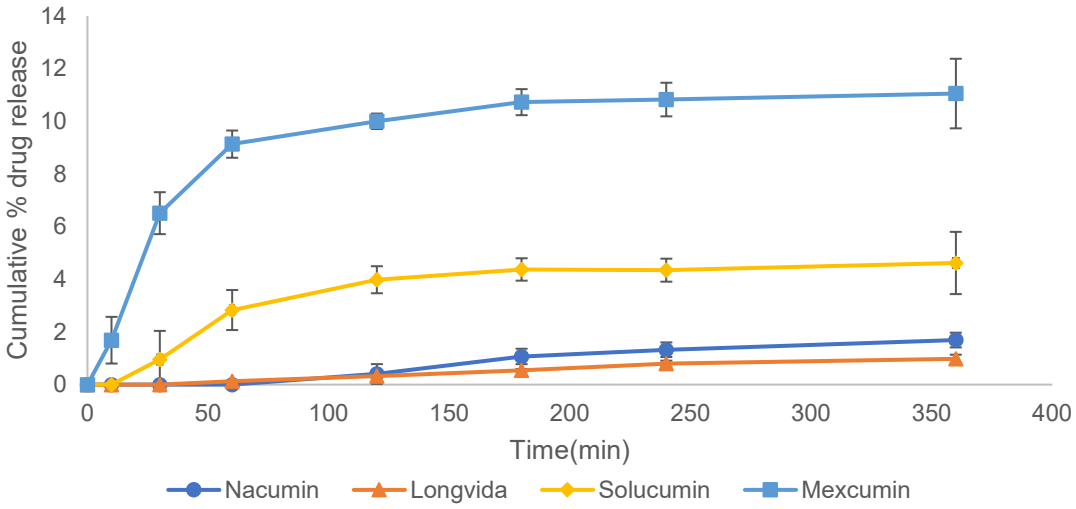

Figure 3.13. Dissolution profile of demethoxycurcumin release in pH6.8 from Nacumin® (●), Longvida® (▲), Solucumin (♦) and Mexcumin (■) (n=6, mean ± SD)

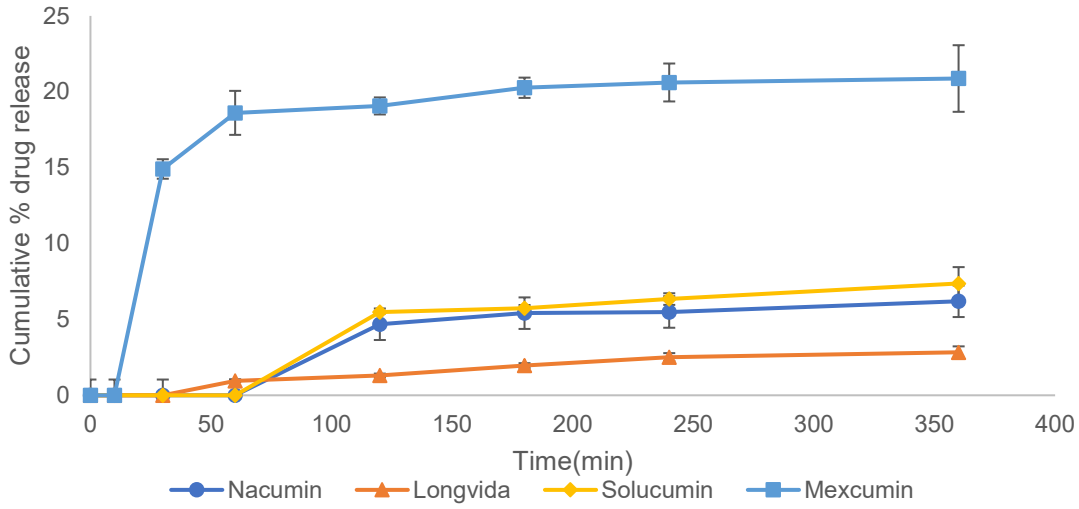

Figure 3.14. Dissolution profile of bisdemethoxycurcumin release in pH6.8 from Nacumin® (●), Longvida® (▲), Solucumin (♦) and Mexcumin (■) (n=6, mean ± SD)

	Actual amount of curcumin(mg)	Amount of the formulation(mg)
Solucumin	40	593.47
Mexcumin	40	448.93
Longvida®	40	130.42
Nacumin®	40	559.44

Table 3.3. The amount of curcumin contained in each formulation and the actual amount of each formulation added in the dissolution study

Among all the samples tested, Solucumin showed the highest percentage of dissolution of curcumin. As shown in Figure 3.12, no dissolution of curcumin was detected from Solucumin at 10 minutes. Then it showed significantly higher percentage of curcumin dissolution than other tested samples at every subsequent time point ($p \leq 0.05$). The dissolution of curcumin increased steadily from 0% to 9.81 ± 1.16% from time points 0 to 180 minutes. Then the dissolution rate slowed down, with 10.50 ± 1.37% curcumin dissolved at 360 minutes. As shown in Figure 3.13, no demethoxycurcumin dissolution was detected at 10 minutes from Solucumin. At 30 minutes, it showed 0.95 ± 0.18% of demethoxycurcumin dissolution, which was significantly higher than Longvida® and Nacumin® ($p \leq 0.05$). Subsequently, the percentage dissolution of demethoxycurcumin from Solucumin increased steadily and reached to 4.37 ± 0.43% at 180 minutes. The dissolution rate then slowed down and eventually 4.62 ± 1.18% of demethoxycurcumin was dissolved at 360 minutes. Solucumin showed significantly higher percentage of bisdemethoxycurcumin dissolution than Longvida® and Nacumin® from 30 to 360 minutes ($p \leq 0.05$). As shown in Figure 3.14, no bisdemethoxycurcumin dissolution was detected from Solucumin from 10 to 60 minutes. It reached to 5.47 ± 0.09% at time point 120 minutes and eventually increased to 7.37 ± 1.08% at 360 minutes. There were no significant differences between Solucumin and Nacumin® from 180 to 360 minutes ($p > 0.05$). Overall, in contrast to curcumin dissolution, dissolution of demethoxycurcumin and bisdemethoxycurcumin from Solucumin was much lower.

Mexcumin exhibited the highest release of demethoxycurcumin and bisdemethoxycurcumin among all the samples tested. In contrast, curcumin had much lower percentage dissolution from Mexcumin. As shown in Figure 3.12, Mexcumin showed 0.11 ± 0.07% of dissolution of curcumin at 10 minutes, which was significantly higher than all other tested samples ($p \leq 0.05$). It showed much lower dissolution of curcumin than Solucumin at the following time points and only 1.01 ± 0.08 % of curcumin was dissolved at the end of the *in vitro* dissolution test. No significant differences were found between Mexcumin, Longvida® and Nacumin® in terms of the percentage of curcumin dissolution at 240 minutes and 360 minutes ($p > 0.05$). In contrast to curcumin, demethoxycurcumin and bisdemethoxycurcumin were much more readily dissolved from Mexcumin. As shown in Figure 3.13 and 3.14, Mexcumin showed demethoxycurcumin dissolution of 1.69 ± 0.89% at 10 minutes while no bisdemethoxycurcumin dissolution was detected. At 30 minutes, bisdemethoxycurcumin dissolution from Mexcumin has increased to 14.91 ± 0.64%, which was significantly higher than other tested samples ($p \leq 0.05$). In the following time points, demethoxycurcumin and bisdemethoxycurcumin were rapidly released and eventually reached to 9.13 ± 0.52% and 18.61 ± 1.45% respectively at 60 minutes. Then the percentage of the curcuminoids dissolution slowed down and finally reached to 11.05 ± 1.32 % and 20.87 ± 2.19% respectively, at the end of 360 minutes. Mexcumin showed significantly higher percentage of demethoxycurcumin dissolution than all other tested samples at every time point throughout the *in vitro* dissolution test ($p \leq 0.05$). It also showed significantly higher percentage of bisdemethoxycurcumin dissolution than other tested samples from 30 to 360 minutes ($p \leq 0.05$).

For Longvida® and Nacumin®, curcumin dissolution was not detected from before 120 minutes. At 120 minutes, percentage curcumin dissolution from Longvida® and Nacumin® increased to 0.02 ± 0.00% and 0.06 ± 0.02%, respectively. They exerted very poor dissolution of curcumin in the following time points with only 0.07 ± 0.01% and 0.10 ± 0.02% of curcumin dissolved at the end of the *in vitro* dissolution test. No significant differences were found between Longvida® and Nacumin® in terms of the percentage of curcumin

dissolution from 120 to 360 minutes (p> 0.05). Likewise, demethoxycurcumin dissolution was not detected from Longvida® and Nacumin® from 10 to 30 minutes and 10 to 60 minutes, respectively. Demethoxycurcumin dissolution was detected from Longvida® at 60 minutes and Nacumin® at 120 minutes, with 0.13 ± 0.03% and 0.40 ± 0.37%, respectively. During the remaining time points, the dissolution of demethoxycurcumin and bisdemethoxycurcumin was slow, with only 0.98 ± 0.16% and 1.69 ± 0.82 % being dissolved at the end of the *in vitro* dissolution test. There were no significant differences between Longvida® and Nacumin® in terms the percentage of demethoxycurcumin dissolution from 120 to 360 minutes (p> 0.05). As for bisdemethoxycurcumin dissolution, it was neither detected from Longvida® from 10 to 30 minutes nor from Nacumin® from 10 to 60 minutes. Bisdemethoxycurcumin dissolution was detected from Longvida® at 60 minutes and Nacumin® at 120 minutes, with 0.95 ± 0.09 % and 4.68 ± 0.51%, respectively. After 120 minutes, the curve of the percentage of bisdemethoxycurcumin release became stable and eventually reached to 2.83 ± 0.39% from Longvida® and 6.20 ± 0.35% from Nacumin® at the end of the *in vitro* dissolution test. From 120 to 360 minutes, Longvida® showed significantly lower percentage of bisdemethoxycurcumin dissolution than all other samples (p> 0.05).

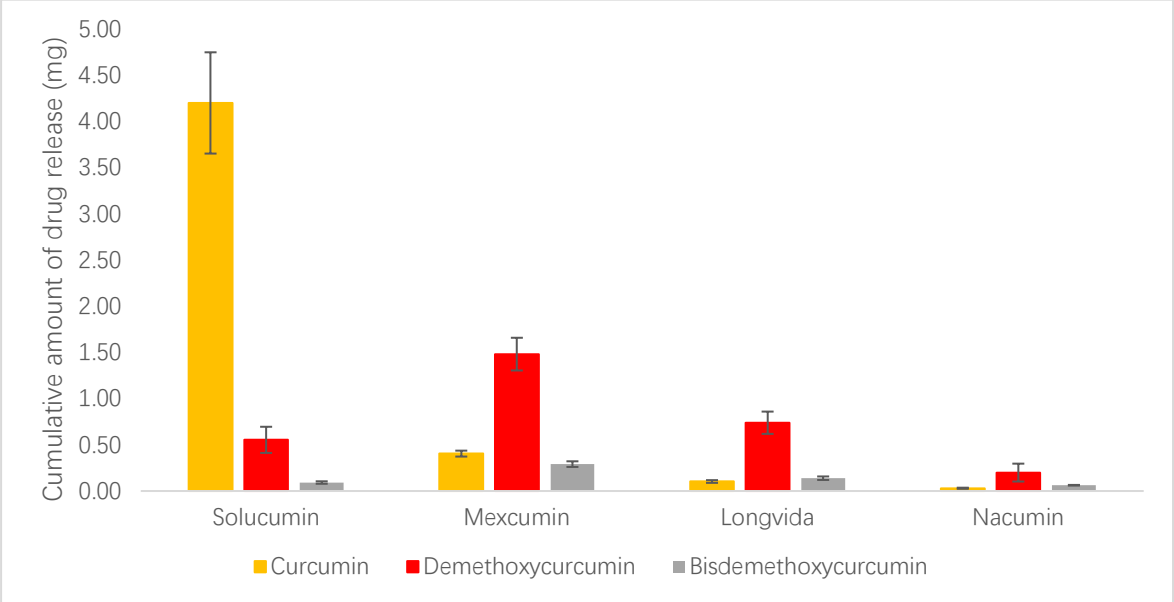

Figure 3.15. Cumulative amount of curcuminoids dissolved from each formulation at the end of the *in vitro* dissolution test (n=6, mean ± SD)

As shown in Table 3.2, the curcumin content was higher than the other two curcuminoids in each tested sample. This means that the measured percentage of demethoxycurcumin or bis-demethoxycurcumin dissolved from a tested sample might be higher than that of curcumin but does not necessarily mean they were dissolved in higher amounts than curcumin. As result, the amount of curcuminoids dissolved at the end of the *in vitro* dissolution was calculated for each sample.

As shown in Figure 3.15, Solucumin showed the significantly higher cumulative amount of dissolved curcumin (4.20 ± 0.55 mg) than all other samples ($p \leq 0.05$). In contrast, Mexcumin showed significantly higher cumulative amount of dissolved demethoxycurcumin (1.48 ± 0.18 mg) and bisdemethoxycurcumin (0.29 ± 0.03 mg) than all other samples ($p \leq 0.05$). The amount of dissolved bisdemethoxycurcumin from Mexcumin was significantly lower than curcumin (0.40±0.03 mg) ($p \leq 0.05$). This was expected as Mexcumin contained much higher amount of curcumin than bisdemethoxycurcumin, as shown in Table 3.2.

Despite having the highest curcumin content among all the tested samples, Longvida® showed significantly lower amount of dissolved curcumin than Solucumin and Mexcumin ($p \leq 0.05$). On the other hand, it exhibited significantly higher amount of dissolved demethoxycurcumin and bisdemethoxycurcumin than Solucumin ($p \leq 0.05$). As for Nacumin®, it exhibited the lowest dissolution amount of all the curcuminoids.

3.5. Discussion

3.5.1. *In vitro* dissolution study

In this study, the *in vitro* dissolution tests with dissolution media to mimic gastrointestinal fluids provided insight of how the curcumin formulations would dissolve when administered orally into the human body. No dissolution of curcumin, demethoxycurcumin and bisdemethoxycurcumin were detected from all the samples at pH 1.2 dissolution medium while all the samples (except commercial curcumin powder) have released the three curcuminoids when at pH 6.8 dissolution medium. These results suggest that the aqueous solubility of curcumin, demethoxycurcumin and bisdemethoxycurcumin is affected by pH level. A study conducted by Song et al. showed that the aqueous solubility of curcumin is pH dependent. Between pH 1.2 and 4.5, the solubility of curcumin was less than 0.01 μg/ml. As the pH exceeded 4.5, it began to increase rapidly, eventually reaching approximately 0.10 μg/ml between pH 6.8 and 7.4 (Song et al., 2016). The increase in curcumin aqueous solubility is associated with deprotonation of the phenolic groups of curcumin, which occurs when the pH reaches neutral-alkaline levels (Jagannathan et al., 2012; Treesinchai & Pitaksuteepong, 2020). The resulting anionic curcumin is more soluble in water than the neutral form (Priyadarsini, 2014). It is currently unknown whether the phenolic groups in demethoxycurcumin and bis-demethoxycurcumin are deprotonated at neutral or basic pH. However, it has been reported that demethoxycurcumin and bisdemethoxycurcumin have higher aqueous solubility at neutral pH than at acidic pH. An *in vitro* dissolution study on the curcuminoids by Ferreira et al. showed that the percentage of dissolved curcumin, demethoxycurcumin and bis-demethoxycurcumin in pH6.8 phosphate buffer was nearly two-fold than in pH1.2 HCL buffer, after 90 minutes dissolution (Ferreira et al., 2019).

Solucumin has showed highest percentage of cumulative curcumin dissolution and the second highest demethoxycurcumin and bisdemethoxycurcumin cumulative dissolution among all the tested samples. In addition, the percentage of dissolution of curcumin from Solucumin was higher

than other samples at every sampling time point. This shows that the combination of Soluplus and Vitamin E TPGs has not only increased the solubility of curcumin, but also the dissolution rate.

It was worth noting that sink condition was not maintained during the in vitro dissolution tests. As shown in Figures 3.12 and 3.13, the curves of curcumin and demethoxycurcumin dissolved from Solucumin have become stable at 180 minutes and there were no statistically significant differences among the drug dissolution at 180, 240 and 360 minutes ($p > 0.05$). In Figure 3.13, the curve of bisdemethoxycurcumin has become stable at 120 minutes and no statistically significant differences were found among the drug dissolution at 120, 180, 240 and 360 minutes ($p > 0.05$). It was possible that the dissolution of the curcuminoids from Solucumin have reached saturation during the dissolution tests which might explain the relatively low percentage dissolution of the curcuminoids measured. Nevertheless, the data from the dissolution tests was still valuable as it proved that Solucumin has significantly improved the drug dissolution of curcumin, demethoxycurcumin and bisdemethoxycurcumin.

Lee et al., developed an amorphous solid formulation prepared by Soluplus/Vitamin E TPGs and it has demonstrated considerable improvement on the solubility of poorly water soluble valsartan due to the conversion of crystalline valsartan into an amorphous form (Lee et al., 2015). The increase in the dissolution rate of curcumin observed from Solucumin was possibly due to the conversion of crystalline curcumin into an amorphous form in the solid dispersion system (Gui et al., 2021; Moneghini et al., 2010; Paul et al., 2019; Qian et al., 2021). Amorphous drugs generally possess higher dissolution than their crystalline counterparts due to the lack of long-order molecular arrangement which provides them higher molecular mobility and free energy (Yu, 2001). A decrease in drug solubility can usually occur in amorphous drugs dissolution due to recrystallisation/precipitation. However, such phenomenon did not occur since a decrease in the percentage of cumulative drug release was not observed during the dissolution test. This suggests that Soluplus was able to maintain the already increased solubility of curcumin over a period of

time. Polymers can interact with amorphous drug in solid dispersion systems. This can limit the mobility of drug molecules and prevent them from recombining into the long-order molecular arrangement of the crystal lattice, thus preventing a reduction in the solubility of the drug due to recrystallisation (Sahoo et al., 2020). An illustration of how polymer inhibit recrystallisation of amorphous drug was shown in Figure 3.16. Combining surfactants with polymers in the formulations might also have contributed to the drug release. Surfactants can lower surface tension, improve drug wettability and form micelles thus further increasing the dissolution of poorly water-soluble drugs (Heng et al., 1990; Schott et al., 1982).

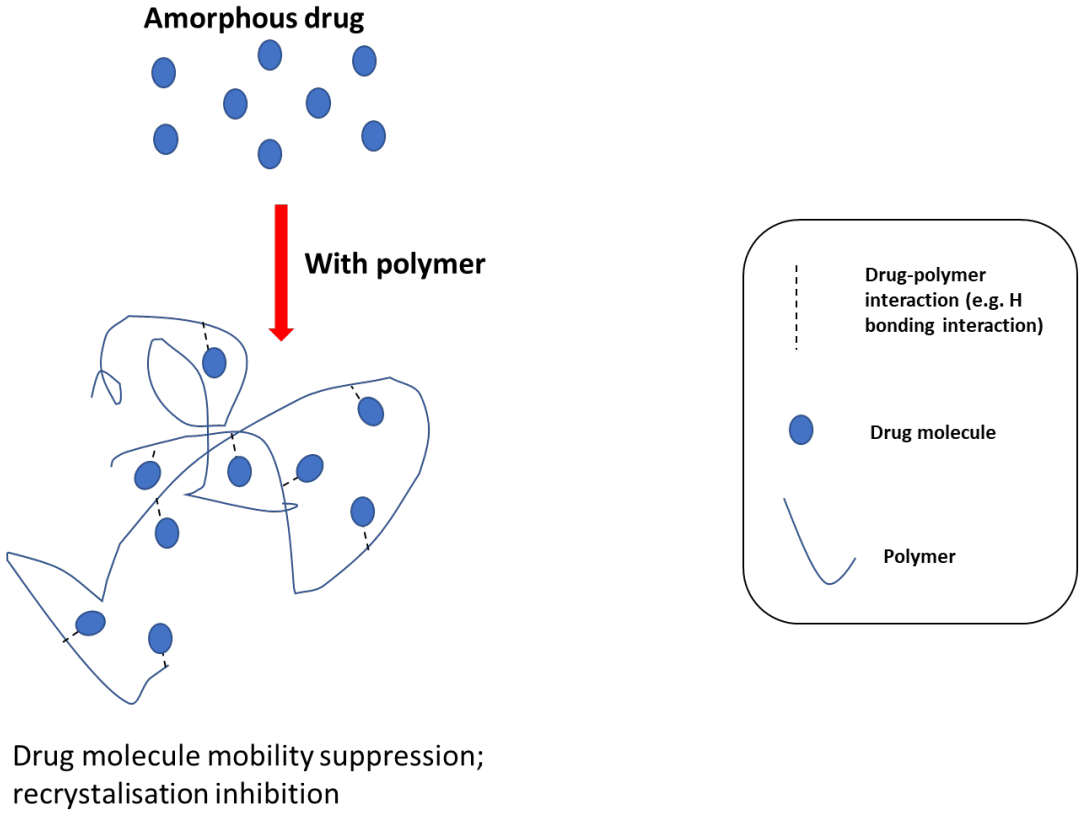

Figure 3.16. The illustration of how polymer inhibit recrystallisation of amorphous drug

Mexcumin was prepared by a melting and mixing method, which is a classic way to prepare amorphous solid dispersion (Chiou & Riegelman, 1971; Sekiguchi & Obi, 1961). However, it was unlikely that Mexcumin formed an amorphous solid dispersion system due to the long cooling time. Although the dissolution of curcumin from Mexcumin was relatively low, it has exhibited the highest cumulative dissolution of demethoxycurcumin and bisdemethoxycurcumin among all the tested samples. As shown in Figures 3.13 and 3.14, the dissolution of demethoxycurcumin and bisdemethoxycurcumin might have reached saturation since 180 minutes as there were no significant differences between the drug dissolution at 180, 240 and 360 minutes ($p>0.05$). Nevertheless, the data obtained from the dissolution tests was still valuable as it showed that Mexcumin has higher percentage of dissolution of demethoxycurcumin and bisdemethoxycurcumin than other samples at every sampling time points. This indicates that Mexcumin has much higher dissolution rate for these two curcuminoids when compared to other formulations. This interesting phenomenon might be related to the chemical structures of the curcuminoids and drug-polymer interactions. It was reported that curcumin is capable of forming hydrogen bonding with PEG400 (Sharma & Pathak, 2016). The methoxy groups in curcumin act as an acceptor of proton, which can form hydrogen bonding with hydroxyl groups (–OH) and hydrogen (–H) atoms contained in PEG400 molecules (Palusiak & Grabowski, 2002). A comparative study has reported that solid products with drug-polymer hydrogen bonding interaction exhibited poorer drug dissolution than those without (Saboo et al., 2020). Therefore, the lack of methoxy groups in demethoxycurcumin and bisdemethoxycurcumin might account for the higher drug dissolution than curcumin, as they are less likely to form hydrogen bonds with PEG400. Further studies could be carried out to investigate the reasons for the considerable increase in demethoxycurcumin and bisdemethoxycurcumin dissolution from Mexcumin.

The release of curcumin, demethoxycurcumin and bisdemethoxycurcumin varied between the tested samples, which can lead to different absorption of the curcuminoids and may result in different therapeutic effects for different

health conditions. A clinical trial on Longvida® has found that 800 mg of Longvida® per day was effective and safe in pain relief in patients suffering from knee osteoarthritis when administered for 90 days. Besides, the result was comparable to 400 mg ibuprofen per day for the same duration of 90 days (Gupte et al., 2019).This study has shown that demethoxycurcumin was the most abundant curcuminoid dissolved from Longvida®. These observations suggest that pain relief effect was most likely from demethoxycurcumin.

Curcuminoids exert their therapeutic effect on Alzheimers disease by acting as an inhibitor of acetylcholinesterase and butyrylcholinesterase, which lead to an increase in acetylcholine concentrations and restoring communication between nerve cells (Ahmed & Gilani, 2009; Kalaycıoğlu et al., 2017). A comparative study conducted by Kalaycıoğlu et al. has showed that the acetylcholinesterase inhibition activity of curcuminoids ranked from bisdemethoxycurcumin, followed by demethoxycurcumin, whereas curcumin showed very little effect on acetylcholine inhibition. As for the butyrylcholinesterase inhibition activity, bisdemethoxycurcumin showed inhibition effect against butyrylcholinesterase while curcumin and demethoxycurcumin exhibited no inhibitory activity (Kalaycıoğlu et al., 2017). As the formulation with the highest amount of dissolved bisdemethoxycurcumin, Mexcumin might have the potential to be used for treatment of Alzheimer's disease as it has been reported that increased bisdemethoxycurcumin solubility lead to improved effect in reducing neuroinflammation in patients with Alzheimer's disease (Gagliardi et al., 2022).

The antioxidant and anti-inflammatory activities of the curcuminoids were ranked from high to low as follows: curcumin > demethoxycurcumin > bis-demethoxycurcumin (Jayaprakasha et al., 2006; Kalaycıoğlu et al., 2017; Sandur et al., 2007). The phenolic methoxy groups in the curcuminoids are responsible for the antioxidant and anti-inflammatory effects. They are essential for the free radical scavenging activity of curcuminoids as antioxidants (Menon & Sudheer, 2007). For the anti-inflammatory activities, the phenolic methoxy groups are responsible for inhibiting TNF-α induced NF-κB activation, thereby

suppressing the production of inflammatory cytokines such as interleukin 1 (IL-1) and interleukin 6 (IL-6) (Liu et al., 2017; Sandur et al., 2007). Therefore, this could probably be the reason why curcumin (two phenol methoxy groups) has stronger antioxidant and anti-inflammation effects than demethoxycurcumin (one phenol methoxy group) and bisdemethoxycurcumin (no phenol methoxy group). As the formulation with the highest dissolution of curcumin, Solucumin might allow more curcumin to be absorbed and exhibit higher antioxidant activity and anti-inflammatory effect than other tested samples. It has the potential to be an anti-inflammatory agent for patients with pro-inflammatory diseases such as osteoarthritis, cancer or obesity (Hewlings & Kalman, 2017) and antioxidant agent for lower risk of chronic oxidative stress related diseases like cardiovascular diseases and Alzheimer disease (Menon & Sudheer, 2007).

Huang et al., have investigated the anti-proliferation effects of curcumin, demethoxycurcumin and bisdemethoxycurcumin on osteosarcoma (HOS and U2OS), breast (MDA-MB-231) and melanoma (A2058) cancer cells. It was found that bisdemethoxycurcumin exhibited much poorer anti-proliferation potency than curcumin and demethoxycurcumin have shown much in MDA-MB-231 and A2058 cancer cells (Huang et al., 2020). This was due to the lack of phenyl methoxy groups in bisdemethoxycurcumin. It was reported that the phenyl methoxy groups in curcuminoids are responsible for inhibiting TNF-α induced NF-κB activation in cancer cells. By suppressing NF-κB pathway, it reduces tumor cell proliferation and promotes apoptosis. Curcumin and demethoxycurcumin contain either two or one phenyl methoxy groups thereby showing stronger inhibition effect on TNF-α induced NF-κB activation than bisdemethoxycurcumin (Sandur et al., 2007). Solucumin and Mexcumin are the formulations with highest dissolution of curcumin and demethoxycurcumin, respectively. The release of curcumin and demethoxycurcumin from these two formulations were also high than bisdemethoxycurcumin. This suggests that Solucumin and Mexcumin might exert better anti-tumor effect than other tested samples for breast and melanoma cancers. However, curcumin, demethoxycurcumin and bisdemethoxycurcumin have shown the same potency in inhibiting the growth of other cancer cells which include U937

(histiocytic myeloid lymphoma), KBM-5 (chronic myeloid leukemia), Jurkat (T cell leukemia), H1299 (lung adenocarcinoma), Calu-6 (non-small cell lung carcinoma), A549 (lung adenocarcinoma), SCC-4 (squamous cell carcinoma), Panc-1 (pancreatic duct cell carcinoma), MCF-7 (breast adenocarcinoma), DU145 (prostate carcinoma) and A293 (embryonic kidney carcinoma) and HOS and U2OS cells (osteosarcoma carcinoma) (Huang et al., 2020; Sandur et al., 2007). This suggests that the NF-κB-suppressive effect of the curcuminoids was not correlated to their anti-proliferative effect to these cancer cells. It was still unclear why the proliferative effects of the curcuminoids differ in different cancer cells. Overall, one thing that is now certain is that small differences in chemical structure can strongly influence the biological activities of the curcuminoids, which could result in different therapeutic effects for different health conditions.

3.6. Conclusion

In conclusion, Solucumin has exhibited significantly higher dissolution of curcumin in pH 6.8 dissolution medium than two marketed curcumin products and another polymer-surfactant based curcumin formulation. This suggests that it is a formulation that can both enhance the solubility and dissolution rate of curcumin, making it a promising formulation for improving the oral bioavailability. Curcumin presented in an amorphous state was suspected to be the reason for the increased dissolution of curcumin. To determine whether curcumin did actually present in an amorphous state in Solucumin, characterisation studies including Fourier transform infrared spectroscopy (FTIR), differential scanning calorimetry (DSC), X-ray powder diffraction (XRD) are carried out and discussed in Chapter 4.

Chapter 4. Characterisation studies on different physicochemical properties of Solucumin and the comparators

4.1. Introduction

In this chapter, several characterisation studies were carried out to assess the physical and chemical properties of Solucumin and its comparators. Some properties measured from the characterisation studies can help to explain the effect on the drug solubility and dissolution of the formulations. The characterisation studies that have been conducted in this study include FTIR, DSC, XRD, DLS, Zeta-potential and a short-term stability test.

4.1.1. Fourier transform infrared spectroscopy (FTIR)

Fourier transform infrared spectroscopy (FTIR) is an analytical technique using infrared (IR) light. It works by detecting the absorption of infrared light caused by vibrational transitions. A beam of IR (infrared) light is generated by a fitting light source and passes through a beam splitter. The light is split into two separate beams that direct into a fixed mirror and a movable mirror respectively. Then the two light beams travel back to the splitter, re-combine into one and direct towards a sample. When the IR light is passed through the sample, some light is absorbed by the sample (absorption) while some passes through (transmittance). The absorption of IR light with specific wavelengths leads to the vibration of specific molecular bonds (stretching or bending). The transmitted IR light finally reaches the detector, generating a spectrum of the sample. Since different bonds and functional groups vibrate at different frequencies, the FTIR spectrum is different for different molecules. As a result, the FTIR spectrum represents a molecular ‘fingerprint’ of the sample (Alawam, 2014; Song et al., 2020). In this study, FTIR was used for determining any

potential interactions between the API and excipients in Solucumin and Mexcumin. This was done by comparing the changes in intensity and position of the functional group peaks representing the API and excipients. Longivdia and Nacumin were not tested by FTIR because their excipients is not known.

4.1.2. Differential scanning calorimetry (DSC)

Differential scanning calorimeter (DSC) is a major technique used for thermal analysis. It measures the change in physical properties of a sample because of a change in temperature. In DSC, a sample in a pan is either heated or cooled and the heat flow is measured as a function of time and temperature. An empty pan is used as a reference to counteract any heat absorbed by the pan material. Both the sample and the reference pans are heated in the same oven, so the heat flow reflects the thermal properties of the sample (Gill et al., 2010). When a sample undergoes a physical transformation such as phase transition or glass transition, more heat will need to flow to it than to the reference to maintain both at the same temperature. Whether more of less heat must flow to the sample depends on whether the process is exothermic or endothermic. By recording the amount of energy (heat) absorbed or released during the physical transformation, DSC can measure the heat flow into and out of the sample over a temperature range. The results of a DSC test are typically expressed as a curve of heat flow against temperature.

The heat flow is calculated by the thermal equivalent of Ohms law:

$$q = \Delta T / R \qquad \textbf{Equation 4.1}$$

q = Sample heat flow

ΔT= Temperature difference between the sample and reference

R = Resistance of thermoelectric disk

In this study, DSC was used for thermal analysis of Solucumin and Mexcumin. This was to investigate how the change in temperature can lead to changes in the physical nature of the formulations.

4.1.3. X-ray powder diffraction (XRD)

X-ray powder diffraction (XRD) is a powerful non-destructive technique which is primarily used for phase identification of crystalline materials. In an X-ray diffraction experiment, a sample is placed into the center of the instrument and illuminated with a beam of X-rays. The X-ray tube and detector move in a synchronised motion. The signal coming from the sample is recorded, where peaks are observed related to the atomic structure of the sample (Warren, 2003).

The fundamental principle of X-ray diffraction is that when an X-ray encounters an atom, its energy is absorbed by the electrons. Electrons occupy special energy states around an atom since this is not enough energy for the electron to be released. The energy must be re-emitted in the form of a new X-ray, with the same energy as the original. This process is called elastic scattering. In a crystal, the repeating arrangement of atoms form distinct planes with well-defined distances. When the atomic planes are exposed to an X-ray beam, the X-rays are scattered by the regularly space atoms as shown in Figure 4.1. Strong amplification of the emitted signal occurs at very specific angles where the scattered X-ray waves constructively interfere. The effect is called diffraction (Bunaciu et al., 2015).

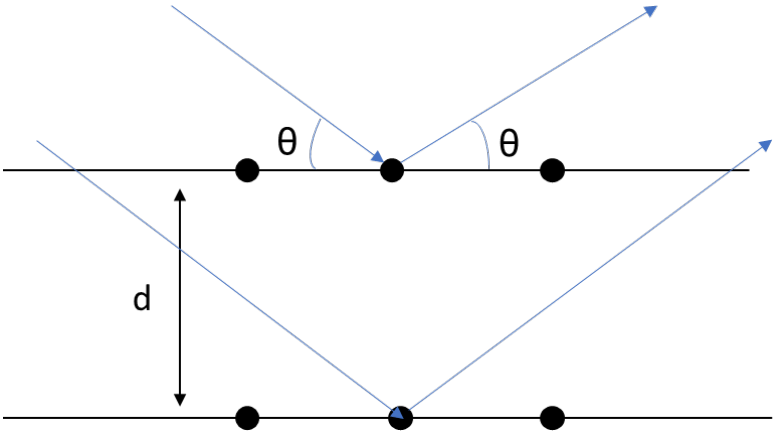

Figure 4.1. Scattering of x-rays from two planes of atoms in a crystal

When constructive interference occurs, the diffraction pattern will be detected and shows a peak, however if the scattered X-ray waves are out of phase, destructive interference will occur and there will be no peak. Diffraction peaks only occur if conditions satisfy Braggs Law (Cullity, 1956) as shown in Equation 4.2 below:

$$n\lambda = 2d \sin\theta \qquad \textbf{Equation 4.2}$$

θ =The angle of incidence of the X-ray
n = An integer defining order of diffracted X-ray beam
λ =The wavelength of the X-ray
d =The spacing between atomic planes

In this study, XRD was used for detecting the crystallinity of Solucumin, Mexcumin, Longvida® and Nacumin®. Whether a drug exists in a crystalline or amorphous form could have a significant impact on its stability and dissolution.

4.1.4. Dynamic Light Scattering (DLS)

Dynamic light scattering (DLS) is a technique that can be used to determine the size and size distribution of small particles in suspension. The principle of DLS is that it measures the Brownian motion of particles in a dispersion and uses this information to determine their hydrodynamic size. Brownian motion is the random movement of particles which result from their collision with solvent molecules. Smaller particles move or diffuse more quickly than larger particles. The rate of Brownian motion is quantified as the diffusion coefficient (D). During a DLS analysis, a beam of laser is directed towards the particles in suspension and the laser is scattered by the particles. The scattered laser will either cancel each other (destructive phases) or combined together creating a light intensity signal (constructive phases). The intensity will keep fluctuating over time as the

particles continue to diffuse. The speed of these intensity fluctuations depends on the particles diffusion rate. The smaller the particle the more quickly it diffuses, which leads to more rapid fluctuation in the scattered laser. An autocorrelator compares the intensity of scattered laser over time and the diffusion coefficients (D) is obtained. The value can then be used in the Stoke Einstein equation to calculate the particle size (Stetefeld et al., 2016). The Stokes-Einstein equation is shown in Equation 4.3 below:

$$D = k_B T / 6 \pi \eta r \qquad \textbf{Equation 4.3}$$

D =Diffusion coefficient

k_B =Boltzmann's constant

T =The absolute temperature

η = The dynamic viscosity

r =The radius of the spherical particle

In this study, DLS was used to measure the particle sizes of Solucumin, Mexcumin, Longvida® and Nacumin®.

4.1.5. Zeta potential

Dispersed particles have two layers of oppositely charged ions surrounding their surface. An internal layer known as stern layer formed by counterions (charged opposite to the surface charge) attracted to the particle surface and an outside layer known as the diffused layer formed by weakly attached ions.

The zeta potential is defined as the voltage at the edge of the double layer. If particles have high positive or negative zeta potentials of the same sign, they

will not agglomerate because the particles will tend to repel each other. Thus, zeta potential can be used as an indicator of the stability of the particles when dispersed in solution (Kaszuba et al., 2010).

During a zeta potential measurement, a sample is loaded into a folded capillary cell, which has conductive points to receive an electric charge. Once placed inside the instrument, a laser measures how fast the particles are moving when they are charged; the faster they move, the higher the absolute value of their zeta potential. Zeta potential cannot be measured directly so it is calculated indirectly by measuring the electrophoretic mobility of charged particles under an applied electric field (Bhattacharjee, 2016). The electrophoretic mobility (μ_e) of the particles is first calculated using Equation 4.4 below:

$$\mu e = \frac{V}{E} \qquad \textbf{Equation 4.4}$$

V = particle velocity (μm/s)

E = electric field strength (Volt/cm)

The zeta potential is then calculated from the obtained μ_e by the Henrys

equation. The Henry's equation is shown in Equation 4.5 below:

$$\mu e = \frac{2\varepsilon r \varepsilon 0 \zeta f(Ka)}{3\eta} \qquad \textbf{Equation 4.5}$$

εr = relative permittivity/dielectric constant

ε0 = permittivity of vacuum

ζ = zeta potential

f(Ka) = Henrys function

η = viscosity at experimental temperature.

In this study, zeta potential of Solucumin, Mexcumin, Longvida® and Nacumin® were measured to determine the potential stability of their particles in aqueous solution.

4.1.6. Short-term Stability test

Drug stability is a crucial factor to be aware of in drug development, as it affects the safety and efficacy of the drug. It is defined as the extent to which a drug substance or product retains, under specified conditions, the same properties and characteristics as when it was manufactured (Ahuja & Dong, 2005). Degradation of drugs can occur under the influence of many environmental factors such as light, pH, temperature, oxygen level and moisture(Zothanpuii et al., 2020). This can lead to adverse effects such as loss of therapeutic effect and reduction in bioavailability (Bajaj et al., 2012).

It has become mandatory to carry out stability studies on new drug products before submission of a registration dossier (Blessy et al., 2014). The major purpose for performing a drug stability study is to verify whether the drug can maintain an acceptable level of quality with time under the influence of different

environmental factors (ICH, 2003) Stability studies include long-term studies (12 months), accelerated stability studies (6 months, at relatively high temperatures and/or humidity) and intermediate studies (6 months, carried out under more moderate conditions than accelerated studies). The International Conference of Harmonization (ICH) guidelines provide uniformed standards for developing drug stability testing methods and analysing drug stability data (ICH, 2003).

Due to time constraints and impact of COVID19, the stability test conducted in this study was a short-term stability test (1 month) for determining the change of the active ingredient (curcumin) content when under room temperature and high temperature.

4.2. Aims

- To determine any potential drug-excipient interactions of Solucumin and Mexcumin using Fourier transform-infra red spectroscopy (FTIR).
- To determine the changes of physical nature at different temperatures of Solucumin and Mexcumin using differential scanning calorimetry (DSC).
- To determine crystallinity of Solucumin, Mexcumin, Longvida® and Naucumin® using X-ray powder diffraction (XRD).
- To determine the particle size and particle size distribution of Solucumin, Mexcumin, Longvida® and Nacumin® using differential light scattering (DLS) technique.
- To determine the potential stability in aqueous solution of the particles of Solucumin, Mexcumin, Longvida® and Nacumin® using zeta-potential.
- To determine the change of active ingredient content in Solucumin and Mexcumin during storage by conducting a short-term stability test.

4.3. Materials and method

4.3.1. Materials

Commercial curcumin powders were obtained from Techbifarm (Hanoi, Vietnam). Soluplus was provided by BASF SE (Ludwigshafen, Germany). Polyethylene glycol (PEG) 400, Poloxamer 407, Vitamin E TPGs, and Microcrystalline cellulose (MCC) were obtained from Sigma-Aldrich Ltd. (Gillingham, Dorset, UK). Magnesium stearate was purchased from Merck (Dorset, UK) and Aerosil from Evonik (Essen, Germany). Longvida® Optimised Curcumin 500 mg capsules were purchased from Igennus Healthcare Nutrition (Cambridge, UK). Nacumin® capsules with average weight 420 mg per capsule was a gift from Techbifarm (Hanoi, Vietnam).

4.3.2. Method

4.3.2.1. Fourier transform infrared spectroscopy (FTIR)

FTIR analysis was performed on a PerkinElmer Spectrum 65 Infra-red spectrophotometer (UK) for commercial curcumin, PEG400, Soluplus, Poloxamer 407, Vitamin E TPGs, MCC, magnesium stearate, Aerosol, Solucumin, Mexcumin and their physical mixtures. A background scan was conducted before each sample was loaded. For each sample, 8 scans were carried out with a resolution of 4 cm^{-1} and a frequency range from 4000 cm^{-1} to 400 cm^{-1}. FT-IR software (PerkinElmer Spectrum version 10.03.07) was used to compare the spectra and calculate the correlations between FTIR spectra. The correlation analysis was used to assess the similarity or dissimilarity between two spectra. The correlation coefficients of Solucumin/Mexcumin, commercial curcumin, their excipients and physical mixtures were calculated by the software. The correlation coefficient ranges from -1 to 1, with values closer to 1 indicating a strong positive correlation, values closer to -1 indicating a strong negative correlation, and values close to 0 indicating no correlation.

4.3.2.2. Differential scanning calorimetry (DSC)

The thermal behaviour of the formulations was determined by DSC Q2000. 4 mg of accurately weighted commercial curcumin, Soluplus, Poloxamer 407, Vitamin E TPGs, MCC, magnesium stearate, aerosol, Solucumin, Mexcumin and their physical mixtures were loaded into a standard aluminium pan separately. The sample pans were sealed with standard aluminium lids. As for PEG400, 30 mg was loaded into an aluminium pan and sealed with a hermetic lid. An empty aluminium pan sealed with a standard aluminium lid was used as reference for samples in solid form while another empty pan sealed with a hermetic lid was used as the reference for the sample in liquid form (PEG400). Each sample was analysed over the temperature range from 20°C to 250°C, with heating rate at 15°C/minute and nitrogen gas flow rate of 40 ml/minute.

4.3.2.3. X-ray powder diffraction (XRD)

X-ray powder diffraction (XRD) study of commercial curcumin powder, Longvida®, Nacumin®, Soluplus, Poloxamer 407, Vitamin E TPGs, MCC, magnesium stearate, aerosol, Solucumin, Mexcumin and their physical mixtures were performed over the range of 2θ (the angle between transmitted X-ray beam and reflected X-ray beam) from 0º to 51.56º by Oxford Diffraction, Xcalibur microfocus NovaT X-ray diffractometer, using Cu Kα radiation. 0.2 mg of each sample was loaded to a 0.7mm diameter capillary and then compaction was applied to the sample-loaded capillary. After compaction, the capillary was placed in the XRD instrument for analysis.

The X-ray diffractometer was combined with a Titan CCD imaging system and the data was processed by CrysalisPro (Agilent Technologies) software. PEG400 was not tested by XRD as it is a liquid under room temperature.

4.3.2.4. Dynamic light scattering (DLS)

Dynamic light scattering study of Solucumin, Mexcumin and commercial curcumin powders was carried out by using Malvern Zetasizer (Nano series, Nano-ZS90). 5 mg of each sample was suspended in 10 ml ultrapure water and sonicated for 5 minutes to ensure homogenous distribution. 1.5ml of the sample suspension was then transferred into a disposable four-sided clear polystyrene cuvette and tested for its size at 25^{o}C, with a 90^{o} angle detector. Samples were measured in triplicate and each run consisted of 30 repeats. The average, polydispersity index (PdI) and standard deviation (SD) were calculated by the zetasizer software (version 2.2).

IBM SPSS Statistics software (Version 24.0; IBM Corp, Armonk, NY, USA) was used for statistical analysis of the data. Brown-Forsythe ANOVA test was applied to compare different mean particle size of the samples as it is commonly applied when there are wide variations in standard deviation. *Post Hoc* Dunnett T3 test was applied for multiple comparison test. It is the multi-comparison test method to use when sample sizes are small (<50 per group) and the homogeneity of variance assumption for One-Way ANOVA is violated (Shingala & Rajyaguru, 2015). Levene's test was conducted to check the homogeneity of variances and the result showed that the significance was 0.05, indicating equal variances are not assumed in the One-way ANOVA (Kim, 2017).

4.3.2.5. Zeta potential

Zeta potential measurement for Solucumin, Mexcumin, Longvida®, Nacumin® and commercial curcumin powders was also conducted in Malvern Zetasizer (Nano series, Nano-ZS90). Sample solutions were prepared under the same method used in the DLS study. The solution of each sample was loaded into a reusable folded capillary cell with gold plated electrodes. Samples were measured in triplicate with each measurement consisting of 12 runs. The

mean zeta potentials were calculated by the Zetasizer software. One-way ANOVA and Post Hoc Tukey test were carried out in IBM SPSS Statistics software (Version 24.0; IBM Corp, Armonk, NY, USA) for analysing the mean values of zeta potential.

4.3.2.6. Short-term stability test

A drug stability test was conducted for determining the change of the curcumin stability in commercial curcumin, Solucumin, Mexcumin, Nacumin® and Longvida® over time at different temperatures. Each sample was sealed in two glass vials, each containing 1 g of the sample powder. The sample containing glass vials were then placed in an oven at 25 °C /60% RH and 40 °C/ 60%RH for 1 month respectively. The change in curcumin content was measured by HPLC. Three replicates of each sample were prepared for each temperature. Sensitivity to moisture or potential for solvent loss is not a concern for drug products packaged in impermeable containers that provide a permanent barrier to passage of moisture or solvent (ICH, 2003). Since the samples were placed in sealed glass vials, the effect of relative humidity was not considered in this stability study.

One-way ANOVA and Post Hoc Dunnett's test were carried out to compare the percentage curcumin content at day 0 and after 1 month. Dunnett's test was selected for comparison because it is the only *post hoc* test that allows comparison of multiple means to a control mean (Field, 2009). In this case, the control mean is the percentage of curcumin content in Day 0.

4.4. Results

4.4.1. Fourier transform infrared spectroscopy (FTIR)

Figure 4.2 shows the FTIR spectra of curcumin, Soluplus, Vitamin E TPGs, Solucumin and the physical mixture of curcumin with the excipients used for preparing Solucumin. Commercial curcumin (Figure 4.2a) showed its characteristic peaks at 3509 cm^{-1} (phenolic O-H stretching), 1626 cm^{-1} (aromatic C=C stretching),1601 cm^{-1} (C=C-C, aromatic ring stretching), 1505 cm^{-1} (C=O and C=C stretching), 1427 cm^{-1} (olefinic C-H bending), 1273 cm^{-1} (aromatic C-O stretching), 1114 cm^{-1} (alkyl-substituted ether, C-O-C stretching) (X. Chen et al., 2015). Soluplus (Figure 4.2b) showed its characteristic peaks at peaks at 2,860 cm^{-1} (aliphatic C–H stretching), 1732 cm^{-1} (ester C=O stretching), 1623 cm^{-1} (amide group, C(O)N) stretching) (Lavra et al., 2017). The Vitamin E TPGs spectrum (Figure 4.2c) has peaks at 3467 cm^{-1} (-OH stretching), 2885 cm^{-1} (aliphatic C-H stretching), 1736 cm^{-1} (ester C=O stretching), 1465 cm^{-1} (aromatic ring, C=C-C stretching), 1240 and 1104 cm^{-1} (ether, C-O-C stretching) (Moneghini et al., 2010). These observations of the characteristic peaks agree with the published literature (X. Chen et al., 2015; Lavra et al., 2017; Moneghini et al., 2010). The representative peaks of Soluplus (1730 cm^{-1}, C=O stretching) and Vitamin E TPGs (2883 $cm^{-}1$, C-H stretching) can be seen at the spectra of Solucumin (Figure 4.2d) and its physical mixture (Figure 4.2e). An OH peak of curcumin was observed in the spectrum of the physical mixture (Figure 4.2e) but was absent in Solucumin (Figure 4.2d).

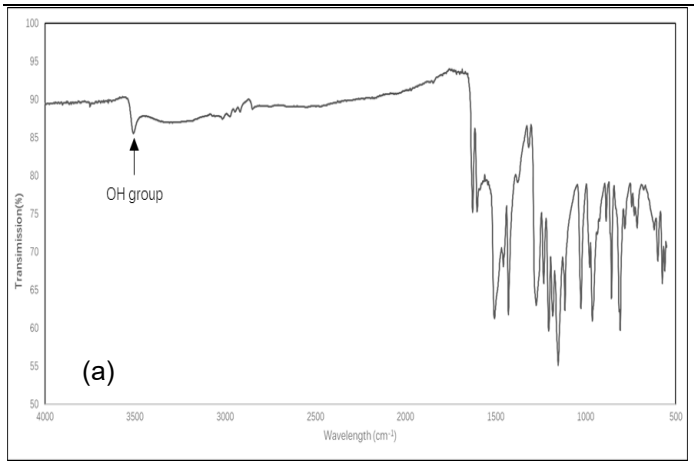
OH group
Transmission(%)
Wavelength (cm-1)
(a)

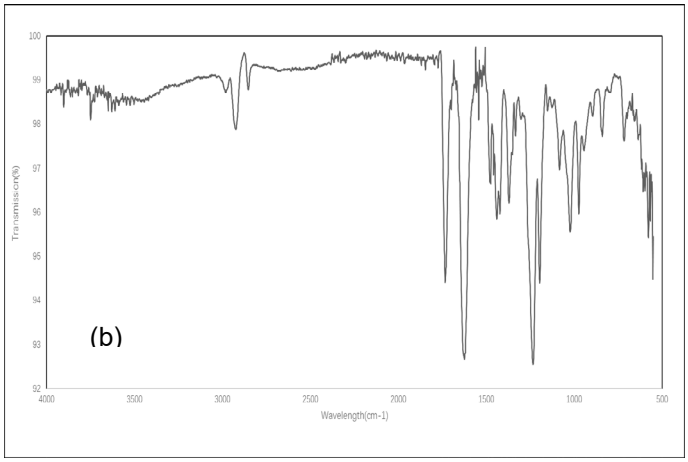
Transmission(%)
Wavelength(cm-1)
(b)

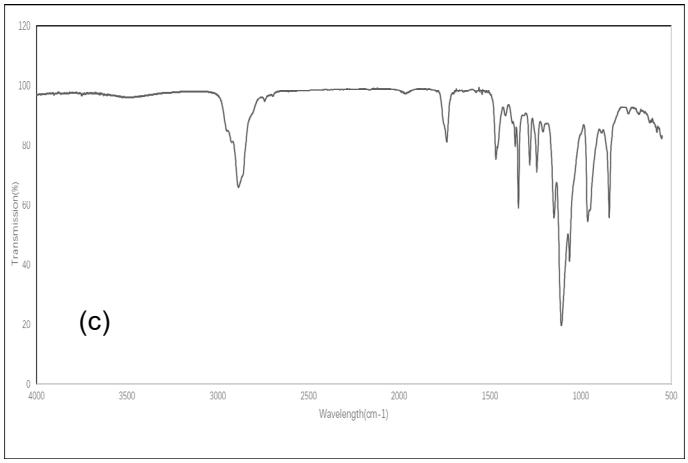
Transmission(%)
Wavelength(cm-1)
(c)

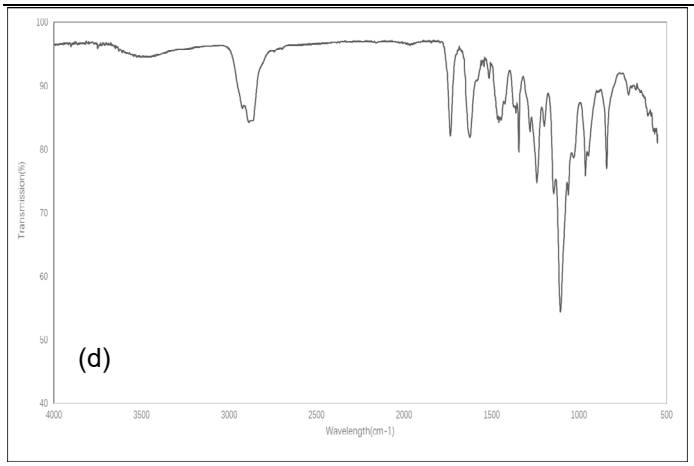

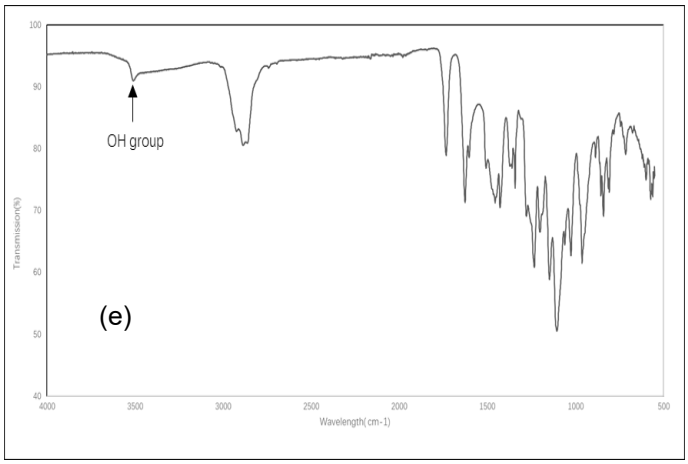

Figure 4.2. FTIR spectrum of (a) Commercial curcumin, (b) Soluplus, (c) Vitamin E TPGs, (d) Solucumin and (e) physical mixture of Solcumin (curcumin:Soluplus:Vitamin E TPGs 1:10:10)

Figure 4.3 shows the FTIR spectra of PEG400, Poloxamer 407, microcrystalline cellulose, aerosil, magnesium stearate, Mexcumin and a physical mixture of Mexcumin. In the spectra of PEG400 (Figure 4.3a), it showed characteristic peaks at 3444 cm^{-1} (O-H stretching), 2865 cm^{-1} (alkyl C-H stretching), 1456 cm^{-1}, 1349 cm^{-1}, 1295 cm^{-1}, 1248 cm^{-1} (alkyl C-H bending) and 1094 cm^{-1} (ether C-O-C stretching) (Alemdar et al., 2005; Lin & Zhou, 2017). Poloxamer 407 (Figure 4.3b) exhibited peaks at 2880 cm^{-1} (C-H alkyl stretching), 1466 cm^{-1} (C-H alkyl bending), 1341 cm^{-1} (in plane O-H bending) and 1098 cm^{-1} (ether C-O-C stretching) (Karolewicz et al., 2017). Microcrystalline cellulose (MCC) (Figure 4.3c) showed characteristic peaks at 3329 cm^{-1} (O-H stretching), 2891 cm^{-1} (C-H alkyl stretching), 1631 cm^{-1} (C=O stretching) and 1315 cm^{-1} (C-O stretching) (Jia et al., 2011). Aerosil (Figure 4.3d) exhibited a sharp peak at 1090 cm^{-1} (Si-O-Si stretching) (Parvinzadeh et al., 2010). The spectrum of magnesium stearate (Figure 4.3e) showed peaks at 3252 cm^{-1} (O-H stretching), 2916 cm^{-1}, 2850 cm^{-1} (C–H stretching vibration), 1571 cm^{-1} and 1466 cm^{-1} (COO-stretching vibration) (Stulzer et al., 2008). The values of the characteristic peaks for these excipients correspond to the results in published literatures (Alemdar et al., 2005; Jia et al., 2011; Karolewicz et al., 2017; Lin & Zhou, 2017; Parvinzadeh et al., 2010; Stulzer et al., 2008). The FTIR spectra of Mexcumin and the physical mixture were shown in Figure 4.3f and Figure 4.3g, respectively.

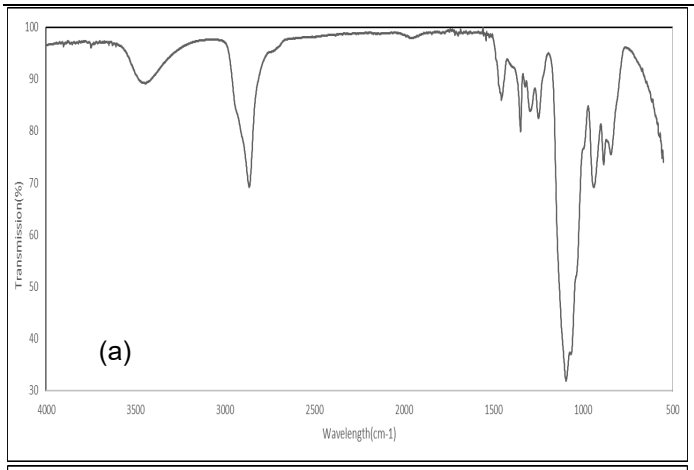
100
90
80
70
60
50
40
30
Transmission(%)
(a)
4000
3500
3000
2500
2000
1500
1000
500
Wavelength(cm-1)

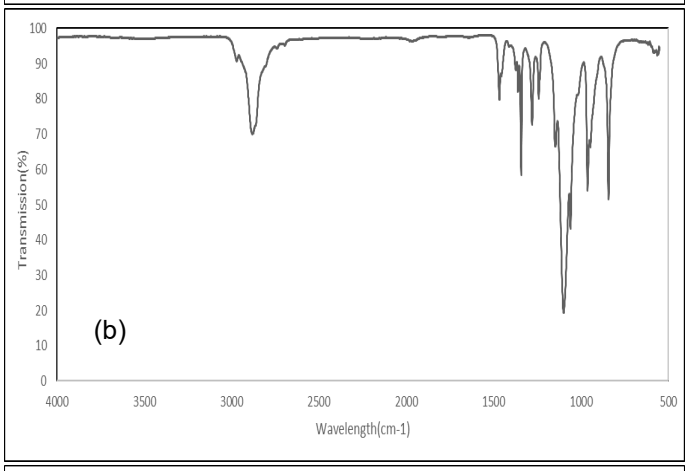
100
90
80
70
60
50
40
30
20
10
0
Transmission(%)
(b)
4000
3500
3000
2500
2000
1500
1000
500
Wavelength(cm-1)

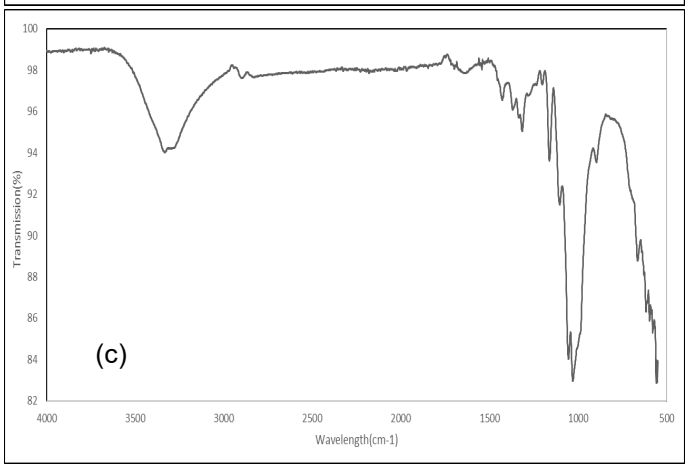
100
98
96
94
92
90
88
86
84
82
Transmission(%)
(c)
4000
3500
3000
2500
2000
1500
1000
500
Wavelength(cm-1)

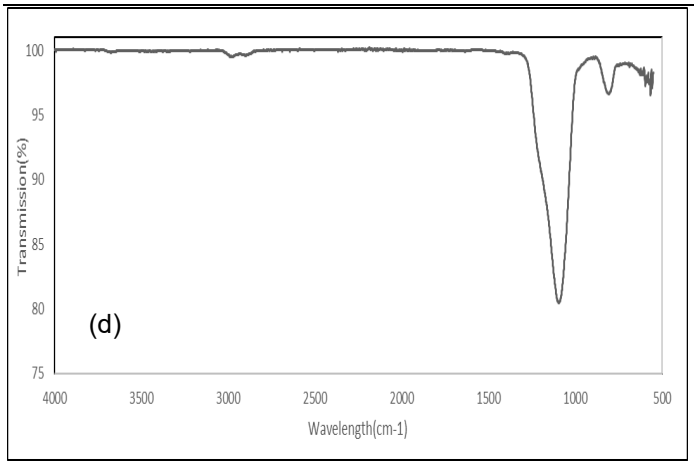
Transmission(%)
100
95
90
85
80
75
(d)
4000
3500
3000
2500
2000
1500
1000
500
Wavelength(cm-1)

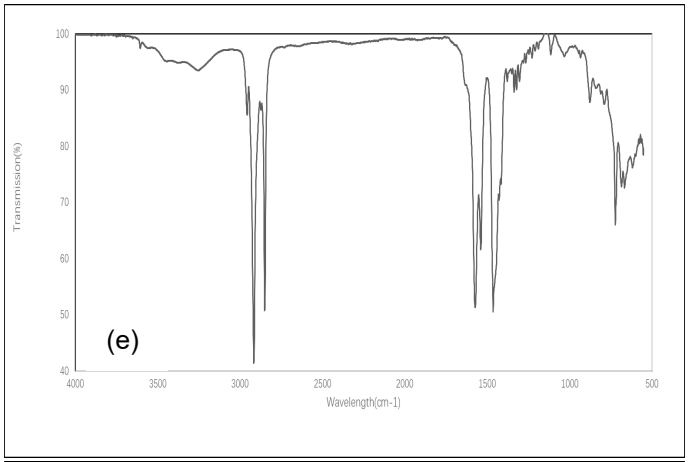
Transmission(%)
100
90
80
70
60
50
40
(e)
4000
3500
3000
2500
2000
1500
1000
500
Wavelength(cm-1)

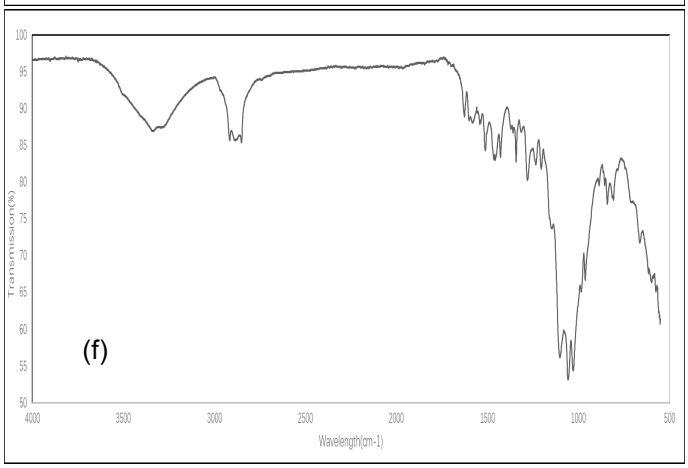
Transmission(%)
100
95
90
85
80
75
70
65
60
55
50
(f)
4000
3500
3000
2500
2000
1500
1000
500
Wavelength(cm-1)

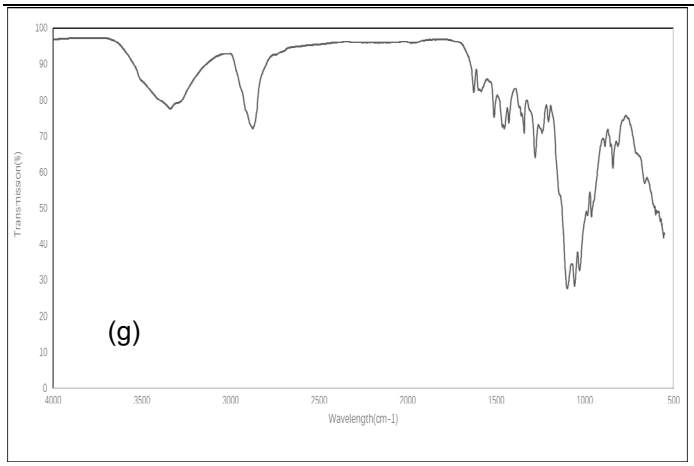

Figure 4.3. FTIR spectrum of the (a) PEG400, (b) Poloxamer 407, (c) MCC, (d) aerosil, (e) Magnesium stearate, (f) Mexcumin, and (g) physical mixture of Mexcumin (Curcumin: PEG400: Poloxamer 407: MCC: aerosil: Magnesium stearate 1:0.5:0.9:5.6:0.1:0.1)

The spectra of Solucumin and Mexcumin were compared with that of the commercial curcumin, their excipients and their physical mixtures. A correlation factor between each comparison batch was calculated, which describes the similarity between the spectra. As shown in Table 4.1 and 4.2, the spectrum of commercial curcumin showed very low similarity to Solucumin and Mexcumin. On the other hand, the spectra of Solucumin and Mexcumin expressed much higher similarities to their correlating excipients and physical mixtures.

Sample to compare with Solucumin	FTIR spectra correlation factor
Commercial curcumin	0.0749
Soluplus	0.6354
Vitamin E TPGs	0.7607
The physical mixture of Solucumin	0.6785

Table 4.1. Summary of FTIR spectra correlation factor between Solucumin to commercial curcumin, Soluplus, Vitamin E TPGs and the physical mixture of Solucumin

Sample to compare with Mexcumin	FTIR spectra correlation factor
Commercial curcumin	0.0621
Poloxamer 407	0.2481
MCC	0.7365
Magnesium stearate	0.0273
Aerosil	0.0067
The physical mixture of Mexcumin	0.8742

Table 4.2. Summary of FTIR spectra correlation between Mexcumin to commercial curcumin, Poloxamer 407, MCC, magnesium stearate, aerosil and the physical mixture of Mexcumin

4.4.2. Differential scanning calorimetry (DSC)

The DSC thermograms of the formulations were compared with commercial curcumin, the excipients, and the physical mixtures of Solucumin and Mexcumin to identify any changes in thermal properties.

Commercial curcumin powder (Figure 4.4a) exhibited a sharp, single endothermic peak at 176.57°C, which corresponded to its melting point (Sayyar & Jafarizadeh-Malmiri, 2019). Since sharp endotherm is expected from a highly crystalline compound, it suggested that commercial curcumin powder is likely to have a crystallised structure (Clas et al., 1999). The DSC thermogram of Soluplus (Figure 4.4b) exhibited a broad glass transition peak around 70°C (Altamimi & Neau, 2017). The DSC curve of Vitamin E TPGs (Figure 4.4c) exhibited a sharp endothermic peak at 35.48°C, corresponding to its melting point (Moneghini et al., 2010). The observed thermograms agree with the results in published literature. The thermogram for Solucumin (Figure 4.4d) revealed the presence of a weaker endothermic peak at 33.50°C corresponding to Vitamin E TPGs. As for the physical mixture, its DSC thermogram showed a similar pattern to Solucumin, only an endothermic peak was observed at 35.80°C (Figure 4.4e).

Poloxamer 407 (Figure 4.5a) showed a sharp endothermic peak at 55.67°C (Newa et al., 2008). Magnesium stearate (Figure 4.5b) showed two endothermic peaks. The peak at 105.08 ℃ was due to evaporation of moisture and the peak at 126.59℃ indicated mesophase transition occurred in magnesium stearate (Haware et al., 2018). MCC (Figure 4.5c) showed glass transition point peaks 119.79°C respectively (Barboza et al., 2009; Delaney et al., 2017). No obvious peaks were observed from PEG400 (Figure 4.5d) and aerosil (Figure 4.5e).

In the thermogram of Mexcumin (Figure 4.5f), a weak endothermic peak at 45.95°C corresponds to the melting point of Poloxamer 407 was observed. The peak shifted to lower temperature and became broader compared with the thermograms of Poloxamer 407. The DSC thermogram of the physical mixture is very similar to Mexcumin, with only one endothermic peak observed at 44.20°C (Figure 4.5g).

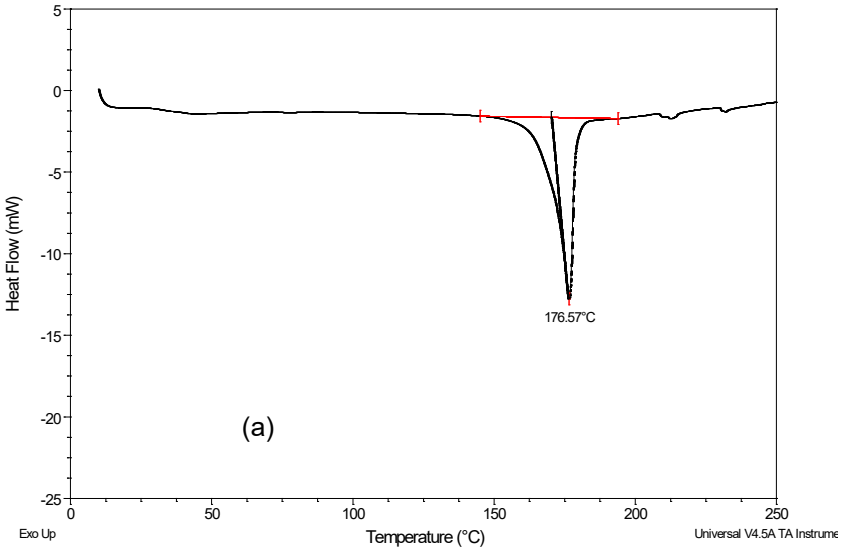
5
0
-5
-10
-15
-20
-25
Heat Flow (mW)
176.57°C
(a)
0
50
100
150
200
250
Exo Up
Temperature (°C)
Universal V4.5A TA Instrume

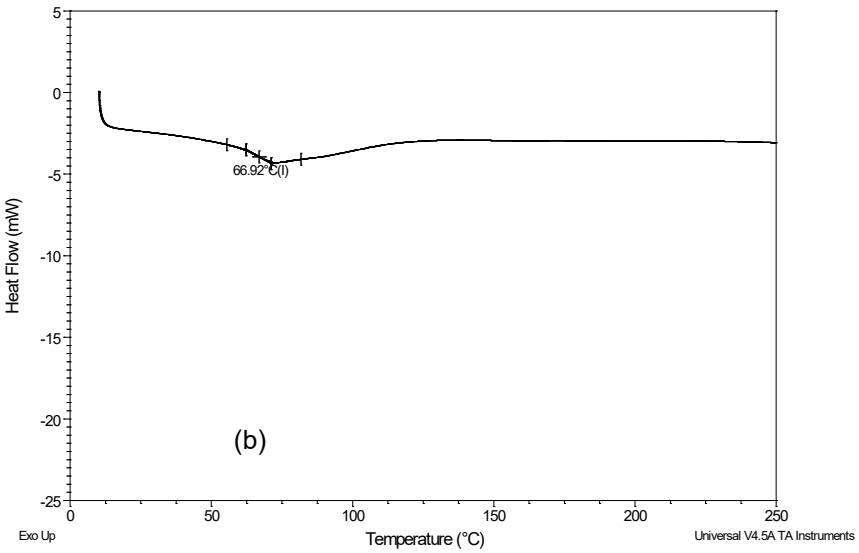
5
0
-5
-10
-15
-20
-25
Heat Flow (mW)
66.92°C(I)
(b)
0
50
100
150
200
250
Exo Up
Temperature (°C)
Universal V4.5A TA Instruments

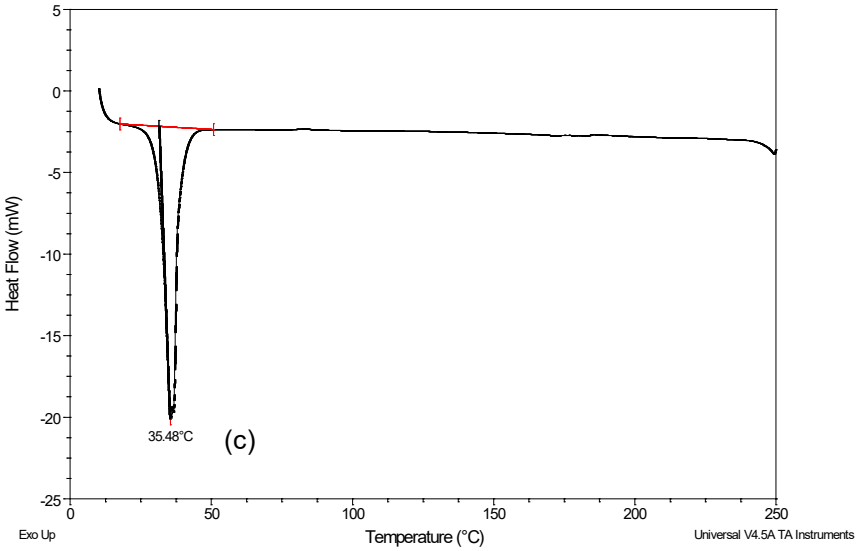
5
0
-5
-10
-15
-20
-25
Heat Flow (mW)
35.48°C
(c)
0
50
100
150
200
250
Exo Up
Temperature (°C)
Universal V4.5A TA Instruments

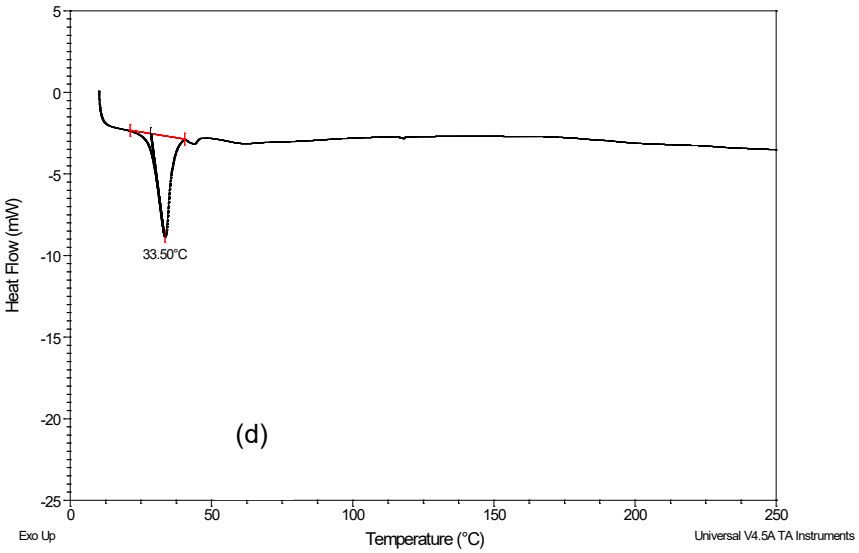
5
0
-5
-10
-15
-20
-25
Heat Flow (mW)
33.50°C
(d)
0
50
100
150
200
250
Exo Up
Temperature (°C)
Universal V4.5A TA Instruments

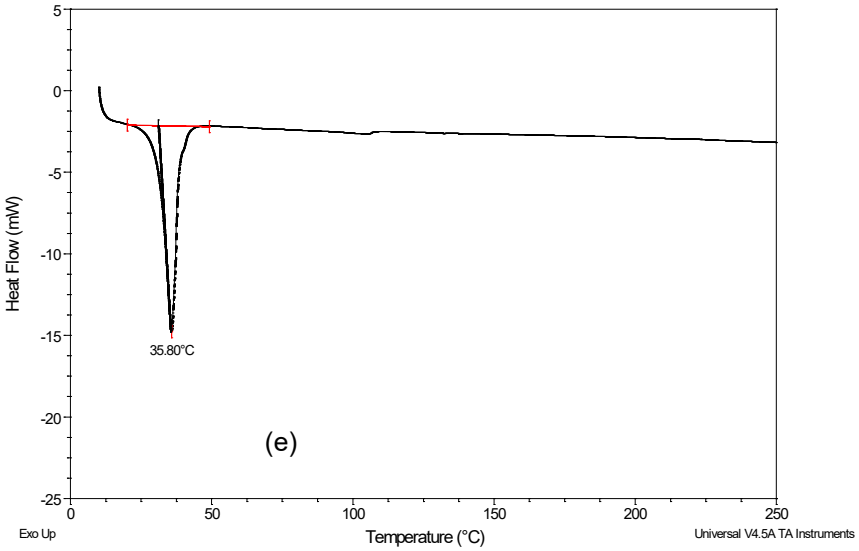

Figure 4.4. DSC thermograms of (a) commercial curcumin, (b) Soluplus, (c) Vitamin E TPGs, (d) Solucumin, (e) physical mixture of Solucumin (curcumin:Soluplus:Vitamin E TPGs 1:10:10)

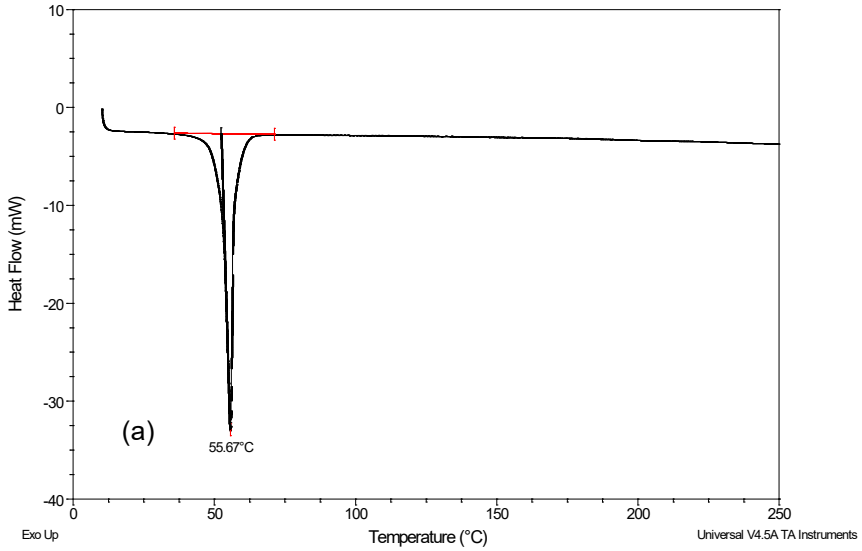
10
0
-10
-20
-30
-40
Heat Flow (mW)
(a)
55.67°C
0
50
100
150
200
250
Exo Up
Temperature (°C)
Universal V4.5A TA Instrumentsl

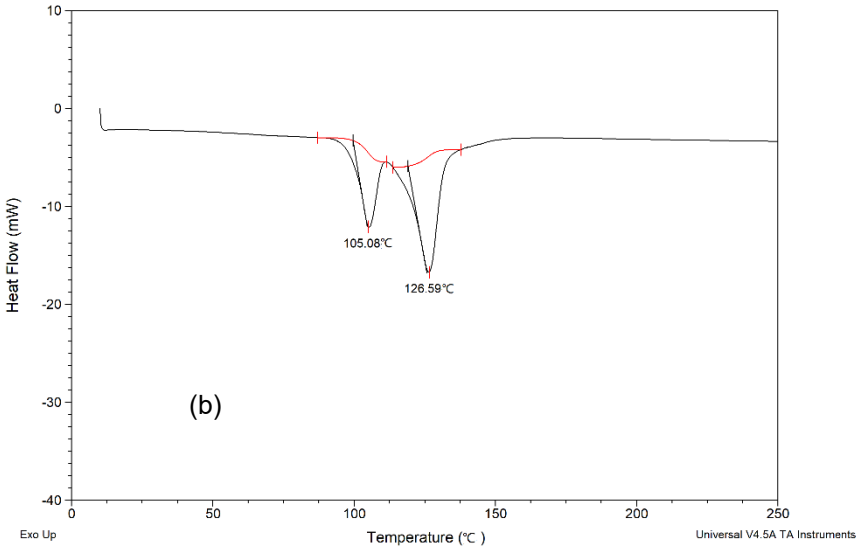
10
0
-10
-20
-30
-40
Heat Flow (mW)
105.08℃
126.59℃
(b)
0
50
100
150
200
250
Exo Up
Temperature (℃)
Universal V4.5A TA Instruments

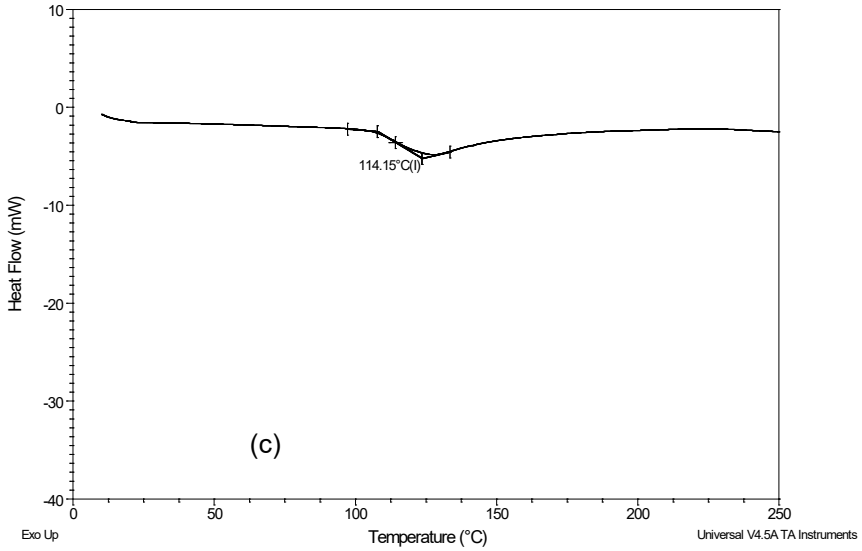
10
0
-10
-20
-30
-40
Heat Flow (mW)
114.15°C(I)
(c)
0
50
100
150
200
250
Exo Up
Temperature (°C)
Universal V4.5A TA Instruments

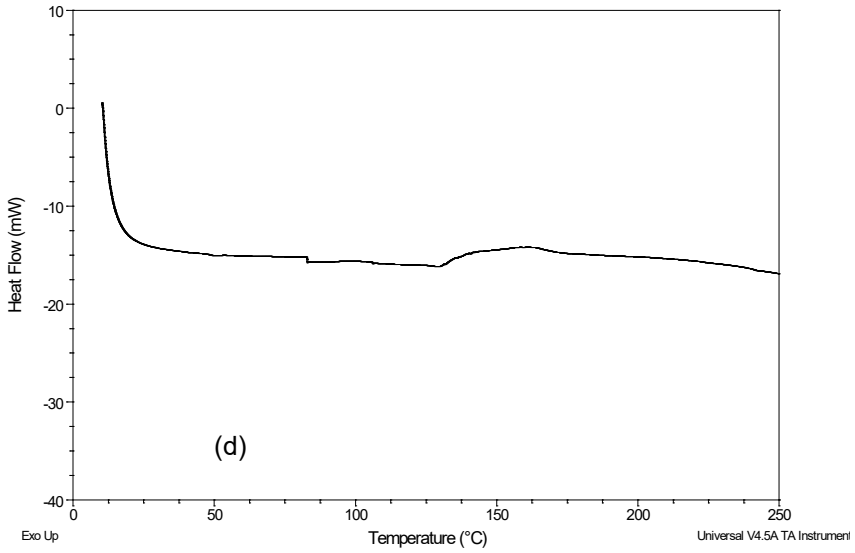
10
0
-10
-20
-30
-40
Heat Flow (mW)
(d)
0
50
100
150
200
250
Exo Up
Temperature (°C)
Universal V4.5A TA Instrumen

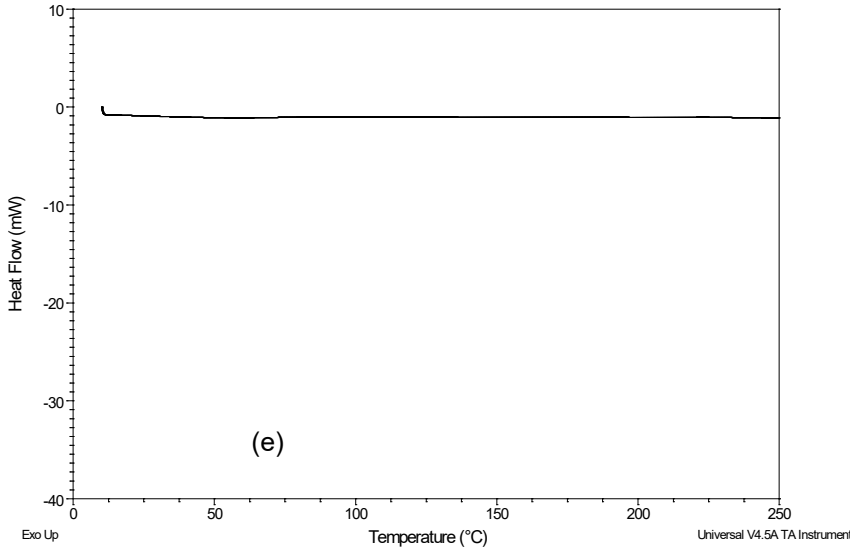
10
0
-10
-20
-30
-40
Heat Flow (mW)
(e)
0
50
100
150
200
250
Exo Up
Temperature (°C)
Universal V4.5A TA Instrument

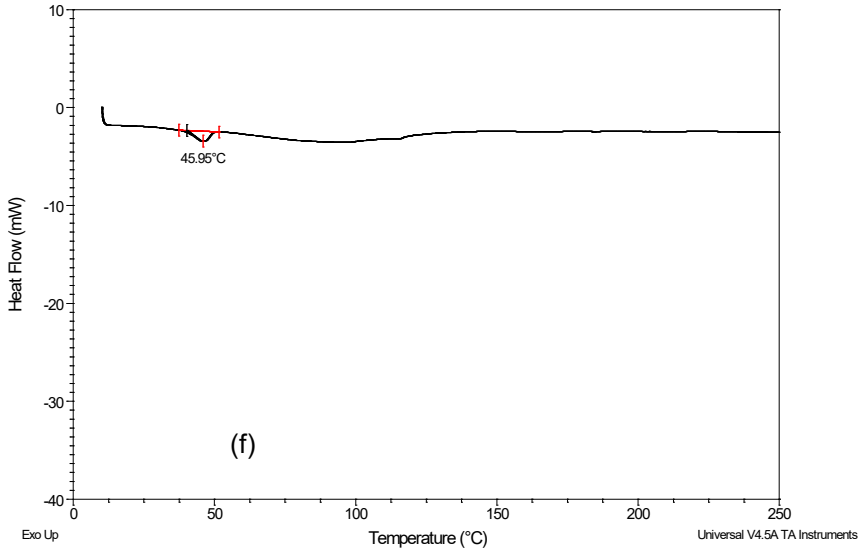
10
0
-10
-20
-30
-40
Heat Flow (mW)
45.95°C
(f)
0
50
100
150
200
250
Exo Up
Temperature (°C)
Universal V4.5A TA Instruments

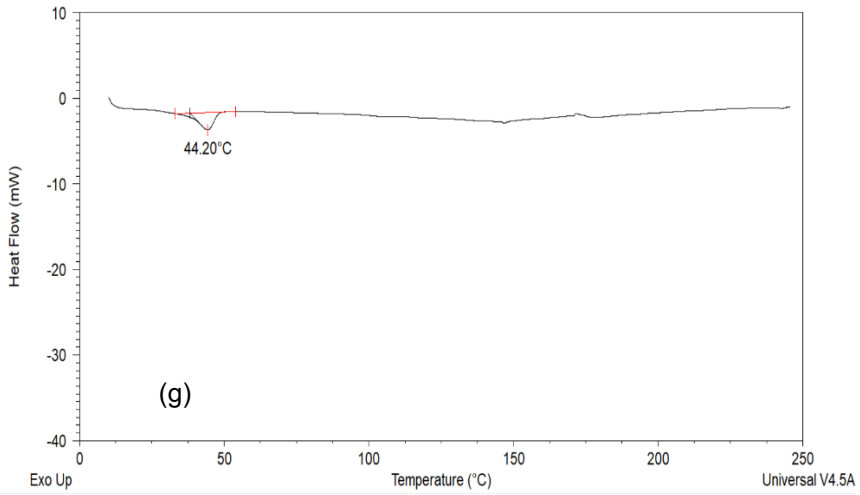

Figure 4.5. DSC thermograms of (a) Poloxamer 407, (b) Magnesium stearate, (c) MCC, (d) PEG400, (e) aerosil, (f) Mexcumin, (g) physical mixture of Mexcumin (Commercial curcumin: PEG 400: Poloxamer 407: MCC: aerosil: magnesium stearate 1:0.5:0.9:5.6:0.1:0.1)

4.4.3. X-ray powder diffraction (XRD)

The XRD spectra of commercial curcumin powder, Soluplus, Vitaimin E TPGs, Solucumin and its physical mixture are shown in Figure 4.6. Commercial curcumin (Figure 4.6a) exhibited several distinct diffraction peaks at 7.94º, 8.93º, 12.26º, 14.64º, 15.9º, 17.35º, 18.26º, 19.55º, 21.48º, 23.47º, 24.65º, 25.68º, 27.46º and 29.18º. For Soluplus (Figure 4.6b), it showed a distinct intense peak at 22.69 º and several less intense peaks at 8.99 º,12.28 º,15.56 º,17.43 º,18.33 º,19.29 º,25.64 º, and 34.73 º. Vitamin E VTPGs (Figure 4.6c) showed two distinct sharp peaks at 19.26 º and 23.31 º. Some broad peaks were observed at 26.59 º, 32.9 º and 36.1 º. For Solucumin (Figure 4.6d), two sharp peaks were found at 19.2 º and 23.28 º. Several broad peaks can be seen at 9.09 º, 14.86 º, 19.1 º, 26.39 º and 35.98 º. The physical mixture of Solucumin (Figure 4.6e) showed sharp peaks at 7.94 º ,8.95 º, 12.26 º, 14.65 º,15.22 º, 15.9 º, 17.44 º,18.29 º,19.25 º, 21.27 º, 23.31 º, 24.65 º, 25.68 º, 26.17 º, 26.91 º, 27.41 º and 29.1 º.

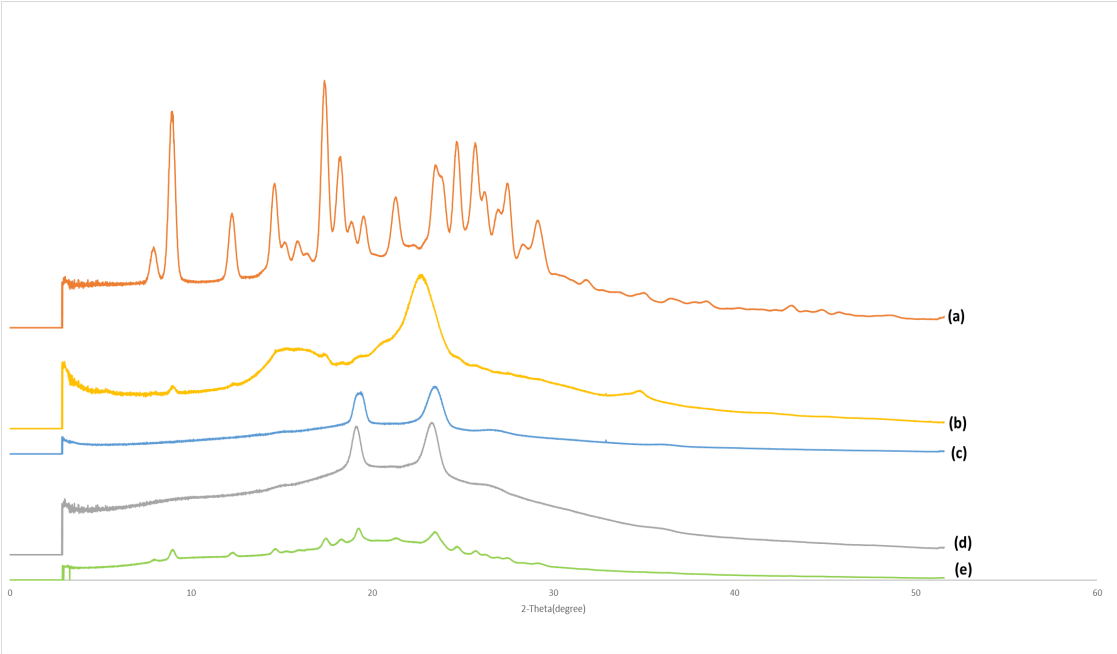

Figure 4.6. XRD spectra of (a) Commercial curcumin powder (b) Soluplus (c) Vitamin E TPGs (d) Solucumin and (e) the physical mixture of Solucumin

The XRD spectra of poloxamer 407, aerosol, magnesium stearate, MCC, Mexcumin and its physical mixture are shown in Figure 4.7. Poloxamer 407 (Figure 4.7a) exhibited two distinct sharp peaks at 19.34 º and 23.52 º. Two less intense sharp peaks were shown at 26.23 º and 33.16 º. Aerosil (Figure 4.7b) showed some intense peaks at 21.03 º, 25.75 º ,26.24 º ,26.29 º, 28.3 º and 29.11 º. Several less intense peaks were found at 30.18 º, 31.59 º, 34.58 º, 36.26 º, 38.12 º, 40.88 º and 43.01 º. Various sharp peaks were observed in magnesium stearate (Figure 4.7c) at 9.98 º, 10.28 º, 18.68 º and 19.96 º. Some less intense peaks can be seen at 23.03 º,24.97 º, 25.62 º, 26.12 º, 26.93 º, 28.44 º ,28.93 º ,30.55 º, 34.3 º and 36.11 º. MCC (Figure 4.7d) illustrated a distinct sharp peak at 22.61 º and a broad peak at 15.6 º. Less intense sharp peaks were found at 12.32 º, 18.24 º, 19.06 º, 25.69 º and 34.65 º. Mexcumin (Figure 4.7e) showed a distinct sharp peak at 22.54 º, a broad peak at 15.32 º, and several less intense sharp peaks at 5.48 º ,8.88 º, 12.26 º, 17.15 º, 18.11 º, 19.1 º, 25.2 º and 34.69 º. The physical mixture of Mexcumin (Figure 4.7f) showed a distinct sharp peak at 22.65 º, a broad peak at 15.37 º, and several less intense peaks at 5.47 º ,8.90 º, 12.21 º ,17.20 º, 18.09 º, 19.08 º, 25.64 º and 34.65 º.

The XRD spectra of Longvida® and Nacumin ®are shown in Figured 4.8 Both exhibited sharp diffraction peaks from 7º to 30 º (Figure 4.8a and 4.8b). Some peaks observed from the XRD spectrum of the commercial curcumin powder (Figure 4.8c) can also be seen in Longvida® (8.93º, 12.26º, 15.9º, 17.35º, 18.26º and 24.65º) and Nacumin® (8.93º, 12.26º, 17.35º and 24.65º).

.

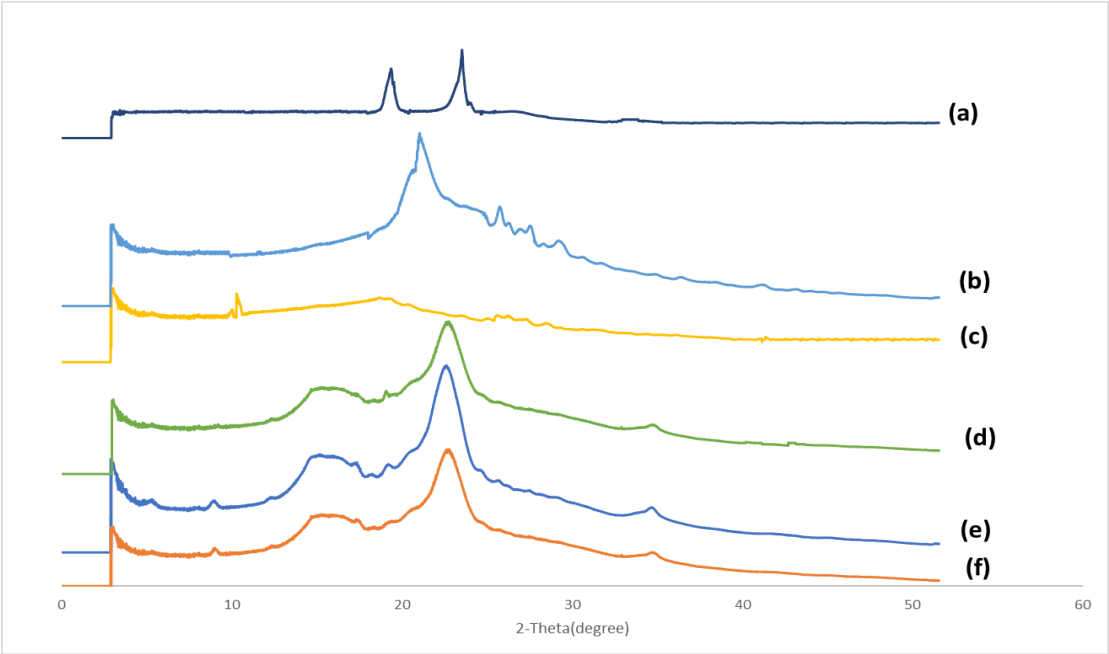

Figure 4.7. XRD spectra of (a) poloxamer 407, (b aerosil (c) magnesium stearate (d) MCC (e) Mexcumin and (f) the physical mixture of Mexcumin

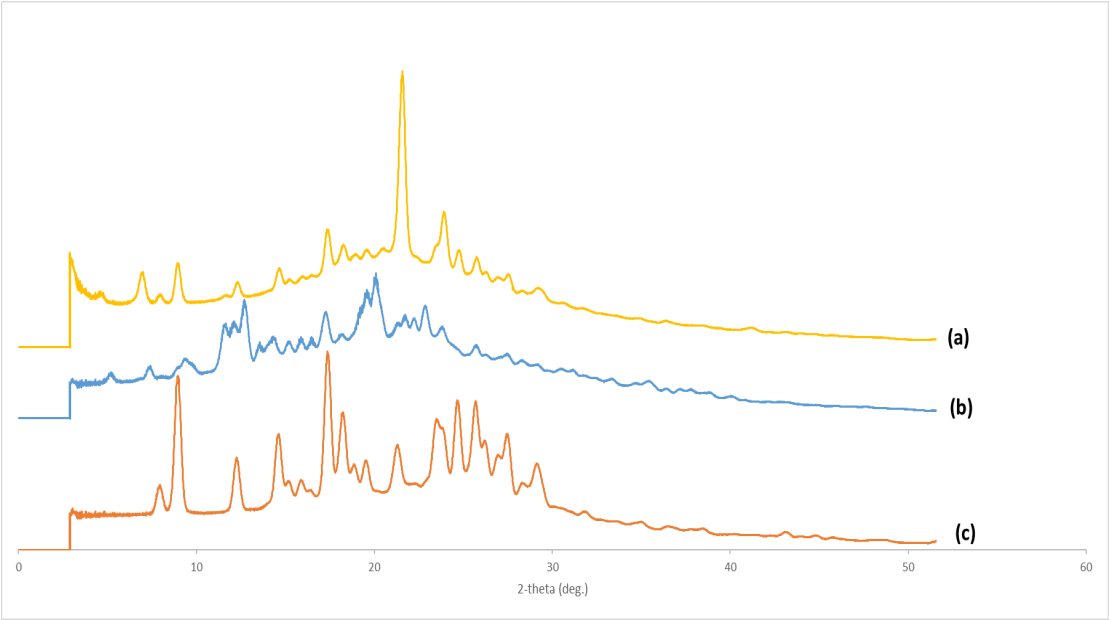

Figure 4.8. XRD spectra of (a) Longvida® (b) Nacumin® and (c) commercial curcumin powders

4.4.4. Dynamic Light Scattering (DLS)

Commercial curcumin powders, Solucumin and Mexcumin were measured for their particle size and particle size distribution using DLS. A summary of the results is shown in Table 4.3. The mean particle size of the commercial curcumin measured from the Zetasizer was 21421.67 ± 2505.71 nm, which is outside the particle size detection range of the Zetasizer (0.3nm to 10 μm). Nevertheless, this value is relatively close to the particle size of curcumin in published literatures. According to previous research studies, the particle size of curcumin ranges from 16.10 μm to 28.96 μm (Arozal et al., 2021; Valeh-e-Sheyda et al., 2015).

Solucumin, Mexcumin, Longvida® and Nacumin® have shown particle sizes of 3407.00±421.01 nm, 1169.67±76.83 nm, 865.67±44.58 nm and 372.67±49.41 nm, respectively. The PdI values for Solucumin, Mexcumin, Longvida® and Nacumin® were 0.424, 0.783, 0.411 and 0.325 respectively. Data analysis using Brown-Forsythe ANOVA test showed significant difference among the particle sizes of the samples tested in DLS ($p \leq 0.05$). Post Hoc Tamhane test results showed that the mean particle size of commercial curcumin was significantly lower than Solucumin, Mexcumin, Longvida® and Nacumin® ($p \leq 0.05$). In addition, the mean particle size of Solucumin, Mexcumin, Longvida® and Nacumin® were significantly different from each other ($p \leq 0.05$).

	Particle size (nm)	PdI
Solucumin	3407.00±421.01	0.424
Mexcumin	1169.67±76.83	0.783
Longvida®	865.67±44.58	0.411
Nacumin®	372.67±49.41	0.325

Table 4.3. The particle size (n=3, Mean±SD) and PdI values of commercial curcumin, Solucumin and Mexcumin

4.4.5. Zeta potential

Zeta potential was measured for commercial curcumin, Solucumin and Mexcumin. The result is shown in Table 4.4. Commercial curcumin showed more negative zeta potential values of -40.96 ± 2.15 mV compared to -12.80 ± 2.43 mV for Solucumin, -20.25 ± 4.46 mV for Mexcumin, -33.57 ± 4.99 mV for Longvida® and -15.27 ± 2.95 mV for Nacumin®.

One-way ANOVA results showed that there is a significant difference between the zeta potential values of the samples. According to the result of Tukey test, it can be found that the mean zeta potential values of commercial curcumin and Longvida® were significantly higher than that of Solucumin, Mexcumin and Nacumin® ($p \leq 0.05$). There was no significant difference between commercial curcumin and Longvida ® ($p > 0.05$). On the other hand, no significant difference was found between Solucumin and Mexcumin ($p > 0.05$), Nacumin® and Solucumin ($p > 0.05$), and Nacumin® and Mexcumin ($p > 0.05$).

	Zeta-potential (mV)
Commercial curcumin	-40.97±2.15
Mexcumin	-20.25±4.46
Solucumin	-12.8±2.43
Longvida®	-33.57±4.99
Nacumin®	-15.27±2.95

Table 4.4. Zeta-potential of commercial curcumin, Mexcumin, Solucumin, Longvida® and Nacumin® (n=3, mean ± SD)

4.4.6. Short-term stability test

A short-term stability test was conducted for determining the change of the curcumin content in commercial curcumin, Solucumin, Mexcumin, Longvida® and Nacumin® at different temperatures over a one-month period. The

percentage of remaining curcumin in each sample is shown in Table 4.5.

According to ICH guidelines, a significant change for a drug product in a stability test is a 5% change of content from its initial value (ICH, 2003). In this stability test, all samples have shown less than 5% change in their initial curcumin content. One-way ANOVA and the *post hoc* Dunnett's test showed that there is no statistically significant difference the percentages of the curcumin content at day 0 and after 1 months when at 25 °C or 40°C for all the samples($p > 0.05$).

It is worth noting that the texture of Solucumin became slightly sticky after being placed at 40 °C for 1 month. This could be due to the melting of the vitamin E TPGs.

	curcumin content (%)		
	Day 0	**After 1 months, under 25 °C**	**After 1 months, under 40°C**
Commercial curcumin	82.54 ± 5.75	78.76 ± 6.27	77.49 ± 4.14
Solucumin	6.55 ± 0.23	6.74 ± 0.45	6.05 ± 0.71
Mexcumin	10.03 ± 0.55	11.12 ± 0.42	10.90 ± 1.36
Nacumin®	7.89 ± 0.91	7.41 ± 0.73	6.58 ± 0.65
Longvida®	30.48 ± 3.32	28.38 ± 4.04	27.64 ± 2.96

Table 4.5. The percentage of the curcumin remaining in day 0, after 1 months under 25 °C and after 1 month under 40°C (n=3, Mean ± SD)

4.5. Discussion

4.5.1. Fourier-transform infrared spectroscopy (FTIR)

In the FTIR spectra of Solucumin (Figure 4.2d) and Mexcumin (Figure 4.3f), the characteristic peak of curcumin (O-H group, 3200-3500 cm $^{-1}$) could not be seen, which suggests that curcumin molecules are entrapped by the excipients rather than adsorbed on the surface of the excipients, thus hiding the characteristic signals of curcumin (Rong et al., 2014). An alternative explanation could be that curcumin content was too low a level to be detect by the instrument. On the other hand, the -OH peak of curcumin was observed in the spectrum of the physical mixture of Solucumin (Figure 4.2e) but was absent in the spectrum of the physical mixture of Mexcumin (Figure 4.3g). A possible explanation for the absence of the -OH peak of curcumin in the physical mixture of Mexcumin could be that there may have been an inhomogeneous mixing of drug and excipients during the preparation of the physical mixture with curcumin only making up to 12% of the physical mixture, while the rest were the excipients. Another possible explanation is that curcumin was dissolved in PEG400 during the preparation of the physical mixture so that its signal cannot been detected. PEG400 was in liquid form under room temperature and it was reported that curcumin is soluble in PEG400 with the solubility of 9.92 ± 0.24 mg/ml (Sharma & Pathak, 2016). However, according to the Mexcumin preparation method mentioned in section 3.3.2.2, 1 g of physical mixture of Mexcumin contains 0.05 ml of PEG400 (0.06 g, density 1.13 g/ml) (Sigma-Aldrich, 2022) and 0.12 g of commercial curcumin. Based on the reported curcumin solubility in PEG400, the amount of PEG400 in the physical mixture is only enough to dissolve around 0.41% of the commercial curcumin. Thus, PEG400 is unlikely the cause for the absence of the -OH peak of curcumin in the physical mixture of Mexcumin.

The correlation factor results showed that the spectra of Solucumin and

Mexcumin showed very low similarity to the spectrum of commercial curcumin, which indicate that either curcumin was encapsulated inside the particles of the excipients or the curcumin content was too low to be detected. Unlike curcumin, the spectra of Soluplus and Vitamin E TPGs showed much higher correlations to Solucumin, while MCC and Poloxamer 407 showed higher correlations to Mexcumin. The higher correlation factor is most likely due to the high content of these excipients in the formulations. The correlation results between the formulations and the physical mixtures showed that Solucumin and Mexcumin have some similarity in chemical structure to their correlating physical mixture, but they are not completely the same. This suggests that changes in chemical structure occurred during the formulation preparation process, which may be due to drug-excipient interactions such as formation of solid dispersion or complex, which can result in improved drug dissolution and bioavailability (Huang et al., 2008; Pugliese et al., 2021).

4.5.2. Differential scanning calorimetry (DSC)

In this study, DSC was used to measure thermal properties and the changes in physical nature of Solucumin and Mexcumin. The DSC thermograms of Solucumin (Figure 4.4d) and its physical mixture (Figure 4.4e) have shown similar patterns i.e., presence of an endothermic peak of Vitamin E TPGs at a range of 33-35°C, absence of the endothermic peak of curcumin and the glass transition point of Soluplus. It is possible that curcumin and Soluplus might have dissolved in the molten Vitamin E TPGs during the DSC measurement since Vitamin E TPGs is amphiphilic and only the endothermic peak corresponding to the melting of Vitamin E TPGs was observed in the DSC thermograms of Solucumin and the physical mixture. The disappearance of the endothermic peak of curcumin was also observed in a solid dispersion composed of curcumin, Vitamin E TPGs and Mannitol at ratio of 1:10:15 (w/w) and it was likely attributed to curcumin dissolving in the molten Vitamin E TPGs

during DSC measurement (Song et al., 2016). The ratio of curcumin to Vitamin E TPGs is also 1:10 in Solucumin, so it should have enough Vitamin E TPGs for curcumin to dissolve into. The body temperature of a human is 37ºC, which is above the measured melting point of Vitamin E TPGs. Vitamin E TPGs is very hydrophilic and dissolves quickly in aqueous solutions (Guo et al., 2013), so if some curcumin has been dissolved in molten Vitamin E TPGs, when they can be quickly released into the intestinal lumen fluid and absorbed by the intestine epithelium as they are already in solution.

In the thermogram of Mexcumin (Figure 4.5f) and the physical mixture (Figure 4.5g), only a weak endothermic peak at range 44-46 °C was observed corresponding to the melting point of Poloxamer 407. The endothermic peaks of curcumin and aerosil and the glass transition point of MCC were all absent from the DSC diagram of Mexcumin and the physical mixture. A possible explanation is the absence of the endothermic peak curcumin might be due to the dissolution of curcumin in the molten poloxamer during heating ramp since and it was reported that curcumin is soluble in poloxamers (Thapa et al., 2020). Aerosil account for less than1.3% of Mexcumin so it is likely that the amount is too little to be detected by DSC. MCC makes up about 70% of Mexcumin, so it is unlikely that all of it is dissolved in molten Poloxamer 407. The disappearance of the glass transition peak of MCC in the DSC thermogram of Mexcumin might be due to the conversion of MCC from its amorphous state to crystalline state during preparation process.

4.5.3. X-ray powder diffraction (XRD)

XRD was used to characterise polymorphic nature of the drug of Solucumin and Mexcumin and to detect if amorphous phase was present in the formulations. When the material is in a crystalline state, it will have a periodic arrangement of its atoms. As a result, the X-rays will be scattered only in certain

directions which leads to highly intense sharp peaks. If a material is in an amorphous state where the atoms are randomly arranged, X-rays will be scattered in many directions leading to a large bump distributed in a wide range resulting in smooth and broad peaks (Cullity, 1956).

The sharp and intense diffraction peaks observed from the XRD spectrum of commercial curcumin (Figure 4.6a) indicate the significant crystallinity of curcumin. Similar XRD spectrum of curcumin was reported in previous studies (Aditya et al., 2015). In this study, there were no distinct peaks of curcumin and Soluplus can be observed in the spectrum of Solucumin (Figure 4.6d). Two distinct sharp peaks were observed at 19.2 º and 23.28 º. It is possible these two sharp peaks observed in the XRD spectrum of Solucumin was due to the presence of the microcrystalline regions on the surface of the sample. These regions might have contributed by the crystalline Vitamin E TPGs, since the position, intensity and height of the sharp peaks observed in Solucumin were almost identical to the peaks observed in Vitamin E TPGs (peak positions at 19.26 º and 23.31 º). Microcrystalline regions can contribute to the overall diffraction pattern observed in XRD analysis, even if the sample as a whole is amorphous or lacking in long-range order, because these regions contain ordered arrangements of molecules on a small scale (Smit et al., 2003). The fact that the absence of all the characteristic peaks for curcumin in Solucumin would suggest curcumin was very amorphous in the formulation, which could be one of the main reasons for the significantly increased solubility and dissolution of curcumin from Solucumin. As other studies have shown, the solubility and dissolution rate of amorphous curcumin was much higher than their crystalline counterparts, due to the lack of long-order molecular arrangement of amorphous compounds which gives them higher molecular mobility and free energy. Although amorphous curcumin underwent

recrystallisation after reaching the peak solubility, which resulted in a decrease in its solubility, it still remained higher than crystalline curcumin. (Pawar et al., 2012). In contrast, the spectra of the physical mixture of Solucumin showed several sharp peaks that indicate the presence of crystalline curcumin (7.94 º, 12.26 º,14.65 º,15.9 º,18.29 º, 24.65, º27.41 º and 29.1 º), crystalline Soluplus (8.95 º, 17.44 º and 25.68 º) and crystalline Vitamin E VTPGs (19.25 º and 23.31 º).

As shown in Figure 4.7, the XRD spectra of Mexcumin and its physical mixture were almost identical to that of MCC. Almost all the characteristic peaks observed in Mexcumin and the physical mixture can be found in MCC. No peaks for curcumin, Poloxamer 407, aerosil and magnesium stearate were observed. Since MCC makes up approximately 70% of the composition in Mexcumin and the physical mixture, it is very likely that the large amount of MCC masked curcumin and other excipients, rendering their characteristic peaks undetectable by XRD. As a result, it is inconclusive to say if the curcumin in Mexcumin was in a crystalline state or an amorphous state.

As for Longvida® and Nacumin®, several sharp peaks of curcumin can be seen in their XRD, which indicated that curcumin in these formulations was very crystalline. The possession of crystalline curcumin is likely to be responsible for their poor dissolution of curcumin shown in the *in vitro* dissolution tests.

4.5.4. Dynamic light diffraction (DLS)

Particle size is an important property that should be studied when creating a new pharmaceutical product. It is crucial for the control of the drug dissolution of a pharmaceutical product since the dissolution rate is inversely proportional to the particle size for poorly water-soluble drugs. Studies have shown that amorphous solid dispersion particles with smaller particle sizes exhibited much

faster drug dissolution than the larger ones (D. Zhang et al., 2018; Zheng et al., 2019).

It has been demonstrated in Chapters 2 and 3 that Solucumin and Mexicumin are more soluble than commercial curcumin. Therefore, some of particles of the formulations could have dissolved in the solvent during the DLS measurement and the dissolved particles cannot be detected by DLS. If this occurred, what DLS actually measured was the size of the particles of the formulations that did not dissolve during the measurement. Then it would appear that the DLS results did not fully reflect the actual particle size of the formulations. However, the results are still valuable as they showed that those formulation particles that were not immediately dissolved in water were still smaller than the particle size of commercial curcumin. The smaller particle size means they might be more soluble than the commercial curcumin.

The reduction in drug particle size was likely to be another reason that is responsible for the improved dissolution due to the larger surface area which allows greater interaction with the solvent. It can possibly also lead to higher drug permeability due to the higher drug dissolution. This will be tested and discussed in Chapter 5. The smaller particle size result in higher solubility, dissolution, and bioavailability has been well documented by many studies (Anderberg et al., 1988; (Charoenchaitrakool et al., 2000) (Foster et al., 2003) Jinno et al., 2006; (Savjani et al., 2012).

The relatively larger particle size of Solucumin compared with other curcumin products could be due to the extra step of freeze-drying. It is not uncommon to see an increase in particle size from freeze-dried products, which is believed to be due to the aggregation of particles during the lyophilisation

process (Lijuan Zhang et al., 2008). Several studies have shown that freeze-dried products exhibited larger particle sizes compared with the ones have not been freeze dried (Luo et al., 2021; Parmar et al., 2011; Seyfoddin et al., 2010). It was reported that the addition of cryoprotectant such as sucrose, glucose and trehalose could effectively reduce the particle size of freeze-dried products (Almalik et al., 2017). It was reported that the sugar-based cryoprotectants prevent aggregation to occur during lyophilisation by forming H-bonding interaction with the particles thus protecting them from the stress of the freezing and drying process (Patil et al., 2010; Rampino et al., 2013).

Interestingly, despite the smaller particle sizes, Mexcumin, Longvida® and Nacumin® all exhibited much poorer curcumin release in the *in vitro* dissolution studies. This suggests that other factors such as polymorphic state of the drug, formulation composition, excipients and preparation method might have played a greater role in influencing the drug release of curcumin. In addition, although larger particles generally have poorer absorption, this is not always the case. For instance, it has been reported that larger anionic polyamidoamine dendrimers have shown higher levels of permeation across Caco-2 cell monolayers compared to smaller sized dendrimers (Bergin & Witzmann, 2013).

In addition to particle size, PdI should also be considered, as it is an indication of the particle size distribution in the suspension. When PdI is equal to 0, this means that the particles have a perfect uniformed size and when it is equal to 1, the particles are completely heterogeneously dispersed (Danaei et al., 2018). It can be noticed from the results that Solucumin, Longvida® and Nacumin® were closer to a monodisperse system, while Mexcumin was closer to a heterodisperse system.

4.5.5. Zeta potential

In general, a zeta-potential magnitude > ± 30 mV indicates sufficient repulsive force between particles and a good stability. For those with a zeta-potential < ± 5 mV will ultimately coagulate by means of different attraction forces between particles, such as van der Waals, hydrophobic interactions and hydrogen bonding (Kumar & Dixit, 2017). In this concept, commercial curcumin and Longvida® were more stable than Solucumin, Mexcumin and Nacumin® in aqueous solution due to the stronger repulsion effect between the particles.

Since the curcumin formulations are not homogenous and contain different excipients. The mean zeta-potential values detected in this study could be an amalgam of many individual values of the drug and excipients. In addition, the solubilsed curcumin from the formulations could affect the values of zeta potential. Since the solvent for Zeta potential measurement is unbuffered ultrapure water, the solublised curcumin could reduce the pH of the solvent as it is a weak acid (Priyadarsini, 2014). A decrease in pH can increase the positive charge on the surface of the particles and make zeta potential values more positive, which might explain why all the formulation samples have showed less negative zeta potential values than commercial curcumin (Bhattacharjee, 2016).

4.5.6. Short-term stability test

It is known that drugs can degrade over time, particularly with poor storage conditions which can accelerate their degradation. From the stability test results, it suggests that curcumin can stay chemically stable at room temperature and 40°C for up to one month in a sealed container. In addition, the chemical stability of curcumin was not diminished by the presence of other excipients in the formulation samples.

Curcumin is tolerant to heat and it was reported in published research studies that it can remain stable against high temperatures of up to 85°C (Dandekar & Patravale, 2009; Peram et al., 2017). The thermal resistance of curcumin probably is the main reason why curcumin was not degraded in the commercial powder and the formulation samples under the condition of this short-term stability study. This information will be helpful to determine the storage conditions.

Other factors such as the excipients may contribute to the stability of curcumin. Rani et al. reported that Soluplus reduced the degradation rate of curcumin and this was attributed to the multiple intermolecular H-bond interactions formed between the two (Rani et al., 2020). However, due to the short duration of this stability study and the fact that only one environmental factor (temperature) was considered, the information that can be derived from the data is limited. To get sufficient data for drug stability, a long-term stability study of at least 12 months and an accelerated stability study (at least 15°C above the long-term storage temperature with higher or lower humidity) of at least 6 months should be carried out in the future if possible.

4.6. Conclusion

In conclusion, this study has undertaken a series of characterisation studies to examine the physical and chemical properties of Solucumin and its comparators. The results of the FTIR analysis showed that the curcumin in Solucumin and Mexcumin was unlikely adsorbed on the surface of the excipients. DSC analysis found that Vitamin E TPGs can melt at temperatures close to the human body temperature and curcumin may dissolve in the melted Vitamin E TPGs, which might lead to rapid release of curcumin from Solucumin once the melted Vitamin E TPGs have been dissolved in aqueous solvent. The X-ray diffraction results confirmed that curcumin in Solucumin is in an amorphous state, while in other comparators such as Longvida® and Nacumin® it remains in a crystalline state. The DLS results showed that the particle sizes of all the formulation samples were smaller than the commercial curcumin powder. Finally, the short-term stability demonstrated the anti-degradation effect of Solucumin and Mexcumin for a one month.

By interpretating the results of the characterisation studies, it was revealed that the reduction in curcumin particle size and the conversion of crystalline curcumin to an amorphous state could be the main reasons for the higher dissolution of curcumin in Solucumin compared to the commercial curcumin and other comparators. In addition, the solubilisation of curcumin by molten Vitamin E TPGs may also contribute to the increase of dissolution of curcumin from Solucumin. In Chapter 5, *in vitro* drug permeability and cellular uptake studies will be conducted and it will be investigated whether these factors also affect the absorption of curcumin.

Chapter 5. *In vitro drug* permeability study using Caco-2 cell model

5.1. Introduction

The effect of Solucumin on the intestinal permeability of curcumin was investigated by *in vitro* drug permeation experiments and cellular uptake tests using a Caco-2 cell monolayer as the model. Commercial curcumin, Longvida®, Nacumin® and Mexcumin were used as the comparators in these experiments.

5.1.1. A brief introduction to drug intestinal permeability

The small intestine is the primary absorption site for many orally administrated drugs or compounds including curcumin (Esatbeyoglu et al., 2012). In the human small intestine, a single layer of epithelial cells covers the inner intestinal wall and forms the barrier for the absorption of dissolved drugs in the intestinal lumen fluids (Balimane et al., 2000). Drug intestinal permeability is a term describing the flow of a drug passing across the intestinal epithelial cells. In other words, how deep can a drug transport through the small intestinal barrier per unit of time (Dahan & Miller, 2012; Dahlgren & Lennernäs, 2019). It is a critical factor that determines the rate and extent of intestinal absorption of orally administrated drugs because drugs dissolved in intestinal lumen fluid need to pass across the epithelial cells of the small intestine so that they can reach systemic circulation (Dahlgren & Lennernäs, 2019; Martinez & Amidon, 2002). In a nutshell, to achieve high bioavailability, the orally administrated drugs need to be soluble in the intestinal lumen fluid and able to sufficiently pass through the small intestinal barrier.

In general, the permeation of drugs across the intestinal epithelial cells can be divided into four pathways: a) Transcellular diffusion, b) Paracellular diffusion, c) Transporter-mediated transcellular transport, and d) Vesicular transport (Hidalgo, 2001). A schematic diagram of the drug permeation is shown in Figure 5.1.

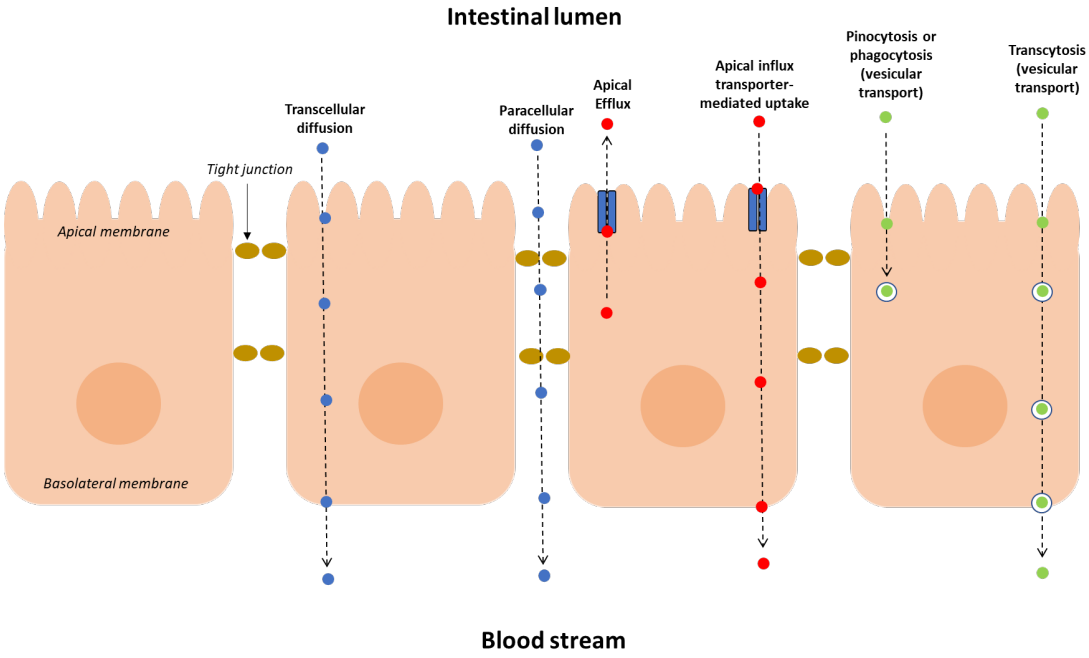

Figure 5.1. Schematic diagram of the drug permeation pathways across the intestinal epithelial cells

In passive diffusion transcellular pathway, the drugs pass through though the apical and basolateral membranes of the intestinal epithelial cells. Due to the lipid structure of intestinal epithelial cell membranes, the transcellular pathway is favoured for the permeation of lipophilic drugs. The driving force for the transcellular diffusion is the concentration gradient of the dissolved drugs between each side of the intestinal membrane, allowing drugs to move from the side with higher concentration to the side with lower concentration (Hidalgo, 2001). In contrast to transcellular transport, drugs transported by paracellular diffusion pathway are permeated through the intercellular space between the intestinal epithelial cells. This is a pathway for the permeation of hydrophilic drugs that are not able to pass through the lipid membrane of the intestinal epithelial cells. Like transcellular passive diffusion pathway, the drug concentration gradient between the intestinal membrane is the driving force for the paracellular passive diffusion pathway. The tight junctions between the cells are the major barrier to paracellular passive diffusion and they are selectively permeable to small hydrophilic molecules (radius < 1.5 nm) and ions (Madara & Pappenheimer, 1987; Salama et al., 2006).

A large number of transporters are expressed at either apical or basolateral membrane of human enterocytes and some of them can mediate the intestinal absorption of the drugs. Each transporter exhibits its own substrate specificity, although it usually exhibits a wide range of substrate specificities (Katsura & Inui, 2003). Some transporters function as influx transporters, which bind to dissolved drugs in intestinal lumen fluid and transport them across the apical membrane of the intestinal epithelial cells. On the other hand, some transporters act as efflux transporters, and they exert the opposite function to influx transporters. Efflux transporters bind the drugs in the cell cytoplasm and transport them to the intestinal lumen, thus reducing the absorption of the drugs. However, some efflux transporters play the opposite role y transporting the drugs from the cell cytoplasm into blood circulation. A schematic diagram of drug transport through the influx and efflux transporters in enterocytes was shown in Figure 5.2. A list of well-studied influx and efflux transporters in intestine is shown in Table 5.1 and 5.2 respectively.

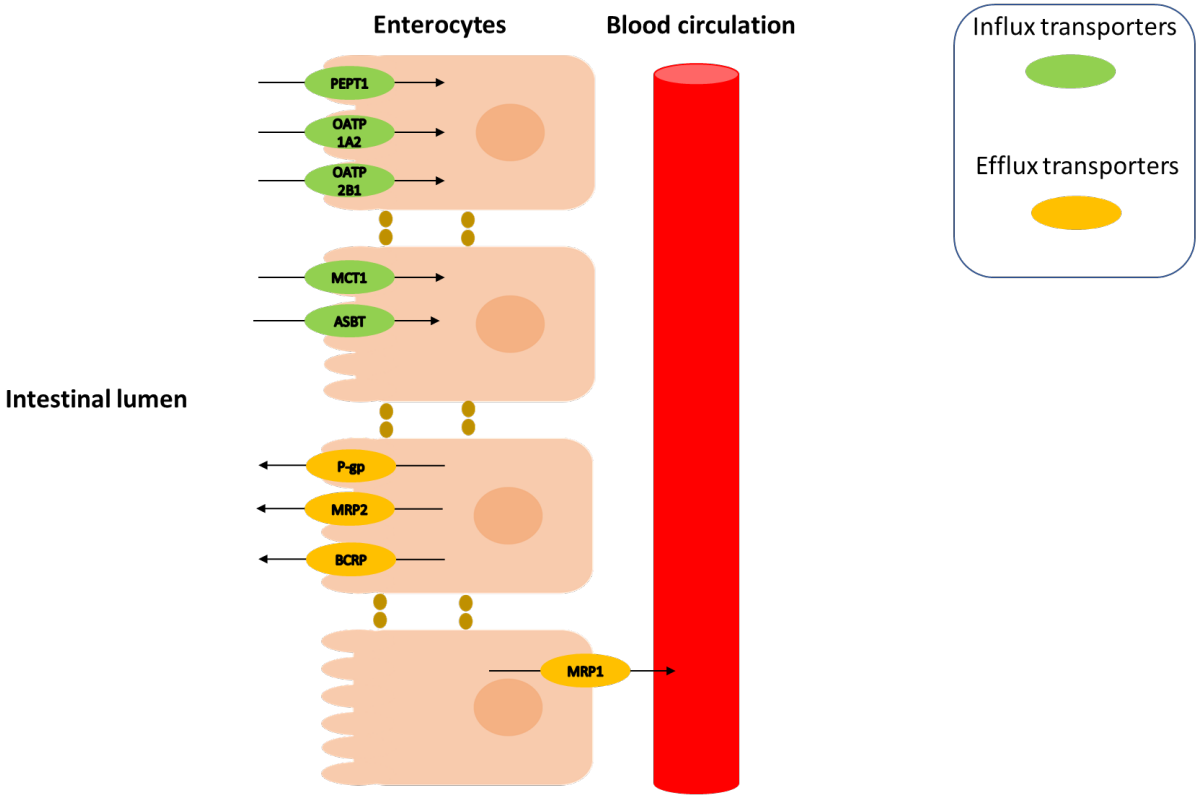

Figure 5.2. A schematic diagram of drug transport through the influx and efflux transporters in human enterocytes

Influx transporters	Examples of uptake drugs/compounds	References
H + /di-tripeptide transporter (PEPT1)	Peptide-like drugs such as angiotensin-converting enzyme inhibitors, β-lactam antibiotics, and renin inhibitor	(Katsura & Inui, 2003)
Anion-transporting polypeptide 1A2 (OATP-1A2)	Erythromycin, Fexofenadine, Imatinib, Levofloxacin, Methotrexate, Ouabain and Pitavastatin	(Kalliokoski & Niemi, 2009)
Anion-transporting polypeptide 2B1 (OATP-2B1)	Atorvastatin, Benzylpenicillin, Bosentan, Fexofenadine, Fluvastatin, Glibenclamide, Pravastatin and Rosuvastatin	(Kalliokoski & Niemi, 2009)
Monocarboxylic acid transporter 1 (mct1)	Lactate, pyruvate, butyrate, acetoacetate, β-hydroxybutyrate	(Vijay & Morris, 2014)
apical sodium–bile acid transporter (ASBT)	Bile acid	(Dawson, 2011)

Table 5.1. List of well-studied influx transporters in human small intestine

Efflux transporters	Examples of efflux drugs/compounds	Reference
P-glycoprotein (P-gp)	Digoxin, vinblastine, saquinavir, indinavir and paclitaxel	(Hochman et al., 2001; Sparreboom et al., 1997; Stephens et al., 2001)
multidrug resistance-associated protein 2 (MRP2)	Epigallocatechin gallate (EGCG) and saquinavir	(Hong et al., 2003; G. C. Williams et al., 2002)
breast cancer resistance protein (BCRP)	Topotecan	(Kruijtzer et al., 2002)
multidrug resistance-associated protein 1(MRP1)	Vincristine, etoposide, anthracyclines, and methotrexate.	(Johnson & Chen, 2017)

Table 5.2. List of well-studied efflux transporters in human small intestine

Vesicular transport is an intestinal permeation pathway that is responsible for the absorption of macromolecules. The mechanism of action of this pathway is to entrap substances within a vesicle and then transport it into cells. There are two types of vesicular transport: Pinocytosis and phagocytosis. Pinocytosis is for relatively small macromolecules solutes (fats, vitamins A, D, E, K and B12) while phagocytosis is for relatively large macromolecule particles (bacteria or whole cells) (Hidalgo, 2001). During the vesicular transport, the macromolecules are first surrounded by an area of the apical cell membrane, which then buds off inside the cell to form a vesicle containing the ingested macromolecules. This transport process is also known as endocytosis (Hidalgo, 2001; van Breemen & Li, 2005). After endocytosis, the macromolecules entrapped in the vesicle are usually destroyed along with the vesicle by lysosomes, a membrane-bound cell organelle that contains digestive enzymes. However, sometimes the vesicle can by-pass the lysosomes, transport across the basolateral membrane and release the entrapped molecules from the vesicle to blood circulation. This phenomenon is known as transcytosis and it could facilitate the intestinal absorption of substances that are unable to pass through the intestinal epithelial cell membrane via passive diffusion or transporter-mediated pathways (Fung et al., 2018; Hidalgo, 2001).

5.1.2. A brief introduction to Caco-2 cell model

Caco-2 cells are human colon epithelial cancer cell line with characteristics like those of intestinal epithelial cells, such as the formation of polarised monolayers with well-defined brush borders and tight junctions. As shown in Figure 5.3 a) and b), Caco-2 cells grown on permeable filters can be used as a model for *in vitro* bidirectional drug permeation experiments (from apical side to basolateral side and basolateral side to apical side) to determine drug intestinal permeability as well as predict the intestinal absorption and intestinal secretion (i.e., basal uptake and apical efflux) of drugs and compounds. The apical and basolateral chambers represent the luminal and blood/mesenteric lymph sides of the gastro-intestinal tract, respectively (Artursson et al., 2001; van Breemen & Li, 2005). More details of the protocol for the determination of drug permeability in Caco-2 monolayers

has been described in section 5.3.6.

Lennernäs et al. (Lennernäs et al., 1996) found that the rate of drug permeation measured in Caco-2 cell models was similar to that measured in human jejunum for drugs predominantly absorbed by transcellular passive diffusion. However, for drugs absorbed by paracellular pathway or transporters, the rate of drug permeation measured in Caco-2 cell models was found to be lower than that measured in human jejunum. This was probably because Caco-2 cell monolayers have narrower tight junctions and the lower expression of apical influx transporters than intestinal epithelial cells (Fine et al., 1995; Lennernäs et al., 1996; Watson et al., 2001).

Most of the human intestinal transporters can be found in Caco-2 monolayers. Influx transporters observed on the apical membrane of Caco-2 cell monolayers include organic anion-transporting polypeptide 2B1 (OATP-B) (Sai et al., 2006), H + /di-tripeptide transporter (PEPT1)(Saito et al., 1997), monocarboxylic acid transporter 1 (MCT1) (Tamai et al., 1995), apical Na+ -dependent bile acid transporter (ASBT)(Hidalgo & Borchardt, 1990) and the organic cation/carnitine transporter (OCTN2) (Elimrani et al., 2003). These transporters facilitate the drug absorption into the cells. On the other hand, efflux transporters such as multidrug resistance protein 1 (MDR1, or P-glycoprotein, P-gp) (Hunter et al., 1993), multidrug resistance-associated protein 2 (MRP2) (Gutmann et al., 1999) and the breast cancer resistance protein (BCRP) (Xia et al., 2005) were also expressed on the apical membrane. Their role is to remove the Intracellular drugs by pumping out to the apical lumen of the Caco-2 cells.

Efflux transporters are also expressed in the basolateral membrane of Caco-2 cell monolayers, but their role is to facilitate the absorption of drugs by transporting the intracellular solutes into the basolateral lumen of the cells. The basolateral efflux transporters observed in Caco-2 cell monolayers include Multidrug resistance proteins MRP1,MRP3, MRP4, MRP6 (Bock-Hennig et al., 2002;

Hirohashi et al., 2000; Prime-Chapman et al., 2004) and organic solute transporter alpha-beta (OSTα-OSTβ) (Okuwaki et al., 2007).

Several metabolic enzymes that are expressed in human intestine can be observed in Caco-2 cell monolayers, such as cytochrome P450 1A (CYP1A) (Lampen et al., 1998), sulfotransferases (SULTs) (Baranczyk-Kuzma et al., 1991), UDP-glucuronyltransferases (UGTs) (Galijatovic et al., 2001) and the glutathione S-transferases (GSTs) (Peters & Roelofs, 1989). However, Cytochrome P450 3A4 (CYP3A4) is poorly expressed in Caco-2 cells (Sun et al., 2008).

As a model for determining intestinal drug permeability, Caco-2 cell monolayers have many advantages over other models. In comparison with biological models such as *in vivo* animal test, *in situ* intestinal segments and inverted gut sacs, Caco-2 cell lines are easier to acquire, less labor and cost-intensive and does not have the ethical issues that normally occur in animal tests or using human tissues (Balimane et al., 2000). In addition, Caco-2 cell models can be used to determine drug permeation via several pathways which include transcellular passive diffusion, paracellular passive diffusion, vesicular transport, active transport and facilitated transport. In contrast, non-biological models such as immobilised artificial membranes, parallel artificial membranes and in silico computer models of membrane diffusion can only work on the presumption that drug absorption is only through transcellular passive diffusion (Balimane et al., 2000; van Breemen & Li, 2005).

Based on the advantages described above, Caco2 cell lines were selected as the model for the *in vitro* drug permeation experiments and cellular uptake tests in this study.

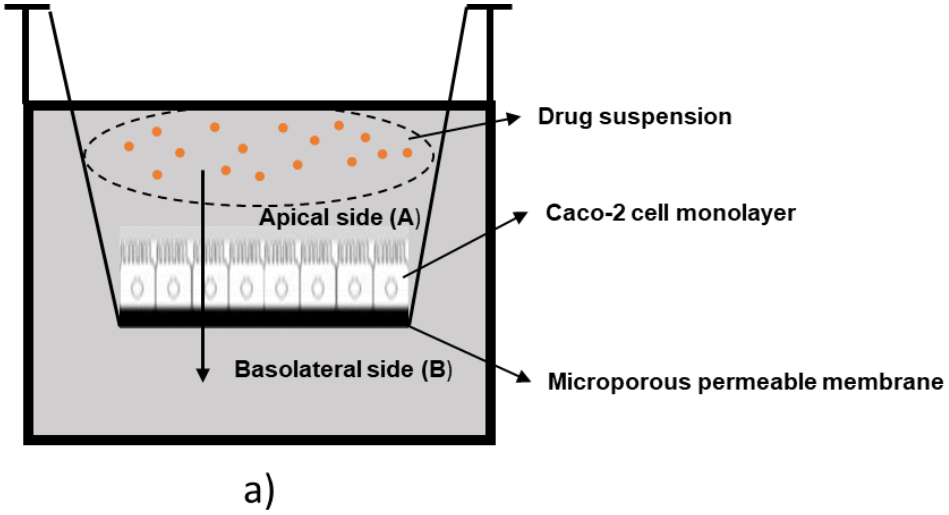

a)

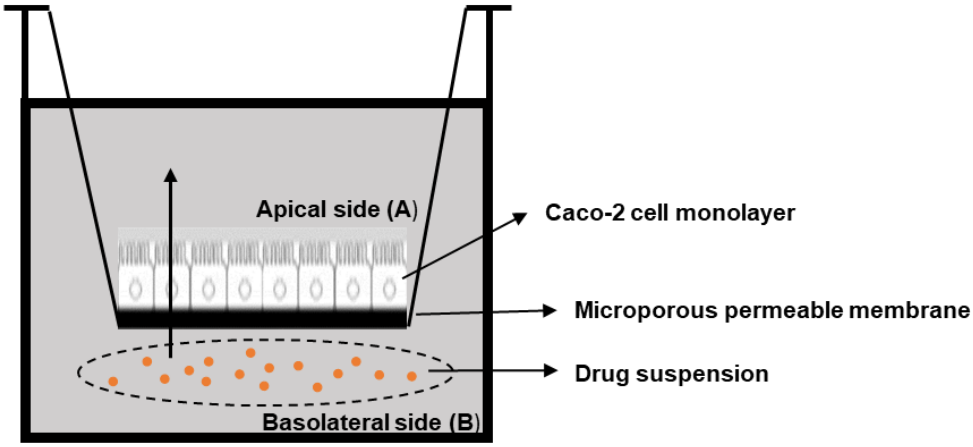

b)

Figure 5.3. Diagrams of drug permeation across the Caco-2 monolayer grown on a permeable filter support from a) Apical side to Basolateral side (A-B) b) Basolateral side to Apical side (B-A)

5.2. Aims

- To determine the least cytotoxic concentration of curcumin on Caco-2 cells by conducting cytotoxicity assays (MTT and LDH assays).
- To determine the intestinal permeability of curcumin from Solucumin, Mexcumin, Longvida® and Nacumin® by conducting *in vitro* drug permeation experiments using Caco-2 cell monolayer as the model.
- To determine the cellular uptake of curcumin (intracellular drug accumulation) from Solucumin, Mexcumin, Longvida® and Nacumin® by conducting cellular uptake tests after completing the *in vitro* drug permeation experiments.

5.3. Materials and methods

5.3.1. Materials

The materials used for the formulations and HPLC analysis were the same as those described in section 3.3.1. The human colon adenocarcinoma cell line, Caco-2 cells, was provided by European Collection of Authenticated Cell Cultures (Salisbury, UK). Gibco® Dulbecco's modified Eagle's medium (DMEM) high glucose with L-glutamine, without Sodium Pyruvate, Fetal bovine serum (FBS), Gibco® MEM Non-Essential Amino Acids (NEAA) solution, Gibco® Penicillin-Streptomycin solution (10,000 U/ml) and Dimethyl Sulfoxide (DMSO) were purchased from Fisher Scientific Ltd. (Loughborough, UK).

Gibco® Trypsin-EDTA (0.25%) solution was obtained from Merck Life Science UK Limited (Gillingham, UK). Hank's balanced salt solution without phenol red (HBSS), HEPES(4-(2-hydroxyethyl)-1-piperazineethanesulfonic acid), L-lactate lithium salt, ß-Nicotinamide adenine dinucleotide (ß-NAD), 1-methoxyphenazine methosulfate (MPMS), Thiazolyl Blue Tetrazolium Bromide (MTT), Tris-HCl buffer (Trizma hydro-chloride buffer solution), 1M, pH 8.0 and Triton X-100 were purchased from Sig-ma-Aldrich Ltd. (Gillingham, Dorset, UK).

5.3.2. Preparation of Solucumin and Mexcumin

Solucumin and Mexcumin were prepared using the same methods mentioned in section 3.3.2.1 and 3.3.2.2.

5.3.3. Caco-2 cell culture

Caco-2 was grown in T-75 cm^2 cell culture flasks (Corning, USA) at 37 °C with 5% CO_2. The cell culture medium consists of DMEM + 10% (v/v) FBS + 1% (v/v) NEAA + 1% (v/v) penicillin-streptomycin solution. Caco-2 cells were passaged every 3 days when the cell density reached 80% confluence at 1:3 split ratio. During passages, the old cell medium was removed from the flasks and the cells were washed with phosphate-buffered saline (PBS). 5 ml of Trypsin-EDTA (0.25%)

was added to each flask and incubated at 37 °C with 5% CO_2 for 2-3 minutes to detach the cells from the flasks. After trypsinisation, 5 ml of the cell medium was added and the suspension containing the Caco-2 cells was centrifuged for 5 minutes at 500 rpm. After removal of the supernatant, the cell pellets were added to new cell culture flasks with fresh cell medium and incubated at 37°C with 5% CO_2. All Caco-2 cells were used between passages 40-50 for MTT assay, LDH assay, drug permeation experiments and cellular uptake tests. It was reported that Caco-2 cells with passage number < 40 showed extremely low P-gp expression (Senarathna & Crowe, 2015). Furthermore, Caco-2 cells with higher passage levels have been reported to express fewer transporters at the apical membrane, which may lead to a reduction in carrier-mediated drug transport (Yu et al., 1997). As a result, Caco-cells with passage numbers 40-50 were used in this study.

5.3.4. Cytotoxicity tests (MTT and LDH assays)

Cytotoxicity of each test sample on Caco-2 cells were measured using MTT ((3-(4,5-dimethylthiazol-2-yl)-2,5-diphenyltetrazolium bromide) and LDH (lactate dehydrogenase) assays. According to the MTT and LDH assay results, the least cytotoxic drug concentration was selected to prepare the donor suspension used in the in vitro drug transport study. DMEM + 10% (v/v) FBS + 1% (v/v) NEAA + 1% (v/v) penicillin-streptomycin solution was used as the cell culture medium in both assays. Weighted powders of Solucumin, Mexcumin, Longvida®, Nacumin® and commercial curcumin were added to 10 ml of the cell culture medium respectively to prepare sample suspensions with curcumin equivalent concentrations of 0.08 mM(equivalent to 29.47 μg/ml), 0.1 mM (equivalent to 36.84 μg/ml) , 0.2 mM(equivalent to 73.68 μg/ml) , 0.5 mM(equivalent to 184.19 μg/ml), 0.8 mM (equivalent to 294.70 μg/ml) and 1 mM (equivalent to 368.38 μg/ml) . The sample suspensions were then sonicated for 1 minute by an ultrasonic pro-processor (Cole-Parmer, USA) to generate homogenised suspensions. The amount of each formulation required for preparing 1ml of the sample suspensions was shown in Table 5.3.

	Commercial curcumin (mg)	**Longvida® (mg)**	**Nacumin® (mg)**	**Solucumin (mg)**	**Mexcumin (mg)**
0.08mM	0.36	0.96	4.12	4.37	3.31
0.1mM	0.45	1.20	5.15	5.47	4.13
0.2mM	0.90	2.40	10.30	10.93	8.27
0.5mM	2.26	6.01	25.76	27.33	20.67
0.8mM	3.62	9.61	41.22	43.72	33.08
1mM	4.52	12.01	51.52	54.66	41.34

Table 5.3. The amount (mg) of each formulation and commercial curcumin required for preparing 1ml of sample suspensions with curcumin equivalent concentrations range from 0.08mM to 1mM

5.3.4.1. MTT assay

Caco-2 cells were seeded at a density of 4×10^4 cells/well in 50 µl cell culture medium in a 96-well plate (Fisher Scientific Ltd., Loughborough, UK) and incubated at 37℃ with 5% CO_2. The culture medium at each well was replaced every day. After 24 hours of incubation, the cell culture medium was replaced with 100 µl of sample suspension in each well. The wells containing Caco-2 cells with no sample suspension contained 100 µl of cell culture medium as the control.

The cells were exposed to the test sample for 24 hours in the incubator at 37 ℃ with 5% CO_2. Subsequently, cell culture medium or sample suspension was removed and 50 µl of 5 mg/ml MTT solution (prepared in PBS) was added to each well and incubated for another 4 h to allow MTT to be metabolized. Finally, the MTT solution was removed and 200 µl of DMSO was added per well. The plate was gently shaken on an orbital shaker for 20 minutes to dissolve the formazan crystals. The formazan concentration was measured by a spectrophotometer plate reader (Perkin Elmer, USA) at 540 nm. The MTT assay was repeated 3 times and in each assay, every sample was tested in six replicates. Percentage of cell viability was calculated using Equation 5.1.

$$\%\ Cell\ viability = \frac{Mean\ absorbance\ from\ sample\ treated\ cells}{Mean\ absorbance\ from\ untreated\ cells\ (control)}\ X\ 100 \quad \textbf{Equation 5.1}$$

5.2.4.2. LDH assay

LDH substrates mixture solution (15 ml) was prepared by mixing the ingredients shown in Table 5.5.

Ingredient	Amount/15 ml
Tris-HCL	13.5 ml
L-lactate	37.5 mg
ß-NAD	37.5 mg
MTT	3.75 mg
MPMS	0.51 mg
1% (v/v) Triton-X100	1.5 ml

Table 5.4. The ingredients for preparing 15 ml of LDH substrates mixture

Caco-2 cells were seeded at a density of 4×10^4 cells/well in 50 µl cell culture medium in a 96-well plate (Fisher Scientific Ltd., Loughborough, UK) and incubated at 37 ℃ with 5% CO2. After 24 h of incubation, the cell culture medium was replaced with 100 µl of sample suspension. In addition, 100 µl of 2% (v/v) Triton-X100 solution (prepared in cell culture medium) was added to the wells with no sample suspension. This is to completely kill the cells so they can be used as positive controls. Wells containing Caco-2 cells with cell culture medium and no sample suspension were used as negative controls.

The plate was incubated for 24 hours after which 50 µl LDH substrate mixture solution was added to each well and incubated at 37℃ with 5% CO_2 for 15 min. The absorbance was measured by spectrophotometer plate reader (Perkin Elmer, USA) at 540 nm. The percentage of LDH release was calculated using Equation 5.2:

$$\%\ LDH\ release = \frac{Mean\ absorbance\ from\ sample\ treated\ cells}{Mean\ absorbance\ from\ completely\ killed\ cells\ (high\ control)}\ X\ 100$$

Equation 5.2

5.3.5. Measurement of transepithelial electrical resistance (TEER)

TEER was measured at room temperature after 21 days of the cell culture with an epithelial volt-ohmmeter equipped with an STX2 “chopstick” electrodes (EVOM2™, World Precision Instruments, USA). TEER reading was also carried out before and after the *in vitro* drug transport experiment. Before measuring the resistance values of each well, the apical and the basolateral chambers were washed twice with pre-warmed HBSS at pH 6.5 (buffered with 0.35 mg/ml $NaHCO_3$ and 10 mM methanesulfonic acid) and at pH 7.4 (buffered with 25 mM HEPES and 0.35 mg/ml $NaHCO_3$), respectively. An apical pH of 6.5 and a basolateral pH of 7.4 was used to mimic the intestinal microclimate. Resistance values of the cell monolayers on the permeable membrane (R_{TOTAL}) and the resistance values of the permeable membrane with no cells (R_{BLANK}) were measured. The specific cell resistance values (R_{TISSUE}) were calculated by the following equations (equation 5.3 and 5.4):

$$R_{TISSUE}\ (\Omega) = R_{TOTAL}\ (\Omega) - R_{BLANK}(\Omega) \qquad \textbf{Equation 5.3}$$

TEER values of the Caco-2 cell monolayers can be calculated using this equation:

$$TEER\ (\Omega * cm^2) = R_{TISSUE}\ (\Omega) \times A_{MEMBRANE}\ (cm^2) \qquad \textbf{Equation 5.4}$$

$A_{MEMBRANE}$ = the area of the permeable membrane of the insert, which is 1.12 cm^2.

To ensure the membrane integrity, Caco-2 cell monolayers with TEER values below 200 Ω cm^2 were discarded.

5.3.6. *In vitro* drug permeation experiments

The transport of curcumin from Solucumin, Mexcumin, Longvida®, Nacumin® and commercial curcumin through Caco-2 cell monolayers was assessed in both apical-to-basolateral (A-B) and basolateral-to-apical (B-A) directions at a curcumin equivalent concentration of 0.1 mM (equivalent to 36.84 µg/ml). The procedure of

the in vitro drug transport test was according to the protocol reported by Hubatsch et al. (Hubatsch et al., 2007). The apical and basolateral sides of the Caco-2 cell monolayer represent the intestinal lumen and blood/mesenteric lymph sides of the intestinal tract, respectively.

Caco-2 cells were seeded onto 12mm polycarbonate cell culture inserts with area of 1.12 cm^2 and pore size of 0.4 μm (Sarstedt, Nümbrecht, Germany) at a concentration of 4×10^5 cells per insert and placed in 12-well cell culture plates (Sarstedt, Nümbrecht, Germany). DMEM + 10% (v/v) FBS + 1% (v/v) NEAA + 1% (v/v) penicillin-streptomycin solution was used as the cell culture medium for the cell seeding process. The apical chamber was filled with 0.5 ml cell suspension containing 8×10^5 cells/ml of Caco-2 cells (prepared by cell culture medium) and the basolateral chamber was filled with 1.5 ml cell culture medium solution. The cell culture plates were incubated at 37℃ with 5% CO_2 for 16 hours. After the incubation, the cell culture medium in the apical chamber was replaced to remove non-adherent cells to reduce the risk of multilayer formation. The plates were incubated again at 37℃ with 5% CO_2 overnight. The following day the cell culture medium in the apical and basolateral chambers was replaced and the plates were incubated for 21 days under the same condition. The cell medium at both compartments was replaced every second day. After 21 days, Caco-2 cell monolayers were observed under a light microscope (Zeiss primovert, Germany) to check the integrity of the Caco-2 cell monolayers. The cell culture medium in both chambers was then removed and the cell monolayers on the inserts were washed twice with warmed HBSS to remove traces of cell culture medium. Subsequently, cells were incubated with pH 6.5 HBSS on the apical side and pH 7.4 HBSS on the basolateral side for 15 minutes at 37℃ with 5% CO_2.

For the A-B drug permeation experiments, donor suspensions of Solucumin, Mexcumin, Longvida®, Nacumin® and commercial curcumin at a curcumin equivalent concentration of 0.1 mM (equivalent to 36.84μg/ml) were prepared in pH 6.5 HBSS (buffered with 0.35 mg/ml NaHCO3 and 10 mM methanesulfonic

acid). For the B-A drug permeation experiments, suspensions were prepared in pH 7.4 HBSS (buffered with 25 mM HEPES and 0.35 mg/ml $NaHCO_3$). The suspensions were sonicated for 1 minute by an ultra-sonic pro processor (Cole-Parmer, U.S) to generate homogenised suspensions. Information on the amount of each formulation and commercial curcumin required to prepare 1 ml of sample suspension containing 0.1 mM of curcumin can be found in Table 5.3, as shown in section 5.3.4.

A-B drug permeation experiments were conducted by adding 1.2 ml pH 7.4 buffered HBSS to the basolateral chamber and 0.4 ml of suspension to the apical chamber. Aliquots (0.05 ml) were immediately withdrawn from each apical compartment (t = 0). The concentration of the dissolved curcumin measured in these samples were known as C_0 (suspension), (A-B) in this study.

Cells were incubated at 37°C in an incubator equipped with an orbital shaker with a speed of 100 rpm to minimise the effect of unstirred water layers (Hubatsch et al., 2007). A sample volume of 0.5 ml was then collected from the basolateral compartment at time points of 10, 30, 60, 90, 120 and 180 minutes and the volume withdrawn was replaced by the same volume of pre-warmed pH 7.4 buffered HBSS. At the end of the A-B drug transport experiment, aliquots of 0.05 ml were withdrawn from the apical chamber (t = 180).

For B-A drug permeation experiments, 1.2 ml pH 7.4 suspension was added to the basolateral chamber and 0.4 ml of pH 6.5 buffered HBSS was added to the apical chamber. Aliquots (0.05 ml) were immediately withdrawn from each basolateral compartment (t = 0). The concentration of the dissolved curcumin measured in these samples were known as C_0 (suspension), (B-A) in this study. Once again, cells were incubated at 37°C in an incubator equipped with an orbital shaker at speed of 100 rpm. A sample volume of 0.2 ml was then collected from the apical compartment at time points of 10, 30, 60, 90, 120 and 180 minutes and the volume withdrawn was replaced by the same volume of pre-warmed pH 6.5

HBSS. At the end of the B-A drug transport experiments, aliquots of 0.05 ml were withdrawn from the basolateral chamber (t = 180).

The concentration of curcumin passing through the Caco-2 cell monolayers, and the initial and final concentrations of curcumin in the donor chambers were measured by HPLC. Samples were analysed using a SphereClone™ C-18 reverse phase silica column (SphereClone™, 150 x 4.6 mm, 5 µm particle size) on an Agilent 1100 HPLC system (Agilent Technologies, US) with a solvent cabinet, pump system, UV–visible detector and manual injection valve. 20 µl of each sample was injected manually onto the HPLC system using a manual syringe (Agilent, needle length 50mm, volume 100µl, Agilent Technologies, US). The mobile phase consisted of a 55:45 mixture of 0.1% v/v ortho-phosphoric acid and acetonitrile solutions, with an isocratic flow rate of 0.8 ml/min and a run time of 15 minutes for each sample. Curcumin was detected at 430 nm using a UV-visible detector. Calibration curves were plotted for curcumin with the concentration range from 0.01 to 1 µg/ml for determining the concentration of curcumin passed through the Caco-2 cell monolayers. In addition, curcumin calibration curves with the concentration range from 0.01 to 20 µg/ml were plotted for determining C_0(suspension). All the calibration curves showed a linear relationship with a correlation coefficient of $R^2 > 0.995$. Examples of the calibration curves of curcumin was shown in Figures 5.4 and 5.5.

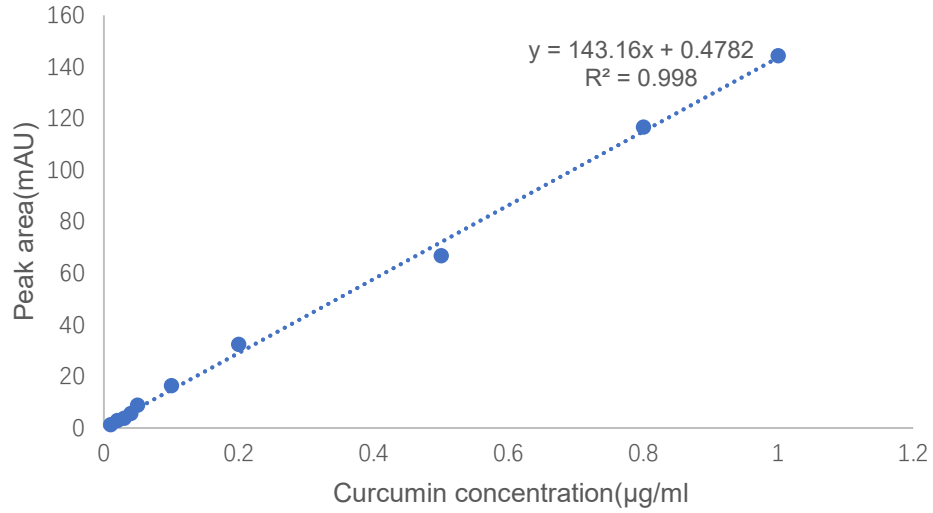

Figure 5.4. Calibration curve of curcumin for determining the concentration of curcumin permeation across the Caco-2 cell monolayer

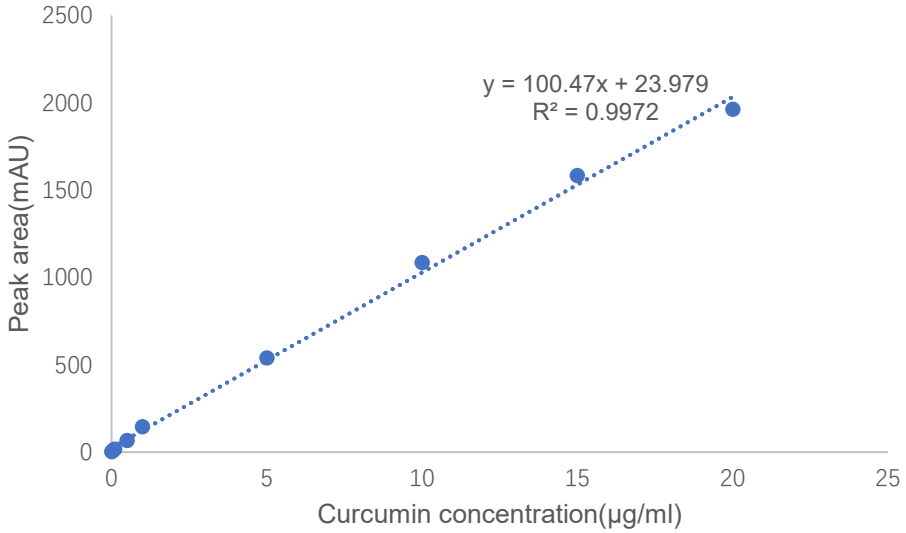

Figure 5.5. Calibration curve of curcumin for determining C_0(suspension)

The *in vitro* drug permeation experiments (A-B and B-A) for all the tested samples were repeated for 3 times on different days. At each drug permeation experiment, each sample was tested in 3 replicates. The averages concentration of permeated curcumin (A-B and B-A) measured from the three repeated experiments were expressed as the mean ± standard deviation (n = 9).

Permeability coefficient (Papp) is also calculated as a quantitative measure of the rate at which a molecule can cross a membrane and an evaluation index of drug permeability. Papp(A-B) and Papp (B-A) were be calculated using by the following equations (Equation 5.5 and 5.6).

$$Papp(A-B) = \frac{dQ}{dt}(A-B)\ X\ \frac{1}{A\ C_{0(A-B)}} \qquad \textbf{Equation 5.5}$$

dQ/dt (A-B) = The change in concentration in the basolateral side over time (μg/ml·s)

A = The surface area of the permeable membrane of the cell culture inserts (cm^2)

$C_{0(A\text{-}B)}$ = The initial drug concentration in the apical side (μg/ml)

$$Papp(B-A) = \frac{dQ}{dt}(B-A)\ X\ \frac{1}{A\ C_{0(B-A)}} \qquad \textbf{Equation 5.6}$$

dQ/dt (B-A) = The change in concentration in the apical side over time (μg/ml·s)

A = The surface area of the permeable membrane of the cell culture inserts (cm^2)

$C_{0(B\text{-}A)}$ = The initial drug concentration in the basolateral side (μg/ml)

The Papp results of each tested sample presented in this study were the averages of the three repeated experiments and were expressed as the mean ± standard deviation (n = 9).

5.3.7. Efflux ratio

Efflux ratio, an index to estimate the magnitude of drug efflux during the drug permeation, was calculated by Equation 5.7.

$$Efflux\ ratio\ (ER) = \frac{Papp\ (B-A)}{Papp\ (A-B)} \qquad \textbf{Equation 5.7}$$

5.3.8. Cellular uptake tests

After completing the *in vitro* drug transport experiment, the Caco-2 cell monolayer of each 12-well transparent membrane insert was washed twice with phosphate buffer pH 7.4 followed by the addition of 0.5 ml of trypsin EDTA solution. The insert was then incubated for 10 minutes at 37°C to allow the Caco-2 cells to detach. An aliquot (1 ml) of DMSO was added to each insert to dissolve any curcumin accumulated in the Caco-2 cells. The collected Caco-2 cell suspension was centrifuged at 1000 rpm for 5 minutes. The solvent layer containing curcumin was then separated from the cell lysate and transferred to a glass vial and DMSO was evaporated to dryness using nitrogen. An aliquot of 1 ml of ethanol was then added to fully dissolve curcumin accumulated in the cells, diluted 1:1 using mobile phase solution and analysed by HPLC to determine the cellular uptake of curcumin for each test sample. The results presented in this study were the average of three individual experiments and expressed as mean ± standard deviation (n = 9).

5.3.9. Statistical analysis

Statistical analysis of the data of the MTT assay, LDH assay, the drug permeation concentration at each time point, C_0(Suspension) and the cellular drug uptake were carried out by One-way ANOVA with Post Hoc Tukey test, respectively. A Tukey test was selected as the Post Hoc multi-comparison because it is the most common for comparing all possible group pairings (Day & Quinn, 1989). Paired t-tests were used for statistical analysis of TEER data, Papp(suspension) and Papp(solution) data, respectively. All statistical analysis was conducted by using IBM SPSS Statistics software (Version 24.0; IBM Corp, Armonk, NY, USA).

5.4. Results

5.4.1. Cytotoxicity tests (MTT and LDH assays)

As shown in Figure 5.6, MTT assay results showed the cell viability of Caco-2 cells decreased in a curcumin concentration-dependent manner. The cell viabilities were higher than 80% when the curcumin concentration was at 0.1 mM and 0.08 mM. There was no significant difference in cell viability at curcumin concentrations of 0.08 mM and 0.1 mM ($p > 0.05$) for all test samples.

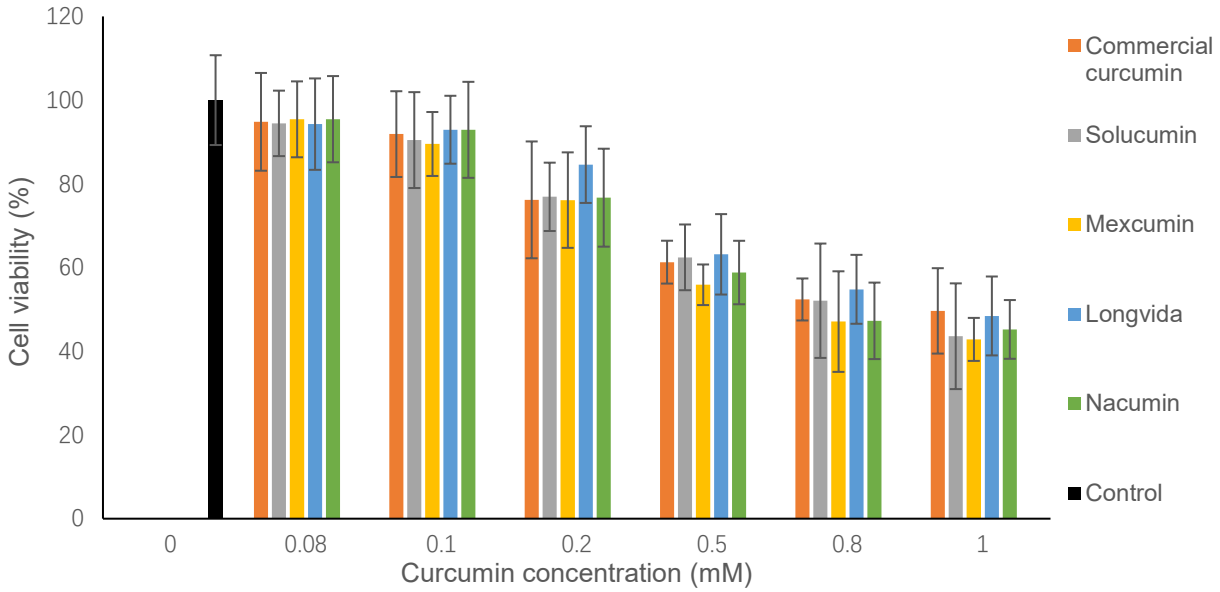

Figure 5.6. Cell viability of Caco-2 cells when exposed to each formulation with equivalent curcumin concentrations from 0.08 to 1 mM (n=18, mean ± SD). No significant differences were found between 0.08 mM and 0.1 mM ($p > 0.05$) for all test samples

The percentage of LDH release into the cell culture medium was used as the indicator of cell death. LDH assay was complementary to MTT assay. As shown in Figure 5.7, the percentage of LDH released from Caco-2 cells increased in a curcumin concentration-dependent manner. The effect of the sample on the LDH release from Caco-2 cells was at a minimum when the curcumin concentration was ≤0.1 mM. All formulations and commercial curcumin showed no significant difference in LDH release at 0.08 mM and 0.1 mM ($p > 0.05$).

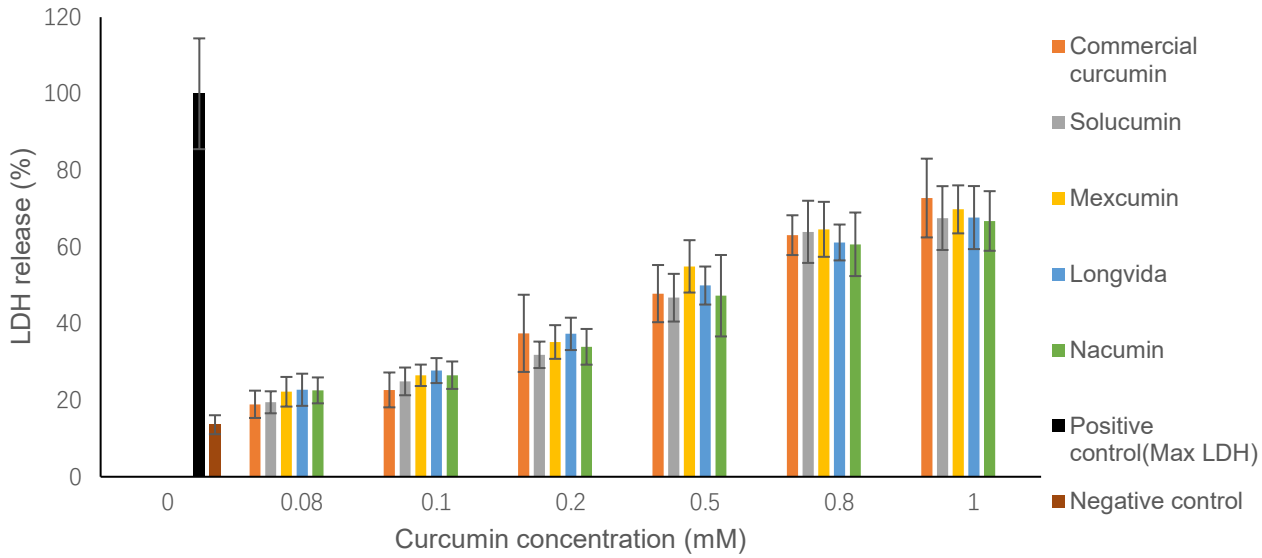

Figure 5.7. The percentage of LDH released from Caco-2 cells when exposed to each formulation with equivalent curcumin concentrations from 0.08 to 1 mM (n=18, mean ± SD). All formulations and commercial curcumin showed no significant difference in LDH release at 0.08 mM and 0.1 mM ($p > 0.05$)

5.4.2. *In vitro* drug permeation experiments and measurement of transepithelial electrical resistance (TEER)

In this study, the *in vitro* permeation of curcumin was studied using Caco-2 cell monolayers. After 21 days, a thin film was formed on the transparent membrane of the inserts. Observation under a light microscope (Zeiss Primostar 1 Upright Compound Microscope, Germany) revealed well-formed cylindrical polarised monolayer of Caco-2 cells (Figure 5.8). Caco-2 cells showed an average TEER value of 299 ± 52 Ω cm^2 during 21 days of cell seeding, indicating that the cells had formed a functional barrier. Those cells with TEER values below 200 Ω cm^2 were discarded due to the damage to membrane integrity.

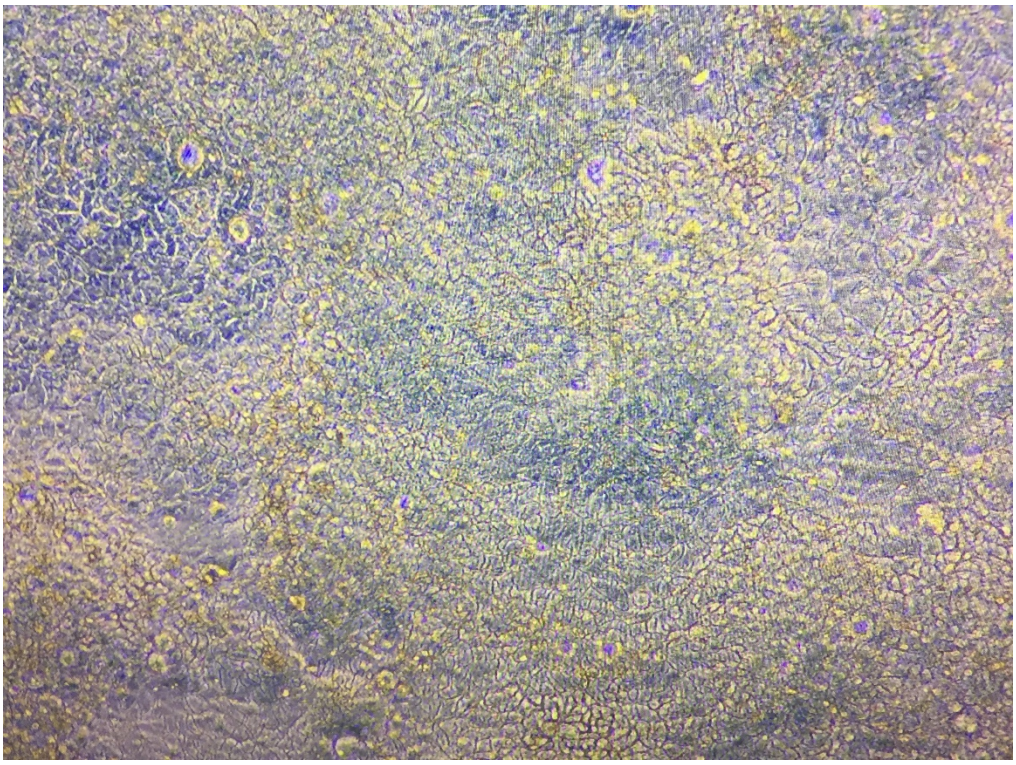

Figure 5.8. Light microscope image of well-formed Caco-2 cell monolayer after 21 days cell culture (20× magnification)

The TEER of the Caco-2 cell monolayers in the *in vitro* drug permeation experiments was measured before and after each experiment. As shown in Table 5.5, at the end of the drug transport experiment, TEER readings significantly decreased ($p \leq 0.05$) for all the test samples.

	At t = 0 min	After t = 180 min
Commercial curcumin	328 ± 23	271 ± 23
Solucumin	330 ± 28	270 ± 28
Mexcumin	316 ± 56	270 ± 50
Longvida®	313 ± 48	257 ± 35
Nacumin®	330 ± 57	271 ± 58

Table 5.5. Average TEER readings of Caco-2 cell monolayers at the start and end of the in vitro drug transport experiment (Ω cm^2) (n=9; mean± S.D)

As shown in Figure 5.9, the concentration of curcumin passing through the Caco-2 cell monolayers and transported into the basolateral side from A-B were seen to increase with the exposure time for Solucumin, Mexcumin, Longvida® and Nacumin®. At the end of the transport experiment (t = 180 min), Solucumin showed the highest curcumin permeation concentration of 0.49 ± 0.07 µg/ml (equivalent to 0.00133 ± 0.00019 mM), followed by Mexcumin of 0.11 ± 0.03 µg/ml (equivalent to 0.00030 ± 0.00008 mM), Nacumin® of 0.09 ± 0.01 µg/ml (equivalent to 0.00024 ± 0.00003 mM) and Longvida® of 0.04 ± 0.00 µg/ml (equivalent to 0.00011± 0.00001 mM). On the other hand, in considering transport in the B-A direction, Solucumin was the only sample that showed curcumin transport with a cumulative total of 0.19 ± 0.04 µg/ml (equivalent to 0.00052 ± 0.00011 mM) (Figure 5.10). Curcumin transport was not detected from commercial curcumin in either the A-B or B-A directions.

According to the results of the One-way ANOVA there were significant differences among the tested samples in terms of the concentration of curcumin permeation either from A to B ($p \leq 0.05$) or B to A ($p \leq 0.05$). Post Hoc Tukey test

results revealed that Solucumin has significantly higher A-B drug permeation concentration compared to other tested samples at every time point ($p \leq 0.05$). On the other hand, there were no significant differences between the A to B drug permeation profiles of Mexcumin and Nacumin® at every time points ($p > 0.05$). Longvida® showed significantly lower A-B drug permeation concentration than Mexcumin and Nacumin® at almost every time point ($p > 0.05$), with only no significant differences when at 60 minutes ($p \leq 0.05$). There was no statistically significant difference among the B to A drug permeation profiles of commercial curcumin, Mexcumin Longvida® and Nacumin® at every time point since no curcumin permeation was detected ($p > 0.05$). In contrast, Solucumin was significantly higher than all other test samples at every time point throughout the study ($p \leq 0.05$).

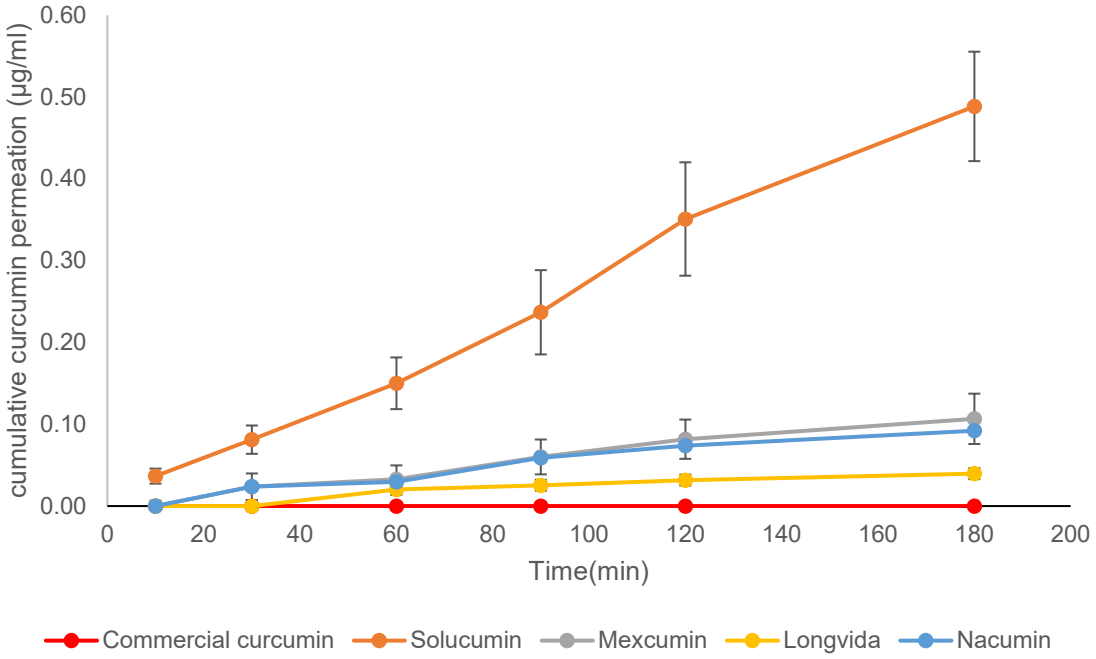

Figure 5.9. Drug permeation profiles (A-B) of each tested sample (n=9, mean ± SD)

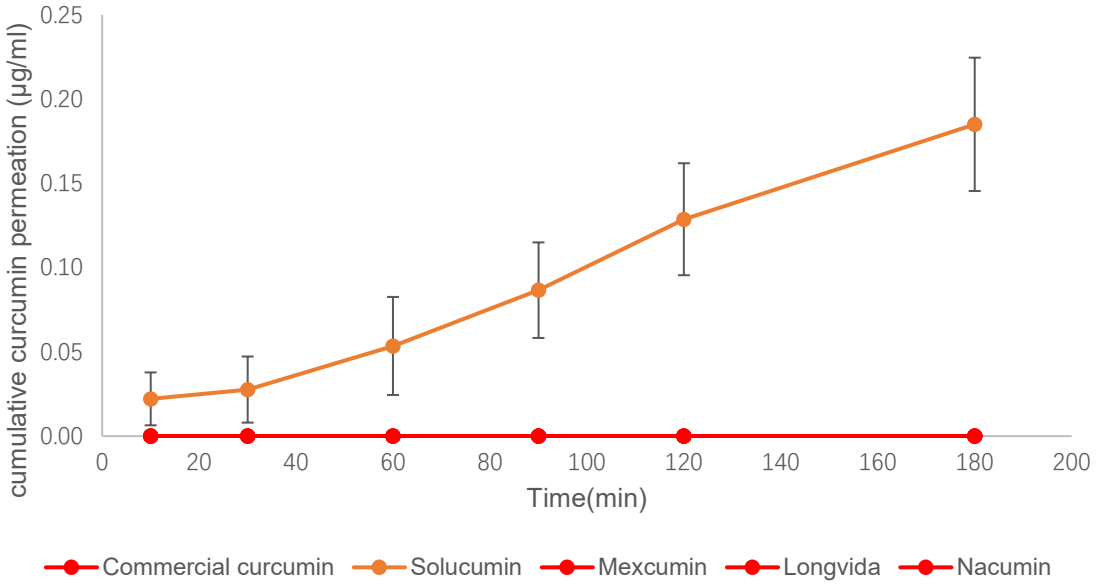

Figure 5.10. Drug permeation profiles (B-A) of each tested sample (n=9, mean ± SD)

The values of the initial curcumin concentration dissolved in donor chamber of each tested sample (C_0 (suspension)) were listed in Table 5.6. Solucumin showed the highest C_0 (suspension), (A-B) of 17 ± 2.95 µg/ml and C_0 (suspension), (B-A) of 15.51 ± 1.46 µg/ml, which were significantly higher than the other formulations ($p \leq 0.05$). Mexcumin exhibited the second highest of C_0 (suspension), (A-B) of 3.72 ± 0.71 µg/ml and C_0 (suspension), (B-A) of 1.88 ± 0.13 µg/ml, which were significantly higher than Longvida®, Nacumin® and commercial curcumin ($p \leq 0.05$). No significant differences between the Longvida®, Nacumin® and commercial curcumin in terms of C_0 (suspension), (A-B) ($p > 0.05$) and C_0 (suspension), (B-A) ($p > 0.05$).

	C_0 (suspension),(A-B) (µg/ml)	**C_0 (suspension), (B-A) (µg/ml)**
Commercial curcumin	0.07 ± 0.01	0.04 ± 0.01
Solucumin	17.00 ± 2.95	15.51 ± 1.46
Mexcumin	3.72 ± 0.71	1.88 ± 0.13
Longvida®	0.31 ± 0.03	0.23 ± 0.04
Nacumin®	0.40 ± 0.05	0.31 ± 0.03

Table 5.6. Concentration of curcumin dissolved in donor chamber at the beginning of the in vitro drug permeation experiments from A-B and B-A (C_0 (suspension),(A-B) and C_0 (suspension), (B-A)) (n=9, mean ± SD)

5.4.3. Permeability coefficient (Papp)

Papp measured in Caco-2 cells is considered a good indicator of drug permeation and a predictor for the oral absorption of passively absorbed drugs in humans (Pade & Stavchansky, 1998). C_0 is defined as the initial drug concentration in the donor chamber, and it is a key factor that affects the values of Papp. In this study, homogeneous donor suspensions were prepared by dispersing the test samples into buffered HBSS. The suspensions were added to the donor chamber at the beginning of the cell permeability experiment. Therefore, it is reasonable to consider that the initial concentration of dissolved curcumin detected in the donor chamber as C_0 (0.1 mM curcumin concentration). However, it is worth noting that most published *in vitro* drug permeability studies prepared the test samples into donor solutions (dissolving test samples completely in organic solvents such as DMSO and then diluting with buffered solutions), rather than donor suspensions. Therefore, C_0 in these studies was the nominal applied dose of the drug (Dempe et al., 2013; Frank et al., 2017; Kamiya et al., 2020; Petri et al., 2004; Volpe et al., 2007; Wahlang et al., 2011; Walgren et al., 1998; Zeng et al., 2017a).

In order to find out which type of C_0 can calculate the Papp that correctly reflects the permeability of curcumin of each tested sample, two types of Papp, Papp(suspension) and Papp(solution) were calculated in this study:

- Papp(suspension) was calculated based on C_0 which represents the initial concentration of curcumin dissolved in the suspension measured in the donor chamber. Here C_0 is referred to as C_0 (suspension). C_0 (suspension) for each test sample is listed in Table 5.6.

- Papp(solution) was calculated based on C_0 which represents the amount of curcumin within each formulation added to the donor chamber. Here C_0 is referred to as C_0 (solution). The values of C_0 (solution) were all the same as all the formulations and commercial curcumin added to the donor

chamber contained the same amount of curcumin (0.1 mM, equivalent to 36.84 μg/ml).

As shown in Table 5.7, the two types of Papp showed the exact opposite trend. The value of Papp(suspension) was significantly higher than Papp(solution) in both A-B (Figure 5.11) and B-A (Figure 5.12) directions ($p \leq 0.05$). This is reasonable because the value of C_0 used for calculating Papp(suspension) was much lower than that for calculating Papp(solution).

For Papp(suspension), (A-B), Nacumin® showed the highest value of 19.58 ± 3.66 $\times 10^{-6}$ cm/s, followed by Longvida® of 10.79 ± 1.42 $\times 10^{-6}$ cm/s, Solucumin of 2.52 ± 0.68 $\times 10^{-6}$ cm/s, and finally Mexcumin of 2.43 ± 0.55 $\times 10^{-6}$ cm/s. Solucumin with the highest A-B drug permeation concentration showed the second lowest value of Papp(suspension), (A-B), while Longvida® and Nacumin®, the two formulations with the lowest A-B drug permeation concentrations, showed Papp values 4.29 and 7.78-fold higher than Solucumin. Mexcumin had the second highest % drug permeation but showed the lowest Papp(suspension), (A-B). It was clear that the trend exhibited by the Papp (suspension) results was contradicted by the results of the drug permeation concentration. The reason for this confusing phenomenon is that Papp (suspension) reflects the rate of permeation of the drug driven by the concentration actually dissolved in the donor compartment rather than the nominally applied drug dose. For instance, Nacumin® and Longvida® have much lower values of Papp (solution) compared to other tested samples due to their limited drug solubility in the donor chamber. On the other hand, they showed much higher values of Papp (suspension) than other tested samples which contradicted the results of the drug permeation concentration. This was because the ratio between the amounts of drug permeation to the amount of drug dissolved in the donor compartment from Longvida® and Nacumin® were actually higher than that of any other samples, which gave them much higher values of Papp (suspension).

On the other hand, Solucumin showed the highest Papp (solution), (A-B) value of 1.12 ± 0.15 $\times 10^{-6}$ cm/s, followed by Mexcumin of 0.24 ± 0.07 $\times 10^{-6}$ cm/s, Nacumin® of 0.21 ± 0.03 $\times 10^{-6}$ cm/s and Longvida® with the lowest Papp value of 0.09 ± 0.01 $\times 10^{-6}$ cm/s. It was clear that Papp (solution) reflects the permeability of the cells to the drug from the applied dose of the drug contained in each test sample and it showed a trend consistent with the data of drug permeation concentrations, i.e., test samples with a higher drug permeation concentration showed higher Papp(solution) values. As a result, Papp(solution) was used as the indicator for the drug permeability and the predictor of *in vivo* drug intestinal absorption in this study.

Zero curcumin permeation from B to A was detected from all tested samples except for Solucumin. For Solucumin, the values of Papp(suspension), (B-A) was 1.00 ± 0.19 $\times 10^{-6}$ cm/s, and Papp(solution), (B-A) 0.42 ± 0.10 $\times 10^{-6}$ cm/s.

	Papp(A-B), (suspension)	**Papp(A-B), (solution)**
1st	Nacumin®	Solucumin
2nd	Longvida®	Mexcumin
3rd	Solucumin	Nacumin®
4th	Mexcumin	Longvida®
5th	Commercial curcumin	Commercial curcumin

Table 5.7. Ranking of sample in terms of Papp(A-B) value (from high to low)

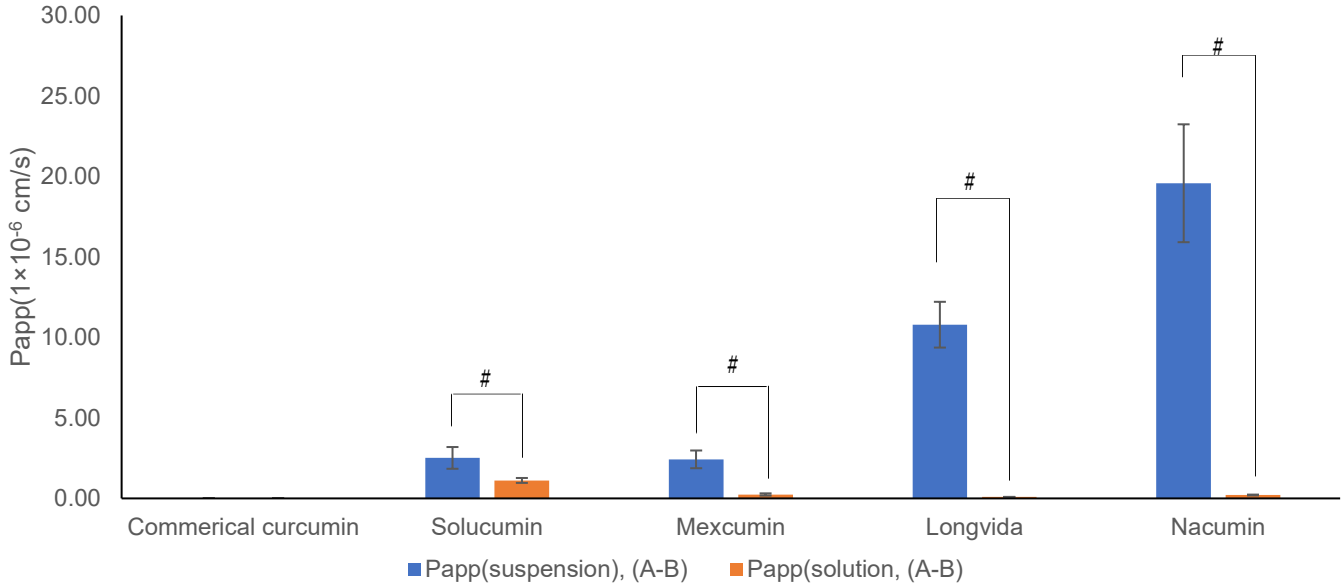

Figure 5.11 Comparison of Papp (suspension), (A-B) and Papp (solution),(A-B) (n=9, mean ± SD). # denotes statistically significant differences between Papp(A-B), (suspension) and Papp(A-B), (solution) of each formulation ($p \leq 0.05$)

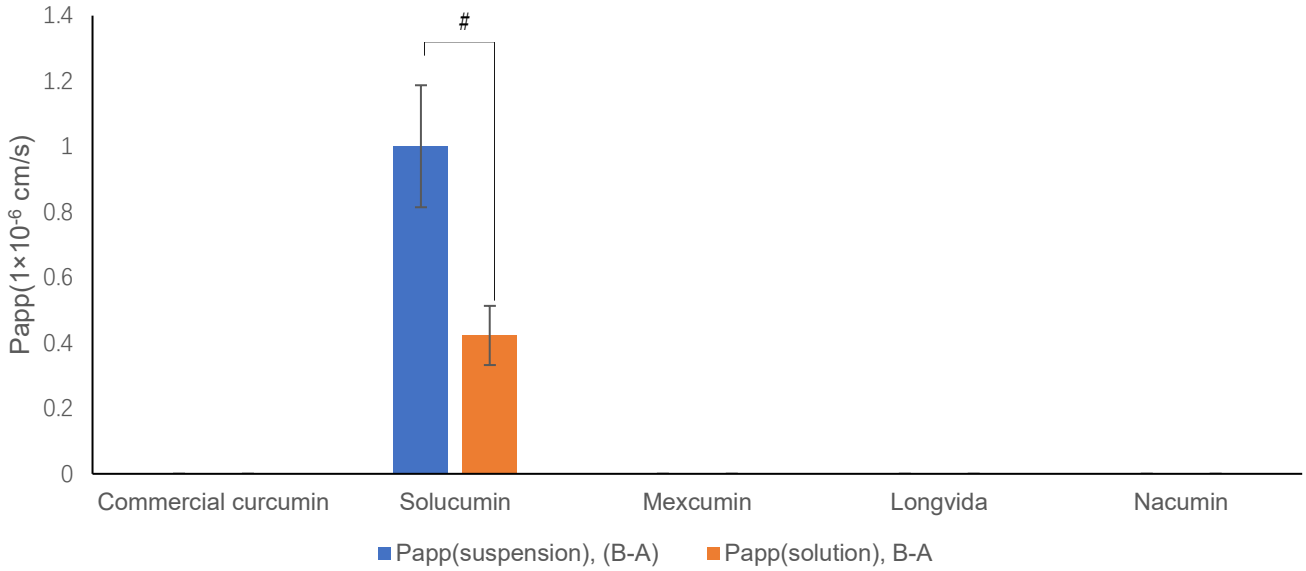

Figure 5.12. Comparison of Papp (suspension), (B-A) and Papp (solution),(B-A) (n=9, mean ± SD) # Denotes statistically significant differences between Papp(B-A), (suspension) and Papp(B-A), (solution) of each formulation (p≤ 0.05)

5.4.4. Efflux ratio

The efflux ratio, defined as the ratio of Papp in the B–A direction to the Papp in the A–B direction, was used to estimate the magnitude of drug efflux. It can also give information about what transport pathway might be involved during the drug transport (Lazorova et al., 2011). The value of efflux ratio of Solucumin was calculated to be 0.38. Other tested samples all have an efflux ratio of 0 since no curcumin was detected at the receiver chamber in the drug transport test from B-A direction.

5.4.5. Cellular uptake tests

Cellular uptake of curcumin in the Caco-2 cells was determined by measuring the concentration of curcumin accumulated in the cells at the end of the *in vitro* drug permeation experiments. Cellular uptake results showed (Figure 5.13) the amount of drug absorbed by the cells but not reaching the basolateral side of the cell monolayer.

For drug cellular uptake measured after the transport experiment from A to B, Solucumin has the highest A-B curcumin accumulation of 0.46 ± 0.09 μg/ml, which was significantly higher than any other test samples ($p \leq 0.05$). Mexcumin exhibited the second highest A-B cellular drug accumulation with 0.10 ± 0.02 μg/ml, followed by Longvida® with 0.04 ± 0.01 μg/ml, Nacumin® with 0.02 ± 0.00 μg/ml and finally commercial curcumin with 0.02 ± 0.00 μg/ml. There were no significant differences between the A to B cellular drug accumulation of Longivda®, Nacumin® and commercial curcumin ($p > 0.05$).

As for drug cellular uptake measured after the transport experiment from B to A, they were all significantly lower than that measured after the drug transport experiment from A to B ($p \leq 0.05$). Solucumin exhibited B-A cellular drug accumulation of 0.12 ± 0.04 μg/ml, which was significantly higher than any other test samples ($p \leq 0.05$). Mexcumin, Nacumin®, Longvida® and commercial curcumin exhibited B-A cellular drug accumulation of 0.05 ± 0.02 μg/ml, 0.06 ±

0.02 µg/ml, 0.04 ± 0.01 µg/ml and 0.02 ± 0.01 µg/ml, respectively. There were no significant differences between their B-A cellular drug accumulation (p> 0.05).

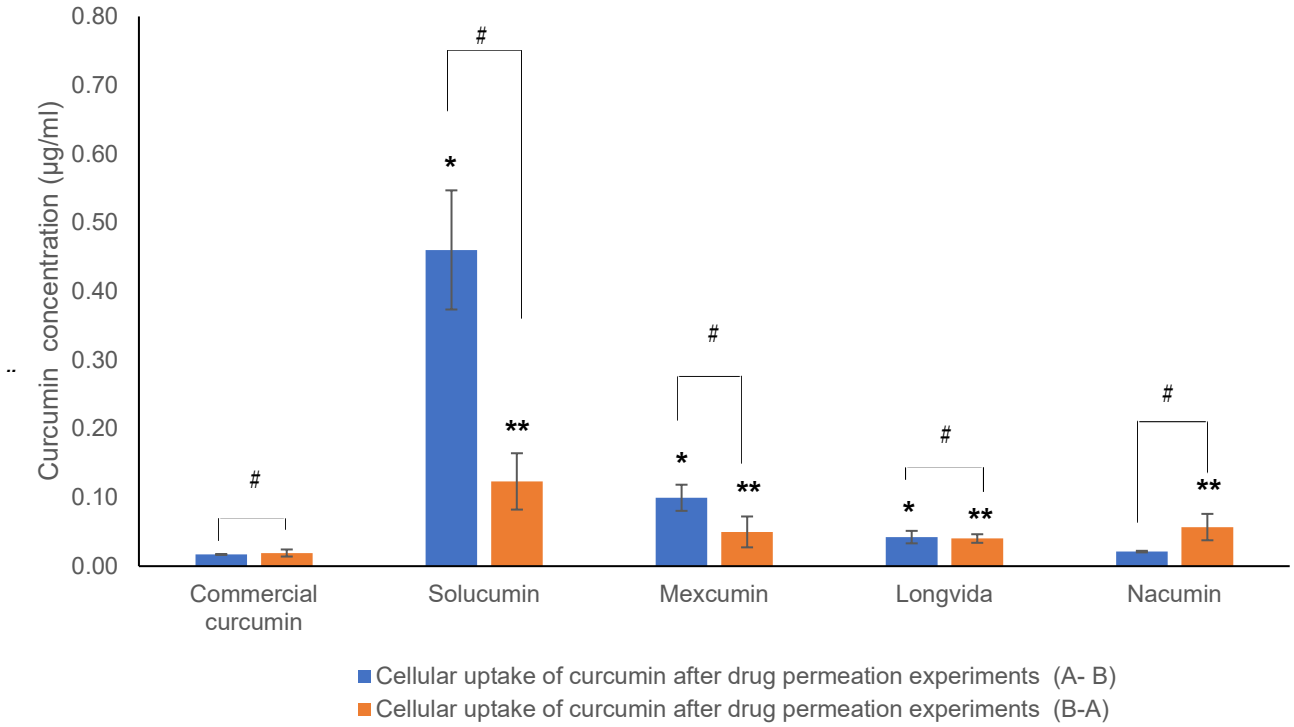

Figure 5.13. Cellular uptake of curcumin in Caco-2 cell after drug permeation experiments (A-B and B-A) (n=9, mean±SD). * denotes statistically significant difference of curcumin cellular accumulation between a formulation sample and the commercial curcumin from A to B. ** denotes statistically significant difference of curcumin cellular accumulation between a formulation sample and the commercial curcumin from B to A. # denotes statistically significant difference between the curcumin cellular accumulation of a test sample from A to B and B to A (p≤ 0.05)

5.5. Discussion

5.5.1. Cytotoxicity tests (MTT and LDH assays)

The MTT assay determines the cell viability in response to extracellular stimuli or therapeutically active agents (Riss et al., 2016). In this study, cell viability was used as an indicator for predicting the cytotoxicity of each formulation towards Caco-2 cells. The MTT assay results showed that the cell viabilities were higher than 80% when the curcumin concentration was at 0.1 mM and 0.08 mM, which indicates that these samples tested should not damage the integrity of the Caco-2 cell monolayers (Zeng et al., 2017a). Similar finding was reported by Faralli et al. that 0.15mM of curcumin solution (prepared in 0.5 M NaOH and phosphate buffer saline) resulted in cell viability ≥ 80% after incubating with Caco-2 cell monolayers (37℃, 5% CO_2) for 24 hours (Faralli et al., 2019).

LDH is an enzyme that is normally found within the cell cytoplasm. This enzyme leaks into the cell culture medium when the cells are dead due to the loss of membrane integrity. In this study, the percentage release of LDH into the cell culture medium was used as the indicator for cell death. Damaged or dead cells that have lost membrane integrity allow the passage of non-permeable molecules and are not suitable to be used in *in vitro* drug permeation and cell uptake studies. It is therefore important to ensure that the samples being tested have minimal negative impact on the cultured cell line. According to the LDH assay results, toxicity of all the tested samples to Caco-2 cells was at a minimum when the curcumin concentration was ≤ 0.1 mM.

Overall, based on the results of the MTT and LDH assays, 0.1 mM (equivalent to 36.84 μg/ml) curcumin was chosen as the drug concentration for the preparation of the donor suspension for the cell permeability and uptake tests, as it was the highest drug concentration that could be used without damaging the Caco-2 cell monolayers.

5.5.2. Measurement of transepithelial electrical resistance (TEER)

TEER is a universally accepted quantitative technique for measuring the integrity of tight junction dynamics of endothelial and epithelial cell monolayers (Srinivasan et al., 2015). It was reported that there is a good correlation between the integrity of the Caco-2 cell monolayers and the TEER value (Duizer et al., 1999). At the end of the drug transport experiment, TEER readings significantly decreased ($p \leq 0.05$) for all the test samples, which might indicate that there was some disruption of the tight junctions and improvement in paracellular permeability (Narai et al., 1997). However, it does not mean the Caco-2 cell monolayer must be damaged or lost its integrity because the difference in TEER values before and after the experiment was less than 100.Ω cm^2, which was within the acceptable limits (Meindl et al., 2015). In addition, the average TEER readings for all samples tested were above 200 Ω cm^2, meaning that the Caco-2 cell monolayer remained intact to limit the diffusion of non-permeable material across the barrier (Srinivasan et al., 2015). In some studies, it was observed that TEER readings decreased after *in vitro* drug permeation experiments without loss of integrity of the cell membrane and no significant cytotoxicity of the test compounds was seen by MTT and LDH assays (Hubatsch et al., 2007; Meindl et al., 2015). Reduction in TEER values when exposed to curcumin solid formulations was found in coculture of Caco-2 cells with other cell lines. After 2 hours exposing to a curcumin loaded, trimyristin based solid lipid nanoparticle formulation, a reduction of 5% of TEER value was observed from a coculture of Caco-2/HT29-MTX cells (seeding at a ratio of 75:25) (data of TEER reading values not shown in the literature) (Guri et al., 2013). Steensma et al. reported that Caco-2 cells showed a decrease in TEER values after exposure to natural compounds other than curcumin, while other cell lines showed no changes. It was observed that TEER value of the Caco-2 cell monolayer decreased from over 1000 Ω cm^2 to less than 800 Ω cm^2after 2 hours of the cellular permeation experiments of 50 µM of genistein and daidzein. Interestingly, the TEER value gradually increased within the next 22 hours and eventually backed to the initial level. In contrast, the TEER values of HCEC (human immortalised colonic cell line) and IEC-18 (a rat small intestinal cell line)

cell monolayers were much lower than Caco-2 cell monolayers (less than 200 Ω cm^2), but they remained constant throughout the experiments. Genistein and Daidzein did not cause damage to Caco-2, HCEC and IEC-18 cells according the LDH assay results. It was suspected that initial decrease of TEER value of Caco-2 cell monolayers was associated with the absence of FBS in the medium. Prior to the permeation experiments, Caco-2 cells were cultured in DMEM containing 10% (v/v) FBS for 21 days. The cell culture medium was then changed into Eagles Minimum Essential Medium contained no FBS when starting the permeation experiments. This resulted in a temporary disruption of the resistance of the Caco-2 cell membrane, leading to a reduction in TEER readings. In contrast, this effect did not occur in IEC-8 and HCEC cells as these cell lines were cultured in media that contained low or zero percentages of FBS (5% FBS for IEC-18 cells and no FBS for HCEC cells) (Steensma et al., 2004). The presence of FBS in the cell culture medium has been reported to stabilise the tight junctions of Caco-2 cells, although the mechanism remains unknown. (Hashimoto & Shimizu, 1993). Similar to Steensma et al's study, Caco-2 cells in the current study were cultured in DMEM contained 10% (v/v) FBS for 21 days prior to the permeation experiments while HBSS with no FBS was used as the medium during the experiments. Therefore, it was possible that reduction of TEER values was caused by the absence of FBS in the medium and it may recover over time. In order to find out whether the TEER values of Caco-2 cell monolayers will return to their initial levels over time, future permeation experiments and TEER readings could be carried out for longer periods (up to 24 hours).

5.5.3. Drug permeability across Caco-2 cell monolayer

In this study, a bidirectional, Caco-2 cell *in vitro* drug permeation experiments were conducted to mimic the intestinal absorption of curcumin and determine its intestinal permeability. In the A-B drug permeation experiments, the donor suspensions of the tested compounds were placed on the apical side of a Caco-2 cell monolayer and the amount of curcumin transported to the basolateral side of

the cells were measured to assess the drug permeability of the monolayer for each tested sample. In the B-A drug permeation experiments, the tested samples were added to the basolateral side and the amount of the drug transported to the apical side were measured, in order to test for the presence of active transport or efflux across the Caco-2 cell monolayer.

From comparison, it was found that the concentrations of curcumin permeation from A-B were significantly higher than that of from B to A for all the tested samples (excluding commercial curcumin) ($p \leq 0.05$). This suggests that the drug influx might be more predominant than the drug efflux across the intestinal epithelium for the tested formulations (except for commercial curcumin). To find more evidence to support this view, the efflux ratio of each test sample was calculated. Solucumin has an efflux ratio of 0.38 while other tested samples all have an efflux ratio of 0. Zero efflux ratio indicates no drug efflux was involved in the drug transport, which could possibly be due to an inhibition of the apical efflux transporters which might have restricted B-A drug transport but could increase the intracellular drug accumulation (Li et al., 2012). For an efflux ratio value of greater than 0 but less than 1, it indicates that absorptive influx transport is more dominant than efflux transport during the drug transport process across the Caco-2 cell monolayer (Zastre et al., 2013).

It was reported that curcumin was absorbed in the small intestine predominantly by passive diffusion (Xue et al., 2017). Thus, the intestinal permeation of curcumin generally follows Fick's first law, in which the rate of diffusion of a solute in solution across unit area (normally a surface or membrane) is proportional to the concentration gradient (Brodin et al., 2010). According to this theory, as the concentration of dissolved curcumin increased in the intestinal lumen fluid, more curcumin molecules can be present at the surface of the intestinal epithelial cells and more drugs per unit time per surface area (flux) can permeate across the cells (Di & Kerns, 2008). In this study, it was found that the tested sample with higher value of $C_{0\ (}$suspension), (A-B) also showed higher

concentration of A-B curcumin permeation and Papp (Solution), (A-B) values. Since the values of $C_{0\ (}$suspension), (A-B) is associated to the aqueous solubility of curcumin, it suggests that there was a positive correlation between the aqueous solubility and the permeability of curcumin across the Caco-2 cell monolayer.

The positive correlation between the drug aqueous solubility and drug permeability was also found in other studies. Frank et al. have developed a nanoscale micellar curcumin formulation based on Tween 80. In an *in vitro* drug permeation study on Caco-2 cell model, at an applied curcumin dose of 320 μg/ml, the nano micellar curcumin formulation showed over 2-fold higher initial concentration of dissolved curcumin at the apical side of the Caco-2 cell monolayer than the curcumin control. At the end of the drug permeation study, it was found that the nano micellar curcumin formulation demonstrated nearly 9.5-fold higher concentration of curcumin permeation from A to B compared to the curcumin control (Frank et al., 2017). In another study, Chanburee and Tiyaboonchai have developed a curcumin-loaded nanostructured lipid carriers with polyethylene glycol 400 (PEG400) and polyvinyl alcohol (PVA) coatings. This formulation increased the curcumin aqueous solubility by 60-fold. In an *in vitro* Caco-2 cell drug permeation test, the formulation resulted in 6.56 % of the applied dose of curcumin (10 μg/ml) permeated to the basolateral side of the Caco-2 monolayer after 6 hours. In contrast, no curcumin permeation was detected from the curcumin control (Chanburee & Tiyaboonchai, 2018). In addition, it was also reported that solublised curcumin (diluted curcumin solution prepared by DMSO) can permeate across the Caco-2 cell monolayers more rapidly. Over 2% of the applied dose of curcumin (20 μg/ml) was transported from A to B through the Caco-2 cell monolayers in 60 minutes. The calculated Papp (A-B) was 7.1×10^{-6} cm/s, which was thought to be a fast permeation rate (Yu & Huang, 2011). In contrast, studies used curcumin dispersed suspension as the test samples in Caco-2 cell drug permeation tests either had no or slow curcumin permeation (Papp(A-B) = 0.56×10^{-6} cm/s) (Chanburee & Tiyaboonchai, 2018; Frank et al., 2017).

Solucumin showed the highest curcumin A-B permeation concentration (0.49 ± 0.07 µg/ml, equivalent to 0.00133 ± 0.00019 mM), Papp (Solution), (A-B) value (1.12 ± 0.15 $\times 10^{-6}$ cm/s) and $C_{0\ (}$suspension), (A-B) value (17.00 ± 2.95 µg/ml). It is clear that the permeability of curcumin from A to B benefits from the increased solubility. The ability of Solucumin to improve the solubility of curcumin has been demonstrated by the solubility test results which is mentioned in section 2.5.4 and the *in vitro* dissolution test results which mentioned in section 3.4.3. The increased solubility of curcumin was attributed to the particle size reduction and conversion of crystalline drug to amorphous, as shown by DLS and XRD results showed in sections 4.5.3 and 4.5.4. Apart from the aqueous solubility, the inhibition of efflux transporters of curcumin can also help to improve the permeability of curcumin from Solucumin. Vitamin E TPGs, one of the excipients of Solcumin, was reported to have the ability to inhibit apical efflux pumps of curcumin such as P-gp (Song et al., 2016), which make less intracellular curcumin to be pumped back to the apical side of the Caco-2 monolayer. In this study, decrease in TEER reading was observed after the permeation experiments. This suggests there could be a disruption of tight junctions. Both Soluplus and Vitamin E TPGS have been shown to have surfactant-like property and it was reported that surfactants can disrupt the tight junctions that hold adjacent epithelial cells together (Brunner et al., 2021; Mine & Zhang, 2003). One of the mechanisms by which surfactants can disrupt tight junctions is by affecting the conformation and function of the transmembrane proteins that make up the tight junctions, such as occludins and claudins. These proteins have extracellular domains that interact with adjacent cells to form the tight junctions, and intracellular domains that interact with cytoskeletal proteins to anchor the junctions to the cell membrane (Buckley & Turner, 2018). Surfactants can affect the interaction of these proteins with other proteins and with the membrane, leading to their mislocalisation or degradation, and ultimately, the disruption of the tight junctions. The disruption of tight junction can lead to increased paracellular transport of molecules across the epithelium (Mine & Zhang, 2003).

As for the comparators, Mexcumin showed the second-highest A-B curcumin permeation concentration (0.11 ± 0.03 µg/ml) and Papp (Solution), (A-B) value (0.24 ± 0.07 ×10-6 cm/s). It also showed the second highest value of C_0 (suspension),(A-B) (3.72 ± 0.71 µg/ml). Interestingly, Nacumin® showed similar A-B curcumin permeation concentration (0.09 ± 0.01 µg/ml) to Mexcumin. However, it has much lower C_0 (suspension), (A-B) value (0.40 ± 0.05 µg/ml) than that of Mexcumin. This suggested that the improved drug permeability from Nacumin® was more likely to be related to factors other than solubility, such as particle size reduction. Nacumin® has a mean particle size of 372.67 ± 49.41 nm, compared to 1169.67 ± 76.83 nm of Mexcumin (shown in Chapter 4.5.4). Nano-sized particles can pass through the lipid bilayer of cell membranes easier than larger particles. In addition, it was reported that nanoparticles < 500nm could be directly transported across the cell barrier into the basolateral compartment via receptor-mediated endocytosis (Rejman et al., 2004). Longvida® exhibited the lowest A-B curcumin permeation concentration (0.04 ± 0.00 µg/ml, equivalent to 0.00011 ± 0.00001 mM), Papp (Solution), (A-B) value (0.09 ± 0.01 ×10-6 cm/s) and C_0 (suspension), (A-B) (0.31 ± 0.03 µg/ml) among all the tested formulations (excluding commercial curcumin). This further confirmed the positive correlation between the solubility and the permeability of curcumin. No drug permeation was found from A to B and B to A for commercial curcumin. As shown in Table 5.7, it exhibited extremely low initial drug solublisation in the donor chamber which was believed to be the main reason for zero drug permeation.

5.5.4. Cellular drug uptake

The results of the cellular drug uptake test provided a prediction for the amount of drug that has been absorbed by the intestinal epithelial cell but has not yet been released to the blood circulation (basolateral side) or efflux back to the intestinal lumen (the apical side) (Derakhshandeh et al., 2011; Joshi et al., 2016).

In this study, it was found the cellular uptake of curcumin absorbed from the apical side was associated with to C_0 (suspension), (A-B). Solucumin showed both

significantly higher $C_{0\,(}$suspension), (A-B) (17.00 ± 2.95 µg/ml) and apical cellular uptake of curcumin (0.46 ± 0.09 µg/ml) than all other tested samples (p≤ 0.05). Next, Mexcumin exhibited the second highest $C_{0\,(}$suspension), (A-B) (3.72 ± 0.71 µg/ml) and apical cellular uptake of curcumin (0.10 ± 0.02 µg/ml) and they were significantly higher than Nacumin®, Longivda® and commercial curcumin (p≤ 0.05). In contrast, Nacumin®, Longvida® and commercial curcumin all exhibited the lowest apical cellular uptake of curcumin and C_0 (suspension), (A-B). There were no significant differences between the three tested samples in terms of the apical cellular uptake of curcumin (p> 0.05) as well as the C_0 (suspension), (A-B) (p> 0.05). Since C_0(suspension), (A-B) is correlated to the aqueous solubility of curcumin, it suggests that the apical cellular uptake of curcumin can be affected by the solubility. This view was further supported by other published studies, which found a positive correlation between the concentration of drugs/natural compounds such as nifedipine and γ-Tocotrienol dissolved in the donor compartment and the *in vitro* apical cellular drug uptake of Caco-2 cells (Alqahtani et al., 2014; Tubtimsri & Weerapol, 2021).

It was unclear whether the uptake of curcumin by the cells from the basolateral side was influenced by the solubility. Solucumin showed the highest C_0(suspension), (B-A) (15.51 ± 1.46 µg/ml) among all the tested samples and it also exhibited the highest basolateral cellular uptake of curcumin (0.12 ± 0.04 µg/ml). On the other hand, Mexcumin has shown significantly higher C_0(suspension), (B-A) (1.88 ± 0.13 µg/ml) than Nacumin®and Longvida®, but they all showed very similar basolateral cellular uptake of curcumin with no significant differences (p> 0.05).

5.6 Conclusion

In this study, *in vitro* drug permeation experiments and cellular uptake tests (using Caco-2 cell monolayers as the model) were carried out to simulate *in vivo* drug absorption across the human intestinal epithelial cells. The results of cytotoxicity assays (MTT and LDH assays) and TEER measurement have shown that all the tested samples were well tolerated by the Caco-2 cell monolayers at the concentrations tested (0.1mM, equivalent to equivalent to 36.84 μg/ml). The TEER values have dropped at the end of the permeation experiments but still within the acceptable limit. The decrease in TEER values might be temporary and was suspected to be related to the absence of FBS in the culture medium during the permeation experiments. Among all the formulations, Solucumin has shown the highest cellular permeation and uptake of curcumin across Caco-2 cell monolayer from A to B, which was attributed to the increased solubility of curcumin and potential inhibition of apical efflux transporters by Vitamin E TPGs. It was also the only formulation that exhibited B-A drug transport, although the drug influx was more predominant than the drug efflux. The ability of Solucumin to improve the solubility and dissolution rate of curcumin has been well demonstrated in Chapters 2 and 3. Combing the significantly improved curcumin intestinal permeability found in this Chapter, it can suggest that Solucumin is a promising formulation that has the potential to increase the oral bioavailability of curcumin.

It has been demonstrated that the permeability of curcumin correlates with its aqueous solubility in this study. It will be very interesting to figure out whether demethoxycurcumin and bis-demethoxycurcumin follow the same trend. Further work could be carried out in the future to investigate how the curcumin formulations will affect the permeability of demethoxycurcumin and bis-demethoxycurcumin and whether they are related to water solubility. This will certainly be helpful for further exploring the potential of these curcumin formulations.

Chapter 6. Application of Solucumin formulation to improve the aqueous dissolution of BCS II and BCS IV compounds

6.1. Introduction

In the previous chapters, Solucumin, the novel solid dispersion curcumin formulation developed in this project, has been proven that it can significantly improve the aqueous solubility, dissolution and permeability of curcumin, which makes it a promising solid formulation for oral drug delivery of curcumin. At this point, another question arises: Can this solid dispersion formulation be applied for other poorly aqueous soluble drugs and make them more soluble? To answer this question, some poorly soluble drugs and plant derived natural compounds were selected and formulated into solid dispersions using the same method for preparing Solucumin. *In vitro* dissolution tests were carried out to investigate the effect on the drug dissolution of including in this solid dispersion formulation. To avoid being confused with Solucumin, the solid dispersion samples prepared in this Chapter were all referred as “novel polymeric-surfactant solid dispersions (NPSSD)”.

The selected drugs were terbinafine, niclosamide, nitrofurantoin and omeprazole and the plant derived natural compounds were quinine, quercetin and rutin. According to biopharmaceutical classification system (BCS) classification, pharmaceutical compounds with poor solubility can be classified into BCS class II (low solubility and high permeability) or BCS class IV (low solubility and low permeability) compounds (Tsume et al., 2014). The BCS classification of the selected drugs and natural compounds are listed in Table 6.1.

BCS Classification	**Drugs and plant derived compounds**
BCS class II	Niclosamide, nitrofurantoin, omeprazole, quinine, terbinafine
BCS Class IV	Quercetin and rutin

Table 6.1. The BCS classification of the selected drugs and natural compounds to be formulated into NPSSD

6.1.1. A brief introduction to biopharmaceutical classification system (BCS)

The biopharmaceutical classification system (BCS) was first proposed by Amidon et al (Amidon et al., 1995). This concept has been widely accepted internationally in industry, academic institutions and public authorities (Chavda et al., 2010). Based on BCS, drug substances or APIs are divided into high/low solubility and intestinal permeability classes as follow:

Class I: High Solubility - High Permeability
Class II: Low Solubility - High Permeability
Class III: High Solubility - Low Permeability
Class IV: Low Solubility - Low Permeability

According to the FDA's guidelines on BCS, drugs with high solubility are those with the highest therapeutic dose completely soluble in ≤ 250 ml of aqueous media over the pH range of 1.2– 6.8 at 37 ± 1°C while high-permeability drugs are generally those with an extent of absorption ≥ 90% of the administrated dose in the gastrointestinal tract (FDA, 2021).

Class I compounds, such as amitriptyline hydrochloride, propranolol

hydrochloride and verapamil hydrochloride, are well absorbed and have neither solubility nor permeability limited absorption. The absorption rate of these compounds is usually faster than excretion (Kasim et al., 2004). Class II compounds, such as phenytoin, glibenclamide, carbamazepine and ibuprofen, are poorly soluble but have high intestinal absorption rate. As a result, the drug dissolution is the rate-limiting step for the drug absorption (Ghadi & Dand, 2017). Normally, the absorption for Class II compounds is slower than Class I. Class III compounds, such as acyclovir, acetylsalicylic acid, amoxicillin, atenolol and fluconazole, are highly soluble, but have low absorption rate thus the gastrointestinal tract permeability is the rate-limiting step for the drug absorption (Kasim et al.,2004). Of all the BCS compounds, Class IV compounds, such as amphotericin B, furosemide, acetazolamide, ritonavir and paclitaxel, have the lowest drug absorption due to the low solubility and permeability, which make them problematic for effective oral administration (Chavda et al., 2010; FDA, 2021; Tsume et al., 2014).

6.1.2. A brief introduction to the selected drugs and natural compounds

6.1.2.1. Niclosamide

Niclosamide is an oral anthelmintic drug which can be used for tapeworm infections. It exerts its anticestodal effect by inhibiting oxidative phosphorylation and stimulating adenosine triphosphatase activity in the mitochondria (Xu et al., 2020). The standard oral dose of niclosamide used for treating tapeworm infections in adults is 2 g/day for 1–7 days (Schweizer et al., 2018). Niclosamide also showed therapeutic potentials for the treatment of diseases other than those caused by parasites, such as cancer, bacterial and viral infection and Type II diabetes (Chen et al., 2018). It is available as tablet for oral administration, although not marketed in U.S and U.K (BNF, 2022b; PubChem, 2020e). Chemically, it is known as 5-chloro-*N*-(2-chloro-4-nitrophenyl)-2-

hydroxybenzamide. It has a molecular weight of 327.12 g/mol, melting point from 225-230°C (PubChem, 2020e) and LogP value of 4.48 (Jurgeit et al., 2012). Niclosamide is a weakly acidic, BCS class II drug with very poor aqueous solubility (1.6 µg/ml) but high permeability (Jara et al., 2021).

Published literature regarding the pharmacokinetics of niclosamide suggested that it has poor oral bioavailability. Chang et al. reported the pharmacokinetic parameters of niclosamide in male sprague-dawley rats when administered orally at 5 mg/kg . It showed C_{max} of 354 ± 152 µg/l and $AUC_{0-\infty}$ of 429 ± 100 µg·h/l (Chang et al., 2006). A study carried out by Andrews er al. showed the maximal serum concentration of niclosamide of 0.25- 6.0 µg/ml when a single oral dose of 2g niclosamide was given to male and female volunteers (Andrews et al., 1982). In another study, a single dose of 500mg niclosamide was given orally to male patients with castration-resistant prostate cancer. The C_{max} and $AUC_{0-\infty}$ were found to be 153.0± 74.1 µg/l and 349.6± 443.0 µg·h/l (Schweizer et al., 2018).

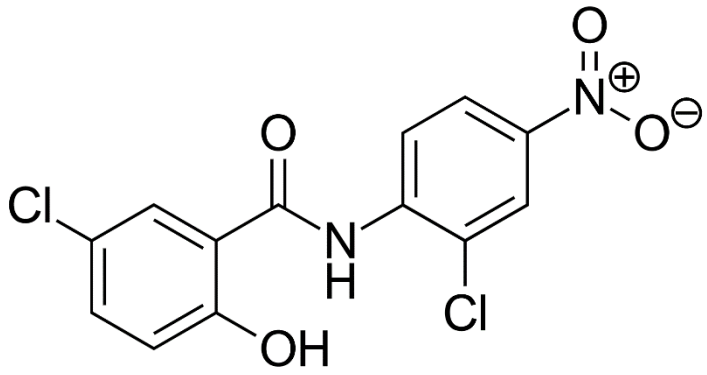

Figure 6.1. Chemical structure of niclosamide

6.1.2.2. Nitrofurantoin

Nitrofurantoin is an antibacterial medication to treat or prevent urinary tract infections. It gets reduced to electrophilic intermediates by bacterial nitrofurantoin reductase, which leads to inhibition of synthesis of DNA, ribosomal RNA and other intracellular components in bacteria (Giedraitiene et al., 2022). The dosage forms of nitrofurantoin available for oral administration include tablets, capsules or suspension (BNF, 2022c; PubChem, 2022g). Chemically, nitrofurantoin is known as 1-[(*E*)-(5-nitrofuran-2-yl)methylideneamino]imidazolidine-2,4-dione. It has a molecular weight of 238.16 g/mol, melting point from 223-263°C and Log P value of -0.47 (PubChem, 2022g).Nitrofurantoin becomes more soluble at aqueous medium with pH> 7 and almost insoluble at pH< 1.2 (Chen et al., 1976).

Nitrofurantoin is very poorly soluble in water (0.19 mg/ml) but highly absorbed in the gastrointestinal tract (Kawahara et al., 2020). As a result, it can be classified as BCS IV drug. A comparative study conducted by Albert et al. showed that nitrofurantoin tablets and capsules showed similar bioavailability. In this study, a single oral dose of 100 mg nitrofurantoin capsule or tablet was given to healthy male volunteers. The pharmacokinetic results showed C_{max} of 986 µg/l for the tablet and 1470 µg/l for the capsule while AUC_{0-t} of 2100 µg·h/l of the tablet and 3280 µg·h/l for the capsule (standard deviation not provided). It was reported that there were no significant differences between the nitrofurantoin capsule and tablet in C_{max} or AUC_{0-t} (Albert et al., 1974). In another study, a single oral dose of 100 mg nitrofurantoin capsule was administrated to healthy human subjects aged from 18-45 years. The subjects had eaten a meal before taking the nitrofurantoin dose. It showed C_{max} of 506.5 37.2 µg/l and AUC_{0-t} of 2401.65 405.34 µg·h/l (Patel et al., 2013).

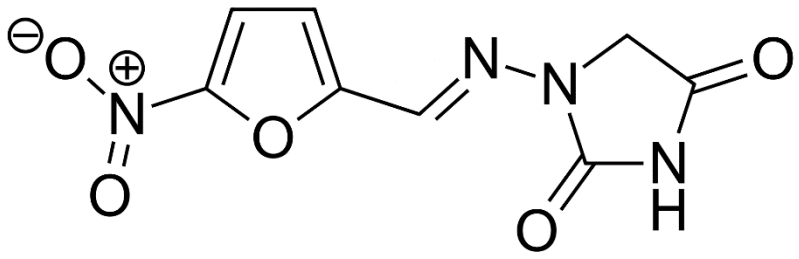

Figure 6.2. Chemical structure of nitrofurantoin

6.1.2.3. Omeprazole

Omeprazole is an antiulcer drug used for the management and treatment of gastric- acid related problems including peptic ulcer disease (PUD), duodenal ulcer, gastric ulcer, eradicating Helicobacter pylori infection, gastroesophageal reflux disease (GORD), uncomplicated heartburns and Zollinger-Ellison syndrome (Frucht et al., 1991; Maton, 1991). Chemically, omeprazole is known as 6-methoxy-2-[(4-methoxy-3,5-dimethylpyridin-2-yl)methylsulfinyl]-1*H*-benzimidazole. It has a molecular weight of 345.4 g/mol, melting point between 155-156°C and Log P value of 2.23 (PubChem, 2022a). Omeprazole is a weak base with low solubility in water (0.15 mg/ml) but high permeability (PubChem, 2022a; Rahman et al., 2017). Thus, it is classified as a BCS class II drug (Amidon et al., 1995; Geng et al., 2019).

The dosage forms of omeprazole for oral administration include tablets, capsules and suspension (PubChem, 2022a). Most dosage forms for oral delivery either contain an enteric coating (tablet and capsule) or buffered with sodium bicarbonate (suspension) in order to protect omeprazole from deteriorating in stomach acid. It was reported that omeprazole would immediately decompose when exposed to an acidic environment of pH less than 2.0, while remains uncharged and stable at pH 7 (Frucht et al., 1991; Maton, 1991). Different dosage form of omeprazole showed different oral bioavailability. In a comparative study by Liu et al., 40 mg of omeprazole capsule was administrated orally to one group of subjects while 40 mg of omeprazole as tablets was given to the other group. Both groups were consisted of healthy male volunteers who were fasting before taking omeprazole. The group that received 40 mg omeprazole tablet showed higher C_{max} and $AUC_{0\text{-}t}$ of 1330.46 ± 758.07 µg/l and 3467.04 ± 3028.47 µg·h/l than the one received 40 mg omeprazole capsule of 1023.67 ± 542.30 µg/l and

3150.80 ± 2760.03 μg·h/l. There were no statistically significant differences between the omeprazole tablet and capsule formulations in C_{max} and AUC_{0-t} (Liu et al., 2012). In a study performed by Vaz-da-Silva et al., an oral dose of one 20mg omeprazole capsule was given to fasting healthy male and female volunteers aged 18-55 years. The measured C_{max} and AUC_{0-t} were 736.7 ± 443.3 μg/l and 1490 ± 1276 μg·h/l (Vaz-da-Silva et al., 2001). In a similar study conducted by Thomson et al., one 20mg omeprazole tablet was given orally to fasting male and female volunteers aged 18-52 years. The measured C_{max} and AUC_{0-t} were 449.36 μg/l and 838.61 μg·h/l (standard deviation not provided) (Thomson et al., 1997). In Zhang et al.'s study, a single dose of buffered omeprazole suspension (contained 20mg omeprazole + 1680mg sodium bicarbonate) was given orally to fasting healthy male and female volunteers aged 18–65 years. The pharmacokinetic results showed C_{max} of 982.01 ± 431.72 μg/l and AUC_{0-t} of 1530.61 ± 1584.30 μg·h/l (Zhang et al., 2022).

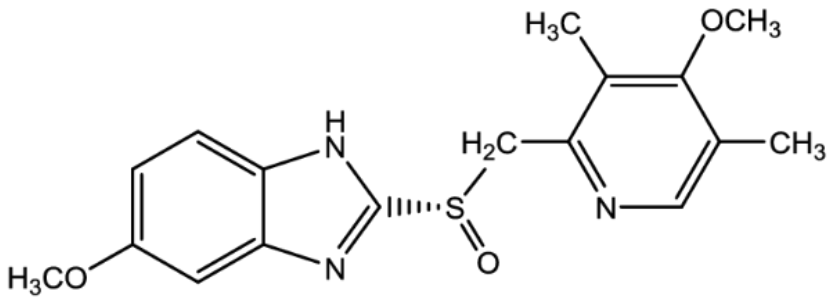

Figure 6.3. Chemical structure of omeprazole

6.1.2.4. Terbinafine

Terbinafine is an antifungal drug that belongs to the allylamine group. At an oral dose of 250 mg/day, terbinafine is generally effective for treating fungal infections of the scalp, body, groin ('jock itch'), feet (athletes foot), fingernails, and toenails (BNF, 2022a; PubChem, 2022d). It exerts the antifungal effect via noncompetitive inhibition of squalene epoxidase that interferes with the synthesis of the fungal cell membrane, ultimately contributing to cell death (Krishnan-Natesan, 2009). Chemically, terbinafine is known as (*E*)-*N*,6,6-trimethyl-*N*-(naphthalen-1-ylmethyl)hept-2-en-4-yn-1-amine. It has a molecular weight of 291.4 g/mol, melting point from 195-205°C and LogP value of 6 (PubChem, 2022d).

Terbinafine is a lipophilic substance with high permeability and it can be readily absorbed from the gastrointestinal tract. On the other hand, it is almost insoluble in water with extremely low solubility of 0.00074 mg/ml (PubChem, 2022d). Due to the low solubility and high permeability, Terbinafine can be classified as BCS II drug.(Kondoros et al., 2022; PubChem, 2022d). Terbinafine alone is not available on the market as an oral drug. It is available as its salt form (terbinafine hydrochloride) as a tablet for oral medical use (EMC, 2022b). Terbinafine is well absorbed after oral administration as terbinafine hydrochloride. A single dose of terbinafine hydrochloride tablet (contained 250 mg terbinafine) was given orally to healthy volunteers in mixed sexes aged 22-35 years, which showed C_{max} of 1146 ± 664 µg/l and AUC_{0-t}: 4406 ± 2279 µg·h/l (Kovarik et al., 1992). In another study, healthy male subjects aged from 20–37 years received a single oral dose of terbinafine hydrochloride tablet (contained 250 mg terbinafine) and similar pharmacokinetics results were observed with C_{max} of 1340 ± 450 µg/l and AUC_{0-t}: 4740 ± 2070 µg·h/l (Kovarik et al., 1995).

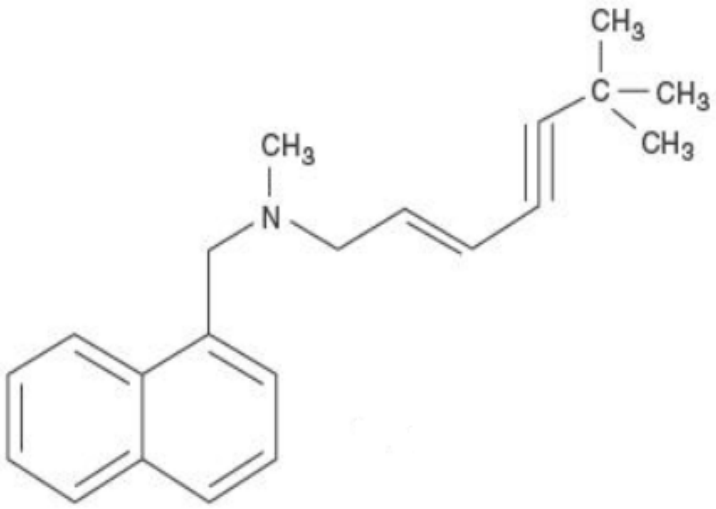

Figure 6.4. Chemical structure of terbinafine

6.1.2.5. Quinine

Quinine, a component of the bark of the cinchona (quina-quina) tree, is used for treating and preventing infectious diseases, specifically malarial infections, for generations (Achan et al., 2011). However, the anti-malarial mechanism of action of quinine is still unknown. Quinine remained the mainstay for treating malaria until the 1940s, when more effective antimalaria drugs such as chloroquine were introduced (Achan et al., 2011). Chemically, quinine is known as 6-methoxy-(S-vinyl- 2-quinuclidyl)-4-quinolinemethanol). It is a cinchona alkaloid that belongs to the aryl amino alcohol group of drugs (Achan et al., 2011). It is a very basic compound with a molecular weight of 324.4 g/mol, melting point from 159 to 177°C and Log P value of 3.44 (Pubchem, 2022c). Quinine is classified as BSC Class II compound due to its poor aqueous solubility (0.5 mg/ml) and high permeability (Strauch et al., 2012). It also has a low therapeutic index and serious adverse effects such as irreversible blindness, skin eruptions, asthma, thrombocytopenia, hepatic injury and psychosis when overdosed (Achan et al., 2011).

Quine alone is not available as drug in the market due to the poor solubility. However, its salt form, quinine sulphate and quinine hydrochloride, are available in the market in the form of tablets and capsules for the treatment of chloroquine-resistant malaria (Drugbank, 2022a; EMC, 2022a). Salts of quinine are reliably absorbed by the oral route and shows similar absorption rate in young and elderly individuals. In a study, an oral dose of 600mg quinine sulphate (2×300 mg quinine sulphate tablets) was given to healthy male and female volunteers. The pharmacokinetics results showed C_{max} of 5.0 ±1.3 mg/l in elderly subjects (aged from 65-78 years) and 5.6 ± 1.2 mg/l in young subjects (aged from 20-25 years); $AUC_{0-\infty}$ of 120.0 ± 30 mg·h/l for the elderly and 87.0 ± 23 mg·h/l for the young. No significant differences were found between the

elderly and young subjects in C_{max} or $AUC_{0-\infty}$ (Wanwimolruk et al., 1991). Giving the quinine salt as a capsule or tablet does not seem to have a significant influence on its bioavailability. In a comparative study, sugar-coated tablets of quinine sulfate containing 540 mg quinine or gelatin capsules of quinine sulfate containing 540 mg quinine were administrated orally to healthy male volunteers every 8 hours for 3 successive days. Blood samples were collected for plasma quinine determination at 2, 4, 8, 16, 24, 40, 48, 64, 72, 84, and 96 hours after the administration of quinine sulfate tablets or capsules. Except for the first 2 hours after the initial dose, the plasma concentration of quinine achieved for tablets and capsule formulations at every time point were not significantly different (Hall et al., 1973). It was reported that hydrochloride and sulphate salts of quinine were similar in terms of the oral bioavailability. In a comparative study, tablets of the quinine hydrochloride or quinine sulphate were given in single oral doses (600 mg quinine equivalent) to healthy male volunteers aged of 20 and 35 years. Quinine hydrochloride showed AUC_{0-t} of 67.9 ± 29.4 μg·h/ml, C_{max} of 5.1 ± 1.3 μg/ml and T_{max} of 1.7 ± 0.9 hours while quinine sulphate showed AUC_{0-t} of 63.5 ± 15.8 μg·h/ml, C_{max} of 4.2 ± 0.9 μg/ml and T_{max} of 2.6 ± 0.7 hours. No statistically significant differences were noted in AUC_{0-t}, C_{max} and T_{max} values between quinine sulphate and quinine hydrochloride (Jamaludin et al., 1988).

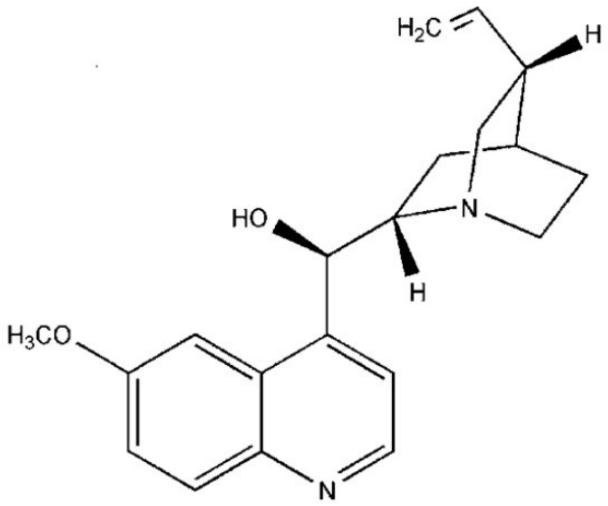

Figure 6.5. Chemical structure of quinine

6.1.2.6. Quercetin

Quercetin is a bioflavonoid that can be found in many fruits, vegetables and plaints. It is often used as an ingredient in dietary supplements, foods and drinks. It also has therapeutic potentials since it exserts antidiabetic, anti-inflammatory, antioxidant, antimicrobial, anti-Alzheimer's, antiarthritic, cardiovascular, and wound-healing effects (Salehi et al., 2020). Chemically, quercetin is known as 2-(3,4-dihydroxyphenyl)-3,5,7-trihydroxychromen-4-one. It has a molecular weight of 302.23g/mol, melting point from 316-318°C (PubChem, 2022f) and LogP value of 1.82 (Rothwell et al., 2005). Quercetin is relatively lipophilic with low water solubility (0.01 mg/ml) and low permeability (Riva et al., 2019). It can be easily oxidised at environment of pH 7.4 and above (Wisudyaningsih et al., 2021). Due to its poor water solubility, chemical instability and low bioavailability, quercetin has not been approved as an agent for therapeutic purposes (Wang et al., 2016). It is currently sold as herbal supplement product in the form of tablets and capsules for oral use (Rasouli et al., 2017).

After quercetin is absorbed from the GI tract, it is quickly metabolised into quercetin sulfate and quercetin glucuronide via conjugation reactions catalysed by sulphotransferases (SULTs) and uridine-5′-diphosphate glucuronosyltransferases (UGTs) (Ulusoy & Sanlier, 2020). In a study carried out by Yang et al., quercetin solution prepared in PEG 400 was administrated orally to male sprague-dawley rats at a dose of 165 μmol/kg (49.87 mg/kg). The plasma concentration of quercetin was too low to be detected. On the other hand, quercetin sulfates and quercetin glucuronide appeared in the blood stream only 5 minutes after the dosing, indicating very rapid metabolism of quercetin after absorption (Yang et al., 2005).

There is currently no pharmacokinetic data available for the oral administration of pure quercetin to human subjects. All the published studies on the pharmacokinetics of quercetin in humans were carried out by giving an oral dose of quercetin derivatives, such as quercetin glycosides or quercetin, which are more hydrophilic than the native quercetin (Almeida et al., 2018; Materska, 2008). Quercetin 7-O-succinyl glucoside, a quercetin derivative, was reported to be approximately 1000 times more water soluble than native quercetin due to the more hydrophilic nature of the glucose moiety (Cao et al., 2022).

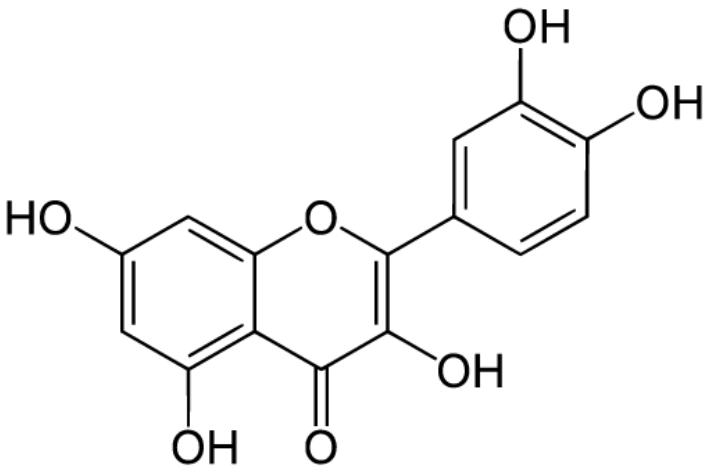

Figure 6.6. Chemical structure of quercetin

6.1.2.7. Rutin

Rutin is a natural flavonoid of the flavonol-type that can be found in many fruits and plants. It possesses various pharmacological activities including antioxidant, anti-inflammatory, anticancer, antimicrobial, antiviral, immunomodulatory and antiulcergenic activities. It is believed that many of the therapeutic effects of rutin was due to its excellent antioxidant and free radical-scavenging properties (Negahdari et al., 2021; Sharma et al., 2013). Chemically, rutin is known as 3,3′,4′,5,7-pentahydroxyflavone-3-rhamnoglucoside. It is a glycoside composed of quercetin, a flavonolic aglycone and the disaccharide rutinose. It has a molecular weight of 610.5 g/mol, melting point at 125°C and LogP value of -2.02(PubChem, 2020b). Rutin is absorbed as quercetin after it is hydrolysed into quercetin by β-glucosidase in small intestine (Bokkenheuser et al., 1987; J. Yang et al., 2019). The maximum dose limit of rutin to act as an antioxidant is reported to be 1000 mg/day (Boyle et al., 2000).

Rutin can be classified as BCS class IV compound due to its low water solubility (0.15 mg/ml) and poor permeability, resulting in poor bioavailability (Abdelkader & Fathalla, 2018; Uzan et al., 2011). In addition, as rutin is absorbed as quercetin, it is quickly metabolised into quercetin glucuronide and quercetin sulphate, which further reduce the bioavailability of rutin (Ulusoy & Sanlier, 2020). In a *in vivo* study, rutin solution prepared by glycofurol was delivered orally at a dose of 328 µmol/kg (99.13 mg/kg) to male sprague-dawley rats. The plasma concentration of quercetin was too low to be detected. On the other hand, quercetin sulfates and quercetin glucuronides were detected from the blood sample after 5 minutes of the administration of rutin solution(Yang et al., 2005). Like quercetin, rutin is not currently approved for medical treatment. It is sold as herbal supplement product in the form of tablets and capsules for oral use (Rasouli et al., 2017).

It has been reported that the stability and solubility of rutin is affected by the pH of the medium. At pH> 10, the particles of rutin were presented in amorphous form and it became partially soluble in aqueous media. When pH< 10 but > 8, the particles of rutin remained in crystalline form and the aqueous solubility became very poor (Rashidinejad et al., 2022).

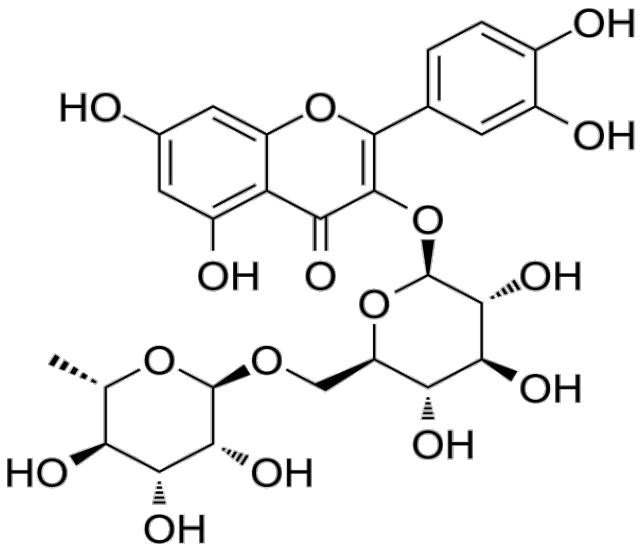

Figure 6.7. Chemical structure of rutin

6.2. Aims

- Preparing NPSSD samples of niclosamide, nitrofurantoin, omeprazole, terbinafine, quinine, quercetin and rutin.
- To determine the effect of the NPSSD samples on the dissolution of niclosamide, nitrofurantoin, omeprazole, terbinafine, quinine, quercetin and rutin by *in vitro* drug dissolution tests at pH 6.8, 37ºC.

6.3. Materials and method

6.3.1. Materials

Omeprazole, terbinafine and rutin powders were obtained from Molekula Ltd. (Darlington, UK). Quinine was purchased from Merck Schuchardt OHG (Hohenbrunn, Germany). Niclosamide, nitrofurantoin and quercetin powders were purchased from Sigma-Aldrich Ltd. (Gillingham, Dorset, UK). Soluplus was provided by BASF SE (Ludwigshafen, Germany). Vitamin E TPGs was obtained from Sigma-Aldrich Ltd. (Gillingham, Dorset, UK). HPLC grade acetone and ethanol were acquired from Fisher Scientific Ltd. (Loughborough, UK).

6.3.2. Method

6.3.2.1. Preparation of the formulated samples

NPSSD samples of niclosamide, nitrofurantoin, omeprazole, terbinafine, quinine, quercetin and rutin were prepared using the same preparation method for Solucumin, as mentioned in section 2.3.2.2.

6.3.2.2. Determination of the wavelength of maximum absorbance (λmax) for each compound

A 10 µg/ml standard solution of each drug was prepared by using acetone. Wavelength of maximum absorption (λmax) of each drug was determined by scanning the standard solutions using UV-visible spectroscopy (Lambda 265 UV/Vis Spectrophotometer, Perkin Elmer) from 200-800 nm. The λmax measured for each drug was used in the UV tests during the *in vitro* dissolution study.

6.3.2.3. *In vitro* dissolution tests

The dissolution profiles the formulated niclosamide, nitrofurantoin,

omeprazole, terbinafine, quinine, quercetin and rutin were determined by using the USP dissolution basket apparatus. The formulated omeprazole, terbinafine, quinine, and rutin were weighed to provide an equivalent dose of 5 mg of the active ingredients. The powders of the weighed samples were then filled in size 0 gelatine capsules. Three replicates were prepared for each compound (n=3). Formulated niclosamide, nitrofurantoin and quercetin were weighed at a dose equivalent to 2.5 mg of the active ingredients and then filled in size 0 gelatine capsules. It was found that at an active ingredient dose of 5 mg, the volume of the NPSSD powders of niclosamide, nitrofurantoin and quercetin powders were too large for all the powder to fill in the 0 sized gelatine capsules. As a result, the applied dose of these NPSSD samples were reduced by half to 2.5 mg. Three replicates were prepared for each compound (n=3).

The baskets were attached to the basket shifts of the dissolution apparatus. During the dissolution test, the capsule-loaded baskets were immersed in 900 ml of phosphate buffer dissolution medium at pH6.8, at 37ºC and 100 rpm rotation. 5ml of sample suspensions were collected at each time (10, 30, 60, 90, 120 and 180 minutes) and filtered through 0.45 µm nylon syringe filters. The dissolution medium was not replaced after collecting sample suspension. The filtered sample solutions were then analysed by UV-visible spectroscopy (Lambda 265 UV/Vis Spectrophotometer, Perkin Elmer) to determine the concentration of the drug dissolved (n=3). The results of the drug dissolution were expressed as the percentage of the drug release of the total amount of the drug in NPSSD samples. The data was presented as mean ± standard deviation (SD).

10 mg of each drug/compound was added to 100 ml of ethanol, yielding 0.1 mg/ml stock solutions. The stock solutions were then diluted by ethanol to

concentrations standard solutions with drug/compound concentrations ranged from 1 to 10 µg/ml and analysed by UV-vis. All calibration curves showed a linear relationship with a correlation coefficient of $R^2 > 0.995$. Examples of the calibration curves for each drug and natural compound are shown in Figures 6.8-6.14.

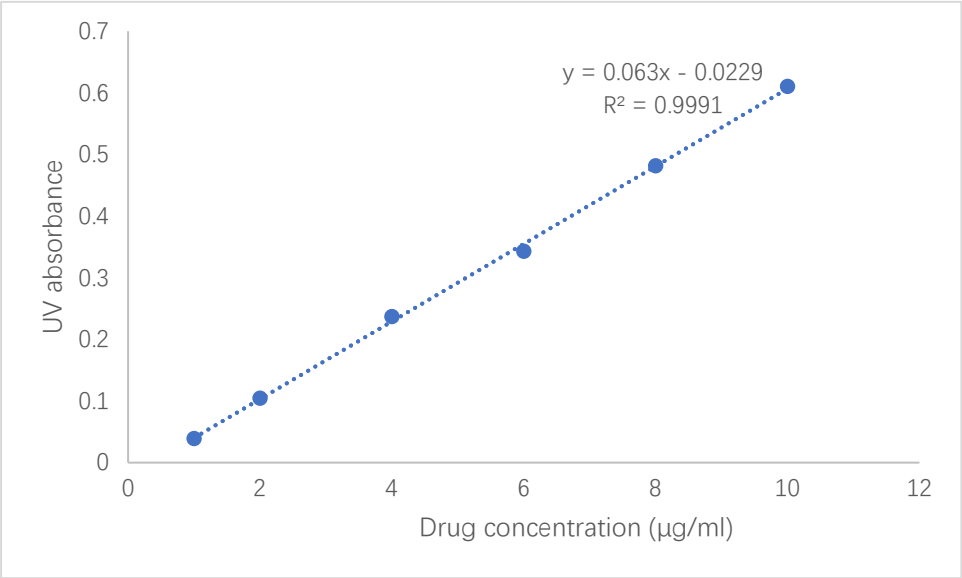

Figure 6.8. Calibration curve of niclosamide with drug concentrations ranged from 1 to 10 µg/ml

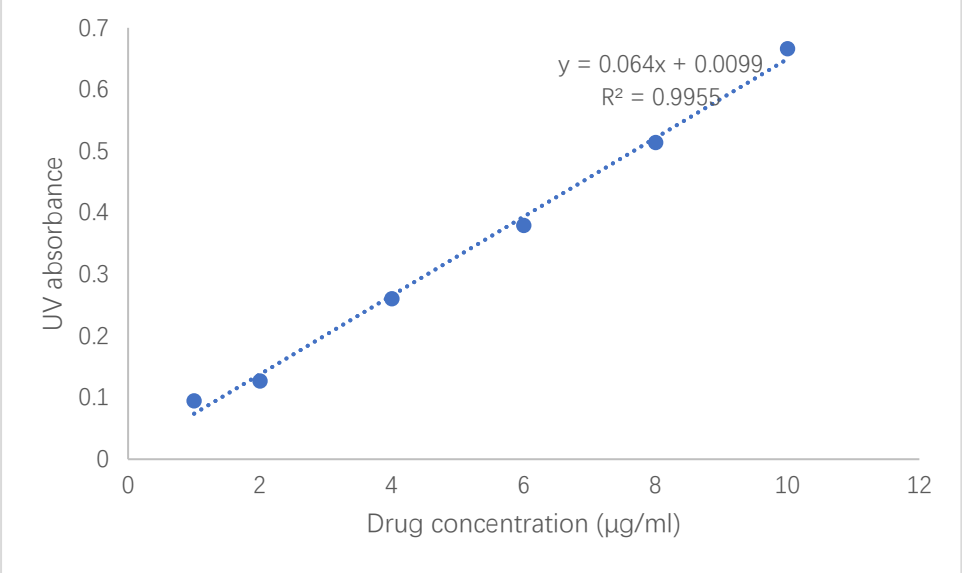

Figure 6.9. Calibration curve of nitrofurantoin with drug concentrations ranged from 1 to 10 µg/ml

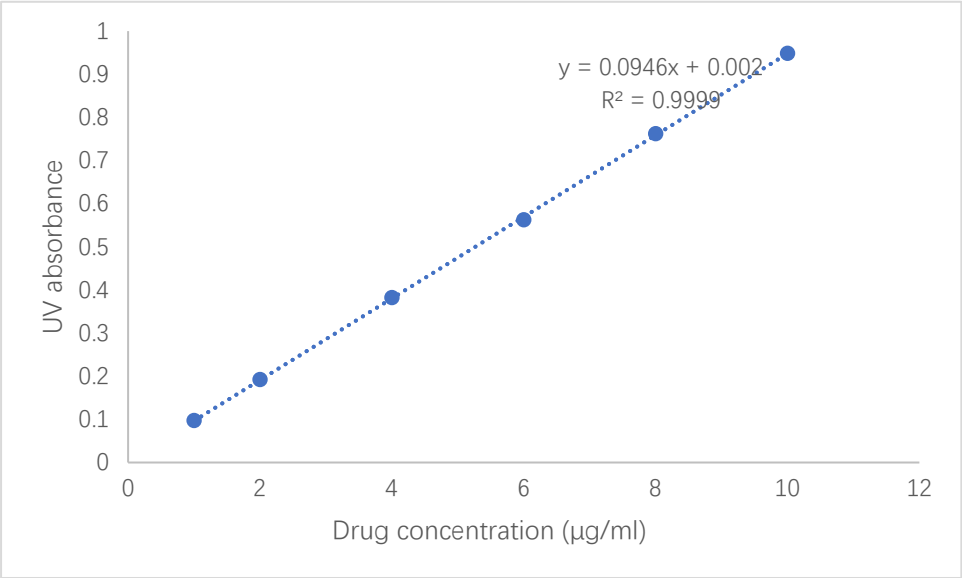

Figure 6.10. Calibration curve of omeprazole with drug concentrations ranged from 1 to 10 µg/ml

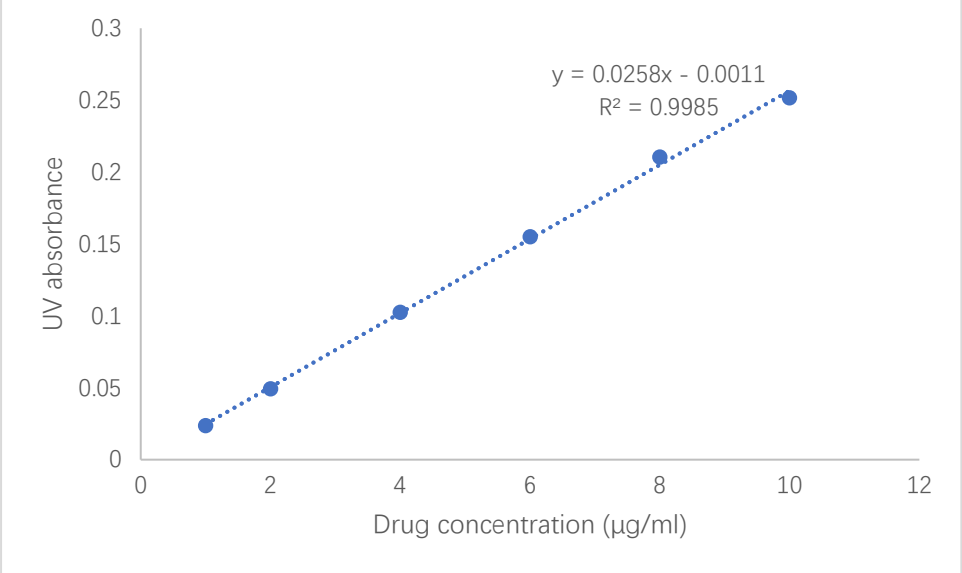

Figure 6.11. Calibration curve of terbinafine with drug concentrations ranged from 1 to 10 µg/ml

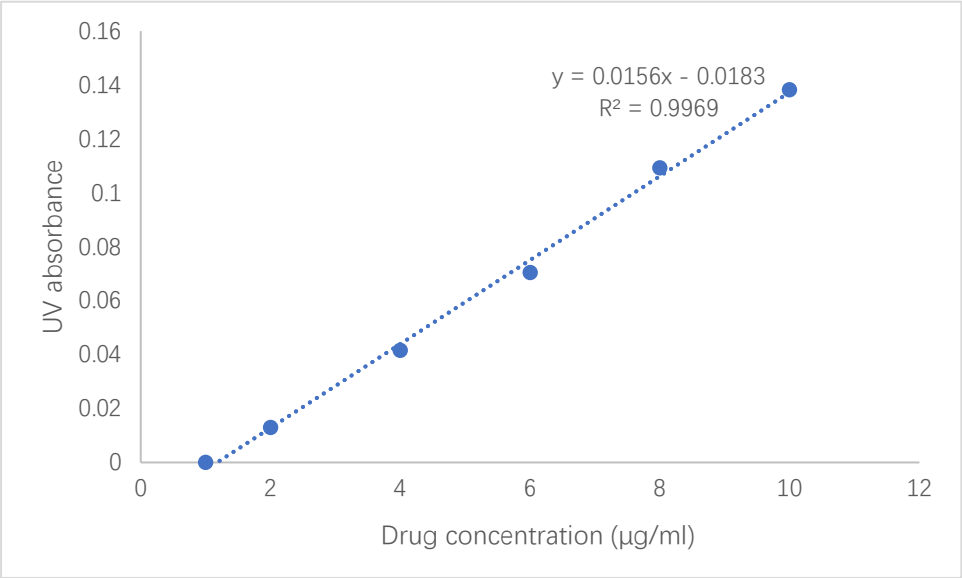

Figure 6.12. Calibration curve of quinine with compound concentrations ranged from 1 to 10 µg/ml

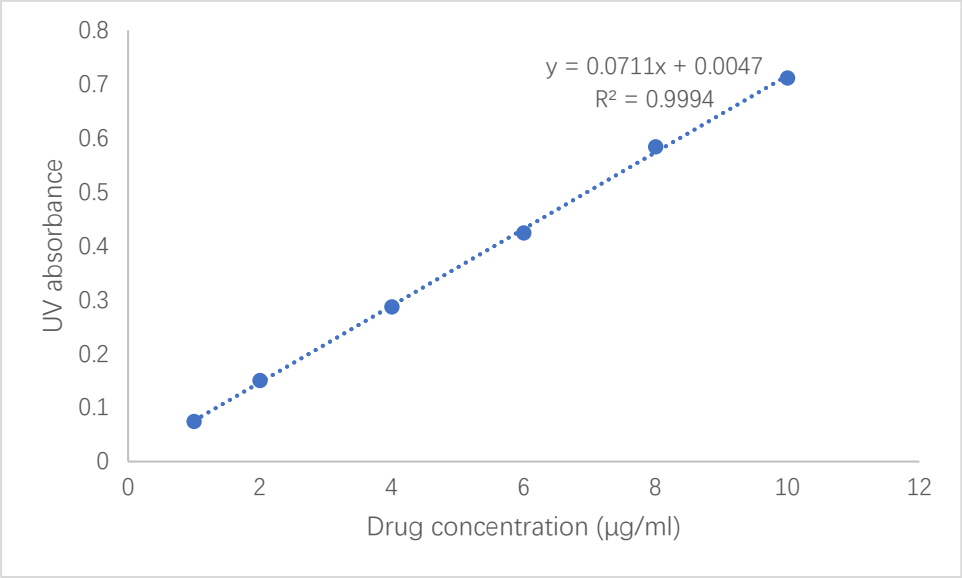

Figure 6.13. Calibration curve of quercetin with compound concentrations ranged from 1 to 10 µg/ml

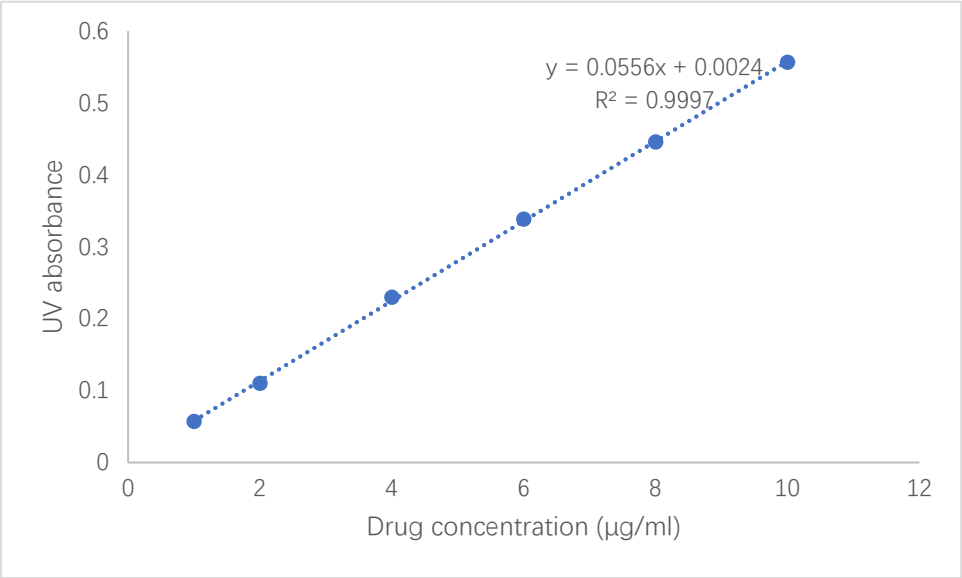

Figure 6.14. Calibration curve of rutin with compound concentrations ranged from 1 to 10 µg/ml

6.3.2.4. Comparison of the dissolution profiles

The percentage of the drug dissolution of the NPSSD and the pure drug/natural compound at each time point were statistically compared by independent sample t-test using the IBM SPSS Statistics software (Version 24.0; IBM Corp, Armonk, NY, USA). The significance value of $p \leq 0.05$ will be considered as significant difference between the percentage drug release from the formulated drug and the pure drug at the same time point.

6.4. Result

6.4.1. Determination of the wavelength of maximum absorbance (λmax) for each drug

The results of UV spectroscopy test of the standard solutions of the drugs showed the maximum characteristic peaks at the wavelength of 331nm for niclosamide, 358nm for nitrofurantoin, 302nm for omeprazole, 282nm for terbinafine, 332nm for quinine, 374nm quercetin and 256nm for rutin. These UV wavelength values were used for the following UV tests in the *in vitro* dissolution study.

6.4.2. *In vitro* dissolution study

Figures 6.15–6.21 illustrates the dissolution profiles for the NPSSD samples compared with the pure drugs at pH 6.8 dissolution medium.

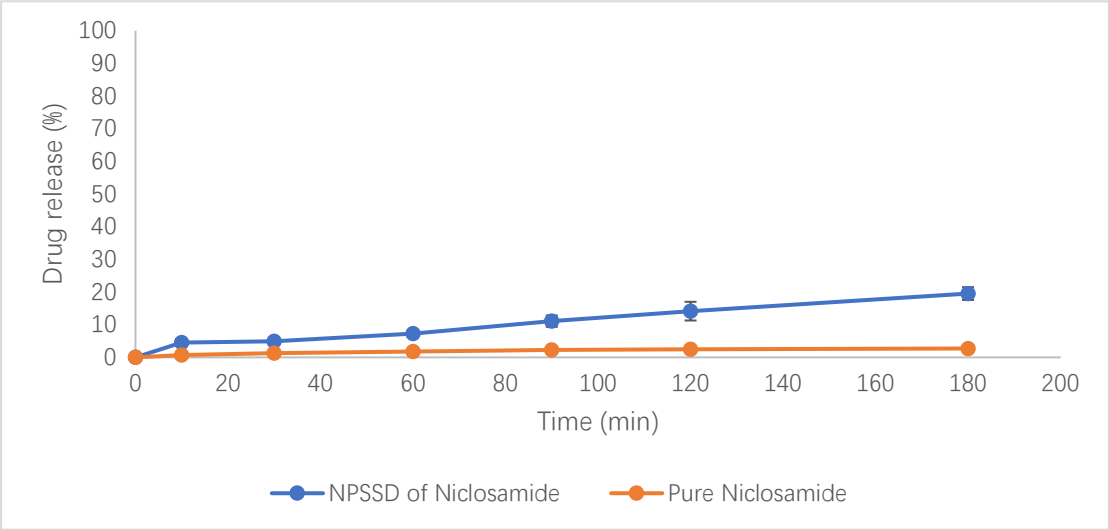

Figure 6.15. Dissolution profile of drug release from the NPSSD of niclosamide and pure niclosamide in pH 6.8 (n=3, mean ± SD)

As shown in Figure 6.15, the NPSSD of niclosamide showed percentage drug release remained stable from 10 to 30 minutes (increased from 4.55 ± 0.07% to 4.89 ± 0.32%), followed by a steady increase from 30 to 180 minutes (increase from 7.24 ± 0.12% to 19.53 ± 1.97%). As for the pure niclosamide, it showed a very low percentage drug release throughout the *in vitro* dissolution test with the cumulative percentage of drug release of only 2.72 ± 0.63% at the end of the dissolution test. The NPSSD of niclosamide showed significantly higher percentage drug release at all the time points compared to pure niclosamide ($p \leq 0.05$).

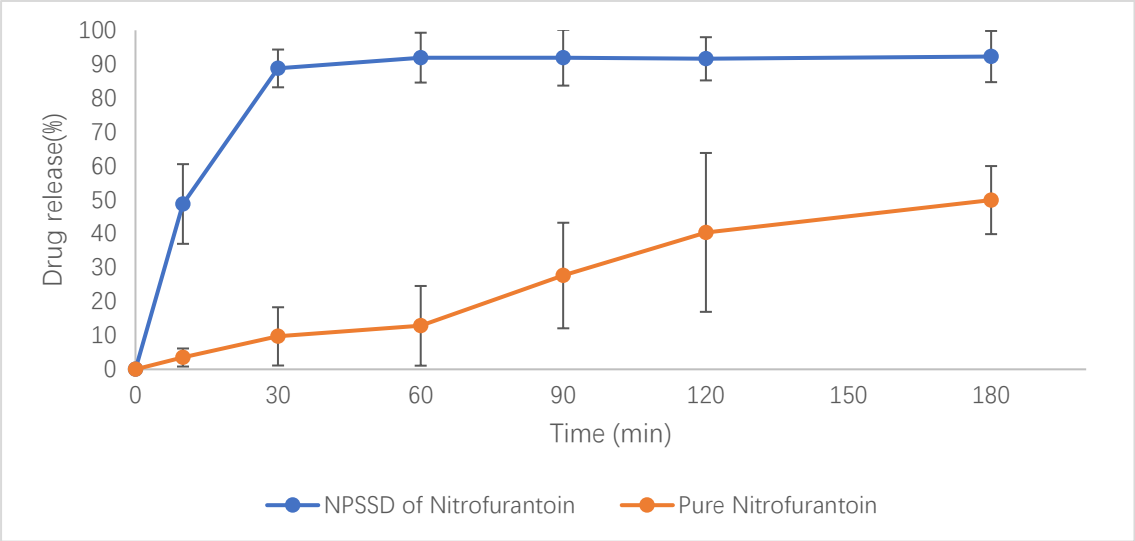

Figure 6.16. Dissolution profile of drug release from the NPSSD of nitrofurantoin and pure nitrofurantoin in pH 6.8 (n=3, mean ± SD)

As shown in Figure 6.16, the NPSSD of nitrofurantoin showed considerable improvement in the amount of the drug dissolved and the rate of the drug dissolution. It was observed that the percentage drug release jumped to 48.77 ± 11.75% at 10 minutes and it rapidly increased to 88.76 ± 5.57% by 30 minutes. Drug dissolution profile became stable and eventually the percentage drug release reached 92.26 ± 7.55%. On the other hand, pure nitrofurantoin showed significantly lower percentage drug release compared with the NPSSD of nitrofurantoin at every time point ($p \leq 0.05$). The percentage drug release of the pure nitrofurantoin increased over time and eventually reached to 49.92 ± 10.04% at the end of the dissolution test.

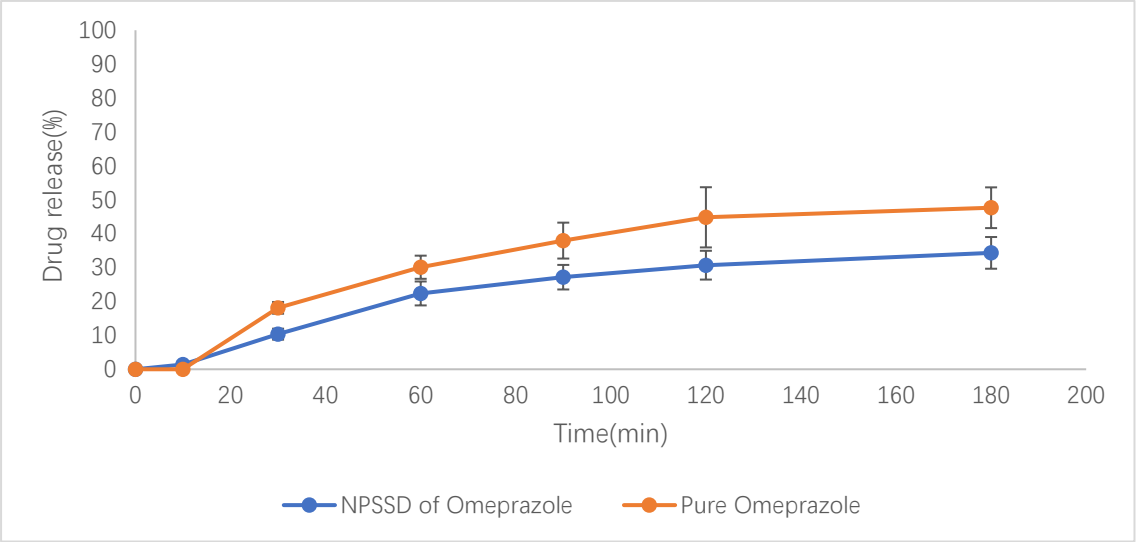

Figure 6.17. Dissolution profile of drug release from the NPSSD of omeprazole and pure omeprazole in pH 6.8 (n=3, mean ± SD)

As shown in Figure 6.17, the percentage of drug release from the NPSSD of Omeprazole and the pure Omeprazole both showed steady increase over time. The the NPSSD of Omeprazole exhibited 1.39 ± 0.92% of the drug release at 10 minutes while no drug was released from the pure omeprazole. However, the percentage of the drug release from the the NPSSD of omeprazole became significantly lower than the pure omeprazole at the subsequent time points ($p \leq 0.05$). At the end of the dissolution test, the NPSSD of omeprazole reached to a percentage of the drug release of 34.33 ± 4.68% which was significantly lower than the pure omeprazole of 47.65 ± 6.01% ($p \leq 0.05$).

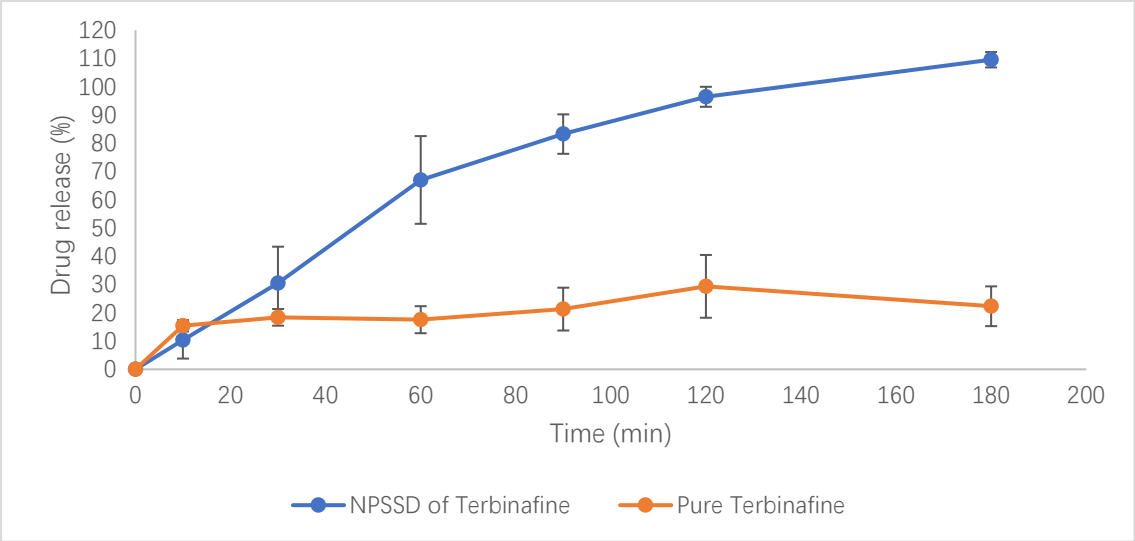

Figure 6.18. Dissolution profile of drug release from the NPSSD of terbinafine and pure terbinafine in pH 6.8 (n=3, mean ± SD)

As shown in Figure 6.18, the NPSSD of terbinafine showed significantly higher percentage of the drug than that of the pure terbinafine at the time points from 60 to 180 minutes ($p \leq 0.05$). Percentage dissolution of the drug increased steadily over time and it eventually reached 109.59 ± 2.72% at the end of the dissolution test. As for the pure terbinafine, it showed much lower dissolution of the drug compared with the formulated terbinafine. Its dissolution profile showed fluctuation over time. The percentage drug release reached 15.40 ± 2.02% at 10 minutes and increased to 18.40 ± 2.94% at 30 minutes. Then it changed to 17.56 ± 4.78% at 60 minutes, 21.32 ± 7.58% at 90 minutes and 29.37 ± 11.12% at 120 minutes. Finally, the percentage of the drug release reached to 22.33 ± 7.04 % at 180minutes.

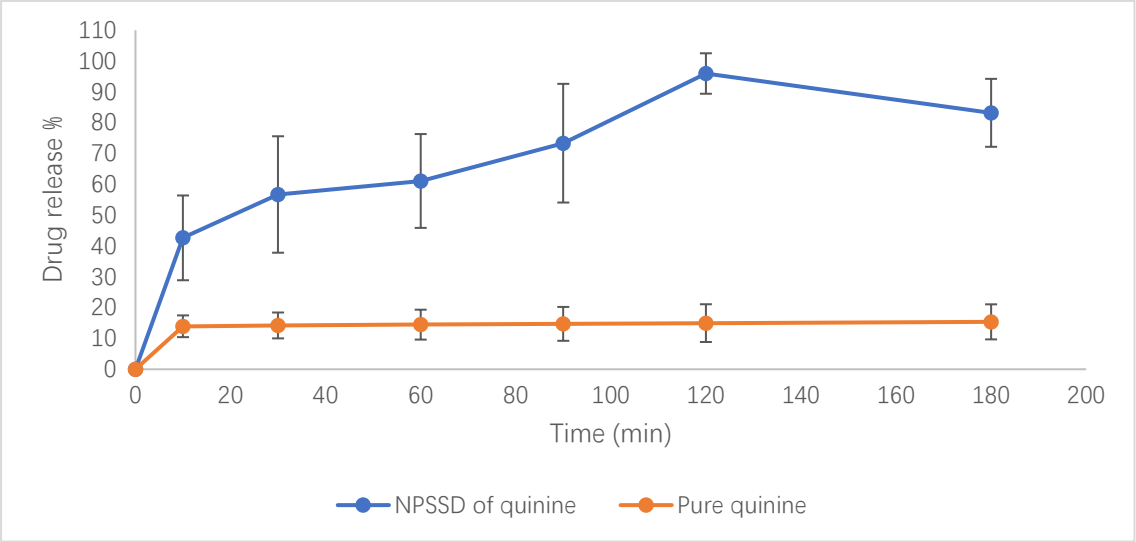

Figure 6.19. Dissolution profile of drug release from the NPSSD of quinine and pure quinine in pH 6.8 (n=3, mean ± SD)

As shown in Figure 6.19, the percentage of the drug release from the pure quinine reached to 13.95 ± 3.53% at 10 minutes and then the dissolution profile became stable. The percentage of drug release eventually reached to 15.38 ± 5.69% at the end of the dissolution test. On the contrary, the NPSSD of quinine showed significantly higher percentage drug release compared to the pure quinine at every time point ($p \leq 0.05$). The drug release had rapidly reached 42.64 ± 13.75 % in 10 minutes and it started to grow steadily which eventually reached to 95.96 ± 6.57% at 120 minutes. The percentage drug release dropped to 83.21 ± 11.02% at 180 minutes. A paired T-test was carried out to compare the data of the percentages of the drug release at 120 minutes and 180 minutes for the NPSSD of quinine and it has been found that there was not significantly different ($p > 0.05$). This indicated that saturated solubility of quinine had been reached at 120 minutes and remained stable throughout the end of the dissolution test.

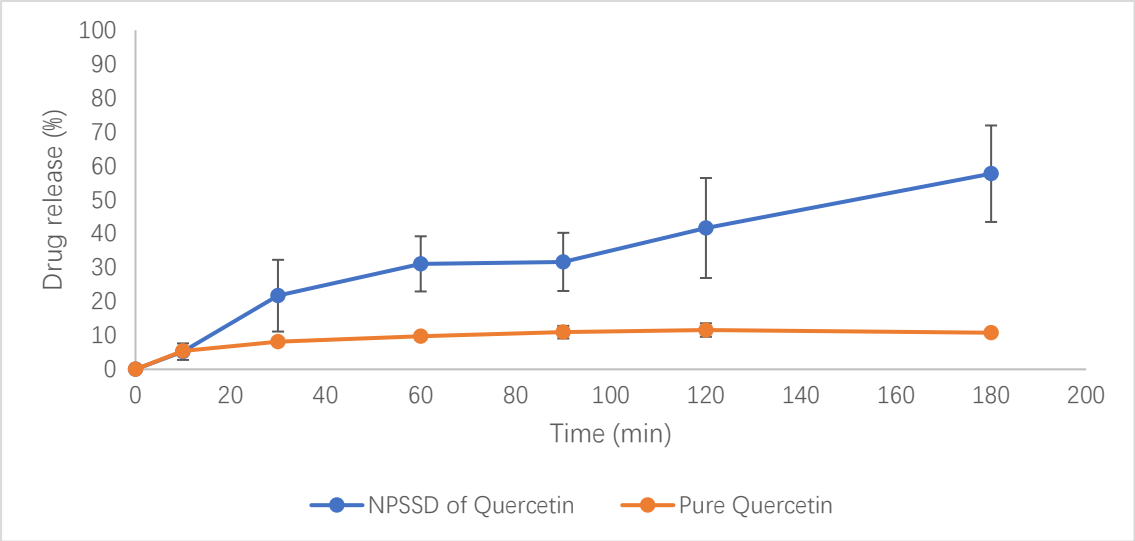

Figure 6.20. Dissolution profile of drug release from the NPSSD of quercetin and pure quercetin in pH 6.8 (n=3, mean ± SD)

As shown in Figure 6.20, the NPSSD of quercetin showed significantly higher percentage drug release compared to the pure quercetin at each time point from 30 to 180 minutes ($p \leq 0.05$). The percentage drug release of the formulated quercetin increased steadily over time and eventually reached to 57.70 ± 14.23% at 180 minutes. As for the pure quercetin, the increase in percentage drug release was much slower compared with the NPSSD of quercetin. It slowly increased over time finally reaching 10.80± 0.78% at 180 minutes.

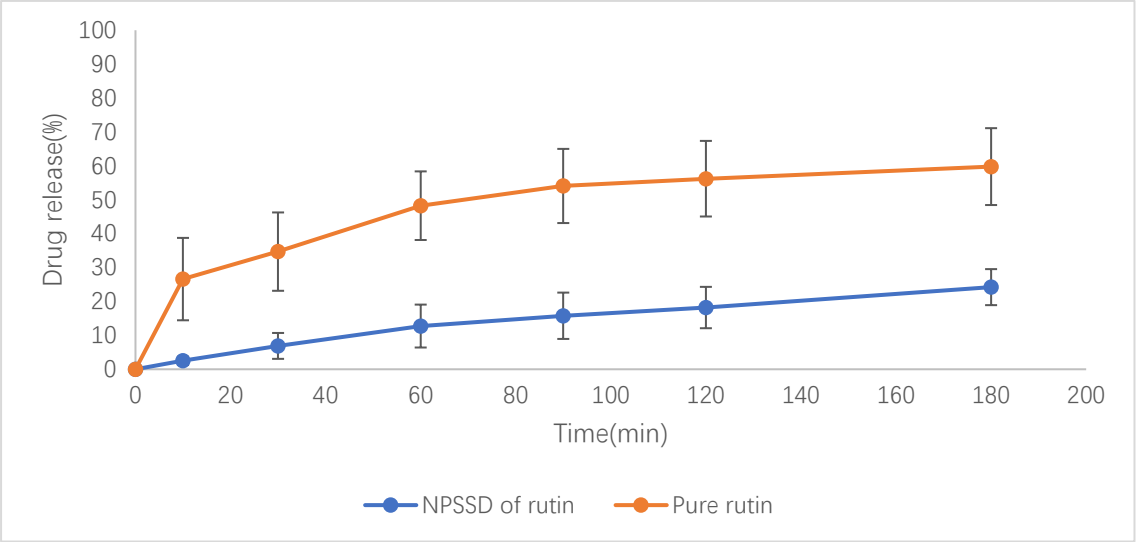

Figure 6.21. Dissolution profile of drug release from the NPSSD of rutin and pure rutin in pH 6.8 (n=3, mean ± SD)

As shown in Figure 6.21, the pure rutin showed significantly higher percentage of drug release compared to the NPSSD of rutin at every time point throughout the dissolution test ($p \leq 0.05$). Percentage drug release of pure rutin rapidly reached to 26.60 ± 12.15% at 10 minutes and then increased steadily over time. At the end of the dissolution test, it reached to 59.78 ±11.34%. As for the NPSSD of rutin, its percentage of the drug release also increased steadily over time and eventually reached to 24.23 ± 5.31% at the end of the dissolution test.

6.5. Discussion

6.5.1. The effect of NPSSD on the dissolution of poorly soluble drugs/natural compounds

As shown in the results of the *in vitro* dissolution tests, the effect of NPSSD on drug dissolution differs for different drugs and natural compounds. It has been demonstrated that NPSSD was able to increase the dissolution of niclosamide, nitrofurantoin, terbinafine, quinine and quercetin while decreasing the dissolution of omeprazole and rutin. Niclosamide, nitrofurantoin, terbinafine and quinine are BCS II compounds, so their drug absorption can certainly be improved by the increased drug dissolution, as drug dissolution is the rate limiting step in the rate of drug absorption for BCS class II compounds (Chavda et al., 2010). Especially for nitrofurantoin, the NPSSD sample has shown immediate drug release as >85% of the total drug had dissolved within first 30 minutes.

The LogP (octanol-water partition coefficient**)** values and BCS classification of each drug/natural compound were analysed to see if the lipophilicity and BCS class of the drug/natural compound might have any influence on the effect of NPSSD on drug dissolution. LogP indicates how readily a compound will partition between an aqueous and organic phase. It is a measure of how lipophilic or hydrophilic a compound is. More positive LogP value indicates higher lipophilicity (Ditzinger et al., 2019).

The extent of increase/decrease of the drug dissolution by NPSSD, BCS classification and the value of Log P of each drug/natural compound are listed in Tables 6.2 and 6.3.

	The extend of Increase of the drug dissolution by NPSSD	**Log P**	**BCS Class**
Quinine	7.39-fold	3.44	II
Quercetin	5.72-fold	1.82	IV
Niclosamide	5.60-fold	4.48	II
Terbinafine	4.90-fold	6	II
Nitrofurantoin	1.84-fold	-0.47	II

Table 6.2. The extend of increase of the drug dissolution by NPSSD, Log P values and BCS classification for the drugs/natural compounds

	The extend of decrease of the drug dissolution by NPSSD	**Log P**	**Class**
Omeprazole	1.38-fold	2.23	II
Rutin	2.46-fold	-2.02	IV

Table 6.3. The extend of decrease of the drug dissolution by NPSSD, Log P values and BCS classification for the drugs/natural compounds

As shown in Table 6.2, niclosamide, terbinafine and quinine are BCS class II drugs/compounds and all have positive Log P values. All of them showed considerable extent of increase in drug dissolution. Quercetin also showed a relatively high increase in drug dissolution by NPSSD and it has a positive Log P value. However, it is a BCS IV compound. Nitrofurantoin is the drug that showed relatively lower extent of increase in drug dissolution by NPSSD compared to other drugs/natural compounds. It is a Class II drug with negative Log P value. In contrast, omeprazole is a Class II drug with positive Log P value while the rutin is a Class IV compound with negative Log P value. As shown in Table 6.3, both of them experienced reduction in drug dissolution by NPSSD. Combining the data of the *in vitro* dissolution test of Solucumin mentioned in section 3.6.3, it was found that NPSSD increased the dissolution of curcumin from 0 to 9.81 ± 1.16% after 3 hours in pH6.8 medium at 37ºC. Curcumin has a Log P value of 3 (Priyadarsini, 2014) and it was classified as a Class IV compound (Paolino et al., 2016; Wahlang et al., 2011).

From the above comparison, it can be noted that among the drugs for which the NPSSD showed an increase in drug dissolution, those with positive Log P values generally showed a higher degree of increase in drug dissolution than those with negative Log P values. In addition, drugs with negative Log P values either showed a relatively small extent of increase in drug dissolution or a decrease in drug dissolution. There might be a positive correlation between lipophilicity of the drug/natural compound and the effect of NPSSD on drug dissolution. However, there is not enough data in the current study to prove in this hypothesis, more data of lipophilicity and dissolution of other drugs/natural compounds will be needed. On the other hand, whether a drug/ natural compound falls into BCS Class II or Class IV does not appear to have an impact on the effect of NPSSD on drug dissolution. This might suggest that the effect of NPSSD on drug dissolution might not be influenced by the BCS class of

poorly soluble drug/compound.

It is possible the increase of the drug dissolution was due to micellar solubilisation as it has been reported that the combination of Soluplus and Vitamin E TPGs could lead to formation of micelles and make the APIs more soluble (Bernabeu et al., 2016; Feng et al., 2020). An interesting finding from this study is that the dissolution of quercetin and rutin, two natural compounds with similar chemical structures, showed the opposite results after being formulated into NPSSD. Rutin is a glycoside composed of quercetin, with the hydroxy group at position C-3 substituted with glucose and rhamnose sugar groups. This means rutin has more H-bond forming groups (e.g. hydroxyl, carbonyl and ether groups) than quercetin, which might give it more chances to form H-bond interactions with Soluplus and/or Vitamin E TPGs. Sabboo et al. has reported that indomethacin-PVPVA solid dispersions with drug-polymer H-bonding interactions exhibited poorer drug dissolution than those without (Saboo et al., 2020). Therefore, it is possible that the dissolution of rutin was reduced by NPSSD due to the formation of H-bond interactions between the drug and the excipients. The other drugs/natural compounds might also have drug: excipient H-bond interactions after being formulated into NPSSD, as they all contain groups that can form H-bonds (e.g. hydroxyl, methoxy, amine and/or ester groups) with the excipients. Like rutin, the reduced dissolution of omeprazole might be related to H-bonding interactions of the drug and excipients. However, it might also be caused by other factors, such as the failure of NPSSD to convert the crystalline drug into an amorphous form or the adsorption of the drug onto the surface of the excipient(Fathima et al., 2011; Teja et al., 2016). In order to verify these hypotheses, future characterisation studies such as FTIR, DSC, XRD should be carried out.

6.6. Conclusion

In summary, it has been proven that NPSSD can not only enhance the dissolution of curcumin, but also several other poorly water-soluble drugs and natural compounds. The lipophilicity of the drug/compound is a factor that might influence the effect of NPSSD on drug dissolution. However, more data of other drugs/natural compounds are needed to prove this view. On the other hand, whether a drug/compound is a BCS Class II or IV does not seem to have a direct correlation with whether NPSSD will increase or decrease the drug dissolution.

Apart from the lipophilicity the drugs/natural compounds, other factors might contribute to the change of the drug dissolution such as reduction of particle size and conversion of crystalline form of the drugs into amorphous state. Published studies have reported that the drug dissolution of quercetin, niclosamide and nitrofurantoin have been significantly increased by formulating into amorphous solid dispersions (Ali & Gorashi, 1984; Jara et al., 2021; Kakran et al., 2011). To verify whether other factors have attributed to the effect of NPSSD on drug dissolution, further characterisation studies such as XRD, DLS, DSC and FTIR should be conducted in the future. Further studies on solubility, stability and permeability could be carried out in the future to further explore the potential of NPSSD.

Chapter 7. General discussion, limitation and future work

7.1. Introduction

In this chapter, it will begin with an outline of the work that has been covered in each chapter of this thesis. Then there will be a general discussion of the study. The purpose of the general discussion is to find interpretations and explanations of the observations from the experimental results and to try to relate them to the hypothesis and aims of this study. It will also discuss the new findings observed from the experiments. At the end of the chapter, the limitations of this study and proposed future work will be discussed.

7.2. Outline

Among all the drug administration routes, the oral route is the most widely used(Gupta et al., 2009). However, a major challenge for orally administered drugs is their low bioavailability and poor solubility as one of the main causes of poor oral bioavailability (Savjani et al., 2012). For any orally delivered drug to be absorbed, it must first dissolve and form a solution in the lumen of gastrointestinal tract. Unfortunately, many drugs have poor aqueous solubility which limits their drug absorption (Savjani et al., 2012).

Curcumin is a yellow, crystalline and odourless powder that is obtained from the roots of turmeric (Esatbeyoglu et al., 2012). Decades of scientific research have confirmed that curcumin has numerous medicinal properties. To this day it continues to attract the interest of researchers worldwide. However, despite its excellent medical potential, curcumin is still not approved for use as a drug due to its poor aqueous solubility which leads to extremely low oral bioavailability (Paolino et al., 2016).

Solid dispersions are commonly used to improve the solubility and the oral bioavailability of poorly soluble drugs/natural compounds. It is a solid product where the drugs can be molecularly or amorphously dispersed in a matrix formed by the excipients (normally polymers) (Chiou & Riegelman, 1971). As mentioned in section 2.1.1.2.4, solid dispersions are a very promising strategy with many advantages over other techniques for improving the solubility and bioavailability of poorly water-soluble drugs, such as milling, formation of salts and emulsions. As a result, it was chosen as the strategy for improving the solubility and oral bioavailability of curcumin.

In this study, the main aim was to develop a novel polymer-surfactant based solid dispersion (NPSSD) to improve the solubility and oral bioavailability of

curcumin, using a combination of excipients that have not been previously used in curcumin solid dispersion formulations. A novel solid dispersion of curcumin, which named as Solucumin, was developed. It consisted of curcumin + Soluplus + Vitamin E TPGs (1:10:10) and was prepared by a solvent evaporation plus freeze-drying method. From a series of experiments, Solucumin has demonstrated a significant increase in the solubility, dissolution and permeability of curcumin. The performance of Solucumin for improving drug dissolution and permeability of curcumin was also compared with two marketed curcumin products (Longvida® and Nacumin®) and another polymer-surfactant based curcumin solid product developed in a previous study (Mexcumin). From comparison, it was revealed that Solucumin was more effective in improving the dissolution and permeability of curcumin than the comparators.

At the beginning of the study, five excipient candidates (Soluplus, Vitamin E TPGs, HPMCAS L, M and H grades) were proposed. After a screening process, Soluplus and Vitamin E TPGs were selected as the final excipients for the preparation of Solucumin, which was described and discussed in Chapter 2 of this thesis. This chapter also presented the effect of Solucumin on the aqueous solubility of curcumin in the pH levels similar to those in the gastrointestinal lumen. Chapter 3 presented *in vitro* dissolution tests to evaluate the effect of Solucumin on drug dissolution of curcumin and how it compared with the other formulations. The results of a series of characteristics studies of Solucumin and the comparators were presented and interpreted in Chapter 4. *In vitro* drug permeation experiments and cellular drug uptake tests were performed using Caco-2 cell model to predict the intestinal absorption of curcumin from Solucumin and the comparators, which was covered by Chapter 5. The potential application of Solucumin technology on other poorly water-soluble drugs and natural compounds was investigated in another *in vitro*

dissolution test. The experimental results and the conclusions were presented in Chapter 6. A general outline of the content that covered in each chapter is shown in Table 7.1.

Chapter 1
✧ **Background information of curcumin** ✧ **Hypothesis of the study** · Using polymer and surfactants to form an amorphous solid dispersion formulation for curcumin to improve its aqueous solubility and eventually enhance the oral bioavailability. ✧ **Aims of the study** · Developing a novel polymer-surfactant based solid dispersion (NPSSD) to improve the solubility and oral bioavailability of curcumin. · Evaluating the effect of the novel solid dispersion formulation on curcumin dissolution & permeability and comparing with marketed curcumin products. · Investigating the effect of the novel solid formulation on the drug dissolution of poorly water-soluble drugs/natural compounds other than curcumin.

Chapter 2
✧ **Preliminary screening study (Literature review)** · Soluplus, HPMCAS (L, M and H grades) and Vitamin E TPGs were chosen as the excipient candidates. ✧ **Secondary screening study (Solubility study)** · Curcumin+Solplus+Vitamin E TPGs (1:10:10) prepared by solvent evaporation+freeze drying was chosen as the novel solid dispersion formulation for curcumin (Solucumin).

Chapter 3
✧ ***In vitro* dissolution tests of Solucumin and the comparators (Mexcumin, Longvida® and Nacumin®)** · Solucumin showed the highest percentage and amount of dissolution of curcumin after 6 hours at pH6.8 buffer. · Mexcumin was found being more effective in dissolving other curcuminoids as it showed the highest percentage and amount of demethoxycurcumin and bisdemethoxycurcumin respectively after 6 hours at pH 6.8 buffer.

Chapter 4

✧ **Characterisation studies of Solucumin and Mexucumin (FTIR, DSC, XRD, DLS, zeta potential and short-term stability test)**

✧ **Solucumin**

- Particle size: 3407.00±421.01 nm.
- Zeta potential: -12.80±2.43 mV.
- Curcumin presented in an amorphous state.
- No API adhered on the surface of the excipients.
- Can keep curcumin from degradation at 25 °C /60% RH and 40 °C /60% RH for at least one month.

✧ **Mexcumin**

- Particle size: 1169.67±76.83 nm.
- Zeta potential: -20.25±4.46 mV.
- It was unclear that if curcumin presented in a crystalline state or an amorphous state.
- No API adhered on the surface of the excipients.
  Can keep curcumin from degradation at 25 °C /60% RH and 40 °C /60% RH for at least one month.

Chapter 5

✧ ***In vitro* permeation experiments on Solucumin and other comparators (Mexcumin, Longvida® and Nacumin®), using Caco2 cell monolayers as the model**

- Solucumin showed the highest curcumin permeation from the apical to basolateral sides (A-B) among all the tested samples.
- Solucumin was the only sample that showed curcumin transported from the basolateral to apical side (B-A), indicating the presence of drug efflux.

✧ **Cellular drug uptake tests conducted at the end of the *in vitro* permeation experiments**

- Solucumin showed both higher apical cellular uptake and basolateral cellular uptake of curcumin than all other tested samples.
- There was a positive correlation between the apical cellular uptake of curcumin and the solubility of curcumin.

Chapter 6

✧ ***In vitro* dissolution tests on NPSSD when the active ingredients changed from curcumin to other poorly water-soluble drugs/natural compounds**

- NPSSD has demonstrated the effect on increasing the drug dissolution of Terbinafine, Nicolosamide, quinine, quercetin and Nitrofurantoin.
- Decreased the drug dissolution of Omerprazole and rutin.

Chapter 7
✧ **Outline** ✧ **General discussion** ✧ **Limitations of the study** ✧ **Future work**

Table 7.1. A general outline of the work covered in each chapter of the thesis

7.3. General discussion

As mentioned in the outline, the main objective of this study was to develop a solid formulation that can improve the aqueous solubility and eventually the oral bioavailability of curcumin and this objective has been achieved through the development of Solucumin.

As a novel solid dispersion formulation of curcumin, the novelty of Solucumin is reflected in these points:

1). Solucumin used an unprecedented combination of excipients to prepare a solid dispersion formation for curcumin. It is the first amorphous solid dispersion formulation of curcumin that was made from a combination of Soluplus and Vitamin E TPGs.

2) Solucumin was not only better than the commercial grade curcumin in terms of solubility, drug dissolution and Caco-2 cell monolayers permeability, but also better than some commercially available curcumin formulations. In contrast, many published studies on curcumin formulations have only compared them with curcumin and not with other curcumin products (Baek & Cho, 2017; Chaurasia et al., 2015; Cuomo et al., 2018; Dhumal et al., 2015; Govindaraju et al., 2019; Parikh et al., 2018; Patil et al., 2015; Peng et al., 2018; Peng et al., 2017; Petchsomrit et al., 2016; Schiborr et al., 2014; Shukla et al., 2017; Song et al., 2016; Teixeira et al., 2016; Vecchione et al., 2016; Wan et al., 2016; Wang et al., 2015; Wang et al., 2019; Wang et al., 2017b; Q. Zhang et al., 2018).

3) Solucumin technology can not only improve the drug dissolution of curcumin, but also other poorly-water soluble drugs and natural compounds. Terbinafine and quinine, in particular, have showed almost complete drug

dissolution in the *in vitro* dissolution study at pH 6.8 after being formulated into NPSSD.

Curcumin in Solucumin has been successfully converted to the amorphous form. In contrast, curcumin in Longvida® and Nacumin® remain crystalline, which might account for their much lower curcumin dissolution compared with Solucumin. Solucumin has shown considerable increase in the aqueous solubility (938-fold at pH6.8 and 582-fold at pH1.2) and dissolution (from 0% to 10.50 ± 1.37% at pH6.8) of curcumin due to the reduction of particle size and conversion of the crystalline curcumin into amorphous form. The reduced particle size provides a large surface area to contact the medium and amorphous drugs generally possess higher dissolution than their crystalline counterparts due to the lack of long-order molecular arrangement which provides them higher molecular mobility and free energy (Yu, 2001). Solucumin has shown higher increase in the solubilities and dissolution of curcumin when at pH 6.8 than pH 1.2. This suggests that the solublisation of curcumin can be influenced by the pH level of the medium and being formulated into Solucumin did not alter this. It was reported that curcumin is very poorly soluble in aqueous solution with pH of 1-6, which is probably due to the undissociated form of the hydroxy groups in acidic pH level (Esatbeyoglu et al., 2012).

While solubility-enhancing formulations can achieve considerable increases in the drug solubility, they do not always a positive effect on the drug permeability. For example, complexes or micelles can facilitate the solublisation of a drug, but they could also reduce the amount and rate of drug permeation by reducing the free fraction of the drug that permeates the cell membrane (Dahan & Miller, 2012). Several published studies have reported that unchanged or decreased intestinal permeability of drug (dantrolene, digoxin, griseofulvin and ketoconazole) was observed after being prepared into

solubility-enhancing formulations such as micelles (Carrier et al., 2007; Katneni et al., 2006, 2007; Loftsson et al., 2007; Miller et al., 2011; Poelma et al., 1991). Fortunately, in this study, Solucumin had avoided the scenario in which the solubility gain results in permeability loss. In fact, the *in vitro* drug permeation experiments result even suggests that there was a positive correlation between the Caco-2 cell permeation and the solubility of curcumin. Since curcumin was absorbed in the small intestine predominately by passive diffusion (Xue et al., 2017). Thus, the Caco-2 cell permeation of curcumin can generally follows Ficks first law, which rate of permeation is proportional to the concentration gradient (Brodin et al., 2010). As shown in section 5.5.3, it was found that the tested sample with higher value of C_0 (suspension), (A-B) also showed higher concentration of A-B curcumin permeation and Papp (Solution), (A-B). As the formulation with the highest values of C_0 (suspension), (A-B), Solucumin allowed more dissolved curcumin to present at the apical surface of the Caco-2 cell monolayer so that more curcumin can permeate across the cells per unit time per surface area.

In the *in vitro* permeation experiments, Solucumin has shown the highest curcumin permeation concentration of 0.49 ± 0.07 μg/ml from A-B and the highest Papp (A-B solution) of 1.12 ± 0.15 $\times 10^{-6}$ cm/s among all the comparators and the curcumin control. Although curcumin transported from the B-A was observed from Solucumin, the measured curcumin permeation concentration from B-A (0.19 ± 0.04 μg/ml) and Papp(B-A), (Solution) (0.42 ± 0.10 $\times 10^{-6}$ cm/s) were lower than that of measured from A-B. Furthermore, the efflux ratio of Solucumin was calculated to be 0.38, which suggested that the absorptive influx passive diffusion transport is more dominant than efflux transport during the curcumin transport process.

As shown in section 5.4.3, this study has calculated Papp in two different

ways (Papp (suspension) and Papp (solution)) and compared them to find out which one can better reflect the permeability of the drug. This is something that has not been done before in other published studies to date. The Papp(solution),(A-B) of Solucumin was 1.12 $\times 10^{-6}$ cm/s, which was lower when comparing with some other curcumin solid formulation developed in recent years, such as curcumin encapsulated xanthan-chitosan polysaccharides nanofibers developed by Faralli et al. with Papp(A-B) of 1.49×10^{-5} cm/s)(Faralli et al., 2019), polyelectrolyte complex nanoparticles of curcumin developed by Wang et al. with Papp (A-B) of 6.04×10^{-6} cm/s(Wang et al., 2018) and curcumin-loaded lignin based nanoparticles developed by Alqahtani et al. with Papp (A-B) of 8 x 10-6 cm/s (Alqahtani et al., 2019). However, it is worth noting that Solucumin was prepared as donor suspensions for the permeation experiments, unlike other studies that used donor solutions where curcumin was completely dissolved in the solvent. By using donor suspensions instead of donor solutions, the effect of drug solubility on drug permeation was taken into account, which better mimics the *in vivo* permeation of curcumin across the human intestinal enterocytes.

Solubility, dissolution and permeability of drugs are critical factors that can determines the extent and the rate of absorption of orally administrated drugs and can ultimately affect the oral bioavailability of the drugs. The ability of Solucumin to improve the solubility, dissolution and permeability of curcumin has been well demonstrated in this study. Therefore, it can be suggested that Solucumin is a promising solid formulation that has the potential to increase the oral bioavailability of curcumin. It has been reported that formulations that increase the oral absorption of curcumin also tend to increase the absorption of demethoxycurcumin. Jäger et al. reported that a novel water-soluble curcumin formulation developed by OmniActive Health Technologies at a single oral dose of 376 mg curcuminoids showed 28-fold and 3-fold higher oral

absorption of curcumin and demethoxycurcumin (AUC_{0-t} of 307.6 ± 44.6 μg·h/l and 54.5 ± 8.1 μg·h/l) than the unformulated commercial curcumin (AUC_{0-t} of 10.8 ± 1.7 μg·h/l and 18.4 ± 2.3 μg·h/l) in healthy human subjects. On the other hand, the formulation and commercial curcumin showed similar oral absorption of bisdemethoxycurcumin (AUC_{0-t} of 10.2 ± 1.3 μg·h/l and 9.3 ± 0.8 μg·h/l)(Jäger et al., 2014). A similar trend was found in another comparative study. A novel γ-cyclodextrin curcumin complex was given orally to healthy human volunteers at a single oral dose of 376 mg of curcuminoids showed 17-fold and 2-fold higher oral absorption of curcumin and demethoxycurcumin (AUC_{0-t} of 327.7 ± 58.1 μg·h/l and 51.5 ± 9.0 μg·h/l) than the unformulated commercial curcumin (AUC_{0-t} of 19.7 ± 2.6 μg·h/l and 21.8 ± 3.1 μg·h/l). The formulated curcumin and commercial curcumin both showed similar oral absorption of bisdemethoxycurcumin (AUC_{0-t} of 9.4 ± 1.3 μg·h/l and 10.6 ± 1.4 μg·h/l) (Purpura et al., 2018). In these studies, the absorption of curcumin was ranked from highest to lowest as curcumin > demethoxycurcumin > bismethoxycurcumin, which was consistent with their percentage content in commercial grade curcumin. (approximately 77% curcumin, 17% demethoxycurcumin and 3% bisdemethoxycurcumin) (Esatbeyoglu et al., 2012). Therefore, the higher absorption of curcumin from the formulations than demethoxycurcumin and bisdemethoxycurcumin was likely due to the higher proportion of curcumin in the commercial curcumin than the other two curcuminoids. The reasons why the oral absorption of bisdemethoxycurcumin was hardly affected by the formulations remain unknown, but a possible explanation is that bisdemethoxycurcumin is less similar in chemical structure to curcumin (relative to demethoxycurcumin) which might make it less affected by the formulations. Both curcumin and demethoxycurcumin contain methoxy in their benzene rings whereas bisdemethoxycurcumin does not (Sandur et al., 2007). Patients with pro-inflammatory diseases such as osteoarthritis, cancer or obesity (Hewlings & Kalman, 2017) and lower risk of chronic oxidative stress

related diseases like cardiovascular diseases could be benefited by improved absorption of both curcumin and demethoxycurcumin, as they are more potent antioxidants and anti-inflammatory agents than bisdemethoxycurcumin (Jayaprakasha et al., 2006; Kalaycıoğlu et al., 2017; Sandur et al., 2007).

Compared to curcumin, the dissolution of demethoxycurcumin (0% to 4.62 ± 1.18%) and bisdemethoxycurcumin (0% to 7.37 ± 1.08% at pH6.8) in Solucumin was much lower. Interestingly, in contrast to Solucumin, Mexcumin showed much lower dissolution of curcumin (from 0% to 1.01 ± 0.08 % at pH6.8) but much higher dissolution of demethoxycurcumin (from 0% to 11.05 ± 1.32 % at pH6.8) and bisdemethoxycurcumin (from 0% to 20.87 ± 2.19% at pH6.8). As mentioned in section 3.5.1, the higher dissolution of demethoxycurcumin and bisdemethoxycurcumin than curcumin in Mexcumin might be related to the lack of methoxy groups in demethoxycurcumin and bisdemethoxycurcumin. In a Tween 80 based curcumin micellar formulation developed by Frank et al., it increased the solubility, and Papp(A-B) of curcumin across Caco-2 cell monolayers. The micellar formulation also exhibited increased Papp(A-B) of demethoxycurcumin and bisdemethoxycurcumin. However, since the solubility results for demethoxycurcumin and bisdemethoxycurcumin were not presented in the literature, it is not known whether the increased permeation across Caco-2 cell monolayers of demethoxycurcumin and bisdemethoxycurcumin was associated with increased solubility.(Frank et al., 2017). In other cell line models, bisdemethoxycurcumin showed that its cellular permeability was related to the solubility. Gagliardi et al. reported that a bisdemethoxycurcumin-loaded H-Ferritin nanoparticle formulation that increased the solubility of bisdemethoxycurcumin also increased the percentage of bisdemethoxycurcumin permeation across the blood brain barrier model based on bEnd.3 cell (a type of mouse brain endothelial cell) monolayers. (Gagliardi et al., 2022). If the Caco-2 cell monolayer permeability of demethoxycurcumin

and bisdemethoxycurcumin is related to their aqueous solubility, as is the case with curcumin, then Mexcumin, the formulation with the highest solublisation effect on demethoxycurcumin and bis-demethoxycurcumin, could show higher intestinal permeability for these curcuminoids than for curcumin. Demethoxycurcumin and bisdemethoxycurcumin are more potent acetylcholinesterase inhibitors than curcumin, making them more effective in relieving neuroinflammation in patients with Alzheimers disease (Gagliardi et al., 2022; Kalaycıoğlu et al., 2017). Alzheimers disease patients with this symptom may benefit from taking Mexcumin if it can provide considerable improvement in the oral absorption of bisdemethoxycurcumin and demethoxycurcumin. Overall, Mexcumin is a very interesting formulation that worth to be further studied in the future as demethoxycurcumin and bisdemethoxycurcumin were much less studied than curcumin.

The application of Solucumin technology or NPSSD to other poorly water-soluble drugs/compounds was also investigated. The results of *in vitro* dissolution tests showed that NPSSD improved the dissolution of niclosamide, nitrofurantoin, terbinafine, quinine and quercetin, but reduced the drug dissolution of omerprazole and rutin. It was found that the lipophilicity of the drug/compound might have a positive correlation to the effect of NPSSD on drug dissolution. However, there was not enough data in the current study to prove this point. More data of the LogP and dissolution of other drugs/natural compounds are needed. Niclosamide, nitrofurantoin, terbinafine and quinine are BCS II compounds so their drug/compound absorption can certainly be improved by increasing the solubility of the drug/compound, as drug/compound dissolution is the limiting step in the rate of drug/compound absorption for BCS II compounds(Chavda et al., 2010). As demonstrated section 6.5.1, whether the drug/natural compound is BCS Class II or Class IV does not have influence on the whether NPSSD would increase or decrease the drug dissolution. In other

words, the effect of NPSSD on drug dissolution is not associated to the BCS classification of poorly soluble drug/natural compound.

7.4. Limitation

7.4.1. DLS and Zeta potential study

The limitation of the DLS analysis was that some of particles of the formulations could have dissolved in the solvent during the measurement which could affect the results of the particle size as the dissolved particles cannot be detected. As mentioned in section 4.5.4, the DLS results might not fully reflect the actual particle size of the formulations, but they are still valuable as they showed that those formulation particles that were not immediately dissolved in water were still significantly smaller than the particle size of commercial curcumin. The smaller particle size means they might be more soluble than the commercial curcumin. To avoid the effect of solubilised drugs to the particle size measurement, techniques that do not involve solvent such as scanning electron microscopy (SEM) could be used.

A limitation of the zeta-potential study was that it did not exam the change of zeta potential at different pH conditions. In aqueous media, the pH level is an important factor that affects the zeta potential of the samples (Thakur et al., 2020). It was reported that the same sample may have completely opposite zeta potential values at different pH values (Vuddanda et al., 2014). In the current zeta-potential study, an unbuffered ultra-pure water was used as the aqueous medium and its pH was 6.98. This means that the zeta-potential results in current study only reflect the stability of the particles in an aqueous medium with a neutral pH. But the pH of the gastrointestinal tract is not neutral. The pH of the stomach is reported to be 1-2.5 and the pH of the small intestine ranged from 6.6-7.5 (Evans et al., 1988). As a formulation developed for oral

administration, the information of zeta potential in different pH environments is needed to reflect the particle stability of Solucumin in the gastrointestinal tract fluids. Another limitation of the zeta-potential study was that the solubilsed curcumin from the formulations could affect the values of zeta potential as it can reduce the pH of the unbuffered solvent which results in more positive zeta potential values (Priyadarsini, 2014). To avoid the dramatic change of pH of the medium by the solublised curcumin, the medium used for the zeta-potential study for should be prepared as buffer.

7.4.2. Stability test

In this study, only a short-term stability test with a time length of 1 month was conducted to determine the degradation of curcumin due to time constraints and the impact of COVID19 lockdown. The result of this short-term stability test only showed that Solucumin, Mexcumin, Longvida® and Nacumin® were able to keep its drug from degradation for at least one month under the storage conditions of 25 °C/60% RH and 40 °C/60% RH. Drug stability tests with longer time length need to be carried in the future in order to get more information about the effect of the curcumin formulations on drug degradation during storage.

Although it is not a legal requirement document, ICH guideline provides professional advice and uniformed standards for conducting safe, effective and high-quality stability tests for newly developed drug products/formulations. As a result, it can be used as a guide when designing the future drug stability tests. According to ICH guideline Q1A(R2), in order to get sufficient data of drug stability, a long-term stability study of at least 12 months and an accelerated stability study (at least 15°C above the long-term storage temperature with higher or lower humidity) of at least 6 months are advised to be carried out for at least three batches of a newly development pharmaceutical product. If ≥ 5%

loss of the initial drug content is observed in an accelerated stability study, an additional testing is advised to be carried out at a more moderate condition than that of accelerated stability study (ICH, 2003).

7.4.3. *In vitro* drug dissolution study

In this study, sink condition was not maintained during the *in vitro* drug dissolution as the amount of curcuminoids added to the dissolution media. Although maintaining sink condition is not a mandatory requirement for *in vitro* dissolution study, it is preferable to maintain it as it prevents saturation of the drug during the dissolution process, which can result in a relatively low percentage of drug dissolution.

To determine the percentage of drug dissolution of curcumin that not affected by the drug saturation in dissolution media, an *in vitro* dissolution study can be carried out using the same methodology but with sink condition. To meet the requirements of the sink condition, a smaller amount of curcumin needed be added to 900 ml of dissolution media. Based on the saturation solubility results of commercial curcumin from Solucumin in section 2.4.4, 70.325 x 900 = 63292.5 µg = 63.292 mg of commercial curcumin can be dissolved in a pH6.8 dissolution medium, which is equivalent to 63.292 x 81.46% = 51.558 mg of curcumin. Since sink condition is the ability of the dissolution media to dissolve at least 3 times the amount of drug that is in your dosage form(FDA, 1997; WHO, 2020). This means that formulations containing no more than 51.558/3 = 17.186 mg of curcumin should be added to the pH6.8 dissolution medium to maintain the sink condition during the dissolution study.

7.4.4. *In vitro* permeation experiments using Caco-2 cells model

In this study, Caco2 cell lines was used to resemble human intestinal epithelial cells as they are phenotypically similar. Caco2 cell lines exhibit a well-

differentiated brush border on the apical surface and uniform tight junctions form between adjacent cells. In addition, various transporters, enzymes, and nuclear receptors that exist in human intestinal epithelium are also present in the Caco-2 cells. There has been a good correlation between drug absorption in human small intestine and Caco-2 cells, especially for passively absorbed drugs (Sun et al., 2008).

However, caution must be taken when analysing the results as the cell lines do not completely imitate the primary cell. For Caco2 cell lines, they have higher expression level of some transporter proteins (glucose transporter 1, OATP4A1, MRP2, MRP1, and OATP2B1) and lower expression of some cytochrome P450 metabolite enzymes (CYP1A1, CYP3A5 and CYP3A4) compared with human jejunum (Vaessen et al., 2017). If possible, *in vivo* studies conducted by giving oral dose of Solucumin to in animal models such as mice or rats should be carried out in the future. *In vitro* studies do not completely mimic a living organism thus providing only partial information regarding the drug absorption and efficacy. Although *in vivo* studies in animal models have some major disadvantages such as ethical issues and considerable physiological differences between humans and animals, they can still generate detailed information regarding the pharmacokinetics, pharmacodynamics, toxicology and therapeutic efficacy of the tested formulation, which could be crucial for future clinical trials. In addition, *in vivo* studies can provide other important information such as drug interactions, mechanism of action and interaction with organ systems (Xu et al., 2021).

7.5. Future work

A series of further works should be performed in the future to obtain more understanding about the property and performance of Solucumin. It can be formulated into a dosage form like tablets or capsules whose performance can be characterised. If possible, *in vivo* animal studies could be conducted to study the pharmacokinetics of Solucumin to help to predict the oral bioavailability when administered into human bodies. If the results of *in vivo* studies confirm that Solucumin improves the oral bioavailability of curcumin, then efficacy trials can be conducted to study the therapeutic effects of Solucumin on a specific health condition such as Alzheimers disease or osteoarthritis. In addition, studies on the use of Solucumin technology on other poorly soluble drugs other than curcumin should be continued. Further experiments including solubility tests, characterisation studies, stability studies and permeability tests need to be carried out to obtain more information on the effects of Solucumin technology on different drugs.

As for stability studies, only a short-term drug stability with the time length of 1 months was conducted in the current study. In the future, at least a long-term stability study and an accelerated stability study that meet the standard of ICH guidelines should be performed in order to fully understand the drug stability profile of Solucumin, Mexcumin, Longvida® and Nacumin®. Furthermore, the detection of change of its particle size, size distribution and surface charge over time could also be conducted and it should be considered as a part of the stability study.

As amorphous drugs tend to recrystallise during storage, the anti-crystallisation effect of Solucumin during storage should also be investigated. Solucumin can be stored under the same storage conditions used in the long-term stability test and the samples will be taken at different times for XRD

analysis to determine the change in the crystallinity of curcumin over time. In addition, changes in the aqueous solubility of curcumin over time should be measured in order to study the effect of drug recrystallisation on drug solubility.

The current study was focused on the formulation development for increasing the solubility and oral bioavailability of curcumin thus less attention was given to demethoxycurcumin and bisdemethoxycurcumin in this study. For instance, Mexcumin showed relatively poor dissolution of curcumin but demonstrated significantly higher dissolution of demethoxycurcumin and bisdemethoxycurcumin, but no further experiments were carried out to in this study to investigate and explain this observation. In the future, further studies such as solubility, permeability and *in vivo* drug absorption tests could be carried out on Mexcumin. Furthermore, it will be interesting to compare this formulation with Solucumin in terms of therapeutic efficacy for certain health conditions such as neuroinflammation in Alzheimer's disease patients.

It is worth mentioning that this study focused only on improving the oral bioavailability of curcumin by improving its water solubility. In addition to poor solubility, the high metabolic rate in the small intestine and liver is another factor contributing to the low oral bioavailability of curcumin. As mentioned in section 1.8.1, co-administration of adjuvants like piperine, quercetin, resveratrol and silibinin could reduce the metabolism of curcumin which eventually increased the absorption of curcumin (Anand et al., 2007; Grill et al., 2014; Lund & Pantuso, 2014; Shoba et al., 1998; Zeng et al., 2017b). Therefore, a future work or new project could be to investigate whether the combination of the two strategies: "co-administration of adjuvants" and "Solucumin technology" will lead to a synergistic enhancement of curcumin oral bioavailability.

7.6. Conclusion

The novel polymeric-surfactant solid dispersion, Solucumin, developed in this study has demonstrated considerable improvement on the aqueous solubility and dissolution of curcumin at environment with pH levels similar to the human gastrointestinal tract. It was found that the effect of Solucumin to improve the aqueous solubility and dissolution of curcumin was associated with the reduction in particle size and the conversion of crystalline curcumin into an amorphous form. The increased solubility of curcumin by Solucumin ultimately helped the improvement of the permeation of curcumin across the Caco-2 cellular model of human intestinal epithelium. Compared to some of the curcumin products currently on the market (Longvida® and Nacumin®) and another polymeric-surfactant based solid formulation (Mexcumin), Solucumin showed significantly higher solubility, dissolution and permeability of curcumin. In addition to curcumin, Solucumin technology could also increase the dissolution of other poorly soluble drugs/natural compounds which include niclosamide, nitrofurantoin, terbinafine, quinine and quercetin.

Overall, it can be concluded that Solucumin is a novel solid dispersion formulation that has the potential to improve the oral bioavailability of not only curcumin but also several different drugs and natural compounds. Undoubtedly, further studies should be carried out to demonstrate and evidence for this potential.

References

Abdelkader, H., & Fathalla, Z. (2018). Investigation into the emerging role of the basic amino acid L-lysine in enhancing solubility and permeability of BCS class II and BCS class IV drugs. *Pharmaceutical research*, *35*(8), 1-18. https://doi.org/10.1007/s11095-018-2443-0

Achan, J., Talisuna, A. O., Erhart, A., Yeka, A., Tibenderana, J. K., Baliraine, F. N., Rosenthal, P. J., & DAlessandro, U. (2011). Quinine, an old anti-malarial drug in a modern world: role in the treatment of malaria. *Malaria journal*, *10*(1), 1-12. https://doi.org/10.1186/1475-2875-10-144

Adhikari, A., & Polli, J. E. (2020). Characterization of grades of HPMCAS spray dried dispersions of itraconazole based on supersaturation kinetics and molecular interactions impacting formulation performance. *Pharmaceutical research*, *37*(10), 1-15. https://doi.org/10.1007/s11095-020-02909-6

Aditya, N., Yang, H., Kim, S., & Ko, S. (2015). Fabrication of amorphous curcumin nanosuspensions using β-lactoglobulin to enhance solubility, stability, and bioavailability. *Colloids and Surfaces B: Biointerfaces*, *127*, 114-121. https://doi.org/10.1016/j.colsurfb.2015.01.027

Adriani, N., Rahayu, D., & Saepudin, E. (2020). Activity of hydrogenated curcuminoid on Pd/C catalyst and its antibacterial activity against Staphylococcus aureus and Streptococcus mutans. *IOP Conference Series: Materials Science and Engineering, 902* (1):012068. https://doi.org/10.1088/1757-899X/902/1/012068

Aggarwal, B. B., Sundaram, C., Malani, N., & Ichikawa, H. (2007). Curcumin: the Indian solid gold. *The molecular targets and therapeutic uses of curcumin in health and disease*, 1-75. https://doi.org/10.1007/978-0-387-46401-5_1

Aggarwal, B. B., Takada, Y., & Oommen, O. V. (2004). From chemoprevention to chemotherapy: common targets and common goals. *Expert opinion on investigational drugs*, *13*(10), 1327-1338. https://doi.org/https://doi.org/10.1517/13543784.13.10.1327

Ahn, J.-S., Kim, K.-M., Ko, C.-Y., & Kang, J.-S. (2011). Absorption enhancer and polymer (Vitamin E TPGS and PVP K29) by solid dispersion improve dissolution and bioavailability of eprosartan mesylate. *Bulletin of the Korean Chemical Society*, *32*(5), 1587-1592. https://doi.org/10.5012/bkcs.2011.32.5.1587

Ahsan, H., Parveen, N., Khan, N. U., & Hadi, S. (1999). Pro-oxidant, anti-oxidant and cleavage activities on DNA of curcumin and its derivatives demethoxycurcumin and bisdemethoxycurcumin. *Chemico-biological interactions*, *121*(2), 161-175. https://doi.org/10.1016/S0009-2797(99)00096-4

Ahmed, T., & Gilani, A.-H. (2009). Inhibitory effect of curcuminoids on acetylcholinesterase activity and attenuation of scopolamine-induced amnesia may explain medicinal use of turmeric in Alzheimers disease. *Pharmacology Biochemistry and Behavior*, *91*(4), 554-559. https://doi.org/10.1016/j.pbb.2008.09.010

Ahuja, S., & Dong, M. (2005). *Handbook of pharmaceutical analysis by HPLC* (M. W. D. Satinder Ahuja, Ed.). Elsevier.

Al-Obaidi, H., Brocchini, S., & Buckton, G. (2009). Anomalous properties of spray dried solid dispersions. *Journal of pharmaceutical sciences*, *98*(12), 4724-4737. https://doi.org/10.1002/jps.21782

Alopaeus, J. F., Hagesæther, E., & Tho, I. (2019). Micellisation mechanism and behaviour of Soluplus®–furosemide micelles: Preformulation studies of an oral nanocarrier-based system. *Pharmaceuticals*, *12*(1), 15. https://doi.org/doi:10.3390/ph12010015

Alshahrani, S. M., Lu, W., Park, J.-B., Morott, J. T., Alsulays, B. B., Majumdar, S., Langley, N., Kolter, K., Gryczke, A., & Repka, M. A. (2015). Stability-enhanced hot-melt extruded amorphous solid dispersions via combinations of Soluplus® and HPMCAS-HF. *AAPS PharmSciTech*, *16*(4), 824-834. https://doi.org/10.1208/s12249-014-0269-6

Alshetaili, A., Alshahrani, S. M., Almutairy, B. K., & Repka, M. A. (2020). Hot melt extrusion processing parameters optimization. *Processes*, *8*(11), 1516. https://doi.org/https://doi.org/10.3390/pr8111516

Alawam, K. (2014). Application of proteomics in diagnosis of ADHD, schizophrenia, major depression, and suicidal behavior. In R. Donev (Ed.), *Advances in protein chemistry and structural biology* (Vol. 95, pp. 283-315). Academic Press. https://doi.org/10.1016/B978-0-12-800453-1.00009-9

Alemdar, A., Güngör, N., Ece, O., & Atici, O. (2005). The rheological properties and characterization of bentonite dispersions in the presence of non-ionic polymer PEG. *Journal of Materials Science*, *40*(1), 171-177. https://doi.org/10.1007/s10853-005-5703-4

Altamimi, M. A., & Neau, S. H. (2017). Investigation of the in vitro performance difference of drug-Soluplus® and drug-PEG 6000 dispersions when prepared using spray drying or lyophilization. *Saudi Pharmaceutical Journal*, *25*(3), 419-439. https://doi.org/10.1016/j.jsps.2016.09.013

Almalik, A., Alradwan, I., Kalam, M. A., & Alshamsan, A. (2017). Effect of cryoprotection on particle size stability and preservation of chitosan nanoparticles with and without hyaluronate or alginate coating. *Saudi Pharmaceutical Journal*, *25*(6), 861-867. https://doi.org/10.1016/j.jsps.2016.12.008

Alqahtani, S., Alayoubi, A., Nazzal, S., Sylvester, P. W., & Kaddoumi, A. (2014). Enhanced solubility and oral bioavailability of γ-Tocotrienol using a self-emulsifying drug delivery system (SEDDS). *Lipids*, *49*(8), 819-829. https://doi.org/10.1007/s11745-014-3923-6

Ali, A., & Gorashi, A. (1984). Absorption and dissolution of nitrofurantoin from different experimental formulations. *International journal of pharmaceutics*, *19*(3), 297-306.

Albert, K., Sedman, A., Wilkinson, P., Stoll, R., Murray, W., & Wagner, J. (1974). Bioavailability studies of acetaminophen and nitrofurantoin. https://doi.org/10.1002/j.1552-4604.1974.tb02312.x

Alqahtani, M. S., Alqahtani, A., Al-Thabit, A., Roni, M., & Syed, R. (2019). Novel lignin nanoparticles for oral drug delivery. *Journal of Materials Chemistry B*, *7*(28), 4461-4473. https://doi.org/10.1039/C9TB00594C

Almeida, A. F., Borge, G. I. A., Piskula, M., Tudose, A., Tudoreanu, L., Valentová, K., Williamson, G., & Santos, C. N. (2018). Bioavailability of quercetin in humans with a focus on interindividual variation. *Comprehensive Reviews in Food Science and Food Safety*, *17*(3), 714-731. https://doi.org/10.1111/1541-4337.12342

Amidon, G. L., Lennernäs, H., Shah, V. P., & Crison, J. R. (1995). A theoretical basis for a biopharmaceutic drug classification: the correlation of in vitro drug product dissolution and in vivo bioavailability. *Pharmaceutical research*, *12*(3), 413-420. https://doi.org/10.1023/a:1016212804288

Andrews, P., Thyssen, J., & Lorke, D. (1982). The biology and toxicology of molluscicides, Bayluscide. *Pharmacology & Therapeutics*, *19*(2), 245-295. https://doi.org/https://doi.org/10.1016/0163-7258(82)90064-X

Anderson, P. S. (2017). *Curcumin Monograph for Intravenous Use* Retrieved 15th August from https://www.consultdranderson.com/wp-content/uploads/securepdfs/2019/04/12-Curcumin-IV-Monograph-Anderson.pdf

Anand, P., Kunnumakkara, A. B., Newman, R. A., & Aggarwal, B. B. (2007). Bioavailability of curcumin: problems and promises. *Molecular pharmaceutics*, *4*(6), 807-818.https:///doi.org/10.1021/mp700113r

Anderberg, E., Bisrat, M., & Nyström, C. (1988). Physicochemical aspects of drug release. VII. The effect of surfactant concentration and drug particle size on solubility and dissolution rate of felodipine, a sparingly soluble drug. *International journal of pharmaceutics*, *47*(1-3), 67-77. https://doi.org/10.1016/0378-5173(88)90216-5

Araiza-Calahorra, A., Akhtar, M., & Sarkar, A. (2018). Recent advances in emulsion-based delivery approaches for curcumin: From encapsulation to bioaccessibility. *Trends in Food Science & Technology*, *71*, 155-169. https://doi.org/10.1016/j.tifs.2017.11.009

Araújo, M. C. P., Antunes, L. M., & Takahashi, C. S. (2001). Protective effect of thiourea, a hydroxyl-radical scavenger, on curcumin-induced chromosomal aberrations in an in vitro mammalian cell system. *Teratogenesis, carcinogenesis, and mutagenesis*, *21*(2), 175-180. https://doi.org/10.1002/1520-6866(2001)21:2-

Artursson, P., & Karlsson, J. (1991). Correlation between oral drug absorption in humans and apparent drug permeability coefficients in human intestinal epithelial (Caco-2) cells. *Biochemical and biophysical research communications*, *175*(3), 880-885. https://doi.org/10.1016/0006-291x(91)91647-u.

Arozal, W., Louisa, M., Rahmat, D., Chendrana, P., & Sandhiutami, N. M. D. (2021). Development, characterization and pharmacokinetic profile of chitosan-sodium tripolyphosphate nanoparticles based drug delivery systems for curcumin. *Advanced pharmaceutical bulletin*, *11*(1), 77. https://doi.org/10.34172/apb.2021.008

Artursson, P., Palm, K., & Luthman, K. (2001). Caco-2 monolayers in experimental and theoretical predictions of drug transport. *Advanced drug delivery reviews*, *46*(1-3), 27-43. https://doi.org/10.1016/S0169-409X(00)00128-9

Asai, A., & Miyazawa, T. (2000). Occurrence of orally administered curcuminoid as glucuronide and glucuronide/sulfate conjugates in rat plasma. *Life sciences*, *67*(23), 2785-2793. https://doi.org/10.1016/s0024-3205(00)00868-7.

Ashland. (2019). *AquaSolveTM hydroxypropylmethylcellulose acetate succinate: Physical and chemical properties handbook*. https://www.ashland.com/file_source/Ashland/Industries/Pharmaceutical/Links/PC-12624.6_AquaSolve_HPMCAS_Physical_Chemical_Properties.pdf.

Atal, C., Dubey, R. K., & Singh, J. (1985). Biochemical basis of enhanced drug bioavailability by piperine: evidence that piperine is a potent inhibitor of drug metabolism. *Journal of Pharmacology and Experimental Therapeutics*, *232*(1), 258-262.

Baird, J. A., & Taylor, L. S. (2012). Evaluation of amorphous solid dispersion properties using thermal analysis techniques. *Advanced drug delivery reviews*, *64*(5), 396-421. https://doi.org/https://doi.org/10.1016/j.addr.2011.07.009

Barmpalexis, P., Kachrimanis, K., & Georgarakis, E. (2011). Solid dispersions in the development of a nimodipine floating tablet formulation and optimization by artificial neural networks and genetic programming. *European Journal of Pharmaceutics and Biopharmaceutics*, *77*(1), 122-131. https://doi.org/10.1016/j.ejpb.2010.09.017

BASF. (2019). *Soluplus - For better solubility & bioavailability* https://pharmaceutical.basf.com/en/Drug-Formulation/Soluplus.html

Baek, J.-S., & Cho, C.-W. (2017). Surface modification of solid lipid nanoparticles for oral delivery of curcumin: Improvement of bioavailability through enhanced cellular uptake, and lymphatic uptake. *European Journal of Pharmaceutics and Biopharmaceutics*, *117*, 132-140. https://doi.org/10.1016/j.ejpb.2017.04.013.

Bajaj, S., Singla, D., & Sakhuja, N. (2012). Stability testing of pharmaceutical products. *Journal of Applied Pharmaceutical Science*(Issue), 129-138. https://doi.org/10.7324/JAPS.2012.2322

Barboza, F., Vecchia, D. D., Tagliari, M. P., Silva, M., & Stulzer, H. (2009). Differential scanning calorimetry as a screening technique in compatibility studies of acyclovir extended release formulations. *Pharmaceutical Chemistry Journal*, *43*(6), 363-368. https://doi.org/10.1007/s11094-009-0304-1

Balimane, P. V., Chong, S., & Morrison, R. A. (2000). Current methodologies used for evaluation of intestinal permeability and absorption. *Journal of pharmacological and toxicological methods*, *44*(1), 301-312. https://doi.org/10.1016/S1056-8719(00)00113-1

Balakrishnan, I., Jawahar, N., Venkatachalam, S., & Datta, D. (2020). A brief review on eutectic mixture and its role in pharmaceutical field. *Int. J. Res. Pharm. Sci*, *11*, 3017-3023. https://doi.org/10.26452/ijrps.v11i3.2398

Baranczyk-Kuzma, A., Garren, J. A., Hidalgo, I. J., & Borchardt, R. T. (1991). Substrate specificity and some properties of phenol sulfotransferase from human intestinal Caco-2 cells. *Life sciences*, *49*(16), 1197-1206. https://doi.org/10.1016/0024-3205(91)90568-V

Bernabé-Pineda, M., Ramírez-Silva, M. a. T., Romero-Romo, M., González-Vergara, E., & Rojas-Hernández, A. (2004). Determination of acidity constants of curcumin in aqueous solution and apparent rate constant of its decomposition. *Spectrochimica Acta Part A: Molecular and Biomolecular Spectroscopy*, *60*(5), 1091-1097. https://doi.org/10.1016/S1386-1425(03)00342-1

Bevernage, J., Forier, T., Brouwers, J., Tack, J., Annaert, P., & Augustijns, P. (2011). Excipient-mediated supersaturation stabilization in human intestinal fluids. *Molecular pharmaceutics*, *8*(2), 564-570. https://doi.org/10.1021/mp100377m.

Bergin, I. L., & Witzmann, F. A. (2013). Nanoparticle toxicity by the gastrointestinal route: evidence and knowledge gaps. *International journal of biomedical nanoscience and nanotechnology*, *3*(1-2). https://doi.org/10.1504/IJBNN.2013.054515

Bernabeu, E., Gonzalez, L., Cagel, M., Gergic, E. P., Moretton, M. A., & Chiappetta, D. A. (2016). Novel Soluplus®—TPGS mixed micelles for encapsulation of paclitaxel with enhanced in vitro cytotoxicity on breast and ovarian cancer cell lines. *Colloids and Surfaces B: Biointerfaces*, *140*, 403-411. https://doi.org/10.1016/j.colsurfb.2016.01.003

Bhujbal, S. V., Mitra, B., Jain, U., Gong, Y., Agrawal, A., Karki, S., Taylor, L. S., Kumar, S., & Zhou, Q. T. (2021). Pharmaceutical amorphous solid dispersion: A review of manufacturing strategies. *Acta Pharmaceutica Sinica B*, *11*(8), 2505-2536. https://doi.org/10.1016/j.apsb.2021.05.014

Bhattacharjee, S. (2016). DLS and zeta potential–what they are and what they

are not? *Journal of Controlled Release*, *235*, 337-351. https://doi.org/10.1016/j.jconrel.2016.06.017

Bisht, S., Feldmann, G., Soni, S., Ravi, R., Karikar, C., Maitra, A., & Maitra, A. (2007). Polymeric nanoparticle-encapsulated curcumin (" nanocurcumin"): a novel strategy for human cancer therapy. *Journal of nanobiotechnology*, *5*(1), 1-18. https://doi.org/10.1186/1477-3155-5-3.

Bikiaris, D. N. (2011). Solid dispersions, part I: recent evolutions and future opportunities in manufacturing methods for dissolution rate enhancement of poorly water-soluble drugs. *Expert opinion on drug delivery*, *8*(11), 1501-1519. https://doi.org/10.1517/17425247.2011.618181

Bindhani, S., & Mohapatra, S. (2018). Recent approaches of solid dispersion: a new concept toward oral bioavailability. *Asian J Pharm Clin Res*, *11*(2), 72-78. http://dx.doi.org/10.22159/ajpcr.2018.v11i2.23161

Blessy, M., Patel, R. D., Prajapati, P. N., & Agrawal, Y. (2014). Development of forced degradation and stability indicating studies of drugs—A review. *Journal of pharmaceutical analysis*, *4*(3), 159-165. https://doi.org/10.1016/j.jpha.2013.09.003

BNF. (2022a). *Terbinifine*. National Institute for Health and Care Excellence. Retrieved 18 August from https://bnf.nice.org.uk/drugs/terbinafine/

BNF. (2022b). *Helminth infections*. National Institute for Health and Care Excellence. Retrieved 21st August from https://bnf.nice.org.uk/treatment-summaries/helminth-infections/

BNF. (2022c). *Nitrofurantoin*. National Institute for Health and Care Excellence. Retrieved 24th August from https://bnf.nice.org.uk/drugs/nitrofurantoin/

Boyle, S., Dobson, V., Duthie, S. J., Hinselwood, D., Kyle, J., & Collins, A. (2000). Bioavailability and efficiency of rutin as an antioxidant: a human supplementation study. *European Journal of Clinical Nutrition*, *54*(10), 774-782. https://doi.org/10.1038/sj.ejcn.1601090

Bokkenheuser, V. D., Shackleton, C., & Winter, J. (1987). Hydrolysis of dietary flavonoid glycosides by strains of intestinal Bacteroides from humans. *Biochemical Journal*, *248*(3), 953-956. https://doi.org/https://doi.org/10.1042/bj2480953

Bock-Hennig, B. S., Köhle, C., Nill, K., & Bock, K. W. (2002). Influence of t-butylhydroquinone and β-naphthoflavone on formation and transport of 4-methylumbelliferone glucuronide in Caco-2/TC-7 cell monolayers. *Biochemical pharmacology*, *63*(2), 123-128. https://doi.org/10.1016/S0006-2952(01)00833-4

Breitenbach, J., Schrof, W., & Neumann, J. (1999). Confocal Raman-spectroscopy: analytical approach to solid dispersions and mapping of drugs. *Pharmaceutical research*, *16*(7), 1109-1113. https://doi.org/10.1023/a:1018956304595

Brodin, B., Steffansen, B., & Nielsen, C. U. (2010). Passive diffusion of drug substances: the concepts of flux and permeability. In *Molecular Biopharmaceutics: Aspects of Drug Characterisation, Drug Delivery and Dosage Form Evaluation* (pp. 135-152). Pharmaceutical Press.

Brunner, J., Ragupathy, S., & Borchard, G. (2021). Target specific tight junction modulators. *Advanced drug delivery reviews*, *171*, 266-288. https://doi.org/doi.org/10.1016/j.addr.2021.02.008

Bunaciu, A. A., UdriŞTioiu, E. G., & Aboul-Enein, H. Y. (2015). X-ray diffraction: instrumentation and applications. *Critical reviews in analytical chemistry*, *45*(4), 289-299. https://doi.org/10.1080/10408347.2014.949616

Buckley, A., & Turner, J. R. (2018). Cell biology of tight junction barrier regulation and mucosal disease. *Cold Spring Harbor perspectives in biology*, *10*(1), a029314. https://doi.org/10.1101/cshperspect.a029314

Canaparo, R., Finnström, N., Serpe, L., Nordmark, A., Muntoni, E., Eandi, M., Rane, A., & Zara, G. P. (2007). Expression of CYP3A isoforms and P-glycoprotein in human stomach, jejunum and ileum. *Clinical and experimental pharmacology and physiology*, *34*(11), 1138-1144. https://doi.org/10.1111/j.1440-1681.2007.04691.x.

Carolina Alves, R., Perosa Fernandes, R., Fonseca-Santos, B., Damiani Victorelli, F., & Chorilli, M. (2019). A critical review of the properties and analytical methods for the determination of curcumin in biological and pharmaceutical matrices. *Critical reviews in analytical chemistry*, *49*(2), 138-149. https://doi.org/10.1080/10408347.2018.1489216

Cappon, G. D., Fleeman, T. L., Rocca, M. S., Cook, J. C., & Hurtt, M. E. (2003). Embryo/fetal development studies with hydroxypropyl methylcellulose acetate succinate (HPMCAS) in rats and rabbits. *Birth Defects Research Part B: Developmental and Reproductive Toxicology*, *68*(5), 421-

427.https://doi.org/10.1002/bdrb.10039

Caron, V., Hu, Y., Tajber, L., Erxleben, A., Corrigan, O. I., McArdle, P., & Healy, A. M. (2013). Amorphous solid dispersions of sulfonamide/Soluplus® and sulfonamide/PVP prepared by ball milling. *AAPS PharmSciTech*, *14*(1), 464-474. https://doi.org/10.1208/s12249-013-9931-7

Cao, J.-N., Wang, W.-H., Qu, Y.-J., Xue, G.-L., Wei, Z.-Y., Liu, J.-Q., Han, H.-Y., Zhang, S., & Song, P. (2022). Biosynthesis and evaluation of a novel highly water-soluble quercetin glycoside derivative. *Journal of Asian Natural Products Research*, *24*(8), 754-760. https://doi.org/10.1080/10286020.2021.1981875

Ceballos, A., Cirri, M., Maestrelli, F., Corti, G., & Mura, P. (2005). Influence of formulation and process variables on in vitro release of theophylline from directly-compressed Eudragit matrix tablets. *Il Farmaco*, *60*(11-12), 913-918. https://doi.org/10.1016/j.farmac.2005.07.002

Chang, M.-T., Tsai, T.-R., Lee, C.-Y., Wei, Y.-S., Chen, Y.-J., Chen, C.-R., & Tzen, J. T. (2013). Elevating bioavailability of curcumin via encapsulation with a novel formulation of artificial oil bodies. *Journal of agricultural and food chemistry*, *61*(40), 9666-9671. https://doi.org/https://doi.org/10.1021/jf4019195.

Chaudhary, P., Kumar, P., Kumar, G., & Varshney, J. (2010). A review on pharmacological activities of turmeric. *Pharmacologyonline*, *3*, 193-199.

Chaurasia, S., Patel, R. R., Chaubey, P., Kumar, N., Khan, G., & Mishra, B. (2015). Lipopolysaccharide based oral nanocarriers for the improvement of

bioavailability and anticancer efficacy of curcumin. *Carbohydrate polymers*, *130*, 9-17. https://doi.org/10.1016/j.carbpol.2015.04.062.

Charoenchaitrakool, M., Dehghani, F., Foster, N., & Chan, H. (2000). Micronization by rapid expansion of supercritical solutions to enhance the dissolution rates of poorly water-soluble pharmaceuticals. *Industrial & engineering chemistry research*, *39*(12), 4794-4802. https://doi.org/10.1021/ie000151a

Chanburee, S., & Tiyaboonchai, W. (2018). Enhanced intestinal absorption of curcumin in Caco-2 cell monolayer using mucoadhesive nanostructured lipid carriers. *Journal of Biomedical Materials Research Part B: Applied Biomaterials*, *106*(2), 734-741. https://doi.org/10.1002/jbm.b.33884

Chavda, H., Patel, C., & Anand, I. (2010). Biopharmaceutics classification system. *Systematic reviews in pharmacy*, *1*(1), 62. https://doi.org/10.4103/0975-8453.59514

Chang, Y.-W., Yeh, T.-K., Lin, K.-T., Chen, W.-C., Yao, H.-T., Lan, S.-J., Wu, Y.-S., Hsieh, H.-P., Chen, C.-M., & Chen, C.-T. (2006). Pharmacokinetics of anti-SARS-CoV agent niclosamide and its analogs in rats. *journal of food and drug analysis*, *14*(4), 15. https://doi.org/10.38212/2224-6614.2464

Chen, L. K., Cadwallader, D. E., & Jun, H. W. (1976). Nitrofurantoin solubility in aqueous urea and creatinine solutions. *Journal of pharmaceutical sciences*, *65*(6), 868-872. https://doi.org/10.1002/jps.2600650617

Chen, W., Mook Jr, R. A., Premont, R. T., & Wang, J. (2018). Niclosamide: Beyond an antihelminthic drug. *Cellular signalling*, *41*, 89-96.

https://doi.org/10.1016/j.cellsig.2017.04.001

Chen, X., Zou, L.-Q., Niu, J., Liu, W., Peng, S.-F., & Liu, C.-M. (2015). The stability, sustained release and cellular antioxidant activity of curcumin nanoliposomes. *Molecules*, *20*(8), 14293-14311. https://doi.org/10.3390/molecules200814293

Chen, J., Ormes, J. D., Higgins, J. D., & Taylor, L. S. (2015). Impact of surfactants on the crystallization of aqueous suspensions of celecoxib amorphous solid dispersion spray dried particles. *Molecular pharmaceutics*, *12*(2), 533-541. https://doi.org/10.1021/mp5006245

Cherukuvada, S., & Guru Row, T. N. (2014). Comprehending the formation of eutectics and cocrystals in terms of design and their structural interrelationships. *Crystal growth & design*, *14*(8), 4187-4198. https://doi.org/10.1021/cg500790q

Chokshi, R., & Zia, H. (2004). Hot-melt extrusion technique: a review. *Iranian journal of pharmaceutical research*, *3*(1), 3-16. https://doi.org/10.22037/ijpr.2010.290

Chiou, W. L., & Riegelman, S. (1971). Pharmaceutical applications of solid dispersion systems. *Journal of pharmaceutical sciences*, *60*(9), 1281-1302. https://doi.org/10.1002/jps.2600600902.

Chuah, A. M., Jacob, B., Jie, Z., Ramesh, S., Mandal, S., Puthan, J. K., Deshpande, P., Vaidyanathan, V. V., Gelling, R. W., & Patel, G. (2014). Enhanced bioavailability and bioefficacy of an amorphous solid dispersion of curcumin. *Food Chemistry*, *156*, 227-233.

https://doi.org/10.1016/j.foodchem.2014.01.108.

Chowdary, K., & Prakasarao, K. (2011). Individual and combined effects of cyclodextrins, Poloxamer and PVP on the solubility and dissolution rate of BCS class II drugs. *Asian J Chem*, *23*(10), 4520-4524.

Chutimaworapan, S., Ritthidej, G., Yonemochi, E., Oguchi, T., & Yamamoto, K. (2000). Effect of water-soluble carriers on dissolution characteristics of nifedipine solid dispersions. *Drug development and industrial pharmacy*, *26*(11), 1141-1150. https://doi.org/10.1081/DDC-100100985

Clas, S.-D., Dalton, C. R., & Hancock, B. C. (1999). Differential scanning calorimetry: applications in drug development. *Pharmaceutical science & technology today*, *2*(8), 311-320. https://doi.org/10.1016/S1461-5347(99)00181-9

Constantinides, P. P. (1995). Lipid microemulsions for improving drug dissolution and oral absorption: physical and biopharmaceutical aspects. *Pharmaceutical research*, *12*(11), 1561-1572. https://doi.org/10.1023/a:1016268311867.

Coltescu, A.-R., Butnariu, M., & Sarac, I. (2020). The importance of solubility for new drug molecules. *Biomedical and Pharmacology Journal*, *13*(2), 577-583.https://dx.doi.org/10.13005/bpj/1920

Craig, D. Q. (2002). The mechanisms of drug release from solid dispersions in water-soluble polymers. *International journal of pharmaceutics*, *231*(2), 131-144. https://doi.org/10.1016/s0378-5173(01)00891-2.

Crowley, M. M., Zhang, F., Repka, M. A., Thumma, S., Upadhye, S. B., Kumar Battu, S., McGinity, J. W., & Martin, C. (2007). Pharmaceutical applications of hot-melt extrusion: part I. *Drug development and industrial pharmacy*, *33*(9), 909-926. https://doi.org/10.1080/03639040701498759

Cui, F., Yang, M., Jiang, Y., Cun, D., Lin, W., Fan, Y., & Kawashima, Y. (2003). Design of sustained-release nitrendipine microspheres having solid dispersion structure by quasi-emulsion solvent diffusion method. *Journal of Controlled Release*, *91*(3), 375-384. https://doi.org/10.1016/S0168-3659(03)00275-X

Cuomo, F., Cofelice, M., Venditti, F., Ceglie, A., Miguel, M., Lindman, B., & Lopez, F. (2018). In-vitro digestion of curcumin loaded chitosan-coated liposomes. *Colloids and Surfaces B: Biointerfaces*, *168*, 29-34. https://doi.org/10.1016/jcolsurfb.2017.11.047.

Cullity, B. D. (1956). *Elements of X-ray Diffraction* (M. Cohen, Ed.). Addison-Wesley Publishing.

Damian, F., Blaton, N., Naesens, L., Balzarini, J., Kinget, R., Augustijns, P., & Van den Mooter, G. (2000). Physicochemical characterization of solid dispersions of the antiviral agent UC-781 with polyethylene glycol 6000 and Gelucire 44/14. *European journal of pharmaceutical sciences*, *10*(4), 311-322. https://doi.org/10.1016/S0928-0987(00)00084-1

Dannenfelser, R.-M., He, H., Joshi, Y., Bateman, S., & Serajuddin, A. T. (2004). Development of clinical dosage forms for a poorly water soluble drug I: application of polyethylene glycol–polysorbate 80 solid dispersion carrier system. *Journal of pharmaceutical sciences*, *93*(5), 1165-1175. https://doi.org/10.1002/jps.20044

Day, R., & Quinn, G. P. (1989). Comparisons of treatments after an analysis of variance in ecology. *Ecological monographs*, *59*(4), 433-463. https://doi.org/10.2307/1943075

Danaei, M., Dehghankhold, M., Ataei, S., Hasanzadeh Davarani, F., Javanmard, R., Dokhani, A., Khorasani, S., & Mozafari, M. (2018). Impact of particle size and polydispersity index on the clinical applications of lipidic nanocarrier systems. *Pharmaceutics*, *10*(2), 57. https://doi.org/10.3390/pharmaceutics10020057

Dandekar, P. P., & Patravale, V. B. (2009). Development and validation of a stability-indicating LC method for curcumin. *Chromatographia*, *69*(9), 871-877. https://doi.org/10.1365/s10337-009-0995-1

Dahan, A., & Miller, J. M. (2012). The solubility–permeability interplay and its implications in formulation design and development for poorly soluble drugs. *The AAPS journal*, *14*(2), 244-251. https://doi.org/10.1208/s12248-012-9337-6

Dahlgren, D., & Lennernäs, H. (2019). Intestinal permeability and drug absorption: Predictive experimental, computational and in vivo approaches. *Pharmaceutics*, *11*(8), 411. https://doi.org/10.3390/pharmaceutics11080411

Dawson, P. A. (2011). Role of the intestinal bile acid transporters in bile acid and drug disposition. *Drug transporters*, 169-203. https://doi.org/10.1007/978-3-642-14541-4_4

Desai, J., Alexander, K., & Riga, A. (2006). Characterization of polymeric dispersions of dimenhydrinate in ethyl cellulose for controlled release.

International journal of pharmaceutics, *308*(1-2), 115-123. https://doi.org/10.1016/j.ijpharm.2005.10.034

De Jong, W. H., & Borm, P. J. (2008). Drug delivery and nanoparticles: applications and hazards. *International journal of nanomedicine*, *3*(2), 133.https://doi.org/10.2147/ijn.s596.

Delaney, S. P., Nethercott, M. J., Mays, C. J., Winquist, N. T., Arthur, D., Calahan, J. L., Sethi, M., Pardue, D. S., Kim, J., & Amidon, G. (2017). Characterization of synthesized and commercial forms of magnesium stearate using differential scanning calorimetry, thermogravimetric analysis, powder X-ray diffraction, and solid-state NMR spectroscopy. *Journal of pharmaceutical sciences*, *106*(1), 338-347. https://doi.org/10.1016/j.xphs.2016.10.004

Dempe, J. S., Scheerle, R. K., Pfeiffer, E., & Metzler, M. (2013). Metabolism and permeability of curcumin in cultured C aco-2 cells. *Molecular nutrition & food research*, *57*(9), 1543-1549. https://doi.org/10.1002/mnfr.201200113

Derakhshandeh, K., Hochhaus, G., & Dadashzadeh, S. (2011). In-vitro cellular uptake and transport study of 9-nitrocamptothecin PLGA nanoparticles across Caco-2 cell monolayer model. *Iranian journal of pharmaceutical research: IJPR*, *10*(3), 425.

Dhumal, D. M., Kothari, P. R., Kalhapure, R. S., & Akamanchi, K. G. (2015). Self-microemulsifying drug delivery system of curcumin with enhanced solubility and bioavailability using a new semi-synthetic bicephalous heterolipid: in vitro and in vivo evaluation. *RSC advances*, *5*(110), 90295-90306. https://doi.org/10.1039/C5RA18112G.

DiNunzio, J. C., Hughey, J. R., Brough, C., Miller, D. A., Williams III, R. O., & McGinity, J. W. (2010). Production of advanced solid dispersions for enhanced bioavailability of itraconazole using KinetiSol® Dispersing. *Drug development and industrial pharmacy*, *36*(9), 1064-1078. https://doi.org/10.3109/03639041003652973

Dimitrova, E., Bogdanova, S., Mitcheva, M., Tanev, I., & Minkov, E. (2000). Development of model aqueous ophthalmic solution of indomethacin. *Drug development and industrial pharmacy*, *26*(12), 1297-1301. https://doi.org/10.1081/DDC-100102312

Di, L., & Kerns, E. (2008). Chapter 7: Solubility. In *Drug-like properties: concepts, structure design and methods from ADME to toxicity optimization*. Academic press.

Ditzinger, F., Price, D. J., Ilie, A.-R., Köhl, N. J., Jankovic, S., Tsakiridou, G., Aleandri, S., Kalantzi, L., Holm, R., & Nair, A. (2019). Lipophilicity and hydrophobicity considerations in bio-enabling oral formulations approaches–a PEARRL review. *Journal of pharmacy and pharmacology*, *71*(4), 464-482. https://doi.org/10.1111/jphp.12984

Djuris, J., Nikolakakis, I., Ibric, S., Djuric, Z., & Kachrimanis, K. (2013). Preparation of carbamazepine–Soluplus® solid dispersions by hot-melt extrusion, and prediction of drug–polymer miscibility by thermodynamic model fitting. *European Journal of Pharmaceutics and Biopharmaceutics*, *84*(1), 228-237. https://doi.org/10.1016/j.ejpb.2012.12.018

Dovigo, L. N., Carmello, J. C., de Souza Costa, C. A., Vergani, C. E., Brunetti, I. L., Bagnato, V. S., & Pavarina, A. C. (2013). Curcumin-mediated

photodynamic inactivation of Candida albicans in a murine model of oral candidiasis. *Sabouraudia*, *51*(3), 243-251. https://doi.org/10.3109/13693786.2012.714081.

Drugbank. (2022a). *Quinine*. Retrieved 21st September from https://go.drugbank.com/drugs/DB00468

Duddu, S. P., & Sokoloski, T. D. (1995). Dielectric Analysis in the Characterization of Amorphous Pharmaceutical Solids. 1. Molecular Mobility in Poly (vinylpyrro1idone)-Water Systems in the Glassy State. *Journal of pharmaceutical sciences*, *84*(6), 773-776. https://doi.org/10.1002/jps.2600840621

Dumortier, G., Grossiord, J. L., Agnely, F., & Chaumeil, J. C. (2006). A review of poloxamer 407 pharmaceutical and pharmacological characteristics. *Pharmaceutical research*, *23*(12), 2709-2728. https://doi.org/10.1007/s11095-006-9104-4

Duizer, E., Gilde, A. J., Versantvoort, C. H., & Groten, J. P. (1999). Effects of cadmium chloride on the paracellular barrier function of intestinal epithelial cell lines. *Toxicology and applied pharmacology*, *155*(2), 117-126. https://doi.org/10.1006/taap.1998.8589

Elimrani, I., Lahjouji, K., Seidman, E., Roy, M.-J., Mitchell, G. A., & Qureshi, I. (2003). Expression and localization of organic cation/carnitine transporter OCTN2 in Caco-2 cells. *American Journal of Physiology-Gastrointestinal and Liver Physiology*, *284*(5), G863-G871. https://doi.org/10.1152/ajpgi.00220.2002

EMC. (2022a). *Quinine*. Retrieved 21st September from www.medicines.org.uk/emc/search?q=quinine"

Ensign, L. M., Cone, R., & Hanes, J. (2012). Oral drug delivery with polymeric nanoparticles: the gastrointestinal mucus barriers. *Advanced drug delivery reviews*, *64*(6), 557-570. https://doi.org/10.1016/j.addr.2011.12.009.

Esatbeyoglu, T., Huebbe, P., Ernst, I. M., Chin, D., Wagner, A. E., & Rimbach, G. (2012). Curcumin—from molecule to biological function. *Angewandte Chemie International Edition*, *51*(22), 5308-5332. https://doi.org/10.1002/anie.201107724

Evans, D., Pye, G., Bramley, R., Clark, A., Dyson, T., & Hardcastle, J. (1988). Measurement of gastrointestinal pH profiles in normal ambulant human subjects. *Gut*, *29*(8), 1035-1041. https://doi.org/10.1136/gut.29.8.1035

Faralli, A., Shekarforoush, E., Ajalloueian, F., Mendes, A. C., & Chronakis, I. S. (2019). In vitro permeability enhancement of curcumin across Caco-2 cells monolayers using electrospun xanthan-chitosan nanofibers. *Carbohydrate polymers*, *206*, 38-47. https://doi.org/10.1016/j.carbpol.2018.10.073

Fathima, N., Mamatha, T., Qureshi, H. K., Anitha, N., & Rao, J. V. (2011). Drug-excipient interaction and its importance in dosage form development. *Journal of Applied Pharmaceutical Science*(Issue), 66-71.

FDA. (2019). *Accessdata.fda.gov.* . https://www.accessdata.fda.gov/scripts/cder/iig/index.cfm?event=browseByLetter.page&Letter=T

FDA. (1997). *Guidance for Industry: Dissolution Testing of Immediate Release Solid Oral Dosage Forms*. Retrieved 25 August from https://www.fda.gov/media/70936/download

FDA. (2022a). *CFR - Code of Federal Regulations Title 21*. Retrieved 21st September from https://www.accessdata.fda.gov/scripts/cdrh/cfdocs/cfcfr/CFRSearch.cfm?fr=172.820

FDA. (2022b). *Inactive Ingredient Search for Approved Drug Products*. Retrieved 25th September from https://www.accessdata.fda.gov/scripts/cder/iig/index.cfm?event=BasicSearch.page

FDA. (2021). *FDA Guidance for industry, waiver of in vivo bioavailability and bioequivalence studies for immediate-release solid oral dosage forms based on a biopharmaceutics classification system*. FDA. Retrieved 21 August from https://www.fda.gov/media/148472/download#:~:text=BCS%2Dbased%20biowaivers%20are%20applicable,and%20reference%20products%20are%20identical.

Ferreira, N. L. O., Rodrigues, M. C. M., Arruda, R. L., Santos, P. A., Bara, M. T. F., & Conceição, E. C. (2019). New formulation containing curcuminoids: Method validation and dissolution profile. *Pharmacognosy Magazine*, *15*(60), 73. https://doi.org/10.4103/pm.pm_50_18

Feng, X., Chen, Y., Li, L., Zhang, Y., Zhang, L., & Zhang, Z. (2020). Preparation, evaluation and metabolites study in rats of novel amentoflavone-loaded TPGS/soluplus mixed nanomicelles. *Drug Delivery*, *27*(1), 137-150.

https://doi.org/doi.org/10.1080/10717544.2019.1709920

Field, A. (2009). *Discovering statistics using SPSS* (3rd edition ed.). SAGE Publications Ltd, Oriental Press.

Figueirêdo, C. B. M., Nadvorny, D., de Medeiros Vieira, A. C. Q., Sobrinho, J. L. S., Neto, P. J. R., Lee, P. I., & Soares, M. F. d. L. R. (2017). Enhancement of dissolution rate through eutectic mixture and solid solution of posaconazole and benznidazole. *International journal of pharmaceutics*, *525*(1), 32-42. https://doi.org/10.1016/j.ijpharm.2017.04.021

Foster, N. R., Dehghani, F., Charoenchaitrakool, K. M., & Warwick, B. (2003). Application of dense gas techniques for the production of fine particles. *AAPS PharmSci*, *5*(2), 32-38. https://doi.org/10.1208/ps050211

Friesen, D. T., Shanker, R., Crew, M., Smithey, D. T., Curatolo, W., & Nightingale, J. (2008). Hydroxypropyl methylcellulose acetate succinate-based spray-dried dispersions: an overview. *Molecular pharmaceutics*, *5*(6), 1003-1019. https://doi.org/10.1021/mp8000793

Fine, K. D., Santa Ana, C. A., Porter, J. L., & Fordtran, J. S. (1995). Effect of changing intestinal flow rate on a measurement of intestinal permeability. *Gastroenterology*, *108*(4), 983-989. https://doi.org/10.1016/0016-5085(95)90193-0

Frank, J., Schiborr, C., Kocher, A., Meins, J., Behnam, D., Schubert-Zsilavecz, M., & Abdel-Tawab, M. (2017). Transepithelial transport of curcumin in Caco-2 cells is significantly enhanced by micellar solubilisation. *Plant Foods for Human Nutrition*, *72*(1), 48-53. https://doi.org/10.1007/s11130-016-0587-9

Frucht, H., Maton, P. N., & Jensen, R. T. (1991). Use of omeprazole in patients with Zollinger-Ellison syndrome. *Digestive diseases and sciences*, *36*(4), 394-404. https://doi.org/10.1007/BF01298865

Fung, K. Y., Fairn, G. D., & Lee, W. L. (2018). Transcellular vesicular transport in epithelial and endothelial cells: Challenges and opportunities. *Traffic*, *19*(1), 5-18. https://doi.org/10.1111/tra.12533

Fukasawa, M., & Obara, S. (2004). Molecular weight determination of hypromellose acetate succinate (HPMCAS) using size exclusion chromatography with a multi-angle laser light scattering detector. *Chemical and Pharmaceutical Bulletin*, *52*(11), 1391-1393. https://doi.org/https://doi.org/10.1248/cpb.52.1391

Gantait, A., Barman, T., & Mukherjee, P. K. (2011). Validated method for estimation of curcumin in turmeric powder.

Gao, D., Liu, H., Lin, J.-M., Wang, Y., & Jiang, Y. (2013). Characterization of drug permeability in Caco-2 monolayers by mass spectrometry on a membrane-based microfluidic device. *Lab on a chip*, *13*(5), 978-985.https://doi.org/10.1039/c2lc41215b.

Gao, P., Akrami, A., Alvarez, F., Hu, J., Li, L., Ma, C., & Surapaneni, S. (2009). Characterization and optimization of AMG 517 supersaturatable self-emulsifying drug delivery system (S-SEDDS) for improved oral absorption. *Journal of pharmaceutical sciences*, *98*(2), 516-528. https://doi.org/10.1002/jps.21451.

Garcea, G., Jones, D., Singh, R., Dennison, A., Farmer, P., Sharma, R., Steward, W., Gescher, A., & Berry, D. (2004). Detection of curcumin and its metabolites in hepatic tissue and portal blood of patients following oral administration. *British journal of cancer*, *90*(5), 1011-1015. https://doi.org/10.1038/sj.bjc.6601623.

Gao, Y., Chen, G., Luan, X., Zou, M., Piao, H., & Cheng, G. (2019). Improved oral absorption of poorly soluble curcumin via the concomitant use of borneol. *AAPS PharmSciTech*, *20*(4), 1-10. https://doi.org/10.1208/s12249-019-1364-5

Gao, Y., Glennon, B., He, Y., & Donnellan, P. (2021). Dissolution kinetics of a bcs class ii active pharmaceutical ingredient: Diffusion-based model validation and prediction. *Acs Omega*, *6*(12), 8056-8067. https://doi.org/10.1021/acsomega.0c05558

García-Rodriguez, J. J., Paloma, M., Vegas-Sánchez, M. C., Torrado-Durán, S., Bolás-Fernández, F., & Torrado-Santiago, S. (2011). Changed crystallinity of mebendazole solid dispersion: improved anthelmintic activity. *International journal of pharmaceutics*, *403*(1-2), 23-28. https://doi.org/10.1016/j.ijpharm.2010.10.002

Galijatovic, A., Otake, Y., Walle, U. K., & Walle, T. (2001). Induction of UDP-glucuronosyltransferase UGT1A1 by the flavonoid chrysin in Caco-2 cells—potential role in carcinogen bioinactivation. *Pharmaceutical research*, *18*(3), 374-379. https://doi.org/10.1023/a:1011019417236

Geng, L., Han, L., Huang, L., Wu, Z., & Wu, Z. (2019). High Anti-Acid Omeprazole Lightweight Capsule for Gastro-Enteric System Acid-Related Disorders Treatment. *J Clin Gastroenterol Treat*, *5*, 068.

https://doi.org/10.23937/2469-584X/1510068

Ghadi, R., & Dand, N. (2017). BCS class IV drugs: Highly notorious candidates for formulation development. *Journal of Controlled Release*, *248*, 71-95. https://doi.org/10.1016/j.jconrel.2017.01.014

Govindaraju, R., Karki, R., Chandrashekarappa, J., Santhanam, M., Shankar, A. K., Joshi, H. K., & Divakar, G. (2019). Enhanced water dispersibility of curcumin encapsulated in alginate-polysorbate 80 nano particles and bioavailability in healthy human volunteers. *Pharmaceutical nanotechnology*, *7*(1), 39-56. https://doi.org/10.2174/2211738507666190122121242.

Goud, N. R., Suresh, K., Sanphui, P., & Nangia, A. (2012). Fast dissolving eutectic compositions of curcumin. *International journal of pharmaceutics*, *439*(1-2), 63-72. https://doi.org/10.1016/j.ijpharm.2012.09.045

Gota, V. S., Maru, G. B., Soni, T. G., Gandhi, T. R., Kochar, N., & Agarwal, M. G. (2010). Safety and pharmacokinetics of a solid lipid curcumin particle formulation in osteosarcoma patients and healthy volunteers. *Journal of agricultural and food chemistry*, *58*(4), 2095-2099. https://doi.org/10.1021/jf9024807

Grancharov, K., Naydenova, Z., Lozeva, S., & Golovinsky, E. (2001). Natural and synthetic inhibitors of UDP-glucuronosyltransferase. *Pharmacology & Therapeutics*, *89*(2), 171-186. https://doi.org/10.1016/S0163-7258(00)00109-1.

Grill, A. E., Koniar, B., & Panyam, J. (2014). Co-delivery of natural metabolic inhibitors in a self-microemulsifying drug delivery system for improved oral

bioavailability of curcumin. *Drug delivery and translational research*, *4*(4), 344-352. https://doi.org/10.1007/s13346-014-0199-6.

Giuliano, E., Paolino, D., Fresta, M., & Cosco, D. (2018). Drug-loaded biocompatible nanocarriers embedded in poloxamer 407 hydrogels as therapeutic formulations. *Medicines*, *6*(1), 7. https://doi.org/10.3390/medicines6010007

Giedraitiene, A., Pereckaite, L., Bredelyte-Gruodiene, E., Virgailis, M., Ciapiene, I., & Tatarunas, V. (2022). CTX-M-producing Escherichia coli strains: resistance to temocillin, fosfomycin, nitrofurantoin and biofilm formation. *Future Microbiology*(0). https://doi.org/10.2217/fmb-2021-0202

Gill, P., Moghadam, T. T., & Ranjbar, B. (2010). Differential scanning calorimetry techniques: applications in biology and nanoscience. *Journal of biomolecular techniques: JBT*, *21*(4), 167.

Gullapalli, R. P., & Mazzitelli, C. L. (2015). Polyethylene glycols in oral and parenteral formulations—A critical review. *International journal of pharmaceutics*, *496*(2), 219-239. https://doi.org/10.1016/j.ijpharm.2015.11.015

Gupta, H., Bhandari, D., & Sharma, A. (2009). Recent trends in oral drug delivery: A review. Recent Pat Drug Deliv Formul 2009; 3: 162-173.

Gurpreet, K., & Singh, S. (2018). Review of nanoemulsion formulation and characterization techniques. *Indian Journal of Pharmaceutical Sciences*, *80*(5), 781-789. https://doi.org/10.4172/pharmaceutical-sciences.1000422.

Guo, Y., Luo, J., Tan, S., Otieno, B. O., & Zhang, Z. (2013). The applications

of Vitamin E TPGS in drug delivery. *European journal of pharmaceutical sciences*, *49*(2), 175-186. https://doi.org/10.1016/j.ejps.2013.02.006

Gupta, M. K., Tseng, Y.-C., Goldman, D., & Bogner, R. H. (2002). Hydrogen bonding with adsorbent during storage governs drug dissolution from solid-dispersion granules. *Pharmaceutical research*, *19*(11), 1663-1672. https://doi.org/10.1023/a:1020905412654

Gupta, S. S., Meena, A., Parikh, T., & Serajuddin, A. T. (2016). Investigation of thermal and viscoelastic properties of polymers relevant to hot melt extrusion-I: Polyvinylpyrrolidone and related polymers. *Journal of Excipients and Food Chemicals*, *5*(1), 1001.

Gui, Y., McCann, E. C., Yao, X., Li, Y., Jones, K. J., & Yu, L. (2021). Amorphous drug–polymer salt with high stability under tropical conditions and fast dissolution: the case of clofazimine and poly (acrylic acid). *Molecular pharmaceutics*, *18*(3), 1364-1372. https://doi.org/10.1021/acs.molpharmaceut.0c01180

Gupte, P. A., Giramkar, S. A., Harke, S. M., Kulkarni, S. K., Deshmukh, A. P., Hingorani, L. L., Mahajan, M. P., & Bhalerao, S. S. (2019). Evaluation of the efficacy and safety of Capsule Longvida® Optimized Curcumin (solid lipid curcumin particles) in knee osteoarthritis: a pilot clinical study. *Journal of inflammation research*, *12*, 145. https://doi.org/10.2147/JIR.S205390

Gutmann, H., Fricker, G., Török, M., Michael, S., Beglinger, C., & Drewe, J. (1999). Evidence for different ABC-transporters in Caco-2 cells modulating drug uptake. *Pharmaceutical research*, *16*(3), 402-407. https://doi.org/10.1023/a:1018825819249

Guri, A., Gülseren, I., & Corredig, M. (2013). Utilization of solid lipid nanoparticles for enhanced delivery of curcumin in cocultures of HT29-MTX and Caco-2 cells. *Food & function*, *4*(9), 1410-1419. https://doi.org/10.1039/C3FO60180C

Haley, B., & Frenkel, E. (2008). Nanoparticles for drug delivery in cancer treatment. Urologic Oncology: Seminars and original investigations, Hassaninasab, A., Hashimoto, Y., Tomita-Yokotani, K., & Kobayashi, M. (2011). Discovery of the curcumin metabolic pathway involving a unique enzyme in an intestinal microorganism. *Proceedings of the National Academy of Sciences*, *108*(16), 6615-6620. https://doi.org/10.1073/pnas.1016217108

Hatcher, H., Planalp, R., Cho, J., Torti, F., & Torti, S. (2008). Curcumin: from ancient medicine to current clinical trials. *Cellular and molecular life sciences*, *65*(11), 1631-1652. https://doi.org/10.1007/s00018-008-7452-4

Ha, E.-S., Baek, I.-h., Cho, W., Hwang, S.-J., & Kim, M.-S. (2014). Preparation and evaluation of solid dispersion of atorvastatin calcium with Soluplus® by spray drying technique. *Chemical and Pharmaceutical Bulletin*, *62*(6), 545-551. https://doi.org/10.1248/cpb.c14-00030

Hancock, B. C., & Zografi, G. (1994). The relationship between the glass transition temperature and the water content of amorphous pharmaceutical solids. *Pharmaceutical research*, *11*(4), 471-477. https://doi.org/10.1023/a:1018941810744

Hasegawa, S., Ke, P., & Buckton, G. (2009). Determination of the structural

relaxation at the surface of amorphous solid dispersion using inverse gas chromatography. *Journal of pharmaceutical sciences*, *98*(6), 2133-2139. https://doi.org/10.1002/jps.21573

Hashimoto, K., & Shimizu, M. (1993). Epithelial properties of human intestinal Caco-2 cells cultured in a serum-free medium. *Cytotechnology*, *13*(3), 175-184. https://doi.org/10.1007/BF00749813

Haware, R. V., Vinjamuri, B. P., Sarkar, A., Stefik, M., & Stagner, W. C. (2018). Deciphering magnesium stearate thermotropic behavior. *International journal of pharmaceutics*, *548*(1), 314-324. https://doi.org/10.1016/j.ijpharm.2018.07.001

Hai, Y., Zhang, Y., Liang, Y., Ma, X., Qi, X., Xiao, J., Xue, W., Luo, Y., & Yue, T. (2020). Advance on the absorption, metabolism, and efficacy exertion of quercetin and its important derivatives: Absorption, metabolism and function of quercetin. *Food Frontiers*, *1*(4), 420-434. https://doi.org/https://doi.org/10.1002/fft2.50

Hall, A. P., Czerwinski, A. W., Madonia, E. C., & Evensen, K. L. (1973). Human plasma and urine quinine levels following tablets, capsules, and intravenous infusion. *Clinical pharmacology & therapeutics*, *14*(4part1), 580-585. https://doi.org/10.1002/cpt1973144part1580

Heng, P. W., Wan, L. S., & Ang, T. S. (1990). Role of surfactant on drug release from tablets. *Drug development and industrial pharmacy*, *16*(6), 951-962. https://doi.org/https://doi.org/10.3109/03639049009114921

Hewlings, S. J., & Kalman, D. S. (2017). Curcumin: A review of its effects on

human health. *Foods*, *6*(10), 92. https://doi.org/10.3390/foods6100092

Hidalgo, I. J. (2001). Assessing the absorption of new pharmaceuticals. *Current topics in medicinal chemistry*, *1*(5), 385-401. https://doi.org/10.2174/1568026013395010

Hidalgo, I. J., & Borchardt, R. T. (1990). Transport of bile acids in a human intestinal epithelial cell line, Caco-2. *Biochimica et Biophysica Acta (BBA)-General Subjects*, *1035*(1), 97-103. https://doi.org/10.1016/0304-4165(90)90179-z

Hirohashi, T., Suzuki, H., Chu, X.-Y., Tamai, I., Tsuji, A., & Sugiyama, Y. (2000). Function and expression of multidrug resistance-associated protein family in human colon adenocarcinoma cells (Caco-2). *Journal of Pharmacology and Experimental Therapeutics*, *292*(1), 265-270.

Hoehle, S. I., Pfeiffer, E., & Metzler, M. (2007). Glucuronidation of curcuminoids by human microsomal and recombinant UDP-glucuronosyltransferases. *Molecular nutrition & food research*, *51*(8), 932-938.https://doi.org/10.1002/mnfr.200600283.

Holder, G. M., Plummer, J. L., & Ryan, A. J. (1978). The metabolism and excretion of curcumin (1, 7-bis-(4-hydroxy-3-methoxyphenyl)-1, 6-heptadiene-3, 5-dione) in the rat. *Xenobiotica*, *8*(12), 761-768. https://doi.org/10.3109/00498257809069589.

Homayun, B., Lin, X., & Choi, H.-J. (2019). Challenges and Recent Progress in Oral Drug Delivery Systems for Biopharmaceuticals. *Pharmaceutics*, *11*(3), 129. https://doi.org/10.3390/pharmaceutics11030129.

Hong, J., Bose, M., Ju, J., Ryu, J.-H., Chen, X., Sang, S., Lee, M.-J., & Yang, C. S. (2004). Modulation of arachidonic acid metabolism by curcumin and related β-diketone derivatives: effects on cytosolic phospholipase A 2, cyclooxygenases and 5-lipoxygenase. *Carcinogenesis*, *25*(9), 1671-1679. https://doi.org/10.1093/carcin/bgh165

Hottot, A., Vessot, S., & Andrieu, J. (2007). Freeze drying of pharmaceuticals in vials: Influence of freezing protocol and sample configuration on ice morphology and freeze-dried cake texture. *Chemical Engineering and Processing: Process Intensification*, *46*(7), 666-674. https://doi.org/10.1016/j.cep.2006.09.003

Hochman, J. H., Chiba, M., Yamazaki, M., Tang, C., & Lin, J. H. (2001). P-glycoprotein-mediated efflux of indinavir metabolites in Caco-2 cells expressing cytochrome P450 3A4. *Journal of Pharmacology and Experimental Therapeutics*, *298*(1), 323-330.

Hong, J., Lambert, J. D., Lee, S.-H., Sinko, P. J., & Yang, C. S. (2003). Involvement of multidrug resistance-associated proteins in regulating cellular levels of (−)-epigallocatechin-3-gallate and its methyl metabolites. *Biochemical and biophysical research communications*, *310*(1), 222-227. https://doi.org/10.1016/j.bbrc.2003.09.007

Hu, J., Johnston, K. P., & Williams III, R. O. (2003). Spray freezing into liquid (SFL) particle engineering technology to enhance dissolution of poorly water soluble drugs: organic solvent versus organic/aqueous co-solvent systems. *European journal of pharmaceutical sciences*, *20*(3), 295-303. https://doi.org/10.1016/s0928-0987(03)00203-3

Hu, J., Rogers, T. L., Brown, J., Young, T., Johnston, K. P., & Williams Iii, R. O. (2002). Improvement of dissolution rates of poorly water soluble APIs using novel spray freezing into liquid technology. *Pharmaceutical research*, *19*(9), 1278-1284. https://doi.org/10.1023/a:1020390422785

Huang, J., Wigent, R. J., & Schwartz, J. B. (2006). Nifedipine molecular dispersion in microparticles of ammonio methacrylate copolymer and ethylcellulose binary blends for controlled drug delivery: effect of matrix composition. *Drug development and industrial pharmacy*, *32*(10), 1185-1197. https://doi.org/10.1080/03639040600832827

Huang, J., Wigent, R. J., & Schwartz, J. B. (2008). Drug–polymer interaction and its significance on the physical stability of nifedipine amorphous dispersion in microparticles of an ammonio methacrylate copolymer and ethylcellulose binary blend. *Journal of pharmaceutical sciences*, *97*(1), 251-262. https://doi.org/10.1002/jps.21072

Huang, Y., & Dai, W.-G. (2014). Fundamental aspects of solid dispersion technology for poorly soluble drugs. *Acta Pharmaceutica Sinica B*, *4*(1), 18-25. https://doi.org/10.1016/j.apsb.2013.11.001

Hung, W.-L., Chang, W.-S., Lu, W.-C., Wei, G.-J., Wang, Y., Ho, C.-T., & Hwang, L. S. (2018). Pharmacokinetics, bioavailability, tissue distribution and excretion of tangeretin in rat. *journal of food and drug analysis*, *26*(2), 849-857. https://doi.org/10.1016/j.jfda.2017.08.003

Huang, C., Lu, H.-F., Chen, Y.-H., Chen, J.-C., Chou, W.-H., & Huang, H.-C. (2020). Curcumin, demethoxycurcumin, and bisdemethoxycurcumin induced

caspase-dependent and–independent apoptosis via Smad or Akt signaling pathways in HOS cells. *BMC complementary medicine and therapies*, *20*(1), 1-11. https://doi.org/10.1186/s12906-020-2857-1

Hubatsch, I., Ragnarsson, E. G., & Artursson, P. (2007). Determination of drug permeability and prediction of drug absorption in Caco-2 monolayers. *Nature protocols*, *2*(9), 2111-2119. https://doi.org/10.1038/nprot.2007.303

Hunter, J., Jepson, M. A., Tsuruo, T., Simmons, N. L., & Hirst, B. H. (1993). Functional expression of P-glycoprotein in apical membranes of human intestinal Caco-2 cells. Kinetics of vinblastine secretion and interaction with modulators. *Journal of Biological Chemistry*, *268*(20), 14991-14997.

Iqbal, Z., Babar, A., & Ashraf, M. (2002). Controlled-release naproxen using micronized ethyl cellulose by wet-granulation and solid-dispersion method. *Drug development and industrial pharmacy*, *28*(2), 129-134. https://doi.org/10.1081/ddc-120002445

Ireson, C., Orr, S., Jones, D. J., Verschoyle, R., Lim, C.-K., Luo, J.-L., Howells, L., Plummer, S., Jukes, R., & Williams, M. (2001). Characterization of metabolites of the chemopreventive agent curcumin in human and rat hepatocytes and in the rat in vivo, and evaluation of their ability to inhibit phorbol ester-induced prostaglandin E2 production. *Cancer research*, *61*(3), 1058-1064.

Ireson, C. R., Jones, D. J., Orr, S., Coughtrie, M. W., Boocock, D. J., Williams, M. L., Farmer, P. B., Steward, W. P., & Gescher, A. J. (2002). Metabolism of the cancer chemopreventive agent curcumin in human and rat intestine.

Cancer Epidemiology Biomarkers & Prevention, *11*(1), 105-111.

ICH. (2003). *STABILITY TESTING OF NEW DRUG SUBSTANCES AND PRODUCTS Q1A(R2)*. Retrieved 28 September from https://database.ich.org/sites/default/files/Q1A%28R2%29%20Guideline.pdf

Involvement of multidrug resistance-associated proteins in regulating cellular levels of (−)-epigallocatechin-3-gallate and its methyl metabolites. *Biochemical and biophysical research communications*, *310*(1), 222-227. https://doi.org/10.1016/j.bbrc.2003.09.007

Jäger, R., Lowery, R. P., Calvanese, A. V., Joy, J. M., Purpura, M., & Wilson, J. M. (2014). Comparative absorption of curcumin formulations. *Nutrition journal*, *13*(1), 1-8. https://doi.org/10.1186/1475-2891-13-11

Jahagirdar, P. S., Gupta, P. K., Kulkarni, S. P., & Devarajan, P. V. (2019). Polymeric curcumin nanoparticles by a facile in situ method for macrophage targeted delivery. *Bioengineering & translational medicine*, *4*(1), 141-151. https://doi.org/10.1002/btm2.10112.

Jantan, I., Bukhari, S. N. A., Lajis, N. H., Abas, F., Wai, L. K., & Jasamai, M. (2012). Effects of diarylpentanoid analogues of curcumin on chemiluminescence and chemotactic activities of phagocytes. *Journal of pharmacy and pharmacology*, *64*(3), 404-412. https://doi.org/10.1111/j.2042-7158.2011.01423.x

Jamwal, R. (2018). Bioavailable curcumin formulations: A review of pharmacokinetic studies in healthy volunteers. *Journal of integrative medicine*, *16*(6), 367-374. https://doi.org/10.1016/j.joim.2018.07.001

Jayaprakasha, G. K., Rao, L. J., & Sakariah, K. K. (2006). Antioxidant activities of curcumin, demethoxycurcumin and bisdemethoxycurcumin. *Food Chemistry*, *98*(4), 720-724. https://doi.org/10.1016/j.foodchem.2005.06.037

Jackson, K., Young, D., & Pant, S. (2000). Drug–excipient interactions and their affect on absorption. *Pharmaceutical science & technology today*, *3*(10), 336-345. https://doi.org/10.1016/S1461-5347(00)00301-1

Jagannathan, R., Abraham, P. M., & Poddar, P. (2012). Temperature-dependent spectroscopic evidences of curcumin in aqueous medium: a mechanistic study of its solubility and stability. *The Journal of Physical Chemistry B*, *116*(50), 14533-14540. https://doi.org/10.1021/jp3050516

Jara, M. O., Warnken, Z. N., & Williams III, R. O. (2021). Amorphous solid dispersions and the contribution of nanoparticles to in vitro dissolution and in vivo testing: Niclosamide as a case study. *Pharmaceutics*, *13*(1), 97. https://doi.org/10.3390/pharmaceutics13010097

Jamaludin, A., Mohamad, M., Navaratnam, V., Selliah, K., Tan, S., Wernsdorfer, W., & Yuen, K. (1988). Relative bioavailability of the hydrochloride, sulphate and ethyl carbonate salts of quinine. *British journal of clinical pharmacology*, *25*(2), 261-263. https://doi.org/10.1111/j.1365-2125.1988.tb03299.x

Jia, N., Li, S.-M., Ma, M.-G., Zhu, J.-F., & Sun, R.-C. (2011). Synthesis and characterization of cellulose-silica composite fiber in ethanol/water mixed solvents. *BioResources*, *6*(2), 1186-1195. https://doi.org/10.15376/biores.6.2.1186-1195

Jinno, J.-i., Kamada, N., Miyake, M., Yamada, K., Mukai, T., Odomi, M., Toguchi, H., Liversidge, G. G., Higaki, K., & Kimura, T. (2006). Effect of particle size reduction on dissolution and oral absorption of a poorly water-soluble drug, cilostazol, in beagle dogs. *Journal of Controlled Release*, *111*(1-2), 56-64. https://doi.org/10.1016/j.jconrel.2005.11.013

Jin, G., Ngo, H. V., Cui, J.-H., Wang, J., Park, C., & Lee, B.-J. (2021). Role of Surfactant Micellization for Enhanced Dissolution of Poorly Water-Soluble Cilostazol Using Poloxamer 407-Based Solid Dispersion via the Anti-Solvent Method. *Pharmaceutics*, *13*(5), 662. https://doi.org/10.3390/pharmaceutics13050662

Jovanovic, S. V., Steenken, S., Boone, C. W., & Simic, M. G. (1999). H-atom transfer is a preferred antioxidant mechanism of curcumin. *Journal of the American Chemical Society*, *121*(41), 9677-9681. https://doi.org/10.1021/ja991446m

Joshi, G., Kumar, A., & Sawant, K. (2016). Bioavailability enhancement, Caco-2 cells uptake and intestinal transport of orally administered lopinavir-loaded PLGA nanoparticles. *Drug Delivery*, *23*(9), 3492-3504. https://doi.org/10.1080/10717544.2016.1199605

Junghanns, J.-U. A., & Müller, R. H. (2008). Nanocrystal technology, drug delivery and clinical applications. *International journal of nanomedicine*, *3*(3), 295. https://doi.org/10.2147/IJN.S595.

Jurgeit, A., McDowell, R., Moese, S., Meldrum, E., Schwendener, R., &

Greber, U. F. (2012). Niclosamide is a proton carrier and targets acidic endosomes with broad antiviral effects. *PLoS pathogens*, *8*(10), e1002976. https://doi.org/10.1371/journal.ppat.1002976

Jug, M., & Mura, P. A. (2018). Grinding as solvent-free green chemistry approach for cyclodextrin inclusion complex preparation in the solid state. *Pharmaceutics*, *10*(4), 189. https://doi.org/10.3390/pharmaceutics10040189

Kadota, K., Okamoto, D., Sato, H., Onoue, S., Otsu, S., & Tozuka, Y. (2016). Hybridization of polyvinylpyrrolidone to a binary composite of curcumin/α-glucosyl stevia improves both oral absorption and photochemical stability of curcumin. *Food Chemistry*, *213*, 668-674. https://doi.org/10.1016/j.foodchem.2016.07.025

Karanth, H., Shenoy, V. S., & Murthy, R. R. (2006). Industrially feasible alternative approaches in the manufacture of solid dispersions: A technical report. *AAPS PharmSciTech*, *7*(4), E31-E38. https://doi.org/10.1208/pt070487

Karavas, E., Ktistis, G., Xenakis, A., & Georgarakis, E. (2006). Effect of hydrogen bonding interactions on the release mechanism of felodipine from nanodispersions with polyvinylpyrrolidone. *European Journal of Pharmaceutics and Biopharmaceutics*, *63*(2), 103-114. https://doi.org/10.1016/j.ejpb.2006.01.016

Kalaycıoğlu, Z., Gazioğlu, I., & Erim, F. B. (2017). Comparison of antioxidant, anticholinesterase, and antidiabetic activities of three curcuminoids isolated from Curcuma longa L. *Natural Product Research*, *31*(24), 2914-2917. https://doi.org/10.1080/14786419.2017.1299727

Karolewicz, B., Gajda, M., Górniak, A., Owczarek, A., & Mucha, I. (2017). Pluronic F127 as a suitable carrier for preparing the imatinib base solid dispersions and its potential in development of a modified release dosage forms. *Journal of Thermal Analysis and Calorimetry*, *130*(1), 383-390. https://doi.org/10.1007/s10973-017-6139-1

Kaszuba, M., Corbett, J., Watson, F. M., & Jones, A. (2010). High-concentration zeta potential measurements using light-scattering techniques. *Philosophical transactions of the royal society a: mathematical, physical and engineering sciences*, *368*(1927), 4439-4451. https://doi.org/10.1098/rsta.2010.0175

Kalliokoski, A., & Niemi, M. (2009). Impact of OATP transporters on pharmacokinetics. *British journal of pharmacology*, *158*(3), 693-705. https://doi.org/10.1111/j.1476-5381.2009.00430.x

Kamiya, Y., Takaku, H., Yamada, R., Akase, C., Abe, Y., Sekiguchi, Y., Murayama, N., Shimizu, M., Kitajima, M., & Shono, F. (2020). Determination and prediction of permeability across intestinal epithelial cell monolayer of a diverse range of industrial chemicals/drugs for estimation of oral absorption as a putative marker of hepatotoxicity. *Toxicology reports*, *7*, 149-154. https://doi.org/10.1016/j.toxrep.2020.01.004

Katsura, T., & Inui, K.-i. (2003). Intestinal absorption of drugs mediated by drug transporters: mechanisms and regulation. *Drug metabolism and pharmacokinetics*, *18*(1), 1-15. https://doi.org/10.2133/dmpk.18.1

Kakran, M., Sahoo, N., & Li, L. (2011). Dissolution enhancement of quercetin through nanofabrication, complexation, and solid dispersion. *Colloids and*

Surfaces B: Biointerfaces, *88*(1), 121-130. https://doi.org/10.1016/j.colsurfb.2011.06.020

Kasim, N. A., Whitehouse, M., Ramachandran, C., Bermejo, M., Lennernäs, H., Hussain, A. S., Junginger, H. E., Stavchansky, S. A., Midha, K. K., & Shah, V. P. (2004). Molecular properties of WHO essential drugs and provisional biopharmaceutical classification. *Molecular pharmaceutics*, *1*(1), 85-96. https://doi.org/10.1021/mp034006h

Kawahara, I., Nishikawa, S., Yamamoto, A., Kono, Y., & Fujita, T. (2020). Assessment of contribution of BCRP to intestinal absorption of various drugs using portal-systemic blood concentration difference model in mice. *Pharmacology Research & Perspectives*, *8*(1), e00544. https://doi.org/10.1002/prp2.544

Katneni, K., Charman, S. A., & Porter, C. J. (2006). Permeability assessment of poorly water-soluble compounds under solubilizing conditions: The reciprocal permeability approach. *Journal of pharmaceutical sciences*, *95*(10), 2170-2185. https://doi.org/10.1002/jps.20687

Katneni, K., Charman, S. A., & Porter, C. J. (2007). Impact of cremophor-EL and polysorbate-80 on digoxin permeability across rat jejunum: delineation of thermodynamic and transporter related events using the reciprocal permeability approach. *Journal of pharmaceutical sciences*, *96*(2), 280-293. https://doi.org/10.1002/jps.20779

Karakucuk, A., & Celebi, N. (2020). Investigation of formulation and process parameters of wet media milling to develop etodolac nanosuspensions. *Pharmaceutical research*, *37*, 1-18. https://doi.org/10.1007/s11095-020-

02815-x

Khan, S., Imran, M., Butt, T. T., Shah, S. W. A., Sohail, M., Malik, A., Das, S., Thu, H. E., Adam, A., & Hussain, Z. (2018). Curcumin based nanomedicines as efficient nanoplatform for treatment of cancer: new developments in reversing cancer drug resistance, rapid internalization, and improved anticancer efficacy. *Trends in Food Science & Technology*, *80*, 8-22. https://doi.org/10.1016/j.tifs.2018.07.026.

Khopde, S. M., Priyadarsini, K. I., Venkatesan, P., & Rao, M. (1999). Free radical scavenging ability and antioxidant efficiency of curcumin and its substituted analogue. *Biophysical chemistry*, *80*(2), 85-91. https://doi.org/10.1016/s0301-4622(99)00070-8.

Kim, M.-K., Choi, G.-J., & Lee, H.-S. (2003). Fungicidal property of Curcuma longa L. rhizome-derived curcumin against phytopathogenic fungi in a greenhouse. *Journal of agricultural and food chemistry*, *51*(6), 1578-1581. https://doi.org/10.1021/jf0210369

Kim, K.-T., Lee, J.-Y., Lee, M.-Y., Song, C.-K., Choi, J.-H., & Kim, D.-D. (2011). Solid dispersions as a drug delivery system. *Journal of pharmaceutical Investigation*, *41*(3), 125-142. https://doi.org/10.4333/KPS.2011.41.3.125

Kim, T. K. (2017). Understanding one-way ANOVA using conceptual figures. *Korean journal of anesthesiology*, *70*(1), 22-26. https://doi.org/10.4097/kjae.2017.70.1.22

Kiss, K., Hegedüs, K., Vass, P., Vári-Mező, D., Farkas, A., Nagy, Z. K., Molnár, L., Tóvári, J., Mező, G., & Marosi, G. (2022). Development of fast-dissolving

dosage forms of curcuminoids by electrospinning for potential tumor therapy application. *International journal of pharmaceutics*, *611*, 121327. https://doi.org/10.1016/j.ijpharm.2021.121327

Klickovic, U., Doberer, D., Gouya, G., Aschauer, S., Weisshaar, S., Storka, A., Bilban, M., & Wolzt, M. (2014). Human pharmacokinetics of high dose oral curcumin and its effect on heme oxygenase-1 expression in healthy male subjects. *BioMed research international*, *2014*. https://doi.org/10.1155/2014/458592

Kolašinac, N., Kachrimanis, K., Homšek, I., Grujić, B., Đurić, Z., & Ibrić, S. (2012). Solubility enhancement of desloratadine by solid dispersion in poloxamers. *International journal of pharmaceutics*, *436*(1-2), 161-170. https://doi.org/10.1016/j.ijpharm.2012.06.060

Kondoros, B. A., Jójárt-Laczkovich, O., Berkesi, O., Szabó-Révész, P., Csóka, I., Ambrus, R., & Aigner, Z. (2022). Development of Solvent-Free Co-Ground Method to Produce Terbinafine Hydrochloride Cyclodextrin Binary Systems; Structural and In Vitro Characterizations. *Pharmaceutics*, *14*(4), 744. https://doi.org/10.3390/pharmaceutics14040744

Kovarik, J., Kirkesseli, S., Humbert, H., Grass, P., & Kutz, K. (1992). Dose-proportional pharmacokinetics of terbinafine and its N-demethylated metabolite in healthy volunteers. *British Journal of Dermatology*, *126*, 8-13. https://doi.org/10.1111/j.1365-2133.1992.tb00002.x

Kovarik, J. M., Mueller, E. A., Zehender, H., Denouël, J., Caplain, H., & Millerioux, L. (1995). Multiple-dose pharmacokinetics and distribution in tissue of terbinafine and metabolites. *Antimicrobial agents and chemotherapy*,

39(12), 2738-2741. https://doi.org/10.1128/AAC.39.12.2738

Krasavage, W. J., & Terhaar, C. J. (1977). d-. alpha.-Tocopheryl poly (ethylene glycol) 1000 succinate: acute toxicity, subchronic feeding, reproduction, and teratologic studies in the rat. *Journal of agricultural and food chemistry*, *25*(2), 273-278. https://doi.org/10.1021/jf60210a002

Kruijtzer, C., Beijnen, J., Rosing, H., ten Bokkel Huinink, W., Schot, M., Jewell, R., Paul, E., & Schellens, J. (2002). Increased oral bioavailability of topotecan in combination with the breast cancer resistance protein and P-glycoprotein inhibitor GF120918. *Journal of Clinical Oncology*, *20*(13), 2943-2950. https://doi.org/10.1200/JCO.2002.12.116

Krishnan-Natesan, S. (2009). Terbinafine: a pharmacological and clinical review. *Expert opinion on pharmacotherapy*, *10*(16), 2723-2733. https://doi.org/10.1517/14656560903307462

Kumar, S., Kesharwani, S. S., Mathur, H., Tyagi, M., Bhat, G. J., & Tummala, H. (2016). Molecular complexation of curcumin with pH sensitive cationic copolymer enhances the aqueous solubility, stability and bioavailability of curcumin. *European journal of pharmaceutical sciences*, *82*, 86-96. https://doi.org/10.1016/j.ejps.2015.11.010

Kumavat, S., Chaudhari, Y., Kenge, D., Kokardekar, R., & Bichave, A. (2014). In vitro and in vivo evaluation of binary Solid dispersion of Curcumin by solvent evaporation technique. *World Journal of Pharmaceutical Sciences*, 1451-1459.

Kumbhar, P. S., Nadaf, S., Manjappa, A. S., Jha, N. K., Shinde, S. S.,

Chopade, S. S., Shete, A. S., Disouza, J. I., Sambamoorthy, U., & Kumar, S. A. (2022). D-α-tocopheryl polyethylene glycol succinate: A review of multifarious applications in nanomedicines. *OpenNano*, 100036. https://doi.org/10.1016/j.onano.2022.100036

Kumar, S., & Gupta, S. K. (2013). Pharmaceutical solid dispersion technology: a strategy to improve dissolution of poorly water-soluble drugs. *Recent patents on drug delivery & formulation*, *7*(2), 111-121. https://doi.org/10.2174/18722113113079990009.

Kunnumakkara, A. B., Anand, P., & Aggarwal, B. B. (2008). Curcumin inhibits proliferation, invasion, angiogenesis and metastasis of different cancers through interaction with multiple cell signaling proteins. *Cancer letters*, *269*(2), 199-225. https://doi.org/10.1016/j.canlet.2008.03.009.

Kurien, B. T., Singh, A., Matsumoto, H., & Scofield, R. H. (2007). Improving the solubility and pharmacological efficacy of curcumin by heat treatment. *Assay and drug development technologies*, *5*(4), 567-576. https://doi.org/10.1089/adt.2007.064.

Kuttan, R., Bhanumathy, P., Nirmala, K., & George, M. (1985). Potential anticancer activity of turmeric (Curcuma longa). *Cancer letters*, *29*(2), 197-202. https://doi.org/10.1016/0304-3835(85)90159-4

Kurien, B. T., Matsumoto, H., & Scofield, R. H. (2017). Nutraceutical value of pure curcumin. *Pharmacognosy Magazine*, *13*(Suppl 1), S161. https://doi.org/10.4103/0973-1296.203988

Kumar, A., & Dixit, C. K. (2017). Methods for characterization of nanoparticles.

In R. C. a. N. G. Surendra Nimesh (Ed.), *Advances in nanomedicine for the delivery of therapeutic nucleic acids* (pp. 43-58). Elsevier. https://doi.org/10.1016/B978-0-08-100557-6.00003-1

Lao, C. D., Demierre, M.-F., & Sondak, V. K. (2006b). Targeting events in melanoma carcinogenesis for the prevention of melanoma. *Expert review of anticancer therapy*, *6*(11), 1559-1568. https://doi.org/10.1586/14737140.6.11.1559

Lao, C. D., Ruffin, M. T., Normolle, D., Heath, D. D., Murray, S. I., Bailey, J. M., Boggs, M. E., Crowell, J., Rock, C. L., & Brenner, D. E. (2006a). Dose escalation of a curcuminoid formulation. *BMC complementary and alternative medicine*, *6*(1), 1-4. https://doi.org/10.1186/1472-6882-6-10

Lavra, Z. M. M., Pereira de Santana, D., & Ré, M. I. (2017). Solubility and dissolution performances of spray-dried solid dispersion of Efavirenz in Soluplus. *Drug development and industrial pharmacy*, *43*(1), 42-54. https://doi.org/10.1080/03639045.2016.1205598

Lampen, A., Bader, A., Bestmann, T., Winkler, M., Witte, L., & BORLAK*, J. (1998). Catalytic activities, protein-and mRNA-expression of cytochrome P450 isoenzymes in intestinal cell lines. *Xenobiotica*, *28*(5), 429-441. https://doi.org/10.1080/004982598239362

Lawrence, M.J. (1994). Surfactant systems: their use in drug delivery. Chemical Society Reviews, 34(9), 881-888.

Lazorova, L., Hubatsch, I., Ekegren, J. K., Gising, J., Nakai, D., Zaki, N. M., Bergström, C. A., Norinder, U., Larhed, M., & Artursson, P. (2011). Structural

features determining the intestinal epithelial permeability and efflux of novel HIV-1 protease inhibitors. *Journal of pharmaceutical sciences*, *100*(9), 3763-3772. https://doi.org/10.1002/jps.22570

Lee, J.-Y., Kang, W.-S., Piao, J., Yoon, I.-S., Kim, D.-D., & Cho, H.-J. (2015). Soluplus®/TPGS-based solid dispersions prepared by hot-melt extrusion equipped with twin-screw systems for enhancing oral bioavailability of valsartan. *Drug design, development and therapy*, *9*, 2745. https://doi.org/10.2147/DDDT.S84070

Lee, S. L., Raw, A. S., & Yu, L. (2008). Dissolution testing. In *Biopharmaceutics applications in drug development* (pp. 47-74). Springer.

Liu, T., Zhang, L., Joo, D., & Sun, S.-C. (2017). NF-κB signaling in inflammation. *Signal transduction and targeted therapy*, *2*(1), 1-9. https://doi.org/10.1038/sigtrans.2017.23

Leuner, C., & Dressman, J. (2000). Improving drug solubility for oral delivery using solid dispersions. *European Journal of Pharmaceutics and Biopharmaceutics*, *50*(1), 47-60. https://doi.org/10.1016/S0939-6411(00)00076-X

Lennernäs, H., Palm, K., Fagerholm, U., & Artursson, P. (1996). Comparison between active and passive drug transport in human intestinal epithelial (Caco-2) cells in vitro and human jejunum in vivo. *International journal of pharmaceutics*, *127*(1), 103-107. https://doi.org/10.1016/0378-5173(95)04204-0

Li, L., Braiteh, F. S., & Kurzrock, R. (2005). Liposome-encapsulated curcumin: in vitro and in vivo effects on proliferation, apoptosis, signaling, and

angiogenesis. *Cancer: Interdisciplinary International Journal of the American Cancer Society*, *104*(6), 1322-1331. https://doi.org/10.1002/cncr.21300

Li, Z.-l., Peng, S.-f., Chen, X., Zhu, Y.-q., Zou, L.-q., Liu, W., & Liu, C.-m. (2018). Pluronics modified liposomes for curcumin encapsulation: Sustained release, stability and bioaccessibility. *Food research international*, *108*, 246-253. https://doi.org/10.1016/j.foodres.2018.03.048

Linn, M., Collnot, E.-M., Djuric, D., Hempel, K., Fabian, E., Kolter, K., & Lehr, C.-M. (2012). Soluplus® as an effective absorption enhancer of poorly soluble drugs in vitro and in vivo. *European journal of pharmaceutical sciences*, *45*(3), 336-343. https://doi.org/10.1016/j.ejps.2011.11.025

Li, C., Li, C., Le, Y., & Chen, J.-F. (2011). Formation of bicalutamide nanodispersion for dissolution rate enhancement. *International journal of pharmaceutics*, *404*(1-2), 257-263. https://doi.org/10.1016/j.ijpharm.2010.11.015

Li, J., Wang, Y., Zhang, W., Huang, Y., Hein, K., & Hidalgo, I. J. (2012). The role of a basolateral transporter in rosuvastatin transport and its interplay with apical breast cancer resistance protein in polarized cell monolayer systems. *Drug metabolism and disposition*, *40*(11), 2102-2108. https://doi.org/10.1124/dmd.112.045666

Lim, H.-T., Balakrishnan, P., Oh, D. H., Joe, K. H., Kim, Y. R., Hwang, D. H., Lee, Y.-B., Yong, C. S., & Choi, H.-G. (2010). Development of novel sibutramine base-loaded solid dispersion with gelatin and HPMC: physicochemical characterization and pharmacokinetics in beagle dogs. *International journal of pharmaceutics*, *397*(1-2), 225-230.

https://doi.org/10.1016/j.ijpharm.2010.07.013

Lin, B., & Zhou, S. (2017). Poly (ethylene glycol)-grafted silica nanoparticles for highly hydrophilic acrylic-based polyurethane coatings. *Progress in Organic Coatings*, *106*, 145-154. https://doi.org/10.1016/j.porgcoat.2017.02.008

Litou, C., Turner, D. B., Holmstock, N., Ceulemans, J., Box, K. J., Kostewicz, E., Kuentz, M., Holm, R., & Dressman, J. (2020). Combining biorelevant in vitro and in silico tools to investigate the in vivo performance of the amorphous solid dispersion formulation of etravirine in the fed state. *European journal of pharmaceutical sciences*, *149*, 105297. https://doi.org/10.1016/j.ejps.2020.105297

Liu, J., Zou, M., Piao, H., Liu, Y., Tang, B., Gao, Y., Ma, N., & Cheng, G. (2015). Characterization and pharmacokinetic study of aprepitant solid dispersions with soluplus®. *Molecules*, *20*(6), 11345-11356. https://doi.org/10.3390/molecules200611345

Liu, P., Zhou, J.-y., Chang, J.-h., Liu, X.-g., Xue, H.-f., Wang, R.-x., Li, Z.-s., Li, C.-s., Wang, J., & Liu, C.-z. (2020). Soluplus-mediated diosgenin amorphous solid dispersion with high solubility and high stability: development, characterization and oral bioavailability. *Drug design, development and therapy*, *14*, 2959. https://doi.org/10.2147/DDDT.S253405

Liu, J., Shentu, J.-z., Wu, L.-h., Dou, J., Xu, Q.-y., Zhou, H.-l., Wu, G.-l., Huang, M.-z., Hu, X.-j., & Chen, J.-c. (2012). Relative bioavailability and pharmacokinetic comparison of two different enteric formulations of omeprazole. *Journal of Zhejiang university science B*, *13*(5), 348-355.

https://doi.org/10.1631/jzus.B1100272

Liu, Y., Friesen, J. B., McAlpine, J. B., Lankin, D. C., Chen, S.-N., & Pauli, G. F. (2018). Natural deep eutectic solvents: properties, applications, and perspectives. *Journal of natural products*, *81*(3), 679-690. https://doi.org/10.1021/acs.jnatprod.7b00945

Liu, P., De Wulf, O., Laru, J., Heikkilä, T., van Veen, B., Kiesvaara, J., Hirvonen, J., Peltonen, L., & Laaksonen, T. (2013). Dissolution studies of poorly soluble drug nanosuspensions in non-sink conditions. *AAPS PharmSciTech*, *14*, 748-756. https://doi.org/10.1208/s12249-013-9960-2

López-Jornet, P., Camacho-Alonso, F., Jiménez-Torres, M. J., Orduña-Domingo, A., & Gómez-García, F. (2011). Topical curcumin for the healing of carbon dioxide laser skin wounds in mice. *Photomedicine and laser surgery*, *29*(12), 809-814. https://doi.org/10.1089/pho.2011.3004.

LoTempio, M. M., Veena, M. S., Steele, H. L., Ramamurthy, B., Ramalingam, T. S., Cohen, A. N., Chakrabarti, R., Srivatsan, E. S., & Wang, M. B. (2005). Curcumin suppresses growth of head and neck squamous cell carcinoma. *Clinical Cancer Research*, *11*(19), 6994-7002. https://doi.org/10.1158/1078-0432.CCR-05-0301.

Loh, Z. H., Samanta, A. K., & Heng, P. W. S. (2015). Overview of milling techniques for improving the solubility of poorly water-soluble drugs. *Asian journal of pharmaceutical sciences*, *10*(4), 255-274. https://doi.org/10.1016/j.ajps.2014.12.006

Lund, K. C., & Pantuso, T. (2014). Combination effects of quercetin,

resveratrol and curcumin on in vitro intestinal absorption. *Journal of Restorative Medicine*, *3*(1), 112-120. https://doi.org/10.14200/jrm.2014.3.0108.

Luo, W.-C., Beringhs, A. O. R., Kim, R., Zhang, W., Patel, S. M., Bogner, R. H., & Lu, X. (2021). Impact of formulation on the quality and stability of freeze-dried nanoparticles. *European Journal of Pharmaceutics and Biopharmaceutics*, *169*, 256-267. https://doi.org/10.1016/j.ejpb.2021.10.014

Madara, J., & Pappenheimer, J. (1987). Structural basis for physiological regulation of paracellular pathways in intestinal epithelia. *The Journal of membrane biology*, *100*(1), 149-164. https://doi.org/10.1007/BF02209147

Martinez, M. N., & Amidon, G. L. (2002). A mechanistic approach to understanding the factors affecting drug absorption: a review of fundamentals. *The Journal of Clinical Pharmacology*, *42*(6), 620-643. https://doi.org/10.1177/00970002042006005

Maniruzzaman, M., Boateng, J. S., Snowden, M. J., & Douroumis, D. (2012). A review of hot-melt extrusion: process technology to pharmaceutical products. *International Scholarly Research Notices*, *2012*. https://doi.org/10.5402/2012/436763

Maton, P. N. (1991). Omeprazole. *New England Journal of Medicine*, *324*(14), 965-975. https://doi.org/10.1056/NEJM199104043241406

Materska, M. (2008). Quercetin and its derivatives: chemical structure and bioactivity-a review. *Polish journal of food and nutrition sciences*, *58*(4).

McClellan, K. J., Wiseman, L. R., & Markham, A. (1999). Terbinafine. *Drugs*,

58(1), 179-202. https://doi.org/10.2165/00003495-199958010-00018

Mai, N. N. S., Otsuka, Y., Kawano, Y., & Hanawa, T. (2020). Preparation and characterization of solid dispersions composed of curcumin, hydroxypropyl cellulose and/or sodium dodecyl sulfate by grinding with vibrational ball milling. *Pharmaceuticals*, *13*(11), 383. https://doi.org/10.3390/ph13110383

McClements, D. J. (2012). Nanoemulsions versus microemulsions: terminology, differences, and similarities. *Soft matter*, *8*(6), 1719-1729. https://doi.org/10.1039/c2sm06903b

McClements, D.J. & Rao, J. (2011). Food-grade nanoemulsions: formulation, fabrication, properties, performance, biological fate, and potential toxicity. Critical Reviews in Food Science and Nutrition, 51(4), 285-330. https://doi.org/10.1080/10408398.2011.559558

Merisko-Liversidge, E., Liversidge, G. G., & Cooper, E. R. (2003). Nanosizing: a formulation approach for poorly-water-soluble compounds. *European journal of pharmaceutical sciences*, *18*(2), 113-120. https://doi.org/10.1016/s0928-0987(02)00251-8.

Mezzomo, N., de Paz, E., Maraschin, M., Martín, Á., Cocero, M. J., & Ferreira, S. R. (2012). Supercritical anti-solvent precipitation of carotenoid fraction from pink shrimp residue: Effect of operational conditions on encapsulation efficiency. *The Journal of Supercritical Fluids*, *66*, 342-349. https://doi.org/10.1016/j.supflu.2011.08.006

Meindl, C., Stranzinger, S., Dzidic, N., Salar-Behzadi, S., Mohr, S., Zimmer, A., & Fröhlich, E. (2015). Permeation of therapeutic drugs in different

formulations across the airway epithelium in vitro. *PloS one*, *10*(8), e0135690. https://doi.org/10.1371/journal.pone.0135690

Menon, V. P., & Sudheer, A. R. (2007). Antioxidant and anti-inflammatory properties of curcumin. *Advances in experimental medicine and biology*, *595*, 105-125. https://doi.org/10.1007/978-0-387-46401-5_3

Miller, D. A., DiNunzio, J. C., Yang, W., McGinity, J. W., & Williams III, R. O. (2008). Enhanced in vivo absorption of itraconazole via stabilization of supersaturation following acidic-to-neutral pH transition. *Drug development and industrial pharmacy*, *34*(8), 890-902. https://doi.org/10.1080/03639040801929273

Miller, J. M., Beig, A., Krieg, B. J., Carr, R. A., Borchardt, T. B., Amidon, G. E., Amidon, G. L., & Dahan, A. (2011). The solubility–permeability interplay: mechanistic modeling and predictive application of the impact of micellar solubilization on intestinal permeation. *Molecular pharmaceutics*, *8*(5), 1848-1856. https://doi.org/10.1021/mp200181v

Miao, L., Liang, Y., Pan, W., Gou, J., Yin, T., Zhang, Y., He, H., & Tang, X. (2019). Effect of supersaturation on the oral bioavailability of paclitaxel/polymer amorphous solid dispersion. *Drug delivery and translational research*, *9*(1), 344-356. https://doi.org/10.1007/s13346-018-0582-9

Mine, Y., & Zhang, J. W. (2003). Surfactants enhance the tight-junction permeability of food allergens in human intestinal epithelial Caco-2 cells. *International archives of allergy and immunology*, *130*(2), 135-142. https://doi.org/doi.org/10.1159/000069009

Modasiya, M., & Patel, V. (2012). Studies on solubility of curcumin. *Int. J. Pharm. Life Sci*, *3*(3), 1490-1497.

Moes, J., Koolen, S., Huitema, A., Schellens, J., Beijnen, J., & Nuijen, B. (2013). Development of an oral solid dispersion formulation for use in low-dose metronomic chemotherapy of paclitaxel. *European Journal of Pharmaceutics and Biopharmaceutics*, *83*(1), 87-94. https://doi.org/10.1016/j.ejpb.2012.09.016

Moneghini, M., De Zordi, N., Solinas, D., Macchiavelli, S., & Princivalle, F. (2010). Characterization of solid dispersions of itraconazole and vitamin E TPGS prepared by microwave technology. *Future medicinal chemistry*, *2*(2), 237-246. https://doi.org/10.4155/fmc.09.166

Mukundan, M., Chacko, M., Annapurna, V., & Krishnaswamy, K. (1993). Effect of turmeric and curcumin on BP-DNA adducts. *Carcinogenesis*, *14*(3), 493-496. https://doi.org/10.1093/carcin/14.3.493

Müller, R. H., Gohla, S., & Keck, C. M. (2011). State of the art of nanocrystals–special features, production, nanotoxicology aspects and intracellular delivery. *European Journal of Pharmaceutics and Biopharmaceutics*, *78*(1), 1-9. https://doi.org/10.1016/jejpb.2011.01.007.

Murugan, P., & Pari, L. (2006). Effect of tetrahydrocurcumin on plasma antioxidants in streptozotocin-nicotinamide induced experimental diabetes. *Journal of basic and clinical physiology and pharmacology*, *17*(4), 231-244. https://doi.org/10.1515/jbcpp.2006.17.4.231.

Mutsuga, M., Chambers, J. K., Uchida, K., Tei, M., Makibuchi, T., Mizorogi, T.,

Takashima, A., & Nakayama, H. (2011). Binding of curcumin to senile plaques and cerebral amyloid angiopathy in the aged brain of various animals and to neurofibrillary tangles in Alzheimers brain. *Journal of Veterinary Medical Science*, 1108250620-1108250620. https://doi.org/10.1292/jvms.11-0307.

Mythri, R. B., Harish, G., Dubey, S. K., Misra, K., & Srinivas Bharath, M. (2011). Glutamoyl diester of the dietary polyphenol curcumin offers improved protection against peroxynitrite-mediated nitrosative stress and damage of brain mitochondria in vitro: implications for Parkinson's disease. *Molecular and cellular biochemistry*, *347*(1), 135-143. https://doi.org/10.1007/s11010-010-0621-4

Nandi, I., Bateson, M., Bari, M., & Joshi, H. N. (2003). Synergistic effect of PEG-400 and cyclodextrin to enhance solubility of progesterone. *AAPS PharmSciTech*, *4*(1), 1-5. https://doi.org/10.1208/pt040101

Narai, A., Arai, S., & Shimizu, M. (1997). Rapid decrease in transepithelial electrical resistance of human intestinal Caco-2 cell monolayers by cytotoxic membrane perturbents. *Toxicology in vitro*, *11*(4), 347-354. https://doi.org/10.1016/S0887-2333(97)00026-X

Newa, M., Bhandari, K. H., Oh, D. H., Kim, Y. R., Sung, J. H., Kim, J. O., Woo, J. S., Choi, H. G., & Yong, C. S. (2008). Enhanced dissolution of ibuprofen using solid dispersion with poloxamer 407. *Archives of pharmacal research*, *31*(11), 1497-1507. https://doi.org/10.1007/s12272-001-2136-8

Negahdari, R., Bohlouli, S., Sharifi, S., Maleki Dizaj, S., Rahbar Saadat, Y., Khezri, K., Jafari, S., Ahmadian, E., Gorbani Jahandizi, N., & Raeesi, S. (2021). Therapeutic benefits of rutin and its nanoformulations. *Phytotherapy*

Research, *35*(4), 1719-1738. https://doi.org/https://doi.org/10.1002/ptr.6904

Nounou, M. M., El-Khordagui, L., Khalafallah, N., & Khalil, S. (2005). Influence of different sugar cryoprotectants on the stability and physico-chemical characteristics of freeze-dried 5-fluorouracil plurilamellar vesicles. *Daru Journal of pharmaceutical sciences*, *13*(4), 133-142.

Okuwaki, M., Takada, T., Iwayanagi, Y., Koh, S., Kariya, Y., Fujii, H., & Suzuki, H. (2007). LXR alpha transactivates mouse organic solute transporter alpha and beta via IR-1 elements shared with FXR. *Pharmaceutical research*, *24*(2), 390-398. https://doi.org/10.1007/s11095-006-9163-6

Onoue, S., Takahashi, H., Kawabata, Y., Seto, Y., Hatanaka, J., Timmermann, B., & Yamada, S. (2010). Formulation design and photochemical studies on nanocrystal solid dispersion of curcumin with improved oral bioavailability. *Journal of pharmaceutical sciences*, *99*(4), 1871-1881. https://doi.org/10.1002/jps.21964.

Overhoff, K. A., Engstrom, J. D., Chen, B., Scherzer, B. D., Milner, T. E., Johnston, K. P., & Williams III, R. O. (2007). Novel ultra-rapid freezing particle engineering process for enhancement of dissolution rates of poorly water-soluble drugs. *European Journal of Pharmaceutics and Biopharmaceutics*, *65*(1), 57-67. https://doi.org/10.1016/j.ejpb.2006.07.012

Orona-Ortiz, A., Velázquez-Moyado, J. A., Pineda-Peña, E. A., Balderas-López, J. L., Tavares Carvalho, J. C., & Navarrete, A. (2021). Effect of the proportion of curcuminoids on the gastroprotective action of Curcuma longa L. in rats. *Natural Product Research*, *35*(11), 1903-1908. https://doi.org/10.1080/14786419.2019.1644504

Overhoff, K. A., Moreno, A., Miller, D. A., Johnston, K. P., & Williams III, R. O. (2007). Solid dispersions of itraconazole and enteric polymers made by ultra-rapid freezing. *International journal of pharmaceutics*, *336*(1), 122-132. https://doi.org/10.1016/j.ijpharm.2006.11.043

Ozeki, T., Yuasa, H., & Kanaya, Y. (2000). Controlled release from solid dispersion composed of poly (ethylene oxide)–Carbopol® interpolymer complex with various cross-linking degrees of Carbopol®. *Journal of Controlled Release*, *63*(3), 287-295. https://doi.org/https://doi.org/10.1016/S0168-3659(99)00202-3

Ozeki, K., Kato, M., Sakurai, Y., Ishigai, M., Kudo, T., & Ito, K. (2015). Evaluation of the appropriate time range for estimating the apparent permeability coefficient (Papp) in a transcellular transport study. *International journal of pharmaceutics*, *495*(2), 963-971. https://doi.org/10.1016/j.ijpharm.2015.09.035.

Pal, S., Choudhuri, T., Chattopadhyay, S., Bhattacharya, A., Datta, G. K., Das, T., & Sa, G. (2001). Mechanisms of curcumin-induced apoptosis of Ehrlichs ascites carcinoma cells. *Biochemical and biophysical research communications*, *288*(3), 658-665. https://doi.org/10.1006/bbrc.2001.5823

Patel, D. S., Sharma, N., Patel, M. C., Patel, B. N., Shrivastav, P. S., & Sanyal, M. (2013). Quantitation of nitrofurantoin in human plasma by liquid chromatography tandem mass spectrometry. *Acta Pharmaceutica*, *63*(2), 141-158. https://doi.org/10.2478/acph-2013-0012

Paolino, D., Vero, A., Cosco, D., Pecora, T. M., Cianciolo, S., Fresta, M., &

Pignatello, R. (2016). Improvement of oral bioavailability of curcumin upon microencapsulation with methacrylic copolymers. *Frontiers in Pharmacology*, *7*, 485. https://doi.org/10.3389/fphar.2016.00485.

Parikh, A., Kathawala, K., Song, Y., Zhou, X.-F., & Garg, S. (2018). Curcumin-loaded self-nanomicellizing solid dispersion system: Part I: Development, optimization, characterization, and oral bioavailability. *Drug delivery and translational research*, *8*(5), 1389-1405. https://doi.org/10.1007/s13346-018-0543-3

Parikh, A., Kathawala, K., Tan, C. C., Garg, S., & Zhou, X.-F. (2016). Development of a novel oral delivery system of edaravone for enhancing bioavailability. *International journal of pharmaceutics*, *515*(1-2), 490-500. https://doi.org/10.1016/j.ijpharm.2016.10.052.

Paarakh, M. P., Jose, P. A., Setty, C., & Christoper, G. (2018). Release kinetics–concepts and applications. *Int. J. Pharm. Res. Technol*, *8*(1), 12-20.

Parsamanesh, N., Moossavi, M., Bahrami, A., Butler, A. E., & Sahebkar, A. (2018). Therapeutic potential of curcumin in diabetic complications. *Pharmacological Research*, *136*, 181-193. https://doi.org/10.1016/j.phrs.2018.09.012

Patil, S., Choudhary, B., Rathore, A., Roy, K., & Mahadik, K. (2015). Enhanced oral bioavailability and anticancer activity of novel curcumin loaded mixed micelles in human lung cancer cells. *Phytomedicine*, *22*(12), 1103-1111. https://doi.org/10.1016/j.phymed.2015.08.006.

Pan, X.-m., Li, J., Gan, R., & Hu, X.-n. (2015). Preparation and in vitro

evaluation of enteric-coated tablets of rosiglitazone sodium. *Saudi Pharmaceutical Journal*, *23*(5), 581-586. https://doi.org/10.1016/j.jsps.2015.02.018

Patil, V., Dandekar, P., Patravale, V., & Thorat, B. (2010). Freeze drying: Potential for powdered nanoparticulate product. *Drying Technology*, *28*(5), 624-635. https://doi.org/10.1080/07373931003788692

Passerini, N., Albertini, B., González-Rodríguez, M. L., Cavallari, C., & Rodriguez, L. (2002). Preparation and characterisation of ibuprofen–poloxamer 188 granules obtained by melt granulation. *European journal of pharmaceutical sciences*, *15*(1), 71-78. https://doi.org/10.1016/s0928-0987(01)00210-x

Paudel, A., Worku, Z. A., Meeus, J., Guns, S., & Van den Mooter, G. (2013). Manufacturing of solid dispersions of poorly water soluble drugs by spray drying: formulation and process considerations. *International journal of pharmaceutics*, *453*(1), 253-284. https://doi.org/10.1016/j.ijpharm.2012.07.015

Paul, S., Islam, M. N., Ali, M. A., Barman, R. K., Wahed, M. I. I., & Rahman, B. M. (2019). Improvement of Dissolution Rate of Gliclazide Using Solid Dispersions with Aerosil 380 and Its Effect on Alloxan Induced Diabetic Rats. *Pharmacology & Pharmacy*, *10*(08), 365. https://doi.org/10.4236/pp.2019.108030

Parmar, J., Singh, D., Lohade, A., Hegde, D. D., Soni, P., Samad, A., & Menon, M. D. (2011). Inhalational system for etoposide liposomes: Formulation development and in vitro deposition. *Indian Journal of Pharmaceutical Sciences*, *73*(6), 656. https://doi.org/10.4103/0250-

474X.100240

Parvinzadeh, M., Moradian, S., Rashidi, A., & Yazdanshenas, M.-E. (2010). Surface characterization of polyethylene terephthalate/silica nanocomposites. *Applied Surface Science*, *256*(9), 2792-2802. https://doi.org/10.1016/j.apsusc.2009.11.030

Pawar, Y. B., Shete, G., Popat, D., & Bansal, A. K. (2012). Phase behavior and oral bioavailability of amorphous Curcumin. *European journal of pharmaceutical sciences*, *47*(1), 56-64. https://doi.org/10.1016/j.ejps.2012.05.003

Pade, V., & Stavchansky, S. (1998). Link between drug absorption solubility and permeability measurements in Caco-2 cells. *Journal of pharmaceutical sciences*, *87*(12), 1604-1607. https://doi.org/https://doi.org/10.1021/js980111k

Peters, W. H., & Roelofs, H. M. (1989). Time-dependent activity and expression of glutathione S-transferases in the human colon adenocarcinoma cell line Caco-2. *Biochemical Journal*, *264*(2), 613-616. https://doi.org/10.1042/bj2640613

Petri, N., Tannergren, C., Rungstad, D., & Lennernäs, H. (2004). Transport characteristics of fexofenadine in the Caco-2 cell model. *Pharmaceutical research*, *21*(8), 1398-1404. https://doi.org/10.1023/b:pham.0000036913.90332.b1

Peng, S., Li, Z., Zou, L., Liu, W., Liu, C., & McClements, D. J. (2018). Enhancement of curcumin bioavailability by encapsulation in sophorolipid-coated nanoparticles: An in vitro and in vivo study. *Journal of agricultural and*

food chemistry, *66*(6), 1488-1497. https://doi.org/10.1021/acs.jafc.7b05478.

Peng, S., Zou, L., Liu, W., Li, Z., Liu, W., Hu, X., Chen, X., & Liu, C. (2017). Hybrid liposomes composed of amphiphilic chitosan and phospholipid: Preparation, stability and bioavailability as a carrier for curcumin. *Carbohydrate polymers*, *156*, 322-332. https://doi.org/10.1016/j.carbpol.2016.09.060.

Peram, M. R., Jalalpure, S. S., Palkar, M. B., & Diwan, P. V. (2017). Stability studies of pure and mixture form of curcuminoids by reverse phase-HPLC method under various experimental stress conditions. *Food science and biotechnology*, *26*(3), 591-602. https://doi.org/10.1007/s10068-017-0087-1

Perkins, S., Verschoyle, R. D., Hill, K., Parveen, I., Threadgill, M. D., Sharma, R. A., Williams, M. L., Steward, W. P., & Gescher, A. J. (2002). Chemopreventive efficacy and pharmacokinetics of curcumin in the min/+ mouse, a model of familial adenomatous polyposis. *Cancer Epidemiology Biomarkers & Prevention*, *11*(6), 535-540.

Petchsomrit, A., Sermkaew, N., & Wiwattanapatapee, R. (2016). Hydroxypropylmethyl cellulose-based sponges loaded self-microemulsifying curcumin: preparation, characterization, and in vivo oral absorption studies. *Journal of Applied Polymer Science*, *133*(6). https://doi.org/10.1002/app.42966

Pfeiffer, E., Hoehle, S. I., Walch, S. G., Riess, A., Sólyom, A. M., & Metzler, M. (2007). Curcuminoids form reactive glucuronides in vitro. *Journal of agricultural and food chemistry*, *55*(2), 538-544. https://doi.org/10.1021/jf0623283.

Pinto, J. M. O., Leão, A. F., Riekes, M. K., França, M. T., & Stulzer, H. K. (2018). HPMCAS as an effective precipitation inhibitor in amorphous solid dispersions of the poorly soluble drug candesartan cilexetil. *Carbohydrate polymers*, *184*, 199-206. https://doi.org/10.1016/j.carbpol.2017.12.052

Poelma, F., Breäs, R., Tukker, J., & Crommelin, D. (1991). Intestinal absorption of drugs. The influence of mixed micelles on on the disappearance kinetics of drugs from the small intestine of the rat. *Journal of pharmacy and pharmacology*, *43*(5), 317-324. https://doi.org/10.1111/j.2042-7158.1991.tb06697.x

Prasad, S., & Tyagi, A. K. (2015). Curcumin and its analogues: a potential natural compound against HIV infection and AIDS. *Food & function*, *6*(11), 3412-3419. https://doi.org/10.1039/C5FO00485C

Prasad, S., Tyagi, A. K., & Aggarwal, B. B. (2014). Recent developments in delivery, bioavailability, absorption and metabolism of curcumin: the golden pigment from golden spice. *Cancer research and treatment: official journal of Korean Cancer Association*, *46*(1), 2-18. https://doi.org/10.4143/crt.2014.46.1.2.

Prime-Chapman, H. M., Fearn, R. A., Cooper, A. E., Moore, V., & Hirst, B. H. (2004). Differential multidrug resistance-associated protein 1 through 6 isoform expression and function in human intestinal epithelial Caco-2 cells. *Journal of Pharmacology and Experimental Therapeutics*, *311*(2), 476-484. https://doi.org/10.1124/jpet.104.068775

Priyadarsini, K. I. (2013). Chemical and structural features influencing the

biological activity of curcumin. *Current pharmaceutical design*, *19*(11), 2093-2100. https://doi.org/10.2174/1381612811319110010

Priyadarsini, K. I. (2014). The chemistry of curcumin: from extraction to therapeutic agent. *Molecules*, *19*(12), 20091-20112. https://doi.org/10.3390/molecules191220091

Pugliese, A., Toresco, M., McNamara, D., Iuga, D., Abraham, A., Tobyn, M., Hawarden, L. E., & Blanc, F. (2021). Drug–polymer interactions in acetaminophen/hydroxypropylmethylcellulose acetyl succinate amorphous solid dispersions revealed by multidimensional multinuclear solid-state NMR spectroscopy. *Molecular pharmaceutics*, *18*(9), 3519-3531. https://doi.org/10.1021/acs.molpharmaceut.1c00427

Pudipeddi, M., & Serajuddin, A. T. (2005). Trends in solubility of polymorphs. Journal of pharmaceutical sciences, 94(5), 929-939. https://doi.org/10.1002/jps.20302

PubChem. (2020b). *Rutin*. Retrieved 25th August from https://pubchem.ncbi.nlm.nih.gov/compound/Rutin

PubChem. (2020e). *Niclosamide*. Retrieved 25th August from https://pubchem.ncbi.nlm.nih.gov/compound/Niclosamide

PubChem. (2022a). *Omeprazole*. PubChem. Retrieved 21st August from https://pubchem.ncbi.nlm.nih.gov/compound/omeprazole

Pubchem. (2022c). *Quinine*. Retrieved 25th August from https://pubchem.ncbi.nlm.nih.gov/compound/Quinine

PubChem. (2022d). *Terbinfaine*. Retrieved 25th August from https://pubchem.ncbi.nlm.nih.gov/compound/Terbinafine

PubChem. (2022f). *Quercetin*. Retrieved 25th August from https://pubchem.ncbi.nlm.nih.gov/compound/Quercetin

PubChem. (2022g). *Nitrofurantoin*. Retrieved 25th August from https://pubchem.ncbi.nlm.nih.gov/compound/Nitrofurantoin

Purpura, M., Lowery, R. P., Wilson, J. M., Mannan, H., Münch, G., & Razmovski-Naumovski, V. (2018). Analysis of different innovative formulations of curcumin for improved relative oral bioavailability in human subjects. *European journal of nutrition*, *57*(3), 929-938. https://doi.org/10.1007/s00394-016-1376-9

Qian, K., Stella, L., Jones, D. S., Andrews, G. P., Du, H., & Tian, Y. (2021). Drug-rich phases induced by amorphous solid dispersion: arbitrary or intentional goal in oral drug delivery? *Pharmaceutics*, *13*(6), 889. https://doi.org/10.3390/pharmaceutics13060889

Ravindranath, V., & Chandrasekhara, N. (1981). Metabolism of curcumn-studies with [3H] curcumin. *Toxicology*, *22*(4), 337-344. https://doi.org/10.1016/0300-483x(81)90027-5.

Ray, B., Bisht, S., Maitra, A., Maitra, A., & Lahiri, D. K. (2011). Neuroprotective and neurorescue effects of a novel polymeric nanoparticle formulation of curcumin (NanoCurc™) in the neuronal cell culture and animal model: implications for Alzheimers di sease. *Journal of Alzheimers disease* , *23*(1),

61-77. https://doi.org/10.3233/jad-2010-101374.

Rahman, M., Ahmad, S., Tarabokija, J., Parker, N., & Bilgili, E. (2020). Spray-dried amorphous solid dispersions of griseofulvin in HPC/Soluplus/SDS: elucidating the multifaceted impact of sds as a minor component. *Pharmaceutics*, *12*(3), 197. https://doi.org/doi:10.3390/pharmaceutics12030197

Rangel-Yagui, C. O., Pessoa Jr, A., & Tavares, L. C. (2005). Micellar solubilization of drugs. *J. Pharm. Pharm. Sci*, *8*(2), 147-163.

Rampino, A., Borgogna, M., Blasi, P., Bellich, B., & Cesàro, A. (2013). Chitosan nanoparticles: Preparation, size evolution and stability. *International journal of pharmaceutics*, *455*(1-2), 219-228. https://doi.org/10.1016/j.ijpharm.2013.07.034

Rani, S., Mishra, S., Sharma, M., Nandy, A., & Mozumdar, S. (2020). Solubility and stability enhancement of curcumin in Soluplus® polymeric micelles: a spectroscopic study. *Journal of Dispersion Science and Technology*, *41*(4), 523-536. https://doi.org/10.1080/01932691.2019.1592687

Rahman, M. S., Yoshida, N., Tsuboi, H., Keila, T., Sovannarith, T., Kiet, H. B., Dararth, E., Zin, T., Tanimoto, T., & Kimura, K. (2017). Erroneous formulation of delayed-release omeprazole capsules: alert for importing countries. *BMC Pharmacology and Toxicology*, *18*(1), 1-11. https://doi.org/10.1186/s40360-017-0138-5

Rashidinejad, A., Jameson, G. B., & Singh, H. (2022). The Effect of pH and Sodium Caseinate on the Aqueous Solubility, Stability, and Crystallinity of

Rutin towards Concentrated Colloidally Stable Particles for the Incorporation into Functional Foods. *Molecules*, *27*(2), 534. https://doi.org/10.3390/molecules27020534

Rasouli, H., Farzaei, M. H., & Khodarahmi, R. (2017). Polyphenols and their benefits: A review. *International Journal of Food Properties*, *20*(sup2), 1700-1741. https://doi.org/10.1080/10942912.2017.1354017

Reddy, R. C., Vatsala, P. G., Keshamouni, V. G., Padmanaban, G., & Rangarajan, P. N. (2005). Curcumin for malaria therapy. *Biochemical and biophysical research communications*, *326*(2), 472-474. https://doi.org/10.1016/j.bbrc.2004.11.051

Rejman, J., Oberle, V., Zuhorn, I. S., & Hoekstra, D. (2004). Size-dependent internalization of particles via the pathways of clathrin-and caveolae-mediated endocytosis. *Biochemical Journal*, *377*(1), 159-169. https://doi.org/10.1042/BJ20031253

Righeschi, C., Bergonzi, M. C., Isacchi, B., Bazzicalupi, C., Gratteri, P., & Bilia, A. R. (2016). Enhanced curcumin permeability by SLN formulation: The PAMPA approach. *LWT-Food Science and Technology*, *66*, 475-483. https://doi.org/10.1016/j.lwt.2015.11.008.

Riss, T. L., Moravec, R. A., Niles, A. L., Duellman, S., Benink, H. A., Worzella, T. J., & Minor, L. (2016). Cell viability assays. *Assay Guidance Manual*.

Riva, A., Ronchi, M., Petrangolini, G., Bosisio, S., & Allegrini, P. (2019). Improved oral absorption of quercetin from quercetin phytosome®, a new delivery system based on food grade lecithin. *European journal of drug*

metabolism and pharmacokinetics, *44*(2), 169-177. https://doi.org/10.1007/s13318-018-0517-3

Rogers, T. L., Johnston, K. P., & Williams III, R. O. (2003). Physical stability of micronized powders produced by spray-freezing into liquid (SFL) to enhance the dissolution of an insoluble drug. *Pharmaceutical Development and Technology*, *8*(2), 187-197. https://doi.org/10.1081/PDT-120018489

Rong, W.-T., Lu, Y.-P., Tao, Q., Guo, M., Lu, Y., Ren, Y., & Yu, S.-Q. (2014). Hydroxypropyl-sulfobutyl-β-cyclodextrin improves the oral bioavailability of edaravone by modulating drug efflux pump of enterocytes. *Journal of pharmaceutical sciences*, *103*(2), 730-742. https://doi.org/10.1002/jps.23807

Rothwell, J. A., Day, A. J., & Morgan, M. R. (2005). Experimental determination of octanol− water partition coefficients of quercetin and related flavonoids. *Journal of agricultural and food chemistry*, *53*(11), 4355-4360. https://doi.org/https://doi.org/10.1021/jf0483669

Ruby, A. J., Kuttan, G., Babu, K. D., Rajasekharan, K., & Kuttan, R. (1995). Anti-tumour and antioxidant activity of natural curcuminoids. *Cancer letters*, *94*(1), 79-83. https://doi.org/10.1016/0304-3835(95)03827-j

Saeidinia, A., Keihanian, F., Butler, A. E., Bagheri, R. K., Atkin, S. L., & Sahebkar, A. (2018). Curcumin in heart failure: a choice for complementary therapy? *Pharmacological Research*, *131*, 112-119. https://doi.org/10.1016/j.phrs.2018.03.009.

Sambuy, Y., De Angelis, I., Ranaldi, G., Scarino, M., Stammati, A., & Zucco, F. (2005). The Caco-2 cell line as a model of the intestinal barrier: influence of cell and culture-related factors on Caco-2 cell functional characteristics. *Cell*

biology and toxicology, *21*(1), 1-26. https://doi.org/10.1007/s10565-005-0085-6

Sandur, S. K., Pandey, M. K., Sung, B., Ahn, K. S., Murakami, A., Sethi, G., Limtrakul, P., Badmaev, V., & Aggarwal, B. B. (2007). Curcumin, demethoxycurcumin, bisdemethoxycurcumin, tetrahydrocurcumin and turmerones differentially regulate anti-inflammatory and anti-proliferative responses through a ROS-independent mechanism. *Carcinogenesis*, *28*(8), 1765-1773. https://doi.org/10.1093/carcin/bgm123.

Sanphui, P., Goud, N. R., Khandavilli, U. R., Bhanoth, S., & Nangia, A. (2011). New polymorphs of curcumin. Chemical Communications, 47(17), 5013-5015. https://doi.org/10.1039/c1cc10204d

Saerens, L., Dierickx, L., Lenain, B., Vervaet, C., Remon, J. P., & De Beer, T. (2011). Raman spectroscopy for the in-line polymer–drug quantification and solid state characterization during a pharmaceutical hot-melt extrusion process. *European Journal of Pharmaceutics and Biopharmaceutics*, *77*(1), 158-163. https://doi.org/10.1016/j.ejpb.2010.09.015

Saffoon, N., Uddin, R., Huda, N. H., & Sutradhar, K. B. (2011). Enhancement of oral bioavailability and solid dispersion: a review. *Journal of Applied Pharmaceutical Science*(Issue), 13-20.

Saharan, V., Kukkar, V., Kataria, M., Gera, M., & Choudhury, P. K. (2009). Dissolution enhancement of drugs. Part I: technologies and effect of carriers. *International Journal of Health Research*, *2*(2). https://doi.org/10.4314/ijhr.v2i2.55401

Salehi, N., Kuminek, G., Al-Gousous, J., Sperry, D. C., Greenwood, D. E., Waltz, N. M., Amidon, G. L., Ziff, R. M., & Amidon, G. E. (2021). Improving Dissolution Behavior and Oral Absorption of Drugs with pH-Dependent Solubility Using pH Modifiers: A Physiologically Realistic Mass Transport Analysis. *Molecular pharmaceutics*, *18*(9), 3326-3341. https://doi.org/10.1021/acs.molpharmaceut.1c00262

Sarabu, S., Kallakunta, V. R., Bandari, S., Batra, A., Bi, V., Durig, T., Zhang, F., & Repka, M. A. (2020). Hypromellose acetate succinate based amorphous solid dispersions via hot melt extrusion: Effect of drug physicochemical properties. *Carbohydrate polymers*, *233*, 115828. https://doi.org/10.1016/j.carbpol.2020.115828

Sareen, S., Mathew, G., & Joseph, L. (2012). Improvement in solubility of poor water-soluble drugs by solid dispersion. *International journal of pharmaceutical investigation*, *2*(1), 12. https://doi.org/10.4103/2230-973X.96921

Savjani, K. T., Gajjar, A. K., & Savjani, J. K. (2012). Drug solubility: importance and enhancement techniques. *International Scholarly Research Notices*, *2012*. https://doi.org/10.5402/2012/195727

Sai, Y., Kaneko, Y., Ito, S., Mitsuoka, K., Kato, Y., Tamai, I., Artursson, P., & Tsuji, A. (2006). Predominant contribution of organic anion transporting polypeptide OATP-B (OATP2B1) to apical uptake of estrone-3-sulfate by human intestinal Caco-2 cells. *Drug metabolism and disposition*, *34*(8), 1423-1431. https://doi.org/10.1124/dmd.106.009530

Saito, H., Motohashi, H., Mukai, M., & Inui, K.-i. (1997). Cloning and

characterization of a pH-sensing regulatory factor that modulates transport activity of the human H+/peptide cotransporter, PEPT1. *Biochemical and biophysical research communications*, *237*(3), 577-582. https://doi.org/10.1006/bbrc.1997.7129

Salama, N. N., Eddington, N. D., & Fasano, A. (2006). Tight junction modulation and its relationship to drug delivery. *Advanced drug delivery reviews*, *58*(1), 15-28. https://doi.org/10.1016/j.addr.2006.01.003

Salehi, B., Machin, L., Monzote, L., Sharifi-Rad, J., Ezzat, S. M., Salem, M. A., Merghany, R. M., El Mahdy, N. M., Kılıç, C. S., & Sytar, O. (2020). Therapeutic potential of quercetin: new insights and perspectives for human health. *Acs Omega*, *5*(20), 11849-11872. https://doi.org/10.1021/acsomega.0c01818

Sayyar, Z., & Jafarizadeh-Malmiri, H. (2019). Temperature effects on thermodynamic parameters and solubility of curcumin O/W nanodispersions using different thermodynamic models. *International Journal of Food Engineering*, *15*(1-2). https://doi.org/10.1515/ijfe-2018-0311

Schweizer, M. T., Haugk, K., McKiernan, J. S., Gulati, R., Cheng, H. H., Maes, J. L., Dumpit, R. F., Nelson, P. S., Montgomery, B., & McCune, J. S. (2018). A phase I study of niclosamide in combination with enzalutamide in men with castration-resistant prostate cancer. *PloS one*, *13*(6), e0198389. https://doi.org/10.1371/journal.pone.0198389

Schiborr, C., Kocher, A., Behnam, D., Jandasek, J., Toelstede, S., & Frank, J. (2014). The oral bioavailability of curcumin from micronized powder and liquid micelles is significantly increased in healthy humans and differs between sexes. *Molecular nutrition & food research*, *58*(3), 516-527.

https://doi.org/10.1002/mnfr.201300724

Schulman, J. H., Stoeckenius, W., & Prince, L. M. (1959). Mechanism of formation and structure of microemulsions by electron microscopy. Journal of Physical Chemistry, 63(9), 1677-1680. https://doi.org/10.1021/j150580a027

Sekiguchi, K., & Obi, N. (1961). Studies on Absorption of Eutectic Mixture. I. A Comparison of the Behavior of Eutectic Mixture of Sulfathiazole and that of Ordinary Sulfathiazole in Man. *Chemical and Pharmaceutical Bulletin*, *9*(11), 866-872.https://doi.org/10.1248/cpb.9.866

Serajuddin, A. T. (2007). Salt formation to improve drug solubility. *Advanced drug delivery reviews*, *59*(7), 603-616. https://doi.org/10.1016/j.addr.2007.05.010

Seo, A., Holm, P., Kristensen, H. G., & Schæfer, T. (2003). The preparation of agglomerates containing solid dispersions of diazepam by melt agglomeration in a high shear mixer. *International journal of pharmaceutics*, *259*(1-2), 161-171. https://doi.org/10.1016/S0378-5173(03)00228-X

Serajuddin, A. T. (1999). Solid dispersion of poorly water-soluble drugs: Early promises, subsequent problems, and recent breakthroughs. *Journal of pharmaceutical sciences*, *88*(10), 1058-1066. https://doi.org/10.1021/js980403l

Sertsou, G., Butler, J., Scott, A., Hempenstall, J., & Rades, T. (2002). Factors affecting incorporation of drug into solid solution with HPMCP during solvent change co-precipitation. *International journal of pharmaceutics*, *245*(1-2), 99-108. https://doi.org/10.1016/S0378-5173(02)00331-9

Sethia, S., & Squillante, E. (2004). Solid dispersion of carbamazepine in PVP K30 by conventional solvent evaporation and supercritical methods. *International journal of pharmaceutics*, *272*(1-2), 1-10. https://doi.org/10.1016/j.ijpharm.2003.11.025

Senft, C., Polacin, M., Priester, M., Seifert, V., Kögel, D., & Weissenberger, J. (2010). The nontoxic natural compound Curcumin exerts anti-proliferative, anti-migratory, and anti-invasive properties against malignant gliomas. *BMC cancer*, *10*(1), 1-8. https://doi.org/10.1186/1471-2407-10-491.

Seo, S.-W., Han, H.-K., Chun, M.-K., & Choi, H.-K. (2012). Preparation and pharmacokinetic evaluation of curcumin solid dispersion using Solutol® HS15 as a carrier. *International journal of pharmaceutics*, *424*(1-2), 18-25. https://doi.org/10.1016/j.ijpharm.2011.12.051.

Seyfoddin, A., Shaw, J., & Al-Kassas, R. (2010). Solid lipid nanoparticles for ocular drug delivery. *Drug Delivery*, *17*(7), 467-489. https://doi.org/10.3109/10717544.2010.483257

Sharma, O. (1976). Antioxidant activity of curcumin and related compounds. *Biochemical pharmacology*, *25*(15), 1811-1812. https://doi.org/10.1016/0006-2952(76)90421-4.

Sharma, S., Ali, A., Ali, J., Sahni, J. K., & Baboota, S. (2013). Rutin: therapeutic potential and recent advances in drug delivery. *Expert opinion on investigational drugs*, *22*(8), 1063-1079. https://doi.org/10.1517/13543784.2013.805744

Sharma, R. A., Euden, S. A., Platton, S. L., Cooke, D. N., Shafayat, A., Hewitt, H. R., Marczylo, T. H., Morgan, B., Hemingway, D., & Plummer, S. M. (2004). Phase I clinical trial of oral curcumin: biomarkers of systemic activity and compliance. *Clinical Cancer Research*, *10*(20), 6847-6854. https://doi.org/10.1158/1078-0432.CCR-04-0744

Shoba, G., Joy, D., Joseph, T., Majeed, M., Rajendran, R., & Srinivas, P. (1998). Influence of piperine on the pharmacokinetics of curcumin in animals and human volunteers. *Planta medica*, *64*(04), 353-356. https://doi.org/10.1055/s-2006-957450

Shukla, M., Jaiswal, S., Sharma, A., Srivastava, P. K., Arya, A., Dwivedi, A. K., & Lal, J. (2017). A combination of complexation and self-nanoemulsifying drug delivery system for enhancing oral bioavailability and anticancer efficacy of curcumin. *Drug development and industrial pharmacy*, *43*(5), 847-861. https://doi.org/10.1080/03639045.2016.1239732.

Shah, N., Iyer, R. M., Mair, H.-J., Choi, D., Tian, H., Diodone, R., Fahnrich, K., Pabst-Ravot, A., Tang, K., & Scheubel, E. (2013). Improved human bioavailability of vemurafenib, a practically insoluble drug, using an amorphous polymer-stabilized solid dispersion prepared by a solvent-controlled coprecipitation process. *Journal of pharmaceutical sciences*, *102*(3), 967-981. https://doi.org/10.1002/jps.23425

Shamma, R. N., & Basha, M. (2013). Soluplus®: a novel polymeric solubilizer for optimization of carvedilol solid dispersions: formulation design and effect of method of preparation. *Powder technology*, *237*, 406-414. https://doi.org/10.1016/j.powtec.2012.12.038

Shi, N.-Q., Lai, H.-W., Zhang, Y., Feng, B., Xiao, X., Zhang, H.-M., Li, Z.-Q., & Qi, X.-R. (2018). On the inherent properties of Soluplus and its application in ibuprofen solid dispersions generated by microwave-quench cooling technology. *Pharmaceutical Development and Technology*, *23*(6), 573-586. https://doi.org/10.1080/10837450.2016.1256409

Singh, R., & Lillard Jr, J. W. (2009). Nanoparticle-based targeted drug delivery. *Experimental and molecular pathology*, *86*(3), 215-223. https://doi.org/10.1016/j.yexmp.2008.12.004.

Siviero, A., Gallo, E., Maggini, V., Gori, L., Mugelli, A., Firenzuoli, F., & Vannacci, A. (2015). Curcumin, a golden spice with a low bioavailability. *Journal of Herbal Medicine*, *5*(2), 57-70. https://doi.org/10.1016/j.hermed.2015.03.001

Siow, C. R. S., Wan Sia Heng, P., & Chan, L. W. (2016). Application of freeze-drying in the development of oral drug delivery systems. *Expert opinion on drug delivery*, *13*(11), 1595-1608. https://doi.org/10.1080/17425247.2016.1198767

Smit, C., Van Swaaij, R., Donker, H., Petit, A., Kessels, W., & Van de Sanden, M. (2003). Determining the material structure of microcrystalline silicon from Raman spectra. *Journal of applied physics*, *94*(5), 3582-3588. https://doi.org/doi.org/10.1063/1.1596364

Solanki, N. G., Lam, K., Tahsin, M., Gumaste, S. G., Shah, A. V., & Serajuddin, A. T. (2019). Effects of surfactants on itraconazole-HPMCAS solid dispersion prepared by hot-melt extrusion I: Miscibility and drug release.

Journal of pharmaceutical sciences, *108*(4), 1453-1465. https://doi.org/10.1016/j.xphs.2018.10.058

Solans, C., Izquierdo, P., Nolla, J., Azemar, N. & Garcia-Celma, M.J. (2005). Nano-emulsions. Current Opinion in Colloid & Interface Science, 10(3-4), 102-110. https://doi.org/10.1016/j.cocis.2005.06.004

Song, I.-S., Cha, J.-S., & Choi, M.-K. (2016). Characterization, in vivo and in vitro evaluation of solid dispersion of curcumin containing d-α-Tocopheryl polyethylene glycol 1000 succinate and mannitol. *Molecules*, *21*(10), 1386. https://doi.org/10.3390/molecules21101386

Srimal, R., & Dhawan, B. (1973). Pharmacology of diferuloyl methane (curcumin), a non-steroidal anti-inflammatory agent. *Journal of pharmacy and pharmacology*, *25*(6), 447-452. https://doi.org/10.1111/j.2042-7158.1973.tb09131.x

Stippler, E., Kopp, S., & Dressman, J. (2004). Comparison of US Pharmacopeia simulated intestinal fluid TS (without pancreatin) and phosphate standard buffer pH 6.8, TS of the International Pharmacopoeia with respect to their use in in vitro dissolution testing. *Dissolution Technologies*, *11*(2), 6-11. https://doi.org/10.14227/DT110204P6

Strauch, S., Dressman, J. B., Shah, V. P., Kopp, S., Polli, J. E., & Barends, D. M. (2012). Biowaiver monographs for immediate-release solid oral dosage forms: quinine sulfate. *Journal of pharmaceutical sciences*, *101*(2), 499-508. https://doi.org/10.1002/jps.22810

Shingala, M. C., & Rajyaguru, A. (2015). Comparison of post hoc tests for

unequal variance. *International Journal of New Technologies in Science and Engineering*, *2*(5), 22-33.

Sigma-Aldrich. (2022). *Poly(ethylene glycol)400*. Retrieved 21st September from https://www.sigmaaldrich.com/GB/en/product/sial/81170

Song, Y., Cong, Y., Wang, B., & Zhang, N. (2020). Applications of Fourier transform infrared spectroscopy to pharmaceutical preparations. *Expert opinion on drug delivery*, *17*(4), 551-571. https://doi.org/10.1080/17425247.2020.1737671

Sparreboom, A., Van Asperen, J., Mayer, U., Schinkel, A. H., Smit, J. W., Meijer, D. K., Borst, P., Nooijen, W. J., Beijnen, J. H., & Van Tellingen, O. (1997). Limited oral bioavailability and active epithelial excretion of paclitaxel (Taxol) caused by P-glycoprotein in the intestine. *Proceedings of the National Academy of Sciences*, *94*(5), 2031-2035. https://doi.org/10.1073/pnas.94.5.2031

Stetefeld, J., McKenna, S. A., & Patel, T. R. (2016). Dynamic light scattering: a practical guide and applications in biomedical sciences. *Biophysical reviews*, *8*(4), 409-427. https://doi.org/DOI10.1007/s12551-016-0218-6

Srinivasan, B., Kolli, A. R., Esch, M. B., Abaci, H. E., Shuler, M. L., & Hickman, J. J. (2015). TEER measurement techniques for in vitro barrier model systems. *SLAS Technology*, *20*(2), 107-126. https://doi.org/https://doi.org/10.1177/2211068214561025

Stephens, R. H., ONeill, C. A., Warhurst, A., Carlson, G. L., Rowland, M., & Warhurst, G. (2001). Kinetic profiling of P-glycoprotein-mediated drug efflux in

rat and human intestinal epithelia. *Journal of Pharmacology and Experimental Therapeutics*, *296*(2), 584-591.

Steensma, A., Noteborn, H. P., & Kuiper, H. A. (2004). Comparison of Caco-2, IEC-18 and HCEC cell lines as a model for intestinal absorption of genistein, daidzein and their glycosides. *Environmental Toxicology and Pharmacology*, *16*(3), 131-139. https://doi.org/10.1016/j.etap.2003.11.008

Stulzer, H., Tagliari, M., Cruz, A., Silva, M., & Laranjeira, M. (2008). Compatibility studies between piroxicam and pharmaceutical excipients used in solid dosage forms. *Pharmaceutical Chemistry Journal*, *42*(4), 215-219. https://doi.org/10.1007/s11094-008-0091-0

Sugiyama, Y., Kawakishi, S., & Osawa, T. (1996). Involvement of the β-diketone moiety in the antioxidative mechanism of tetrahydrocurcumin. *Biochemical pharmacology*, *52*(4), 519-525. https://doi.org/10.1016/0006-2952(96)00302-4.

Sun, J., Zhao, Y., & Hu, J. (2013). Curcumin inhibits imiquimod-induced psoriasis-like inflammation by inhibiting IL-1beta and IL-6 production in mice. *PloS one*, *8*(6), e67078. https://doi.org/10.1371/journal.pone.0067078.

Sun, H., Chow, E. C., Liu, S., Du, Y., & Pang, K. S. (2008). The Caco-2 cell monolayer: usefulness and limitations. *Expert opinion on drug metabolism & toxicology*, *4*(4), 395-411. https://doi.org/10.1517/17425255.4.4.395

Suresh, K., & Nangia, A. (2018). Curcumin: Pharmaceutical solids as a platform to improve solubility and bioavailability. *CrystEngComm*, *20*(24), 3277-3296. https://doi.org/10.1039/C8CE00469B.

Tanaka, N., Imai, K., Okimoto, K., Ueda, S., Tokunaga, Y., Ibuki, R., Higaki, K., & Kimura, T. (2006). Development of novel sustained-release system, disintegration-controlled matrix tablet (DCMT) with solid dispersion granules of nilvadipine (II): in vivo evaluation. *Journal of Controlled Release*, *112*(1), 51-56. https://doi.org/10.1016/j.jconrel.2006.01.020

Tang, X. C., & Pikal, M. J. (2004). Design of freeze-drying processes for pharmaceuticals: practical advice. *Pharmaceutical research*, *21*(2), 191-200. https://doi.org/10.1023/B:PHAM.0000016234.73023.75

Tanida, S., Kurokawa, T., Sato, H., Kadota, K., & Tozuka, Y. (2016). Evaluation of the micellization mechanism of an amphipathic graft copolymer with enhanced solubility of ipriflavone. *Chemical and Pharmaceutical Bulletin*, *64*(1), 68-72. https://doi.org/10.1248/cpb.c15-00655

Tanno, F., Nishiyama, Y., Kokubo, H., & Obara, S. (2004). Evaluation of hypromellose acetate succinate (HPMCAS) as a carrier in solid dispersions. *Drug development and industrial pharmacy*, *30*(1), 9-17. https://doi.org/10.1081/DDC-120027506

Taylor, L. S., & Zografi, G. (1997). Spectroscopic characterization of interactions between PVP and indomethacin in amorphous molecular dispersions. *Pharmaceutical research*, *14*(12), 1691-1698. https://doi.org/10.1023/a:1012167410376

Tamai, I., Takanaga, H., Ogihara, T., Higashida, H., Maeda, H., Sai, Y., & Tsuji, A. (1995). Participation of a proton-cotransporter, MCT1, in the intestinal transport of monocarboxylic acids. *Biochemical and biophysical research*

communications, *214*(2), 482-489. https://doi.org/10.1006/bbrc.1995.2312

Teixeira, C., Mendonça, L., Bergamaschi, M., Queiroz, R. H. C., Souza, G. E. P. d., Antunes, L. M. G., & Freitas, L. A. P. d. (2016). Microparticles containing curcumin solid dispersion: stability, bioavailability and anti-inflammatory activity. *AAPS PharmSciTech*, *17*(2), 252-261. https://doi.org/10.1208/s12249-015-0337-6.

Tekade, A. R., & Yadav, J. N. (2020). A review on solid dispersion and carriers used therein for solubility enhancement of poorly water soluble drugs. *Advanced pharmaceutical bulletin*, *10*(3), 359. https://doi.org/10.34172/apb.2020.044

Techbifarm. (2020). *Nacumin*. Retrieved 29 August from http://www.techbifarm.com.vn/nacumin

Teja, S. B., Patil, S. P., Shete, G., Patel, S., & Bansal, A. K. (2016). Drug-excipient behavior in polymeric amorphous solid dispersions. *Journal of Excipients and Food Chemicals*, *4*(3), 1048.

Thapa, R. K., Cazzador, F., Grønlien, K. G., & Tønnesen, H. H. (2020). Effect of curcumin and cosolvents on the micellization of Pluronic F127 in aqueous solution. *Colloids and Surfaces B: Biointerfaces*, *195*, 111250. https://doi.org/10.1016/j.colsurfb.2020.111250

Thakur, P., Sonawane, S. S., Sonawane, S. H., & Bhanvase, B. A. (2020). Nanofluids-based delivery system, encapsulation of nanoparticles for stability to make stable nanofluids. In B. A. B. a. M. S. Shirish H. Sonawane (Ed.), *Encapsulation of active molecules and their delivery system* (pp. 141-152).

Elsevier. https://doi.org/10.1016/C2018-0-05369-4

Thomson, A., Sinclair, P., Matisko, A., Rosen, E., Andersson, T., & Olofsson, B. (1997). Influence of food on the bioavailability of an enteric-coated tablet formulation of omeprazole 20 mg under repeated dose conditions. *Canadian Journal of Gastroenterology*, *11*(8), 663-667. https://doi.org/10.1155/1997/830856

Tønsberg, H., Holm, R., Bisgaard, J., Jacobsen, J., & Müllertz, A. (2010). Effects of polysorbate 80 on the in-vitro precipitation and oral bioavailability of halofantrine from polyethylene glycol 400 formulations in rats. *Journal of pharmacy and pharmacology*, *62*(1), 63-70. https://doi.org/10.1211/jpp.62.01.0006

Tønsberg, H., Holm, R., Mu, H., Boll, J. B., Jacobsen, J., & Müllertz, A. (2011). Effect of bile on the oral absorption of halofantrine in polyethylene glycol 400 and polysorbate 80 formulations dosed to bile duct cannulated rats. *Journal of pharmacy and pharmacology*, *63*(6), 817-824. https://doi.org/10.1111/j.2042-7158.2011.01286.x

Tong, H. H., Du, Z., Wang, G. N., Chan, H., Chang, Q., Lai, L. C., Chow, A. H., & Zheng, Y. (2011). Spray freeze drying with polyvinylpyrrolidone and sodium caprate for improved dissolution and oral bioavailability of oleanolic acid, a BCS Class IV compound. *International journal of pharmaceutics*, *404*(1-2), 148-158. https://doi.org/10.1016/j.ijpharm.2010.11.027

Treesinchai, S., & Pitaksuteepong, T. (2020). Determination of curcumin stability in various gastro-intestinal pH by Arrhenius equation using HPLC method. *Pharm. Sci. Asia*, *47*, 86-96.

https://doi.org/10.29090/psa.2020.01.019.0013

Türker, S., Onur, E., & Özer, Y. (2004). Nasal route and drug delivery systems. *Pharmacy world and Science*, *26*(3), 137-142. https://doi.org/10.1023/b:phar.0000026823.82950.ff.

Tuomela, A., Hirvonen, J., & Peltonen, L. (2016). Stabilizing agents for drug nanocrystals: effect on bioavailability. *Pharmaceutics*, *8*(2), 16. https://doi.org/10.3390/pharmaceutics8020016

Tubtimsri, S., & Weerapol, Y. (2021). Improvement in solubility and absorption of nifedipine using solid solution: correlations between surface free energy and drug dissolution. *Polymers*, *13*(17), 2963. https://doi.org/10.3390/polym13172963

Tsume, Y., Mudie, D. M., Langguth, P., Amidon, G. E., & Amidon, G. L. (2014). The Biopharmaceutics Classification System: subclasses for in vivo predictive dissolution (IPD) methodology and IVIVC. *European journal of pharmaceutical sciences*, *57*, 152-163.

USP. (2011). *⟨711⟩ DISSOLUTION*. Retrieved 27 August from https://www.usp.org/sites/default/files/usp/document/harmonization/gen-method/stage_6_monograph_25_feb_2011.pdf

USP. (2013). *1092 THE DISSOLUTION PROCEDURE: DEVELOPMENT AND VALIDATION*. https://www.uspnf.com/sites/default/files/usp_pdf/EN/USPNF/gc_1092.pdf

Ulusoy, H. G., & Sanlier, N. (2020). A minireview of quercetin: from its

metabolism to possible mechanisms of its biological activities. *Critical reviews in food science and nutrition*, *60*(19), 3290-3303. https://doi.org/10.1080/10408398.2019.1683810

Uzan, E., Portet, B., Lubrano, C., Milesi, S., Favel, A., Lesage-Meessen, L., & Lomascolo, A. (2011). Pycnoporus laccase-mediated bioconversion of rutin to oligomers suitable for biotechnology applications. *Applied microbiology and biotechnology*, *90*(1), 97-105. https://doi.org/10.1007/s00253-010-3075-4

Vasconcelos, T., Sarmento, B., & Costa, P. (2007). Solid dispersions as strategy to improve oral bioavailability of poor water soluble drugs. *Drug discovery today*, *12*(23-24), 1068-1075. https://doi.org/10.1016/j.drudis.2007.09.005

van Drooge, D.-J., Hinrichs, W. L., Dickhoff, B. H., Elli, M. N., Visser, M. R., Zijlstra, G. S., & Frijlink, H. W. (2005). Spray freeze drying to produce a stable Δ9-tetrahydrocannabinol containing inulin-based solid dispersion powder suitable for inhalation. *European journal of pharmaceutical sciences*, *26*(2), 231-240. https://doi.org/10.1016/j.ejps.2005.06.007

Van Drooge, D., Hinrichs, W., Visser, M., & Frijlink, H. (2006). Characterization of the molecular distribution of drugs in glassy solid dispersions at the nano-meter scale, using differential scanning calorimetry and gravimetric water vapour sorption techniques. *International journal of pharmaceutics*, *310*(1-2), 220-229. https://doi.org/10.1016/j.ijpharm.2005.12.007

van Breemen, R. B., & Li, Y. (2005). Caco-2 cell permeability assays to measure drug absorption. *Expert opinion on drug metabolism & toxicology*,

1(2), 175-185. https://doi.org/10.1517/17425255.1.2.175

Valeh-e-Sheyda, P., Rahimi, M., Adibi, H., Razmjou, Z., & Ghasempour, H. (2015). An insight on reducing the particle size of poorly-water soluble curcumin via LASP in microchannels. *Chemical Engineering and Processing: Process Intensification*, *91*, 78-88. https://doi.org/10.1016/j.cep.2015.03.018

Vaz-da-Silva, M., Hainzl, D., Almeida, L., Dolgner, A., Silveira, P., Maia, J., & Soares-da-Silva, P. (2001). Relative bioavailability of two enteric-coated formulations of omeprazole following repeated doses in healthy volunteers. *Clinical Drug Investigation*, *21*(3), 203-210. https://doi.org/10.2165/00044011-200121030-00006

Vaessen, S. F., van Lipzig, M. M., Pieters, R. H., Krul, C. A., Wortelboer, H. M., & van de Steeg, E. (2017). Regional expression levels of drug transporters and metabolizing enzymes along the pig and human intestinal tract and comparison with Caco-2 cells. *Drug metabolism and disposition*, *45*(4), 353-360. https://doi.org/10.1124/dmd.116.072231

Vecchione, R., Quagliariello, V., Calabria, D., Calcagno, V., De Luca, E., Iaffaioli, R. V., & Netti, P. A. (2016). Curcumin bioavailability from oil in water nano-emulsions: In vitro and in vivo study on the dimensional, compositional and interactional dependence. *Journal of Controlled Release*, *233*, 88-100. https://doi.org/10.1016/j.jconrel.2016.05.004.

Venkatesan, N. (1998). Curcumin attenuation of acute adriamycin myocardial toxicity in rats. *British journal of pharmacology*, *124*(3), 425-427. https://doi.org/10.1038/sj.bjp.0701877.

Venkatesan, N., Punithavathi, D., & Arumugam, V. (2000). Curcumin prevents adriamycin nephrotoxicity in rats. *British journal of pharmacology*, *129*(2), 231-234. https://doi.org/10.1038/sj.bjp.0703067

Vilhelmsen, T., Eliasen, H., & Schæfer, T. (2005). Effect of a melt agglomeration process on agglomerates containing solid dispersions. *International journal of pharmaceutics*, *303*(1-2), 132-142. https://doi.org/10.1016/j.ijpharm.2005.07.012

Vijay, N., & Morris, M. E. (2014). Role of monocarboxylate transporters in drug delivery to the brain. *Current pharmaceutical design*, *20*(10), 1487-1498. https://doi.org/10.2174/13816128113199990462

Volak, L. P., Ghirmai, S., & Cashman, J. R. (2008). Curcuminoids inhibit multiple human cytochromes P450, UDP-glucuronosyltransferase, and sulfotransferase enzymes, whereas piperine is a relatively selective CYP3A4 inhibitor. *Drug metabolism and disposition*, *36*(8), 1594-1605. https://doi.org/10.1124/dmd.108.020552.

Volpe, D. A., Faustino, P. J., Ciavarella, A. B., Asafu-Adjaye, E. B., Ellison, C. D., Yu, L. X., & Hussain, A. S. (2007). Classification of drug permeability with a Caco-2 cell monolayer assay. *Clinical Research and Regulatory Affairs*, *24*(1), 39-47. https://doi.org/10.1080/10601330701273669

Vo, C. L.-N., Park, C., & Lee, B.-J. (2013). Current trends and future perspectives of solid dispersions containing poorly water-soluble drugs. *European Journal of Pharmaceutics and Biopharmaceutics*, *85*(3), 799-813. https://doi.org/https://doi.org/10.1016/j.ejpb.2013.09.007

vs-corp. (2020). *Longvida*®. Retrieved 29 August from https://www.vs-corp.com/longvida

Vuddanda, P. R., Rajamanickam, V. M., Yaspal, M., & Singh, S. (2014). Investigations on agglomeration and haemocompatibility of vitamin E TPGS surface modified berberine chloride nanoparticles. *BioMed research international*, *2014*. https://doi.org/10.1155/2014/951942

Wahlang, B., Pawar, Y. B., & Bansal, A. K. (2011). Identification of permeability-related hurdles in oral delivery of curcumin using the Caco-2 cell model. *European Journal of Pharmaceutics and Biopharmaceutics*, *77*(2), 275-282. https://doi.org/10.1016/j.ejpb.2010.12.006.

Wahlström, B., & Blennow, G. (1978). A study on the fate of curcumin in the rat. *Acta pharmacologica et toxicologica*, *43*(2), 86-92. https://doi.org/10.1111/j.1600-0773.1978.tb02240.x

Wan, K., Sun, L., Hu, X., Yan, Z., Zhang, Y., Zhang, X., & Zhang, J. (2016). Novel nanoemulsion based lipid nanosystems for favorable in vitro and in vivo characteristics of curcumin. *International journal of pharmaceutics*, *504*(1-2), 80-88. https://doi.org/10.1016/j.ijpharm.2016.03.055.

Wan, S., Sun, Y., Qi, X., & Tan, F. (2012). Improved bioavailability of poorly water-soluble drug curcumin in cellulose acetate solid dispersion. *AAPS PharmSciTech*, *13*(1), 159-166. https://doi.org/10.1208/s12249-011-9732-9

Wang, F., Yang, Y., Ju, X., Udenigwe, C. C., & He, R. (2018). Polyelectrolyte complex nanoparticles from chitosan and acylated rapeseed cruciferin protein for curcumin delivery. *Journal of agricultural and food chemistry*, *66*(11), 2685-

2693. https://doi.org/10.1021/acs.jafc.7b05083

Wang, Y. t., Wang, C. y., Zhao, J., Ding, Y. f., & Li, L. (2017). A cost-effective method to prepare curcumin nanosuspensions with enhanced oral bioavailability. *Journal of Colloid and Interface Science*, *485*, 91-98. https://doi.org/10.1016/j.jcis.2016.09.003.

Wang, X., Michoel, A., & Van den Mooter, G. (2005). Solid state characteristics of ternary solid dispersions composed of PVP VA64, Myrj 52 and itraconazole. *International journal of pharmaceutics*, *303*(1-2), 54-61. https://doi.org/10.1016/j.ijpharm.2005.07.002

Wang, J., Ma, W., & Tu, P. (2015). The mechanism of self-assembled mixed micelles in improving curcumin oral absorption: in vitro and in vivo. *Colloids and Surfaces B: Biointerfaces*, *133*, 108-119. https://doi.org/10.1016/j.colsurfb.2015.05.056.

Wang, R., Han, J., Jiang, A., Huang, R., Fu, T., Wang, L., Zheng, Q., Li, W., & Li, J. (2019). Involvement of metabolism-permeability in enhancing the oral bioavailability of curcumin in excipient-free solid dispersions co-formed with piperine. *International journal of pharmaceutics*, *561*, 9-18. https://doi.org/10.1016/j.ijpharm.2019.02.027.

Vishweshwar, P., McMahon, J. A., Bis, J. A., & Zaworotko, M. J. (2006). Pharmaceutical co-crystals. *Journal of pharmaceutical sciences*, *95*(3), 499-516. https://doi.org/10.1002/jps.20578

Wang, Y.-J., Pan, M.-H., Cheng, A.-L., Lin, L.-I., Ho, Y.-S., Hsieh, C.-Y., & Lin, J.-K. (1997). Stability of curcumin in buffer solutions and characterization of its

degradation products. *Journal of pharmaceutical and biomedical analysis*, *15*(12), 1867-1876. https://doi.org/10.1016/s0731-7085(96)02024-9.

Wang, Y., Ke, X., Zhang, C., & Yang, R. (2017a). Absorption mechanism of three curcumin constituents through in situ intestinal perfusion method. *Brazilian Journal of Medical and Biological Research*, *50*. https://doi.org/10.1590/1414-431x20176353.

Wang, W., Sun, C., Mao, L., Ma, P., Liu, F., Yang, J., & Gao, Y. (2016). The biological activities, chemical stability, metabolism and delivery systems of quercetin: A review. *Trends in Food Science & Technology*, *56*, 21-38. https://doi.org/10.1016/j.tifs.2016.07.004

Wang, Y. t., Wang, C. y., Zhao, J., Ding, Y. f., & Li, L. (2017b). A cost-effective method to prepare curcumin nanosuspensions with enhanced oral bioavailability. *Journal of Colloid and Interface Science*, *485*, 91-98. https://doi.org/10.1016/j.jcis.2016.09.003.

Wang, F., Yang, Y., Ju, X., Udenigwe, C. C., & He, R. (2018). Polyelectrolyte complex nanoparticles from chitosan and acylated rapeseed cruciferin protein for curcumin delivery. *Journal of agricultural and food chemistry*, *66*(11), 2685-2693. https://doi.org/10.1021/acs.jafc.7b05083

Wang, Y. t., Wang, C. y., Zhao, J., Ding, Y. f., & Li, L. (2017). A cost-effective method to prepare curcumin nanosuspensions with enhanced oral bioavailability. *Journal of Colloid and Interface Science*, *485*, 91-98. https://doi.org/10.1016/j.jcis.2016.09.003.

Warren, B. E. (2003). *X-ray Diffraction*. Dover Publications Inc.

Zhang, D., Lee, Y.-C., Shabani, Z., Frankenfeld Lamm, C., Zhu, W., Li, Y., & Templeton, A. (2018). Processing impact on performance of solid dispersions. *Pharmaceutics*, *10*(3), 142. https://doi.org/10.3390/pharmaceutics10030142

Walgren, R. A., Walle, U. K., & Walle, T. (1998). Transport of quercetin and its glucosides across human intestinal epithelial Caco-2 cells. *Biochemical pharmacology*, *55*(10), 1721-1727. https://doi.org/10.1016/s0006-2952(98)00048-3

Watson, C., Rowland, M., & Warhurst, G. (2001). Functional modeling of tight junctions in intestinal cell monolayers using polyethylene glycol oligomers. *American Journal of Physiology-Cell Physiology*, *281*(2), C388-C397. https://doi.org/10.1152/ajpcell.2001.281.2.C388

Wanwimolruk, S., Chalcroft, S., Coville, P. F., & Campbell, A. J. (1991). Pharmacokinetics of quinine in young and elderly subjects. *Transactions of the Royal Society of Tropical Medicine and Hygiene*, *85*(6), 714-717. https://doi.org/10.1016/0035-9203(91)90423-V

WHO. (2020). *DISSOLUTION TEST FOR SOLID ORAL DOSAGE FORMS. Draft proposal for revision in The International Pharmacopoeia*. Retrieved 21 August from https://cdn.who.int/media/docs/default-source/medicines/norms-and-standards/current-projects/qas20-837-dissolution-test-for-solid-oral-dosage-forms.pdf?sfvrsn=f712c6df_2

Williams, J. A., Ring, B. J., Cantrell, V. E., Campanale, K., Jones, D. R., Hall, S. D., & Wrighton, S. A. (2002). Differential modulation of UDP-glucuronosyltransferase 1A1 (UGT1A1)-catalyzed estradiol-3-glucuronidation by the addition of UGT1A1 substrates and other compounds to human liver

microsomes. *Drug metabolism and disposition*, *30*(11), 1266-1273. https://doi.org/10.1124/dmd.30.11.1266.

Williams, G. C., Liu, A., Knipp, G., & Sinko, P. J. (2002). Direct evidence that saquinavir is transported by multidrug resistance-associated protein (MRP1) and canalicular multispecific organic anion transporter (MRP2). *Antimicrobial agents and chemotherapy*, *46*(11), 3456-3462. https://doi.org/https://doi.org/10.1128/AAC.46.11.3456-3462.2002

Wisudyaningsih, B., Sallama, S., & Setyawan, D. (2021). The Effect of pH and Cocrystal Quercetin-Isonicotinamide on Quercetin Solubility and its Thermodynamic. *Research Journal of Pharmacy and Technology*, *14*(9), 4657-4661. https://doi.org/10.52711/0974-360X.2021.00809

Won, D.-H., Kim, M.-S., Lee, S., Park, J.-S., & Hwang, S.-J. (2005). Improved physicochemical characteristics of felodipine solid dispersion particles by supercritical anti-solvent precipitation process. *International journal of pharmaceutics*, *301*(1-2), 199-208. https://doi.org/10.1016/j.ijpharm.2005.05.017

Xia, C. Q., Liu, N., Yang, D., Miwa, G., & Gan, L.-S. (2005). Expression, localization, and functional characteristics of breast cancer resistance protein in Caco-2 cells. *Drug metabolism and disposition*, *33*(5), 637-643. https://doi.org/10.1124/dmd.104.003442

Xu, W., Ling, P., & Zhang, T. (2013). Polymeric micelles, a promising drug delivery system to enhance bioavailability of poorly water-soluble drugs. *Journal of drug delivery*, *2013*. https://doi.org/10.1155/2013/340315.

Xu, J., & Liu, C. (2013). Effect of the critical temperature of organic fluids on supercritical pressure Organic Rankine Cycles. *Energy*, *63*, 109-122. https://doi.org/10.1016/j.energy.2013.09.068

Xu, J., Shi, P.-Y., Li, H., & Zhou, J. (2020). Broad spectrum antiviral agent niclosamide and its therapeutic potential. *ACS infectious diseases*, *6*(5), 909-915. https://doi.org/10.1021/acsinfecdis.0c00052

Xu, Y., Shrestha, N., Préat, V., & Beloqui, A. (2021). An overview of in vitro, ex vivo and in vivo models for studying the transport of drugs across intestinal barriers. *Advanced drug delivery reviews*, *175*, 113795. https://doi.org/10.1016/j.addr.2021.05.005

Xue, M., Cheng, Y., Xu, L., & Zhang, L. (2017). Study of the intestinal absorption characteristics of curcumin in vivo and in vitro. *J. Appl. Pharm*, *9*. https://doi.org/10.21065/1920-4159.1000246,

Yadav, V., Mishra, K., Singh, D., Mehrotra, S., & Singh, V. (2005). Immunomodulatory effects of curcumin. *Immunopharmacology and immunotoxicology*, *27*(3), 485-497. https://doi.org/10.1080/08923970500242244

Yang, M., Akbar, U., & Mohan, C. (2019). Curcumin in autoimmune and rheumatic diseases. *Nutrients*, *11*(5), 1004. https://doi.org/10.3390/nu11051004.

Yang, C.-Y., Hsiu, S.-L., Wen, K.-C., Lin, S.-P., Tsai, S.-Y., Hou, Y.-C., & Chao, P.-D. (2005). Bioavailability and metabolic pharmacokinetics of rutin and

quercetin in rats. *journal of food and drug analysis*, *13*(3), 5. https://doi.org/10.38212/2224-6614.2517

Yang, J., Lee, H., Sung, J., Kim, Y., Jeong, H. S., & Lee, J. (2019). Conversion of rutin to quercetin by acid treatment in relation to biological activities. *Preventive nutrition and food science*, *24*(3), 313. https://doi.org/10.3746/pnf.2019.24.3.313

Youssef, K. M., El-Sherbeny, M. A., El-Shafie, F. S., Farag, H. A., Al-Deeb, O. A., & Awadalla, S. A. A. (2004). Synthesis of curcumin analogues as potential antioxidant, cancer chemopreventive agents. *Archiv der Pharmazie: An International Journal Pharmaceutical and Medicinal Chemistry*, *337*(1), 42-54. https://doi.org/10.1002/ardp.200300763

Yu, L. (2001). Amorphous pharmaceutical solids: preparation, characterization and stabilization. *Advanced drug delivery reviews*, *48*(1), 27-42. https://doi.org/10.1016/S0169-409X(01)00098-9

Yu, H., & Huang, Q. (2011). Investigation of the absorption mechanism of solubilized curcumin using Caco-2 cell monolayers. *Journal of agricultural and food chemistry*, *59*(17), 9120-9126. https://doi.org/10.1021/jf201451m

Yu, H., Cook, T. J., & Sinko, P. J. (1997). Evidence for diminished functional expression of intestinal transporters in Caco-2 cell monolayers at high passages. *Pharmaceutical research*, *14*(6), 757-762. https://doi.org/10.1023/a:1012150405949

Zastre, J., Dowd, C., Bruckner, J., & Popovici, A. (2013). Lack of P-glycoprotein-mediated efflux and the potential involvement of an influx

transport process contributing to the intestinal uptake of deltamethrin, cis-permethrin, and trans-permethrin. *toxicological sciences*, *136*(2), 284-293. https://doi.org/10.1093/toxsci/kft193

Zeng, X., Cai, D., Zeng, Q., Chen, Z., Zhong, G., Zhuo, J., Gan, H., Huang, X., Zhao, Z., & Yao, N. (2017b). Selective reduction in the expression of UGTs and SULTs, a novel mechanism by which piperine enhances the bioavailability of curcumin in rat. *Biopharmaceutics & Drug Disposition*, *38*(1), 3-19. https://doi.org/10.1002/bdd.2049.

Zeng, Z., Shen, Z. L., Zhai, S., Xu, J. L., Liang, H., Shen, Q., & Li, Q. Y. (2017a). Transport of curcumin derivatives in Caco-2 cell monolayers. *European Journal of Pharmaceutics and Biopharmaceutics*, *117*, 123-131. https://doi.org/10.1016/j.ejpb.2017.04.004.

Zeng, Z., Shen, Z. L., Zhai, S., Xu, J. L., Liang, H., Shen, Q., & Li, Q. Y. (2017). Transport of curcumin derivatives in Caco-2 cell monolayers. *European Journal of Pharmaceutics and Biopharmaceutics*, *117*, 123-131. https://doi.org/10.1016/j.ejpb.2017.04.004.

Zhang, M., Li, H., Lang, B., O'Donnell, K., Zhang, H., Wang, Z., Dong, Y., Wu, C., & Williams III, R. O. (2012). Formulation and delivery of improved amorphous fenofibrate solid dispersions prepared by thin film freezing. *European Journal of Pharmaceutics and Biopharmaceutics*, *82*(3), 534-544. https://doi.org/10.1016/j.ejpb.2012.06.016

Zhang, L., Liu, L., Qian, Y., & Chen, Y. (2008). The effects of cryoprotectants on the freeze-drying of ibuprofen-loaded solid lipid microparticles (SLM). *European Journal of Pharmaceutics and Biopharmaceutics*, *69*(2), 750-759.

https://doi.org/10.1016/j.ejpb.2007.12.003

Zhang, R., Guo, P., Zhou, J., Li, P., Wan, J., Yang, C., Zhou, J., Liu, Y., & Shi, S. (2022). Pharmacokinetics and Bioequivalence of Two Formulations of Omeprazole and Sodiun bicarbonate powder, for suspension: A Randomized, Single-Dose, Two-Period, Two-Sequence Crossover Study in Healthy Chinese Volunteers. https://doi.org/10.21203/rs.3.rs-1681720/v1

Zheng, K., Lin, Z., Capece, M., Kunnath, K., Chen, L., & Davé, R. N. (2019). Effect of particle size and polymer loading on dissolution behavior of amorphous griseofulvin powder. *Journal of pharmaceutical sciences*, *108*(1), 234-242. https://doi.org/10.1016/j.xphs.2018.11.025

Zhang, L., Gu, F., Chan, J., Wang, A., Langer, R., & Farokhzad, O. (2008). Nanoparticles in medicine: therapeutic applications and developments. *Clinical pharmacology & therapeutics*, *83*(5), 761-769. https://doi.org/10.1038/sj.clpt.6100400.

Zhang, Q., Polyakov, N. E., Chistyachenko, Y. S., Khvostov, M. V., Frolova, T. S., Tolstikova, T. G., Dushkin, A. V., & Su, W. (2018). Preparation of curcumin self-micelle solid dispersion with enhanced bioavailability and cytotoxic activity by mechanochemistry. *Drug Delivery*, *25*(1), 198-209. https://doi.org/10.1080/10717544.2017.1422298.

Zorofchian Moghadamtousi, S., Abdul Kadir, H., Hassandarvish, P., Tajik, H., Abubakar, S., & Zandi, K. (2014). A review on antibacterial, antiviral, and antifungal activity of curcumin. *BioMed research international*, *2014*. https://doi.org/10.1155/2014/186864

Publications

Publication 1

Liu, Z., Smart, J. D., & Pannala, A. S. (2020). Recent developments in formulation design for improving oral bioavailability of curcumin: a review. *Journal of Drug Delivery Science and Technology*, *60*, 102082. https://doi.org/10.1016/j.jddst.2020.102082

Journal of Drug Delivery Science and Technology 60 (2020) 102082

Contents lists available at ScienceDirect

Journal of Drug Delivery Science and Technology

journal homepage: www.elsevier.com/locate/jddst

Review article

Recent developments in formulation design for improving oral bioavailability of curcumin: A review

Zhenqi Liu, John D. Smart, Ananth S. Pannala *

Biomaterials and Drug Delivery Research Group, School of Pharmacy and Biomolecular Science, University of Brighton, Brighton, BN2 4GJ, UK

ARTICLE INFO

Keywords:
Curcumin
Oral bioavailability
Delivery system
Liposomes
Clinical studies
Solupher®
Piperine

ABSTRACT

Curcumin, a yellow-orange substance that is extracted from the spice turmeric (*Curcuma longa, Zingiberaceae*), has been attributed with a wide range of pharmacological activities for the prevention and treatment of several disease conditions such as arthritis, hypertension, diabetes, Alzheimer's, antibacterial and cancer to name a few. However, its potential for use as an orally delivered medicinal product is hindered by its poor solubility and bioavailability. The low oral bioavailability of curcumin is caused by several factors including low aqueous solubility, poor intestinal permeability, unstable at alkaline pH and rapid metabolism. To improve curcumin's poor oral bioavailability, different formulation strategies such as incorporation into nanoparticles, liposomes, micelles, micro/nano-emulsions and solid dispersions as well as co-administration with piperine have been investigated in both animal models as well as human supplementation studies. In this review, novel formulations of curcumin for oral delivery that were developed in recent years are reviewed and discussed.

1. Introduction

Curcumin is a yellow orange coloured crystalline compound that is extracted from the spice turmeric (*Curcuma longa, Zingiberaceae*). Chemically, curcumin is known as diferuloylmethane ($C_{21}H_{20}O_6$) with a molecular mass of 368.37 g/mol. It is a polyphenol compound and has a melting point of 183 °C. The IUPAC name of curcumin is 1,7-bis (4-hydroxy-3-methoxy phenyl)-1,6-heptadiene-3,5-dione (1E-6E). The two aryl rings in curcumin contain *ortho*-methoxy phenolic groups are symmetrically linked to a β-diketone moiety [1,2,3,4]. Curcumin exhibits a pH-dependent keto–enol tautomerism, where in an acidic or neutral solution, the keto form of curcumin is predominant while in an alkaline medium the enol form of curcumin becomes predominant (Fig. 1) [1,5,6]. The colour of curcumin also changes at different pH levels forming a bright yellow coloured solution at pH range 2.5–7.0 with the colour changing to dark red when the pH is increased above 7 [1,4].

The use of turmeric for medical treatment in Asia can be traced back thousands of years [2]. Turmeric has been widely used since ancient times as a herbal medicine for treating many conditions such as cough/inflammation, respiratory diseases, flu, sinusitis, liver disorders, rheumatism and abdominal pain [7,8,9]. In India, turmeric is traditionally used for treating infections, sprains/swelling and healing burn wounds [10], while in China turmeric is regularly used as herbal medication for treating diseases that are associated with abdominal pain [11]. With the advancement of science and technology, it had been discovered that curcumin is the key ingredient that contributes to most of the therapeutic effects of turmeric [12,13]. Curcumin was found to have a wide spectrum of pharmacological activities. Several studies on curcumin showed that it has anti-inflammatory [14], antimicrobial [15,16,17,18], antirheumatic [19], immunomodulatory [20] and anti-tumour effects [21]. The anti-tumour effect of curcumin is associated with the suppression of early growth of response-1-gene product (EGR-1), protein tyrosine kinase cascade and mitogen-activated protein kinases (MAPK) pathway [22]. Curcumin also demonstrates antioxidant property based on its ability to scavenge free radicals due to the electron donating property of the phenolic group [23,24,25,26,27]. The anti-inflammatory effect of curcumin is associated with its ability to inhibit NFκB (Nuclear factor κB) to bind with DNA. The inhibition of NFκB-DNA binding lead to suppression of pro-inflammatory molecules MMP-3 (matrix metalloprotease 3) and MMP-9 (matrix metalloprotease 9). It also results in reduction in pro-inflammatory cytokines, such as TNFα (tumour necrosis factor 1α), IL1β (interleukin 1β) and IL8 (interleukin 8) [4]. In addition, curcumin also exert anti-inflammatory effects by binding to proteins COX-2 (prostaglandin-endoperoxide synthase 2), which leads to reduction in COX-2 expression, prostaglandin and

* Corresponding author. School of Pharmacy and Biomolecular Sciences University of Brighton Lewes Road Brighton, BN2 4GJ, UK.
E-mail address: a.s.v.pannala@brighton.ac.uk (A.S. Pannala).

https://doi.org/10.1016/j.jddst.2020.102082
Received 17 July 2020; Received in revised form 2 September 2020; Accepted 9 September 2020
Available online 13 September 2020

Publication 2

Liu, Z., Lansley, A. B., Duong, T. N., Smart, J. D., & Pannala, A. S. (2022). Increasing Cellular Uptake and Permeation of Curcumin Using a Novel Polymer-Surfactant Formulation. *Biomolecules*, *12*(12), 1739. https://doi.org/10.3390/biom12121739

biomolecules

MDPI

Article

Increasing Cellular Uptake and Permeation of Curcumin Using a Novel Polymer-Surfactant Formulation

Zhenqi Liu [1], Alison B. Lansley [1], Tu Ngoc Duong [2], John D. Smart [1] and Ananth S. Pannala [1,*]

[1] Biomaterials and Drug Delivery Research Group, School of Applied Sciences, University of Brighton, Brighton BN2 4GJ, UK
[2] Vietnam Academy of Science and Technology, 18 Hoang Quoc Viet, Hanoi 100000, Vietnam
* Correspondence: a.s.v.pannala@brighton.ac.uk

Abstract: Several therapeutically active molecules are poorly water-soluble, thereby creating a challenge for pharmaceutical scientists to develop an active solution for their oral drug delivery. This study aimed to investigate the potential for novel polymer-surfactant-based formulations (designated A and B) to improve the solubility and permeability of curcumin. A solubility study and characterization studies (FTIR, DSC and XRD) were conducted for the various formulations. The cytotoxicity of formulations and commercial comparators was tested via MTT and LDH assays, and their permeability by in vitro drug transport and cellular drug uptake was established using the Caco-2 cell model. The apparent permeability coefficients (Papp) are considered a good indicator of drug permeation. However, it can be argued that the magnitude of Papp, when used to reflect the permeability of the cells to the drug, can be influenced by the initial drug concentration (C_0) in the donor chamber. Therefore, Papp (suspension) and Papp (solution) were calculated based on the different values of C_0. It was clear that Papp (solution) can more accurately reflect drug permeation than Papp (suspension). Formulation A, containing Soluplus® and vitamin E TPGs, significantly increased the permeation and cellular uptake of curcumin compared to other samples, which is believed to be related to the increased aqueous solubility of the drug in this formulation.

Keywords: curcumin; Soluplus®; vitamin E TPGs; cell permeability; oral bioavailability; Caco-2 cell; aqueous solubility; Longvida®; Nacumin®; cytotoxicity

check for updates

Citation: Liu, Z.; Lansley, A.B.; Duong, T.N.; Smart, J.D.; Pannala, A.S. Increasing Cellular Uptake and Permeation of Curcumin Using a Novel Polymer-Surfactant Formulation. *Biomolecules* 2022, *12*, 1739. https://doi.org/10.3390/biom12121739

Academic Editor: Vladimir N. Uversky

Received: 28 October 2022
Accepted: 21 November 2022
Published: 23 November 2022

Publisher's Note: MDPI stays neutral with regard to jurisdictional claims in published maps and institutional affiliations.

1. Introduction

Turmeric (*Curcuma longa*, Zingiberaceae) has a long history of use in the treatment of various medical conditions [1,2], such as coughs, inflammation, respiratory diseases, influenza, sinusitis, liver disorders, rheumatism, and abdominal pain [3–5]. Curcumin, a major curcuminoid that occurs naturally in turmeric, is responsible for the wide range of health benefits of turmeric. The IUPAC name of curcumin is 1,7-bis(4-hydroxy-3-methoxy phenyl)-1,6-heptadiene-3,5-dione (1E-6E). The two aryl rings in curcumin contain *ortho*-methoxy phenolic groups that are symmetrically linked to a β-diketone moiety. Curcumin exhibits a pH-dependent keto–enol tautomerism; in an acidic or neutral solution, the keto form of curcumin is predominant, while in an alkaline medium, the enol form of curcumin becomes predominant (Figure 1).